US009364609B2

(12) **United States Patent**
Keenan et al.

(10) **Patent No.: US 9,364,609 B2**
(45) **Date of Patent: Jun. 14, 2016**

(54) **INSULIN ON BOARD COMPENSATION FOR A CLOSED-LOOP INSULIN INFUSION SYSTEM**

(71) Applicant: **MEDTRONIC MINIMED, INC.**, Northridge, CA (US)

(72) Inventors: **Desmond Barry Keenan**, Hollywood, CA (US); **John J. Mastrototaro**, Los Angeles, CA (US); **Benyamin Grosman**, North Hollywood, CA (US); **Neha J. Parikh**, West Hills, CA (US); **Anirban Roy**, Calabasas, CA (US)

(73) Assignee: **Medtronic MiniMed, Inc.**, Northridge, CA (US)

(*) Notice: Subject to any disclaimer, the term of this patent is extended or adjusted under 35 U.S.C. 154(b) by 341 days.

(21) Appl. No.: **13/870,902**

(22) Filed: **Apr. 25, 2013**

(65) **Prior Publication Data**

US 2014/0066892 A1 Mar. 6, 2014

Related U.S. Application Data

(60) Provisional application No. 61/694,950, filed on Aug. 30, 2012, provisional application No. 61/694,961, filed on Aug. 30, 2012, provisional application No. 61/812,874, filed on Apr. 17, 2013.

(51) **Int. Cl.**
G06Q 10/00 (2012.01)
A61M 5/172 (2006.01)
(Continued)

(52) **U.S. Cl.**
CPC ***A61M 5/1723*** (2013.01); ***A61B 5/14503*** (2013.01); ***A61B 5/14532*** (2013.01); ***A61B 5/4839*** (2013.01); ***A61B 5/746*** (2013.01); ***A61M 5/172*** (2013.01); ***G06F 19/3468*** (2013.01)

(58) **Field of Classification Search**
USPC 702/19
See application file for complete search history.

(56) **References Cited**

U.S. PATENT DOCUMENTS

3,631,847 A 1/1972 Hobbs, II
4,212,738 A 7/1980 Henne
(Continued)

FOREIGN PATENT DOCUMENTS

DE 4329229 3/1995
EP 0319268 11/1988
(Continued)

OTHER PUBLICATIONS

Garry M. Steil, et al., The Effect of Insulin Feedback on Closed Loop Glucose Control, Journal of Clinical Endocrinology & Metabolism, May 1, 2011, pp. 1402-1408, vol. 96, Issue No. 5.
(Continued)

Primary Examiner — Valerie Lubin
(74) *Attorney, Agent, or Firm* — Ingrassia Fisher & Lorenz, P.C.

(57) **ABSTRACT**

An electronic controller for an insulin infusion device includes a processor architecture and at least one memory element. The memory element stores executable instructions that, when executed by the processor architecture, provide an insulin on board (IOB) compensation module to estimate a current IOB value that indicates an amount of active insulin in the body of the user, calculate an IOB rate based at least in part on the estimated current IOB value, determine an adjusted insulin infusion rate based at least in part on the calculated IOB rate and an uncompensated insulin infusion rate, select a final insulin infusion rate for the device, and provide the selected final insulin infusion rate to regulate delivery of insulin by the device.

10 Claims, 53 Drawing Sheets

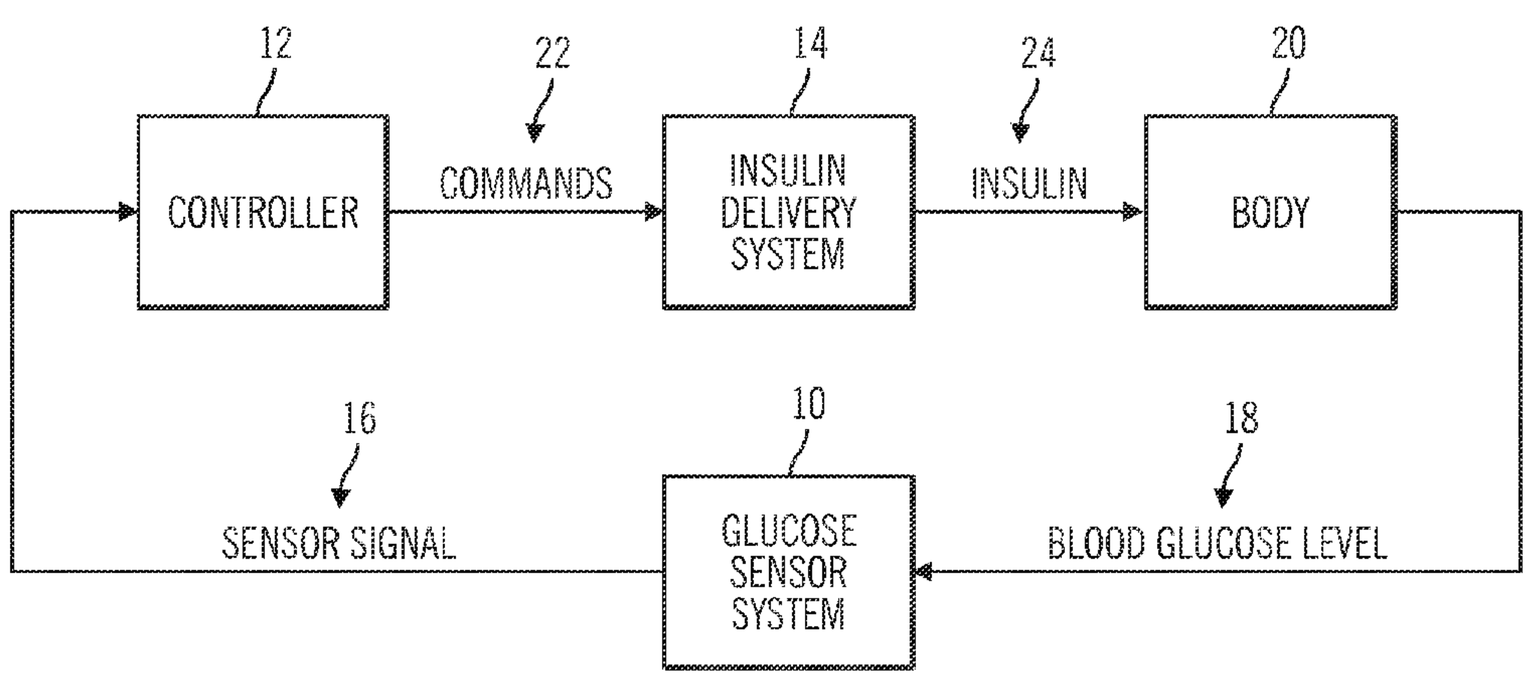

(51) **Int. Cl.**

A61B 5/00	(2006.01)
A61B 5/145	(2006.01)
G06F 19/00	(2011.01)

(56) **References Cited**

U.S. PATENT DOCUMENTS

4,270,532	A	6/1981	Franetzki et al.
4,282,872	A	8/1981	Franetzki et al.
4,373,527	A	2/1983	Fischell
4,395,259	A	7/1983	Prestele et al.
4,433,072	A	2/1984	Pusineri et al.
4,443,218	A	4/1984	DeCant, Jr. et al.
4,494,950	A	1/1985	Fischell
4,533,346	A	8/1985	Cosgrove, Jr. et al.
4,542,532	A	9/1985	McQuilkin
4,550,731	A	11/1985	Batina et al.
4,559,037	A	12/1985	Franetzki et al.
4,562,751	A	1/1986	Nason et al.
4,573,994	A	3/1986	Fischell et al.
4,671,288	A	6/1987	Gough
4,678,408	A	7/1987	Nason et al.
4,685,903	A	8/1987	Cable et al.
4,731,051	A	3/1988	Fischell
4,731,726	A	3/1988	Allen, III
4,755,173	A	7/1988	Konopka et al.
4,781,798	A	11/1988	Gough
4,803,625	A	2/1989	Fu et al.
4,809,697	A	3/1989	Causey, III et al.
4,826,810	A	5/1989	Aoki
4,871,351	A	10/1989	Feingold
4,898,578	A	2/1990	Rubalcaba, Jr.
5,003,298	A	3/1991	Havel
5,011,468	A	4/1991	Lundquist et al.
5,019,974	A	5/1991	Beckers
5,050,612	A	9/1991	Matsumura
5,078,683	A	1/1992	Sancoff et al.
5,080,653	A	1/1992	Voss et al.
5,097,122	A	3/1992	Colman et al.
5,100,380	A	3/1992	Epstein et al.
5,101,814	A	4/1992	Palti
5,108,819	A	4/1992	Heller et al.
5,153,827	A	10/1992	Coutre et al.
5,165,407	A	11/1992	Wilson et al.
5,247,434	A	9/1993	Peterson et al.
5,262,035	A	11/1993	Gregg et al.
5,262,305	A	11/1993	Heller et al.
5,264,104	A	11/1993	Gregg et al.
5,264,105	A	11/1993	Gregg et al.
5,284,140	A	2/1994	Allen et al.
5,299,571	A	4/1994	Mastrototaro
5,307,263	A	4/1994	Brown
5,317,506	A	5/1994	Coutre et al.
5,320,725	A	6/1994	Gregg et al.
5,322,063	A	6/1994	Allen et al.
5,338,157	A	8/1994	Blomquist
5,339,821	A	8/1994	Fujimoto
5,341,291	A	8/1994	Roizen et al.
5,350,411	A	9/1994	Ryan et al.
5,356,786	A	10/1994	Heller et al.
5,357,427	A	10/1994	Langen et al.
5,368,562	A	11/1994	Blomquist et al.
5,370,622	A	12/1994	Livingston et al.
5,371,687	A	12/1994	Holmes, II et al.
5,376,070	A	12/1994	Purvis et al.
5,390,671	A	2/1995	Lord et al.
5,391,250	A	2/1995	Cheney, II et al.
5,403,700	A	4/1995	Heller et al.
5,411,647	A	5/1995	Johnson et al.
5,482,473	A	1/1996	Lord et al.
5,485,408	A	1/1996	Blomquist
5,497,772	A	3/1996	Schulman et al.
5,505,709	A	4/1996	Funderburk et al.
5,543,326	A	8/1996	Heller et al.
5,569,186	A	10/1996	Lord et al.
5,569,187	A	10/1996	Kaiser
5,573,506	A	11/1996	Vasko
5,582,593	A	12/1996	Hultman
5,586,553	A	12/1996	Halili et al.
5,593,390	A	1/1997	Castellano et al.
5,593,852	A	1/1997	Heller et al.
5,594,638	A	1/1997	Illiff
5,609,060	A	3/1997	Dent
5,626,144	A	5/1997	Tacklind et al.
5,630,710	A	5/1997	Tune et al.
5,643,212	A	7/1997	Coutre et al.
5,660,163	A	8/1997	Schulman et al.
5,660,176	A	8/1997	Iliff
5,665,065	A	9/1997	Colman et al.
5,665,222	A	9/1997	Heller et al.
5,685,844	A	11/1997	Marttila
5,687,734	A	11/1997	Dempsey et al.
5,704,366	A	1/1998	Tacklind et al.
5,750,926	A	5/1998	Schulman et al.
5,754,111	A	5/1998	Garcia
5,764,159	A	6/1998	Neftel
5,772,635	A	6/1998	Dastur et al.
5,779,665	A	7/1998	Mastrototaro et al.
5,788,669	A	8/1998	Peterson
5,791,344	A	8/1998	Schulman et al.
5,800,420	A	9/1998	Gross et al.
5,807,315	A	9/1998	Van Antwerp et al.
5,807,336	A	9/1998	Russo et al.
5,814,015	A	9/1998	Gargano et al.
5,822,715	A	10/1998	Worthington et al.
5,832,448	A	11/1998	Brown
5,840,020	A	11/1998	Heinonen et al.
5,861,018	A	1/1999	Feierbach et al.
5,868,669	A	2/1999	Iliff
5,871,465	A	2/1999	Vasko
5,879,163	A	3/1999	Brown et al.
5,885,245	A	3/1999	Lynch et al.
5,897,493	A	4/1999	Brown
5,899,855	A	5/1999	Brown
5,904,708	A	5/1999	Goedeke
5,913,310	A	6/1999	Brown
5,917,346	A	6/1999	Gord
5,918,603	A	7/1999	Brown
5,925,021	A	7/1999	Castellano et al.
5,933,136	A	8/1999	Brown
5,935,099	A	8/1999	Peterson et al.
5,940,801	A	8/1999	Brown
5,951,521	A	9/1999	Mastrototaro et al.
5,954,643	A	9/1999	VanAntwerp et al.
5,956,501	A	9/1999	Brown
5,960,403	A	9/1999	Brown
5,965,380	A	10/1999	Heller et al.
5,972,199	A	10/1999	Heller et al.
5,978,236	A	11/1999	Faberman et al.
5,997,476	A	12/1999	Brown
5,999,848	A	12/1999	Gord et al.
5,999,849	A	12/1999	Gord et al.
6,009,339	A	12/1999	Bentsen et al.
6,011,984	A	1/2000	Van Antwerp et al.
6,032,119	A	2/2000	Brown et al.
6,043,437	A	3/2000	Schulman et al.
6,081,736	A	6/2000	Colvin et al.
6,083,710	A	7/2000	Heller et al.
6,088,608	A	7/2000	Schulman et al.
6,101,478	A	8/2000	Brown
6,103,033	A	8/2000	Say et al.
6,119,028	A	9/2000	Schulman et al.
6,120,676	A	9/2000	Heller et al.
6,121,009	A	9/2000	Heller et al.
6,134,461	A	10/2000	Say et al.
6,143,164	A	11/2000	Heller et al.
6,162,611	A	12/2000	Heller et al.
6,175,752	B1	1/2001	Say et al.
6,183,412	B1	2/2001	Benkowski et al.
6,246,992	B1	6/2001	Brown
6,254,586	B1	7/2001	Mann et al.
6,259,937	B1	7/2001	Schulman et al.
6,329,161	B1	12/2001	Heller et al.
6,408,330	B1	6/2002	DeLaHuerga
6,418,332	B1	7/2002	Mastrototaro et al.

(56) **References Cited**

U.S. PATENT DOCUMENTS

6,424,847	B1	7/2002	Mastrototaro et al.
6,461,331	B1	10/2002	Van Antwerp
6,472,122	B1	10/2002	Schulman et al.
6,484,045	B1	11/2002	Holker et al.
6,484,046	B1	11/2002	Say et al.
6,503,381	B1	1/2003	Gotoh et al.
6,514,718	B2	2/2003	Heller et al.
6,544,173	B2	4/2003	West et al.
6,553,263	B1	4/2003	Meadows et al.
6,554,798	B1	4/2003	Mann et al.
6,558,320	B1	5/2003	Causey, III et al.
6,558,351	B1	5/2003	Steil et al.
6,560,741	B1	5/2003	Gerety et al.
6,565,509	B1	5/2003	Say et al.
6,579,690	B1	6/2003	Bonnecaze et al.
6,591,125	B1	7/2003	Buse et al.
6,592,745	B1	7/2003	Feldman et al.
6,605,200	B1	8/2003	Mao et al.
6,605,201	B1	8/2003	Mao et al.
6,607,658	B1	8/2003	Heller et al.
6,616,819	B1	9/2003	Liamos et al.
6,618,934	B1	9/2003	Feldman et al.
6,623,501	B2	9/2003	Heller et al.
6,641,533	B2	11/2003	Causey, III et al.
6,654,625	B1	11/2003	Say et al.
6,659,980	B2	12/2003	Moberg et al.
6,671,554	B2	12/2003	Gibson et al.
6,676,816	B2	1/2004	Mao et al.
6,689,265	B2	2/2004	Heller et al.
6,728,576	B2	4/2004	Thompson et al.
6,733,471	B1	5/2004	Ericson et al.
6,734,162	B2	5/2004	Van Antwerp et al.
6,746,582	B2	6/2004	Heller et al.
6,747,556	B2	6/2004	Medema et al.
6,749,740	B2	6/2004	Liamos et al.
6,752,787	B1	6/2004	Causey, III et al.
6,809,653	B1	10/2004	Mann et al.
6,881,551	B2	4/2005	Heller et al.
6,892,085	B2	5/2005	McIvor et al.
6,893,545	B2	5/2005	Gotoh et al.
6,895,263	B2	5/2005	Shin et al.
6,916,159	B2	7/2005	Rush et al.
6,932,584	B2	8/2005	Gray et al.
6,932,894	B2	8/2005	Mao et al.
6,942,518	B2	9/2005	Liamos et al.
7,153,263	B2	12/2006	Carter et al.
7,153,289	B2	12/2006	Vasko
7,396,330	B2	7/2008	Banet et al.
7,500,949	B2	3/2009	Gottlieb et al.
2001/0044731	A1	11/2001	Coffman et al.
2002/0013518	A1	1/2002	West et al.
2002/0055857	A1	5/2002	Mault et al.
2002/0082665	A1	6/2002	Haller et al.
2002/0137997	A1	9/2002	Mastrototaro et al.
2002/0161288	A1	10/2002	Shin et al.
2003/0060765	A1	3/2003	Campbell et al.
2003/0078560	A1	4/2003	Miller et al.
2003/0088166	A1	5/2003	Say et al.
2003/0144581	A1	7/2003	Conn et al.
2003/0152823	A1	8/2003	Heller
2003/0176183	A1	9/2003	Drucker et al.
2003/0188427	A1	10/2003	Say et al.
2003/0199744	A1	10/2003	Buse et al.
2003/0208113	A1	11/2003	Mault et al.
2003/0220552	A1	11/2003	Reghabi et al.
2004/0061232	A1	4/2004	Shah et al.
2004/0061234	A1	4/2004	Shah et al.
2004/0064133	A1	4/2004	Miller et al.
2004/0064156	A1	4/2004	Shah et al.
2004/0073095	A1	4/2004	Causey, III et al.
2004/0074785	A1	4/2004	Holker et al.
2004/0093167	A1	5/2004	Braig et al.
2004/0097796	A1	5/2004	Berman et al.
2004/0102683	A1	5/2004	Khanuja et al.
2004/0111017	A1	6/2004	Say et al.
2004/0122353	A1	6/2004	Shahmirian et al.
2004/0152622	A1	8/2004	Keith et al.
2004/0167465	A1	8/2004	Mihai et al.
2004/0263354	A1	12/2004	Mann et al.
2005/0038331	A1	2/2005	Silaski et al.
2005/0038680	A1	2/2005	McMahon et al.
2005/0154271	A1	7/2005	Rasdal et al.
2005/0192557	A1	9/2005	Brauker et al.
2006/0229694	A1	10/2006	Schulman et al.
2006/0238333	A1	10/2006	Welch et al.
2006/0293571	A1	12/2006	Bao et al.
2007/0088521	A1	4/2007	Shmueli et al.
2007/0135866	A1	6/2007	Baker et al.
2007/0173761	A1	7/2007	Kanderian, Jr. et al.
2007/0276279	A1	11/2007	Echauz et al.
2008/0154503	A1	6/2008	Wittenber et al.
2008/0228056	A1*	9/2008	Blomquist et al. 600/365
2008/0269723	A1	10/2008	Mastrototaro et al.
2009/0081951	A1	3/2009	Erdmann et al.
2009/0082635	A1	3/2009	Baldus et al.
2010/0017141	A1*	1/2010	Campbell A61M 5/14244 702/19
2010/0057041	A1	3/2010	Hayter
2010/0121314	A1	5/2010	Iobbi
2010/0185175	A1	7/2010	Kamen et al.
2011/0106011	A1	5/2011	Cinar et al.
2011/0208155	A1	8/2011	Palerm et al.
2011/0208156	A1	8/2011	Doyle, III et al.

FOREIGN PATENT DOCUMENTS

EP	0806738		11/1997
EP	0880936		12/1998
EP	1338295		8/2003
EP	1631036	A2	3/2006
GB	2218831		11/1989
WO	WO 96/20745		7/1996
WO	WO 96/36389		11/1996
WO	WO 96/37246	A1	11/1996
WO	WO 97/21456		6/1997
WO	WO 98/20439		5/1998
WO	WO 98/24358		6/1998
WO	WO 98/42407		10/1998
WO	WO 98/49659		11/1998
WO	WO 98/59487		12/1998
WO	WO 99/08183		2/1999
WO	WO 99/10801		3/1999
WO	WO 99/18532		4/1999
WO	WO 99/22236		5/1999
WO	WO9929230	A1	6/1999
WO	WO 00/10628		3/2000
WO	WO0010628	A2	3/2000
WO	WO 00/19887		4/2000
WO	WO0018449	A2	4/2000
WO	WO0019887	A1	4/2000
WO	WO 00/48112		8/2000
WO	WO0078210	A1	12/2000
WO	WO 02/058537	A2	8/2002
WO	WO 03/001329		1/2003
WO	WO 03/094090		11/2003
WO	WO 2005/065538	A2	7/2005
WO	WO2012/058694	A2	5/2012

OTHER PUBLICATIONS

Mikhail Loutseiko, et al., Closed-Loop Insulin Delivery Utilizing Pole Placement to Compensate for Delays in Subcutaneous Insulin Delivery, Journal of Diabetes Science and Technology, Nov. 1, 2011, pp. 1342-1351, vol. 5, Issue No. 6.

Greet Van Den Berghe G. et al., Intensive Insulin Therapy in Critically Ill Patients, The New England Journal of Medicine, Nov. 8, 2001, pp. 1359-1367, vol. 345, No. 19.

M. Kollind, et al., Insulin clearance during hypoglycemia in patients with insulin-dependent diabetes mellitus, Horm Metab Res, Jul. 1991, pp. 333-335.

(56) **References Cited**

OTHER PUBLICATIONS

Steven E. Khan, et al., Quantification of the Relationship Between Insulin Sensitivity and Beta-Cell Function in Human Subjects. Evidence for a Hyperbolic Function, Diabetes, Nov. 1993, pp. 1663-1672, vol. 42.
Arthur C. Guyton, Insulin, Glucagon, and Diabetes Mellitus, Textbook of Medical Physiology, Eighth Edition, 1991, Chapter 78, pp. 855-867, W. B. Saunders Company.
Antonios E. Panteleon, et al., Evaluation of the Effect of Gain on the Meal Response of an Automated Closed-Loop Insulin Delivery System, Diabetes, Jul. 2006, pp. 1995-2000, vol. 55.
Garry M. Steil, et al., Feasibility of Automating Insulin Delivery for the Treatment of Type I Diabetes, Diabetes, Dec. 2006, pp. 3344-3350, vol. 55.
Stuart A. Weinzimer, et al., Fully Automated Closed-Loop Insulin Delivery Versus Semiautomated Hybrid Control in Pediatric Patients With Type I Diabetes Using an Artificial Pancreas, Diabetes Care, May 2008, pp. 934-939, vol. 31.
Gary M. Steil, et al., Metabolic Modelling and the Closed-Loop Insulin Delivery Problem, Diabetes Research and Clinical Practice, 2006, pp. S183-S186, vol. 74.
PCT Search Report (PCT/US02/03299), Oct. 31, 2002, Medtronic Minimed, Inc.
(Animas Corporation, 1999). Animas . . . bringing new life to insulin therapy.
Bode B W, et al. (1996). Reduction in Severe Hypoglycemia with Long-Term Continuous Subcutaneous Insulin Infusion in Type I Diabetes. Diabetes Care, vol. 19, No. 4, 324-327.
Boland E (1998). Teens Pumping it Up! Insulin Pump Therapy Guide for Adolescents. 2nd Edition.
Brackenridge B P (1992). Carbohydrate Gram Counting a Key to Accurate Mealtime Boluses in Intensive Diabetes Therapy. Practical Diabetology, vol. 11, No. 2, pp. 22-28.
Brackenridge, B P et al. (1995). Counting Carbohydrates How to Zero in on Good Control. MiniMed Technologies Inc.
Farkas-Hirsch R et al. (1994). Continuous Subcutaneous Insulin Infusion: A Review of the Past and Its Implementation for the Future. Diabetes Spectrum From Research to Practice, vol. 7, No. 2, pp. 80-84, 136-138.
Hirsch I B et al. (1990). Intensive Insulin Therapy for Treatment of Type I Diabetes. Diabetes Care, vol. 13, No. 12, pp. 1265-1283.
Kulkarni K et al. (1999). Carbohydrate Counting A Primer for Insulin Pump Users to Zero in on Good Control. MiniMed Inc.
Marcus A O et al. (1996). Insulin Pump Therapy Acceptable Alternative to Injection Therapy. Postgraduate Medicine, vol. 99, No. 3, pp. 125-142.
Reed J et al. (1996). Voice of the Diabetic, vol. 11, No. 3, pp. 1-38.
Skyler J S (1989). Continuous Subcutaneous Insulin Infusion [CSII] With External Devices: Current Status. Update in Drug Delivery Systems, Chapter 13, pp. 163-183. Futura Publishing Company.
Skyler J S et al. (1995). The Insulin Pump Therapy Book Insights from the Experts. MiniMed•Technologies.
Strowig S M (1993). Initiation and Management of Insulin Pump Therapy. The Diabetes Educator, vol. 19, No. 1, pp. 50-60.
Walsh J, et al. (1989). Pumping Insulin: The Art of Using an Insulin Pump. Published by MiniMed•Technologies.
(Intensive Diabetes Management, 1995). Insulin Infusion Pump Therapy. pp. 66-78.
Disetronic My Choice™ D-TRON™ Insulin Pump Reference Manual. (no date).
Disetronic H-TRON® plus Quick Start Manual. (no date).
Disetronic My Choice H-TRONplus Insulin Pump Reference Manual. (no date).
Disetronic H-TRON® plus Reference Manual. (no date).
(MiniMed, 1996). The MiniMed 506. 7 pages. Retrieved on Sep. 16, 2003 from the World Wide Web: http://web.archive.org/web/19961111054527/www.minimed.com/files/506_pic.htm.
(MiniMed, 1997). MiniMed 507 Specifications. 2 pages. Retrieved on Sep. 16, 2003 from the World Wide Web: http://web.archive.org/web/19970124234841/www.minimed.com/files/mmn075.htm.
(MiniMed, 1996). FAQ: The Practical Things . . . pp. 1-4. Retrieved on Sep. 16, 2003 from the World Wide Web: http://web.archive.org/web/19961111054546/www.minimed.com/files/faq_pract.htm.
(MiniMed, 1997). Wanted: a Few Good Belt Clips! 1 page. Retrieved on Sep. 16, 2003 from the World Wide Web: http://web.archive.org/web/19970124234559/www.minimed.com/files/mmn002.htm.
(MiniMed Technologies, 1994). MiniMed 506 Insulin Pump User's Guide.
(MiniMed Technologies, 1994). MiniMed™ Dosage Calculator Initial Meal Bolus Guidelines / MiniMed™ Dosage Calculator Initial Basal Rate Guidelines Percentage Method. 4 pages.
(MiniMed, 1996). MiniMed™ 507 Insulin Pump User's Guide.
(MiniMed, 1997): MiniMed™ 507 Insulin Pump User's Guide.
(MiniMed, 1998). MiniMed 507C Insulin Pump User's Guide.
(MiniMed International, 1998). MiniMed 507C Insulin Pump for those who appreciate the difference.
(MiniMed Inc., 1999). MiniMed 508 Flipchart Guide to Insulin Pump Therapy.
(MiniMed Inc., 1999). Insulin Pump Comparison / Pump Therapy Will Change Your Life.
(MiniMed, 2000). MiniMed® 508 User's Guide.
(MiniMed Inc., 2000). MiniMed® Now [I] Can Meal Bolus Calculator / MiniMed® Now [I] Can Correction Bolus Calculator.
(MiniMed Inc., 2000). Now [I] Can MiniMed Pump Therapy.
(MiniMed Inc., 2000). Now [I] Can MiniMed Diabetes Management.
(Medtronic MiniMed, 2002). The 508 Insulin Pump A Tradition of Excellence.
(Medtronic MiniMed, 2002). Medtronic MiniMed Meal Bolus Calculator and Correction Bolus Calculator. International Version.
Abel, P., et al., "Experience with an implantable glucose sensor as a prerequiste of an artificial beta cell," Biomed. Biochim. Acta 43 (1984) 5, pp. 577-584.
Bindra, Dilbir S., et al., "Design and in Vitro Studies of a Needle-Type Glucose Sensor for a Subcutaneous Monitoring," American Chemistry Society, 1991, 63, pp. 1692-1696.
Boguslavsky, Leonid, et al., "Applications of redox polymers in biosensors," Sold State Ionics 60, 1993, pp. 189-197.
Geise, Robert J., et al., "Electropolymerized 1,3-diaminobenzene for the construction of a 1,1'-dimethylferrocene mediated glucose biosensor," Analytica Chimica Acta, 281, 1993, pp. 467-473.
Gernet, S., et al., "A Planar Glucose Enzyme Electrode," Sensors and Actuators, 17, 1989, pp. 537-540.
Gernet, S., et al., "Fabrication and Characterization of a Planar Electromechanical Cell and its Application as a Glucose Sensor," Sensors and Actuators, 18, 1989, pp. 59-70.
Gorton, L., et al., "Amperometric Biosensors Based on an Apparent Direct Electron Transfer Between Electrodes and Immobilized Peroxiases," Analyst, Aug. 1991, vol. 117, pp. 1235-1241.
Gorton, L., et al., "Amperometric Glucose Sensors Based on Immobilized Glucose-Oxidizing Enymes and Chemically Modified Electrodes," Analytica Chimica Acta, 249, 1991, pp. 43-54.
Gough, D. A., et al., "Two-Dimensional Enzyme Electrode Sensor for Glucose," Analytical Chemistry, vol. 57, No. 5, 1985, pp. 2351-2357.
Gregg, Brian A., et al., "Cross-Linked Redox Gels Containing Glucose Oxidase for Amperometric Biosensor Applications," Analytical Chemistry, 62, pp. 258-263.
Gregg, Brian A., et al., "Redox Polymer Films Containing Enzymes. 1. A Redox-Conducting Epoxy Cement: Synthesis, Characterization, and Electrocatalytic Oxidation of Hydroquinone," The Journal of Physical Chemistry, vol. 95, No. 15, 1991, pp. 5970-5975.
Hashiguchi, Yasuhiro, MD, et al., "Development of a Miniaturized Glucose Monitoring System by Combining a Needle-Type Glucose Sensor With Microdialysis Sampling Method," Diabetes Care, vol. 17, No. 5, May 1994, pp. 387-389.
Heller, Adam, "Electrical Wiring of Redox Enzymes," Acc. Chem. Res., vol. 23, No. 5, May 1990, pp. 128-134.
Jobst, Gerhard, et al., "Thin-Film Microbiosensors for Glucose-Lactate Monitoring," Analytical Chemistry, vol. 68, No. 18, Sep. 15, 1996, pp. 3173-3179.
Johnson, K.W., et al., "In vivo evaluation of an electroenzymatic glucose sensor implanted in subcutaneous tissue," Biosensors & Bioelectronics, 7, 1992, pp. 709-714.

(56) **References Cited**

OTHER PUBLICATIONS

Jönsson, G., et al., "An Electromechanical Sensor for Hydrogen Peroxide Based on Peroxidase Adsorbed on a Spectrographic Graphite Electrode," Electroanalysis, 1989, pp. 465-468.
Kanapieniene, J. J., et al., "Miniature Glucose Biosensor with Extended Linearity," Sensors and Actuators, B. 10, 1992, pp. 37-40.
Kawamori, Ryuzo, et al., "Perfect Normalization of Excessive Glucagon Responses to Intraveneous Arginine in Human Diabetes Mellitus With the Artificial Beta-Cell," Diabetes vol. 29, Sep. 1980, pp. 762-765.
Kimura, J., at al., "An Immobilized Enzyme Membrane Fabrication Method," Biosensors 4, 1988, pp. 41-52.
Koudelka, M., et al., "In-vivo Behaviour of Hypodermically Implanted Microfabricated Glucose Sensors," Biosensors & Bioelectronics 6, 1991, pp. 31-36.
Koudelka, M., et al., "Planar Amperometric Enzyme-Based Glucose Microelectrode," Sensors & Actuators, 18, 1989, pp. 157-165.
Mastrototaro, John J., et al., "An electroenzymatic glucose sensor fabricated on a flexible substrate," Sensors & Actuators, B. 5, 1991, pp. 139-144.
Mastrototaro, John J., et al., "An Electroenzymatic Sensor Capable of 72 Hour Continuous Monitoring of Subcutaneous Glucose," 14th Annual International Diabetes Federation Congress, Washington D.C., Jun. 23-28, 1991.
McKean, Brian D., et al., "A Telemetry-Instrumentation System for Chronically Implanted Glucose and Oxygen Sensors," IEEE Transactions on Biomedical Engineering, Vo. 35, No. 7, Jul. 1988, pp. 526-532.
Monroe, D., "Novel Implantable Glucose Sensors," ACL, Dec. 1989, pp. 8-16.
Morff, Robert J., et al., "Microfabrication of Reproducible, Economical, Electroenzymatic Glucose Sensors," Annuaal International Conference of teh IEEE Engineering in Medicine and Biology Society, Vo. 12, No. 2, 1990, pp. 483-484.
Moussy, Francis, et al., "Performance of Subcutaneously Implanted Needle-Type Glucose Sensors Employing a Novel Trilayer Coating," Analytical Chemistry, vol. 65, No. 15, Aug. 1, 1993, pp. 2072-2077.
Nakamoto, S., et al., "A Lift-Off Method for Patterning Enzyme-Immobilized Membranes in Multi-Biosensors," Sensors and Actuators 13, 1988, pp. 165-172.
Nishida, Kenro, et al., "Clinical applications of teh wearable artifical endocrine pancreas with the newly designed needle-type glucose sensor," Elsevier Sciences B.V., 1994, pp. 353-358.
Nishida, Kenro, et al., "Development of a ferrocene-mediated needle-type glucose sensor covereed with newly designd biocompatible membrane, 2-methacryloyloxyethylphosphorylcholine-co-n-butyl nethacrylate," Medical Progress Through Technology, vol. 21, 1995, pp. 91-103.
Poitout, V., et al., "A glucose monitoring system for on line estimation oin man of blood glucose concentration using a miniaturized glucose sensor implanted in the subcutaneous tissue adn a wearable control unit," Diabetologia, vol. 36, 1991, pp. 658-663.
Reach, G., "A Method for Evaluating in vivo the Functional Characteristics of Glucose Sensors," Biosensors 2, 1986, pp. 211-220.
Shaw, G. W., et al., "In vitro testing of a simply constructed, highly stable glucose sensor suitable for implantation in diabetic patients," Biosensors & Bioelectronics 6, 1991, pp. 401-406.
Shichiri, M., "A Needle-Type Glucose Sensor—A Valuable Tool Not Only for a Self-Blood Glucose Monitoring but for a Wearable Artiffical Pancreas," Life Support Systems Proceedings, XI Annual Meeting ESAO, Alpbach-Innsbruck, Austria, Sep. 1984, pp. 7-9.
Shichiri, Motoaki, et al., "An artificial endocrine pancreas—problems awaiting solution for long-term clinical applications of a glucose sensor," Frontiers Med. Biol. Engng., 1991, vol. 3, No. 4, pp. 283-292.
Shichiri, Motoaki, et al., "Closed-Loop Glycemic Control with a Wearable Artificial Endocrine Pancreas—Variations in Daily Insulin Requirements to Glycemic Response," Diabetes, vol. 33, Dec. 1984, pp. 1200-1202.
Shichiri, Motoaki, et al., "Glycaemic Control in a Pacreatectomized Dogs with a Wearable Artificial Endocrine Pancreas," Diabetologia, vol. 24, 1983, pp. 179-184.
Shichiri, M., et al., "In Vivo Characteristics of Needle-Type Glucose Sensor—Measurements of Subcutaneous Glucose Concentrations in Human Volunteers," Hormone and Metabolic Research, Supplement Series vol. No. 20, 1988, pp. 17-20.
Shichiri, M., et al., "Membrane design for extending the long-life of an implantable glucose sensor," Diab. Nutr. Metab., vol. 2, No. 4, 1989, pp. 309-313.
Shichiri, Motoaki, et al., "Normalization of the Paradoxic Secretion of Glucagon in Diabetes Who Were Controlled by the Artificial Beta Cell," Diabetes, vol. 28, Apr. 1979, pp. 272-275.
Shichiri, Motoaki, et al., "Telemetry Glucose Monitoring Device with Needle-Type Glucose Sensor: A useful Tool for Blood Glucose Monitoring in Diabetic Individuals," Diabetes Care, vol. 9, No. 3, May-Jun. 1986, pp. 298-301.
Shichiri, Motoaki, et al., "Wearable Artificial Endocrine Pancreas with Needle-Type Glucose Sensor," The Lancet, Nov. 20, 1982, pp. 1129-1131.
Shichiri, Motoaki, et al., "The Wearable Artificial Endocrine Pancreas with a Needle-Type Glucose Sensor: Perfect Glycemic Control in Ambulatory Diabetes," Acta Paediatr Jpn 1984, vol. 26, pp. 359-370.
Shinkai, Seiji, "Molecular Recognitiion of Mono- and Di-saccharides by Phenylboronic Acids in Solvent Extraction and as a Monolayer," J. Chem. Soc., Chem. Commun., 1991, pp. 1039-1041.
Shults, Mark C., "A Telemetry-Instrumentation System for Monitoring Multiple Subcutaneously Implanted Glucose Sensors," IEEE Transactions on Biomedical Engineering, vol. 41, No. 10, Oct. 1994, pp. 937-942.
Sternberg, Robert, et al., "Study and Development of Multilayer Needle-type Enzyme-based Glucose Microsensors," Biosensors, vol. 4, 1988, pp. 27-40.
Tamiya, E., et al., "Micro Glucose Sensors using Electron Mediators Immobilized on a Polypyrrole-Modified Electrode," Sensors and Actuators, vol. 18, 1989, pp. 297-307.
Tsukagoshi, Kazuhiko, et al., "Specific Complexation with Mono- and Disaccharides that can be Detected by Circular Dichroism," J. Org. Chem., vol. 56, 1991, pp. 4089-4091.
Urban, G., et al., "Miniaturized multi-enzyme biosensors integrated with pH sensors on flexible polymer carriers for in vivo applciations," Biosensors & Bioelectronics, vol. 7, 1992, pp. 733-739.
Ubran, G., et al., "Miniaturized thin-film biosensors using covalently immobilized glucose oxidase," Biosensors & Bioelectronics, vol. 6, 1991, pp. 555-562.
Velho, G., et al., "In vivo calibration of a subcutaneous glucose sensor for determination of subcutaneous glucose kinetics," Diab. Nutr. Metab., vol. 3, 1988, pp. 227-233.
Wang, Joseph, et al., "Needle-Type Dual Microsensor for the Simultaneous Monitoring of Glucose and Insulin," Analytical Chemistry, vol. 73, 2001, pp. 844-847.
Yamasaki, Yoshimitsu, et al., "Direct Measurement of Whole Blood Glucose by a Needle-Type Sensor," Clinics Chimica Acta, vol. 93, 1989, pp. 93-98.
Yokoyama, K., "Integrated Biosensor for Glucose and Galactose," Analytica Chimica Acta, vol. 218, 1989, pp. 137-142.
C. Choleua, et al., Calibration of a Subcutaneous Amperometric Glucose Sensor Part 1 Effect of Measurement Uncertainties on the Determination of Sensor Sensitivity and Background Current, Aug. 1, 2002, pp. 641-646, vol. 17, Issue No. 8.
Gianni Marchetti, et al., An Improved PID Switching Control Strategy for Type 1 Diabetes, Mar. 1, 2008, pp. 857-865, vol. 35, Isue No. 3.
Roman Hovorka, et al., Nonlinear Model Predictive Control of Glucose Concentration in Subjects With Type 1 Diabetes, Physiological Measurement, 2004, pp. 905-920, vol. 25.
Marchetti et al: "A feedforward-feedback glucose control strategy for type 1 diabetes mellitus", Journal of Process Control, Oxford, GB, vol. 18, No. 2, Oct. 24, 2007, pp. 149-162, XP022455375, ISSN: 0959-1524, DOI: 10.1016/J.JPROCONT.2007.07.008 chapter 3: equations (1)-(4); chapter 7: "Feedforward-feedback control".
Patek S D et al: "Modular Closed-Loop Control of Diabetes", IEEE Transactions on Biomedical Engineering, IEEE Service Center, Piscataway, NJ, USA, vol. 59, No. 11, Apr. 3, 2012, pp. 2986-2999, XP011490242, ISSN: 0018-9294, DOI: 10.1109/TBME.2012.2192930 section III.A and III.B.1-III.B.2 (pp. 2988-2990).

* cited by examiner

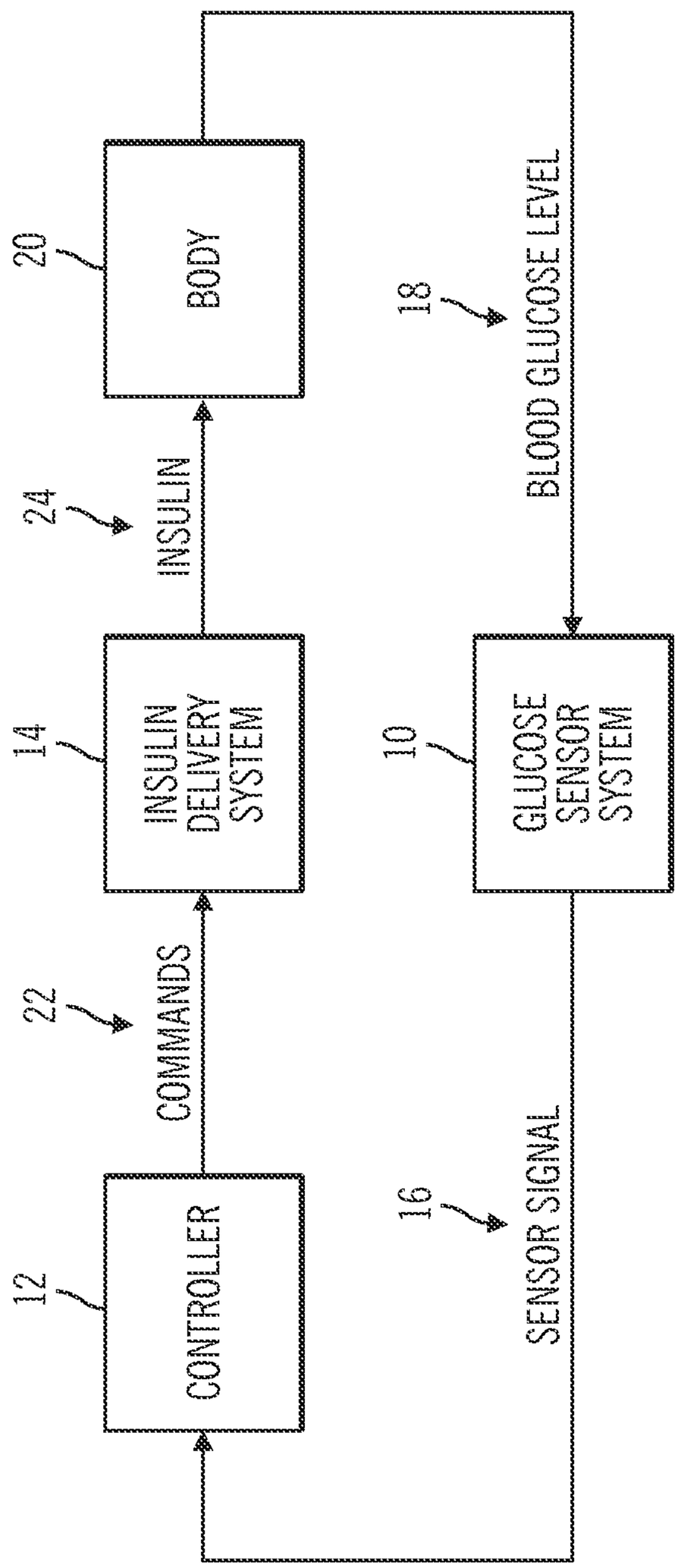
20
BODY
18
BLOOD GLUCOSE LEVEL
24
INSULIN
14
INSULIN DELIVERY SYSTEM
10
GLUCOSE SENSOR SYSTEM
22
COMMANDS
16
SENSOR SIGNAL
12
CONTROLLER

FIG. 1

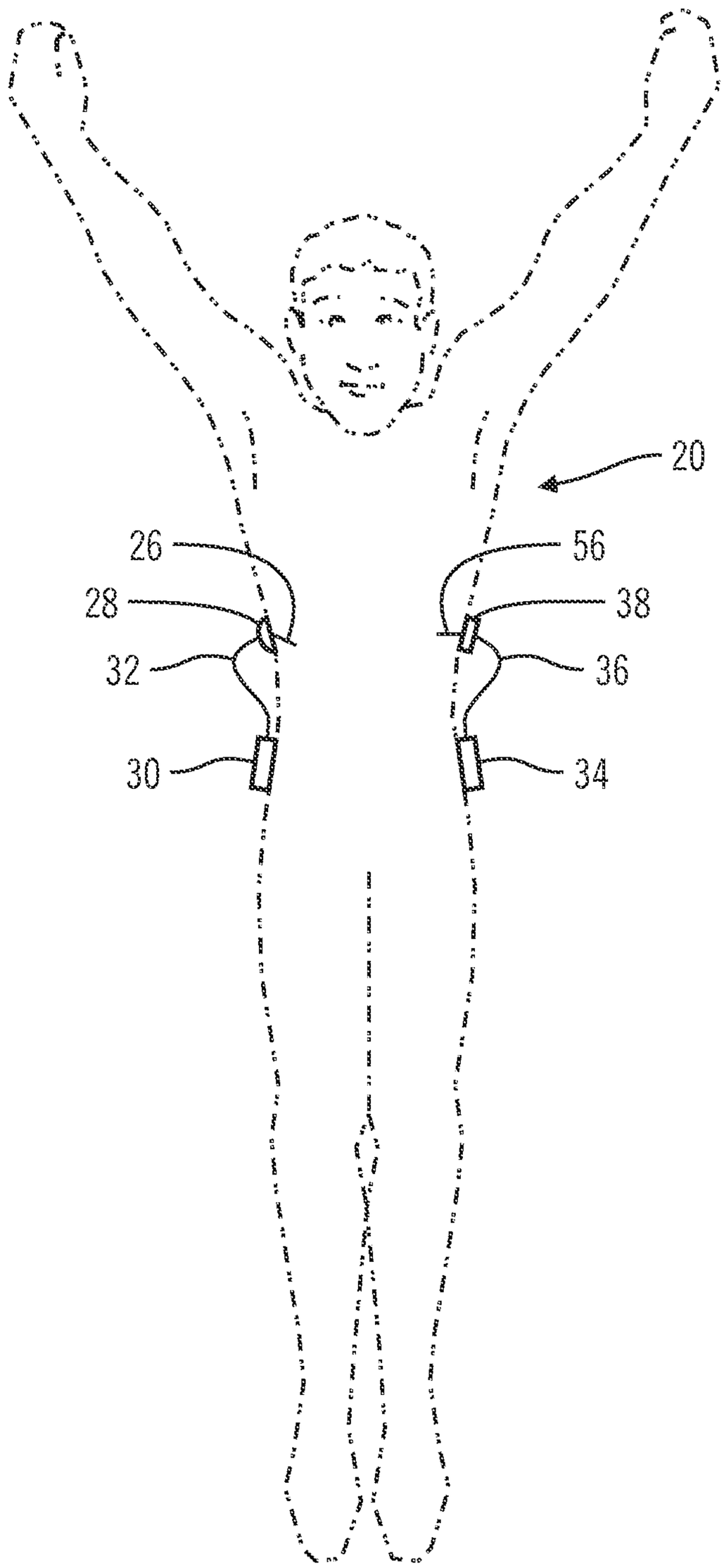

FIG. 2

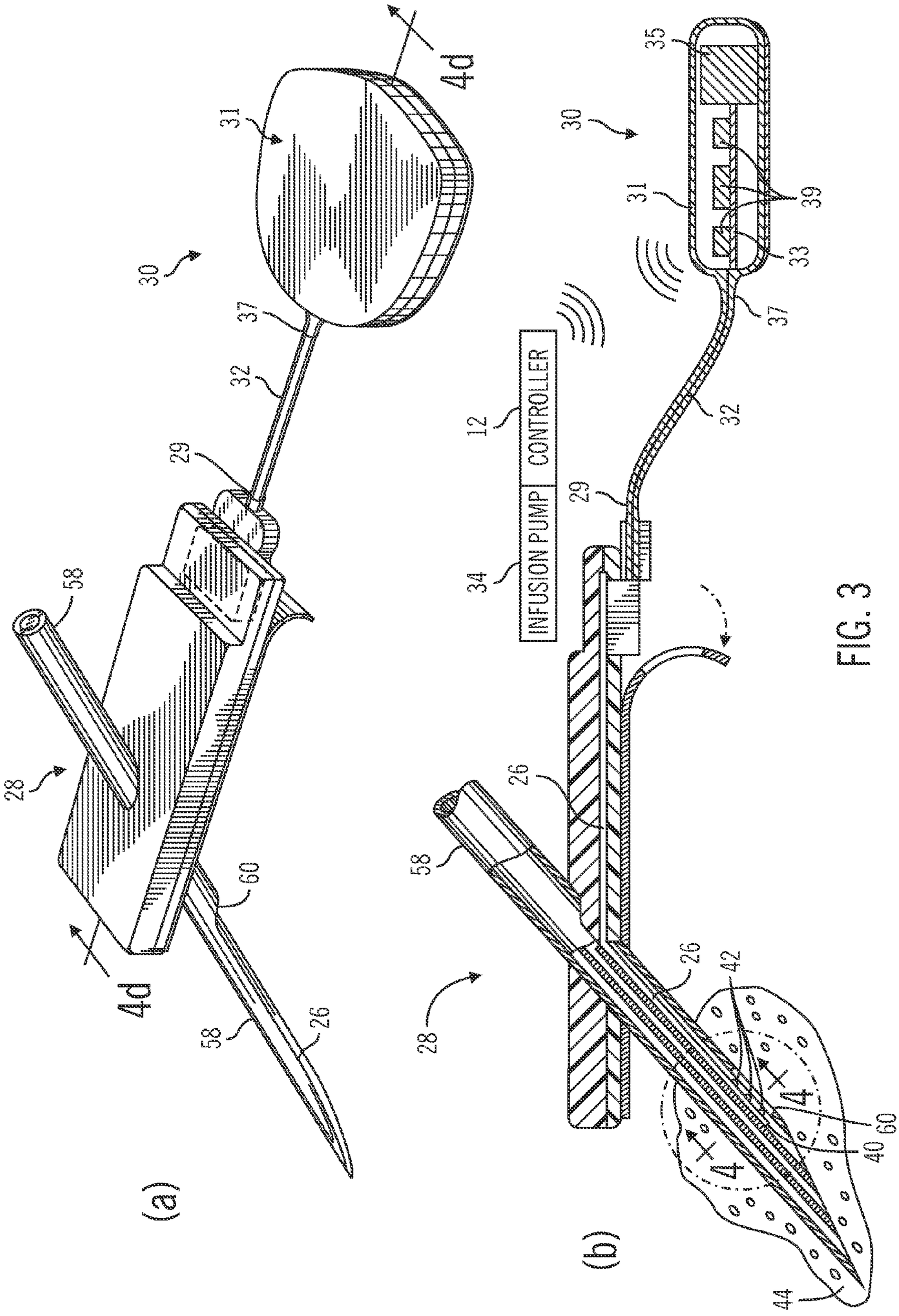
(a)
(b)
INFUSION PUMP
CONTROLLER
12
26
28
29
30
31
32
33
34
35
37
39
40
42
44
58
60
4d
4

FIG. 3

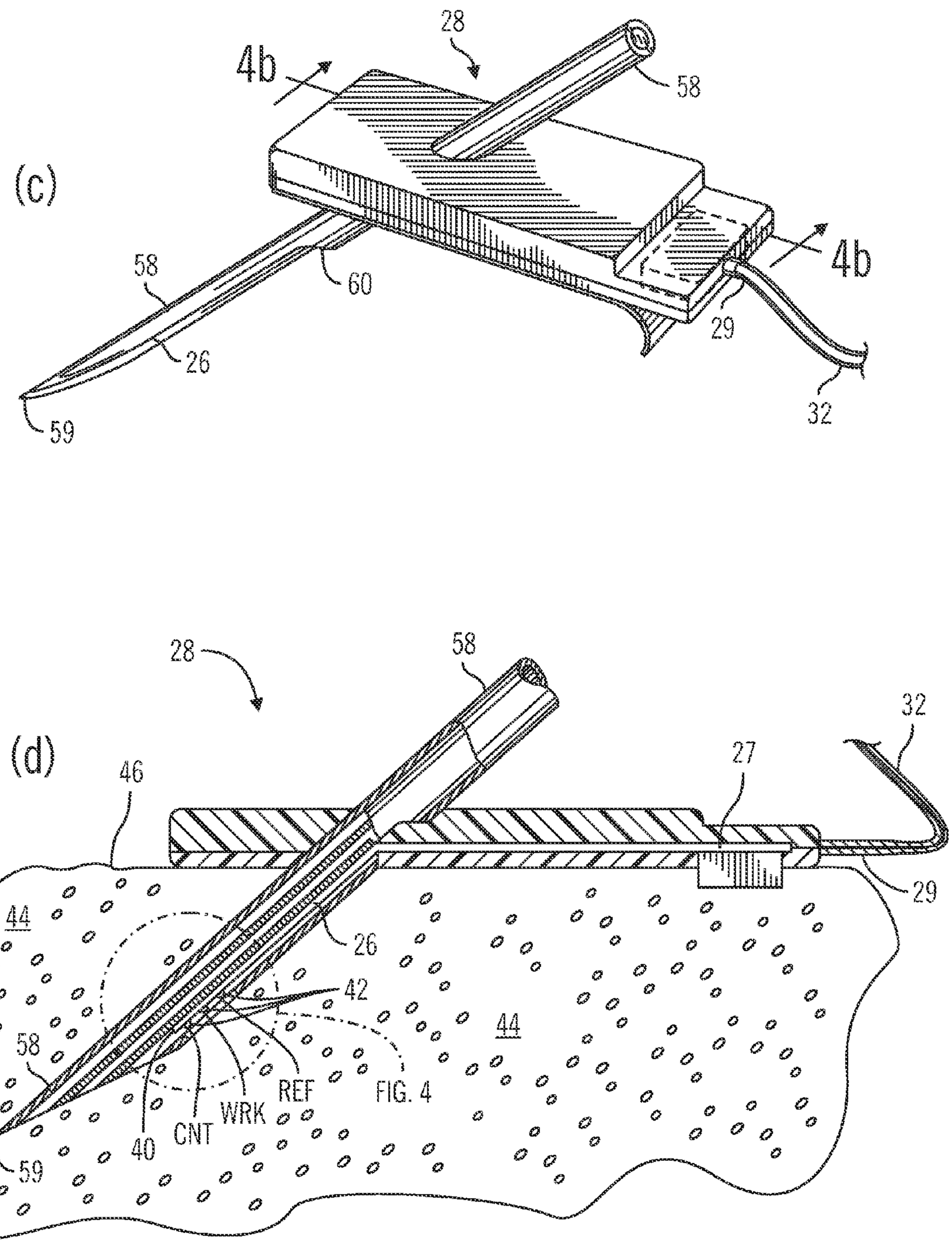
(c)
28
4b
58
58
60
4b
29
26
32
59
(d)
28
58
32
46
27
29
44
26
42
44
58
REF
FIG. 4
WRK
CNT
40
59

FIG. 3

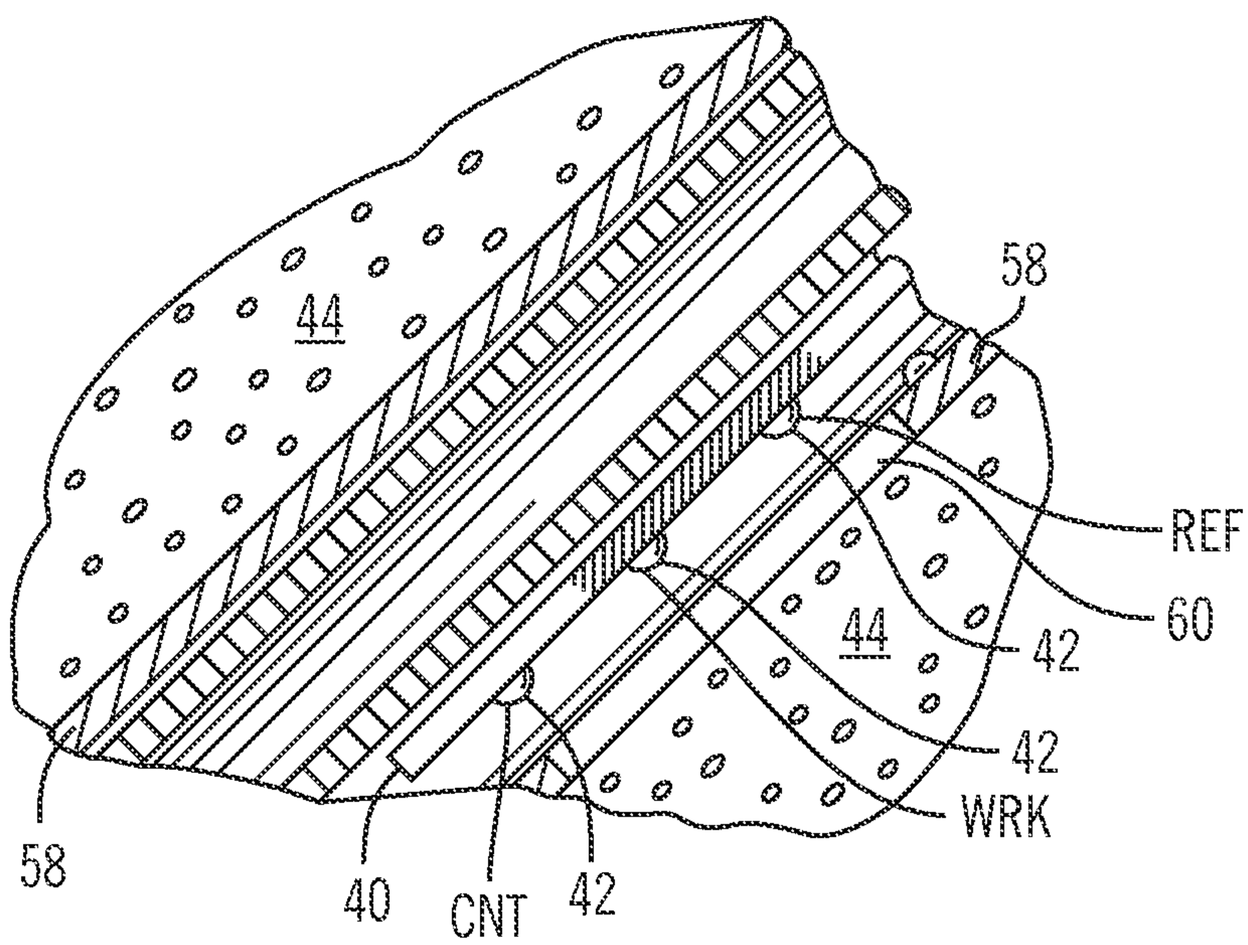

FIG. 4

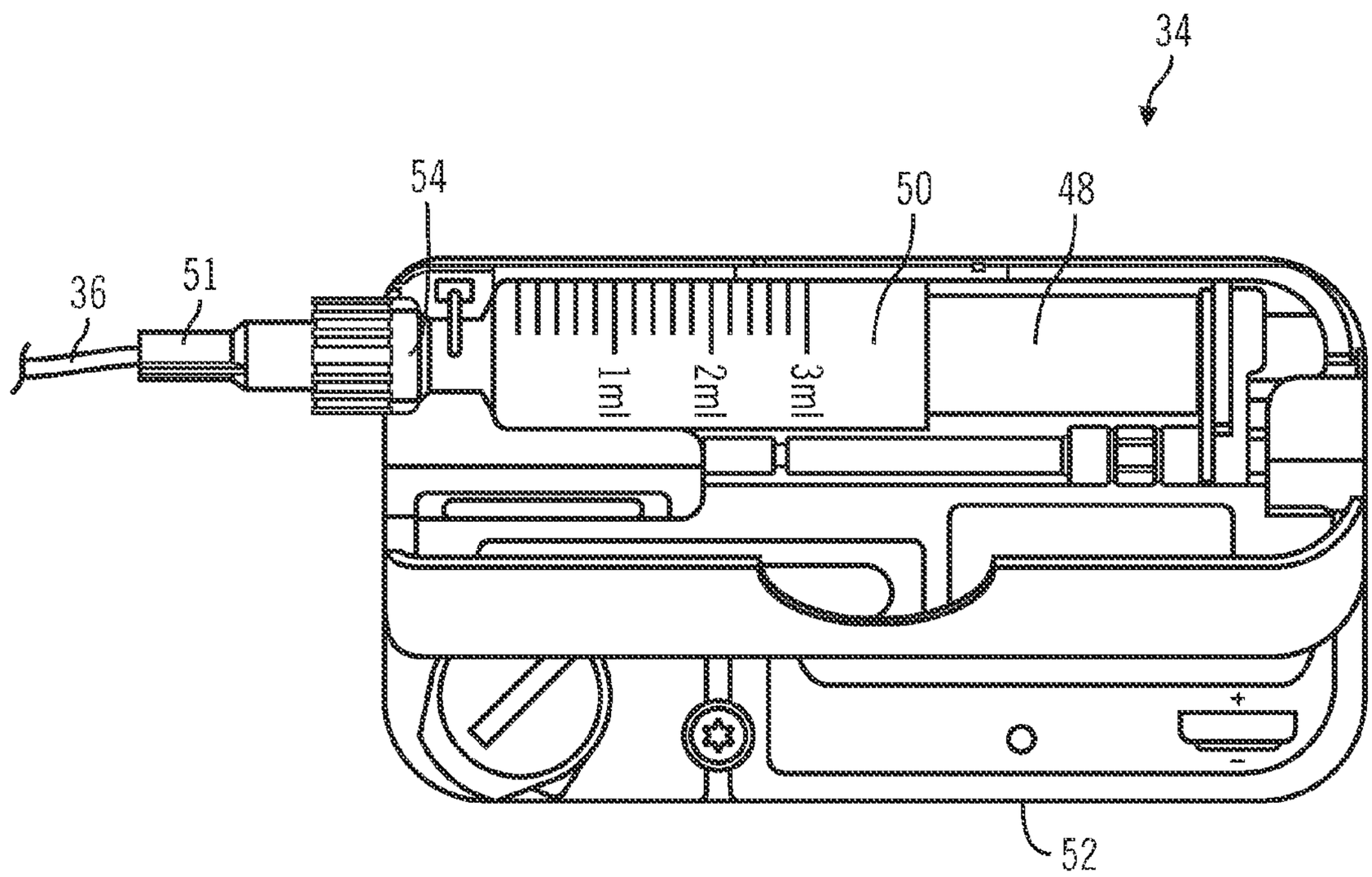

FIG. 5

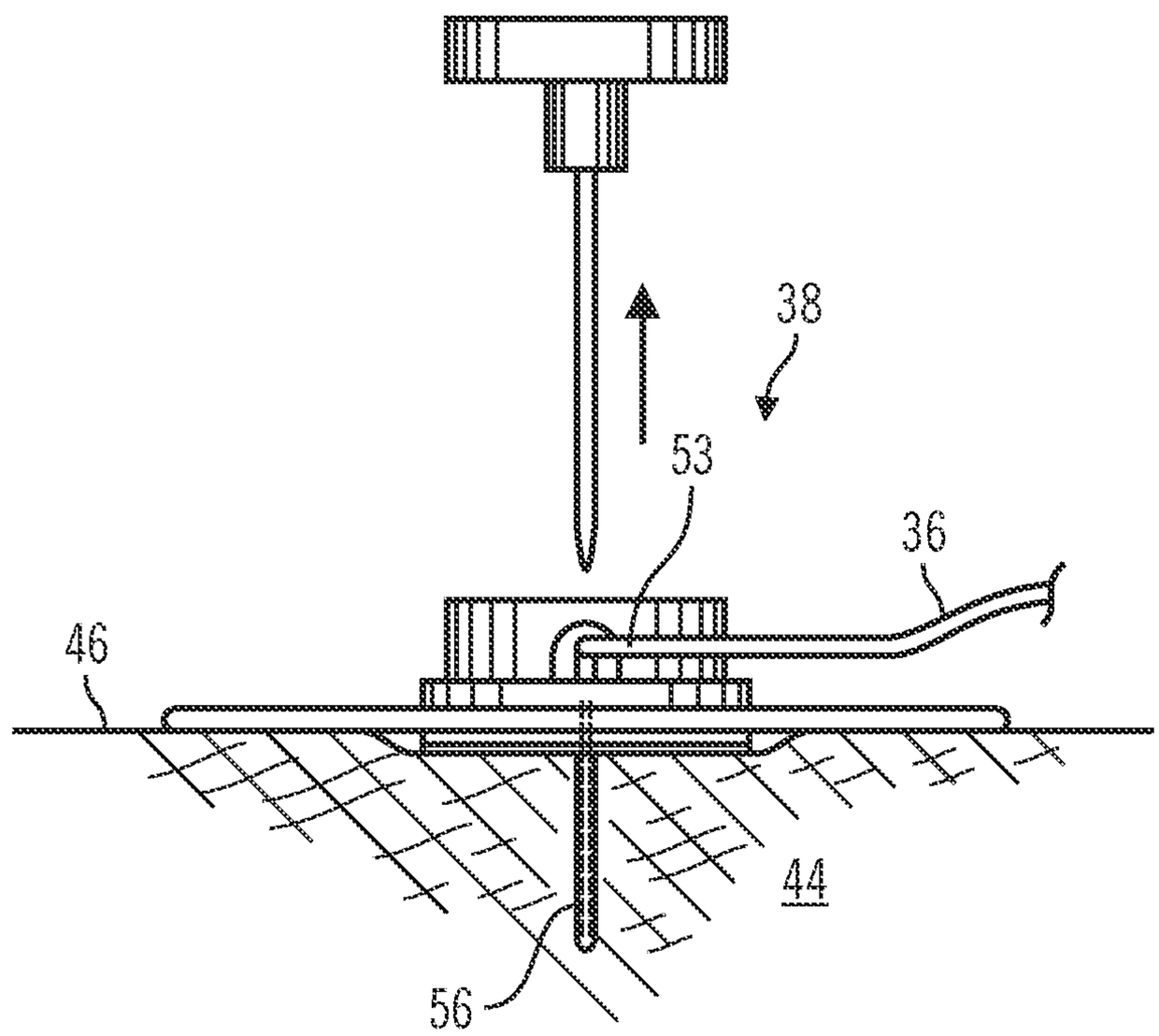

FIG. 6

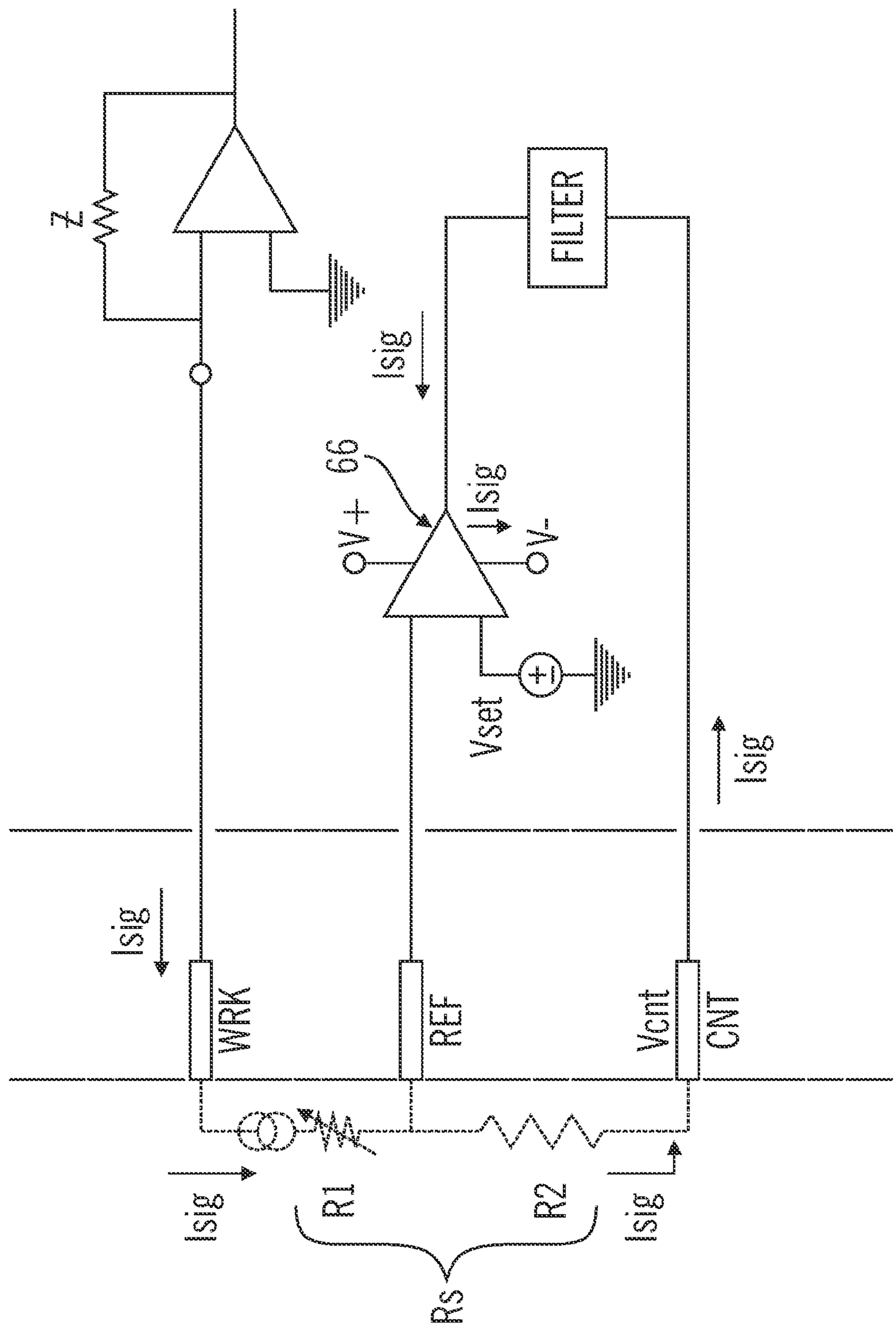
Z
Isig
FILTER
66
V+
Isig
V-
Vset
Isig
Isig
WRK
REF
Vcnt
CNT
Isig
R1
R2
Isig
Rs

FIG. 7

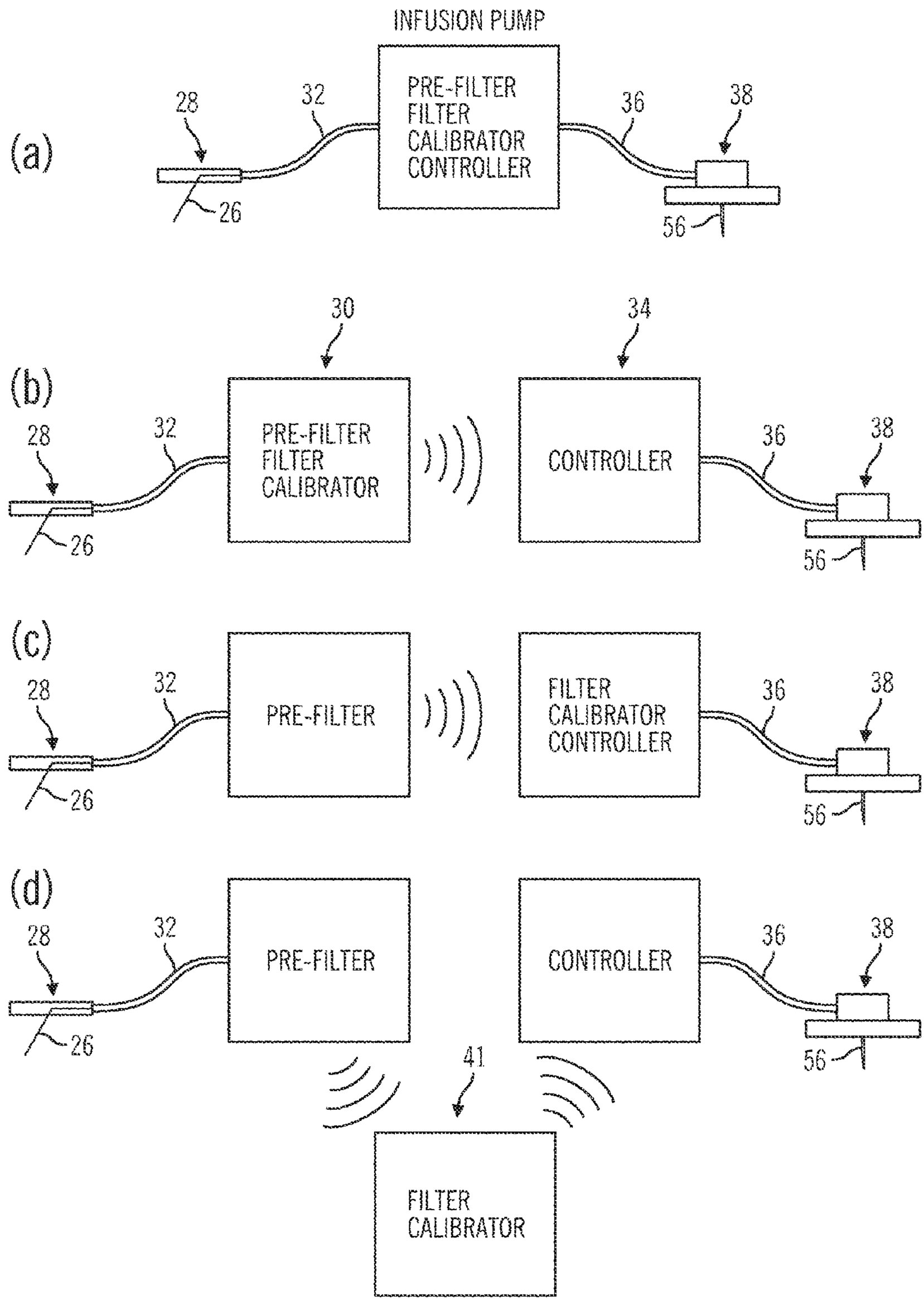
INFUSION PUMP
PRE-FILTER
FILTER
CALIBRATOR
CONTROLLER
(a)
28
32
36
38
26
56
30
34
(b)
PRE-FILTER
FILTER
CALIBRATOR
CONTROLLER
(c)
PRE-FILTER
FILTER
CALIBRATOR
CONTROLLER
(d)
PRE-FILTER
CONTROLLER
41
FILTER
CALIBRATOR

FIG. 8

COMPONENTS	ALTERNATIVE, FIG. 8(a)		PREFERRED EMBODIMENT, FIG. 8(b)		ALTERNATIVE, FIG. 8(c)		ALTERNATIVE, FIG. 8(d)		
	TELEMETERED CHARACTERISTIC MONITOR TRANSMITTER	INFUSION PUMP	TELEMETERED CHARACTERISTIC MONITOR TRANSMITTER	INFUSION PUMP	TELEMETERED CHARACTERISTIC MONITOR TRANSMITTER	INFUSION PUMP	TELEMETERED CHARACTERISTIC MONITOR TRANSMITTER	SUPPLEMENTAL DEVICE	INFUSION PUMP
PRE-FILTERS		X	X		X		X		
FILTERS		X	X			X		X	
CALIBRATOR		X	X			X		X	
CONTROLLER		X		X		X			X

FIG. 9

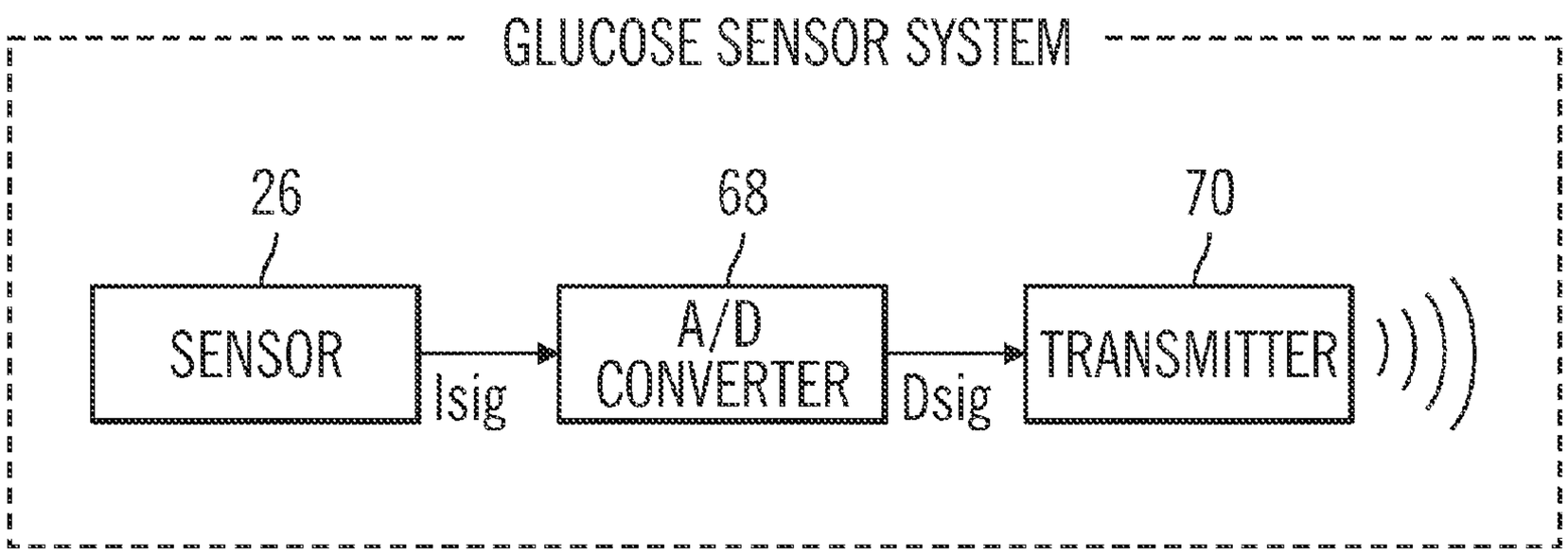
GLUCOSE SENSOR SYSTEM
26
68
70
SENSOR
Isig
A/D CONVERTER
Dsig
TRANSMITTER

FIG. 10

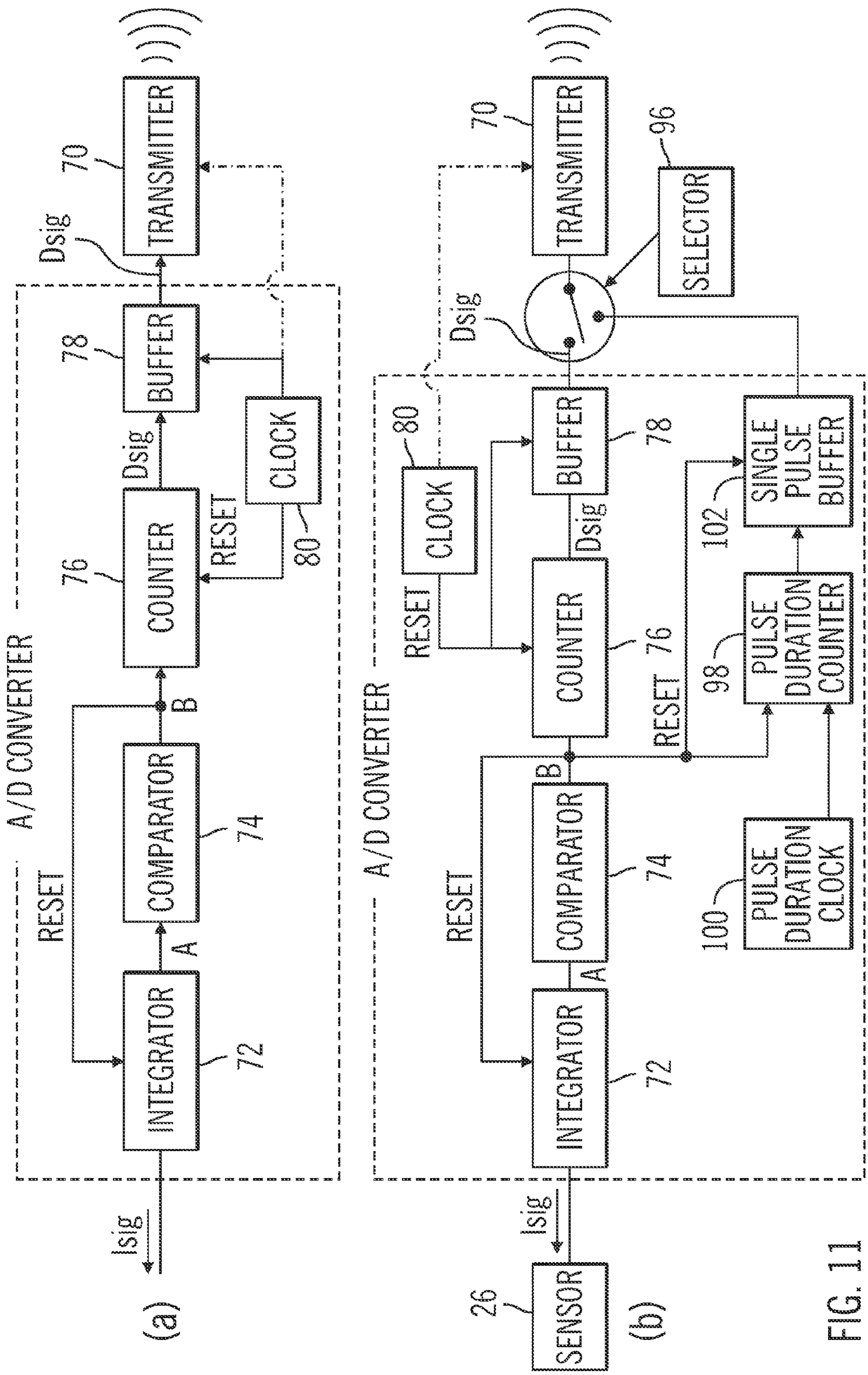
A/D CONVERTER
TRANSMITTER
70
Dsig
BUFFER
78
COUNTER
76
CLOCK
80
RESET
COMPARATOR
74
INTEGRATOR
72
A
B
Isig
(a)
SELECTOR
96
SINGLE PULSE BUFFER
102
PULSE DURATION COUNTER
98
PULSE DURATION CLOCK
100
SENSOR
26
(b)

FIG. 11

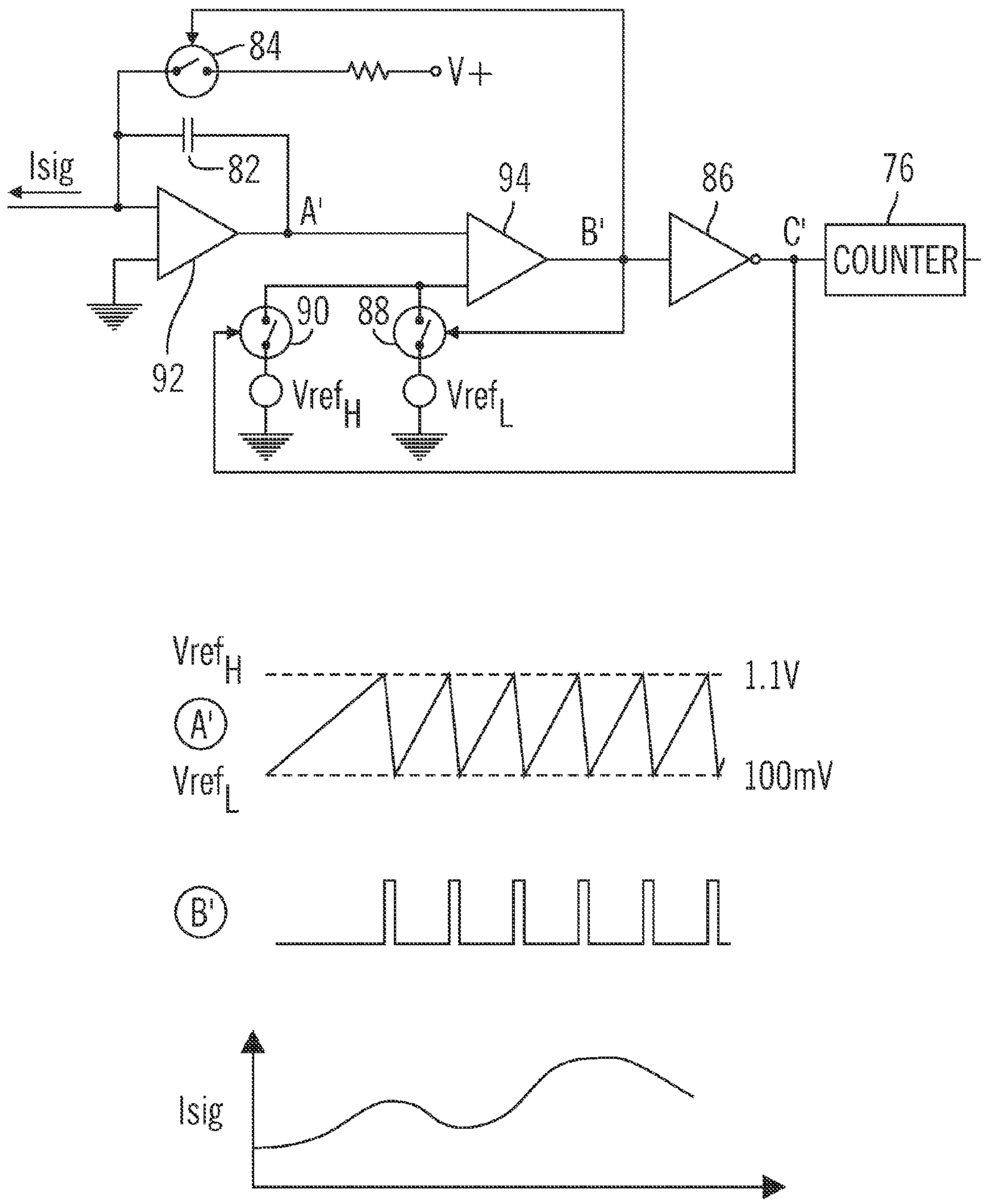
84
V+
82
Isig
A'
94
B'
86
C'
76
COUNTER
90
88
92
Vref$_H$
Vref$_L$
Vref$_H$
A'
Vref$_L$
1.1V
100mV
B'
Isig

FIG. 12

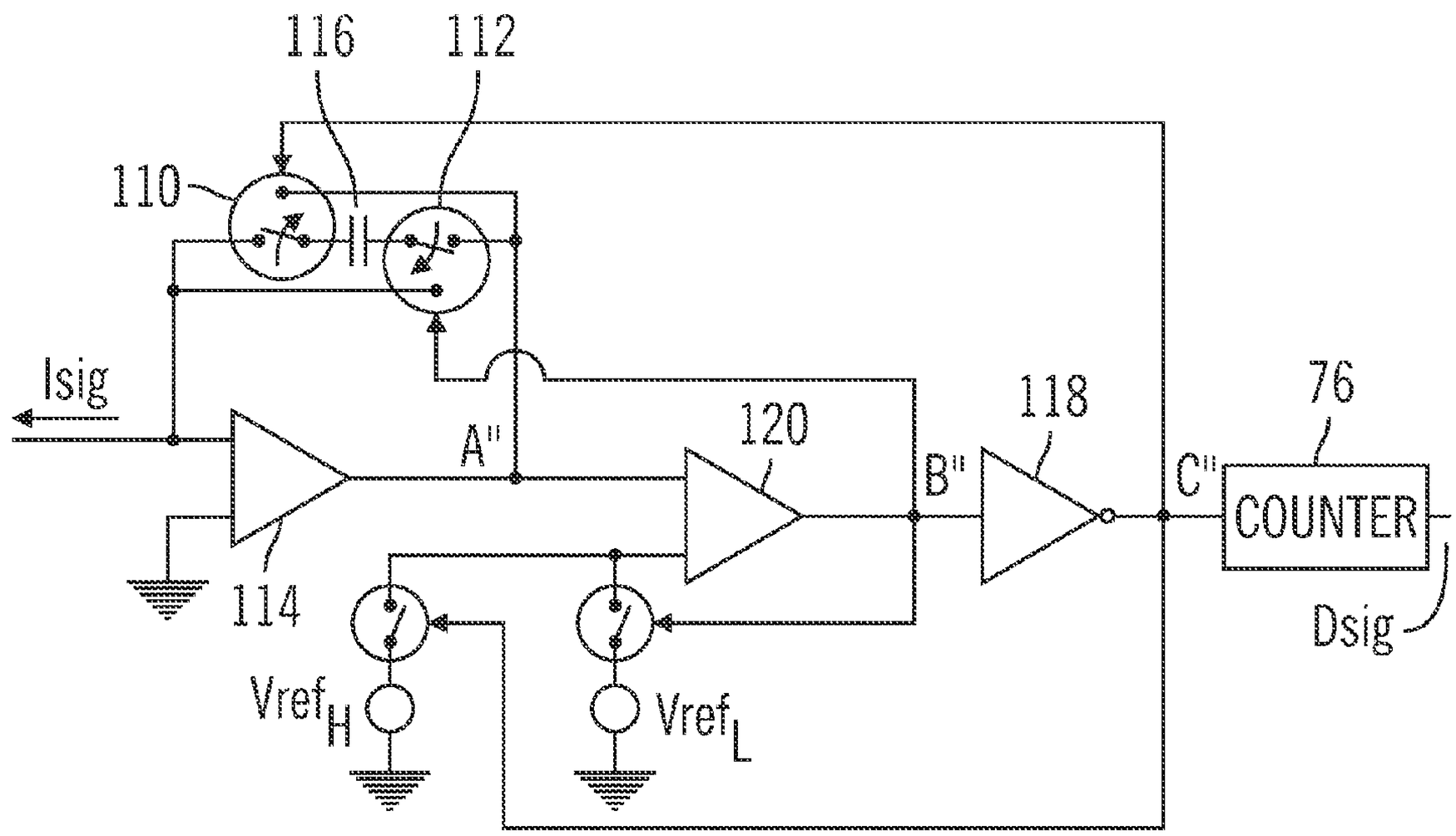
116
112
110
Isig
A"
120
118
76
B"
C"
COUNTER
114
Dsig
VrefH
VrefL

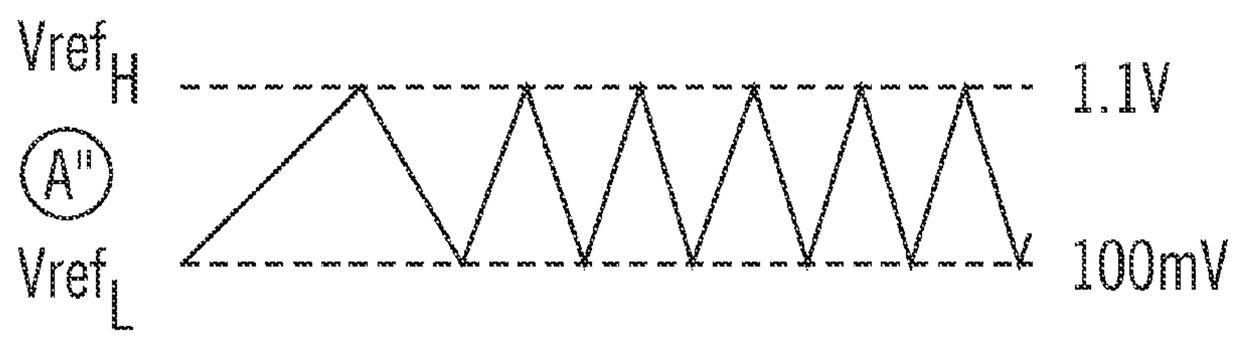
VrefH
1.1V
A"
VrefL
100mV

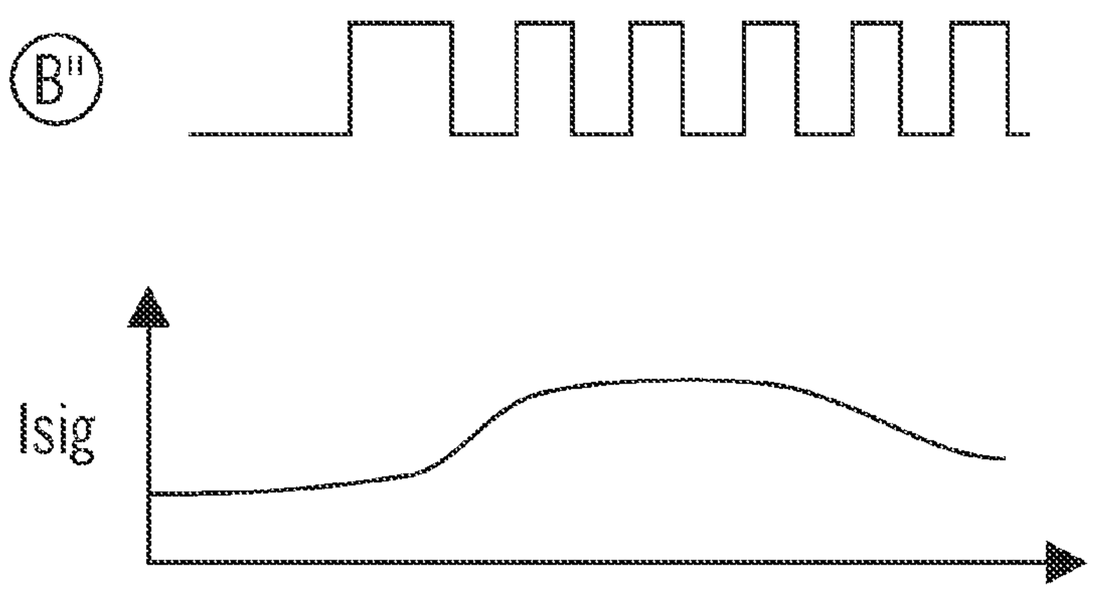
B"
Isig

FIG. 13

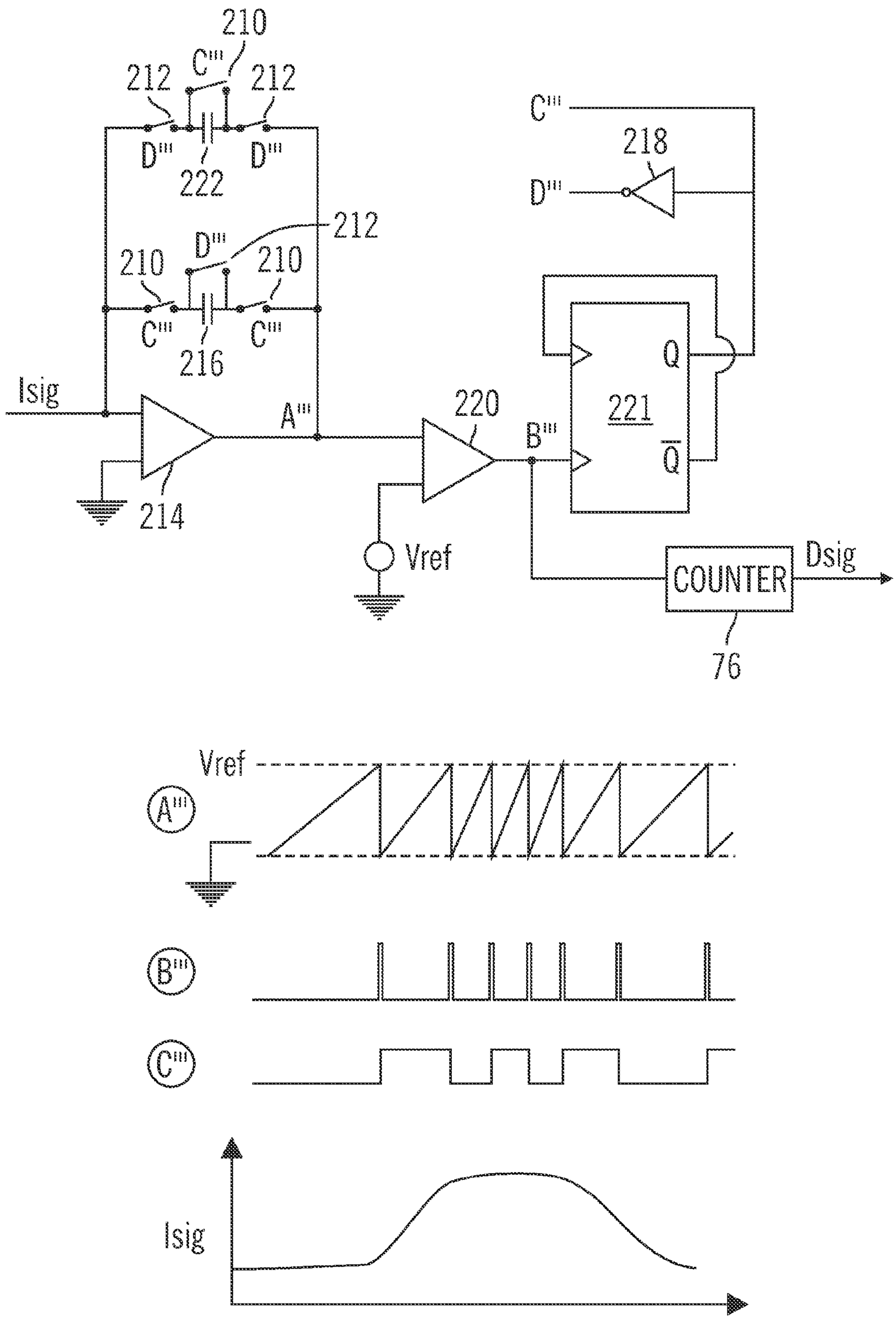
210
C'''
212
212
D'''
D'''
222
212
D'''
210
210
C'''
C'''
216
Isig
A'''
220
B'''
C'''
218
D'''
Q
221
Q̄
214
Vref
COUNTER
Dsig
76
Vref
A'''
B'''
C'''
Isig

FIG. 14

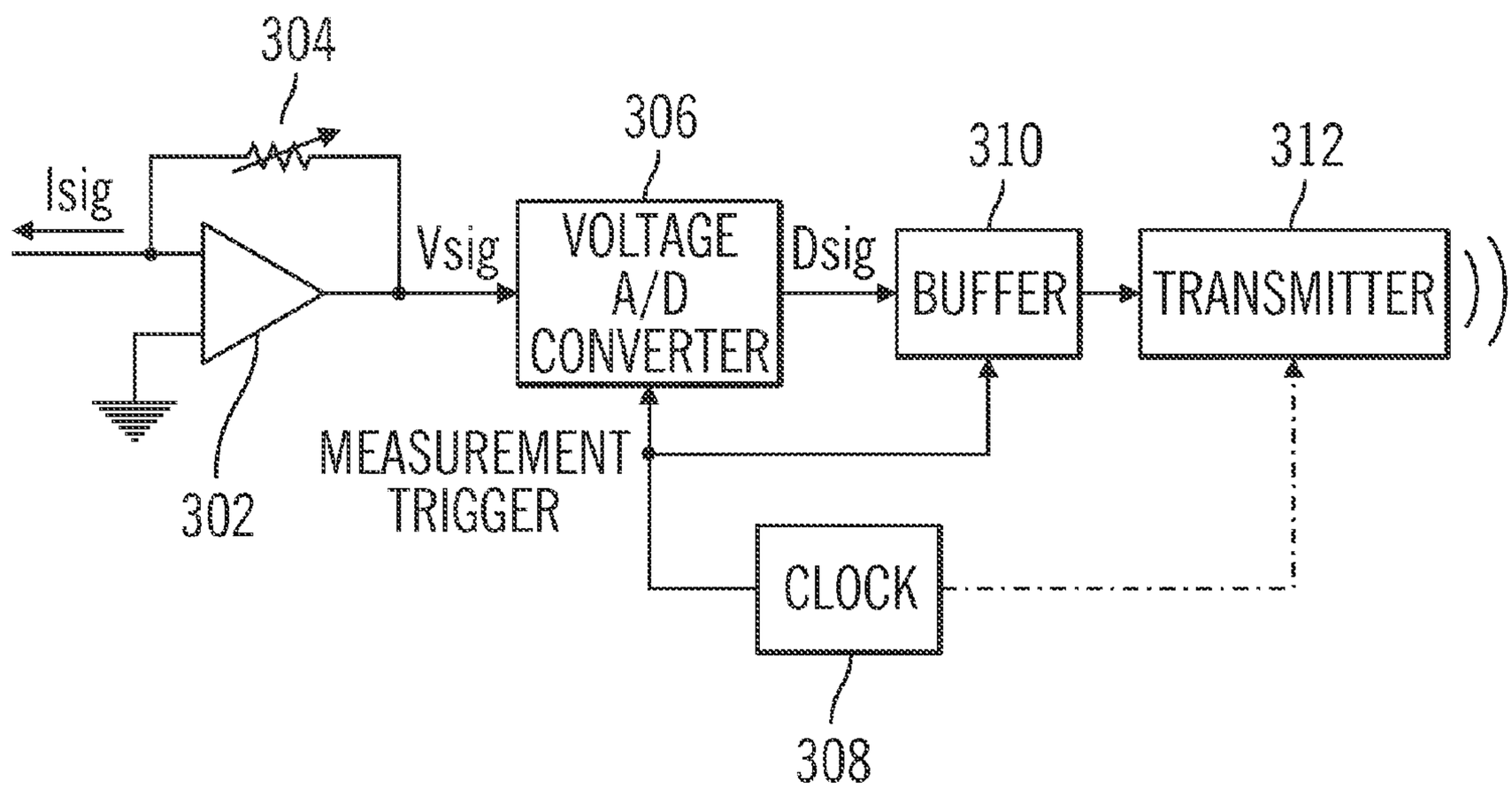
304
Isig
306
VOLTAGE
A/D
CONVERTER
Vsig
Dsig
310
BUFFER
312
TRANSMITTER
302
MEASUREMENT
TRIGGER
CLOCK
308

FIG. 15

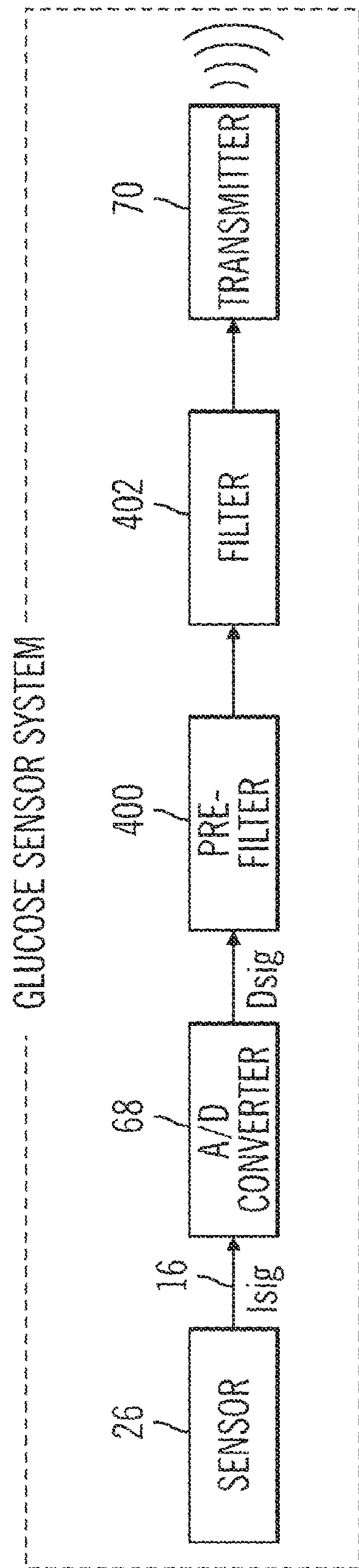
GLUCOSE SENSOR SYSTEM
26
SENSOR
16
Isig
68
A/D CONVERTER
Dsig
400
PRE-FILTER
402
FILTER
70
TRANSMITTER

FIG. 16

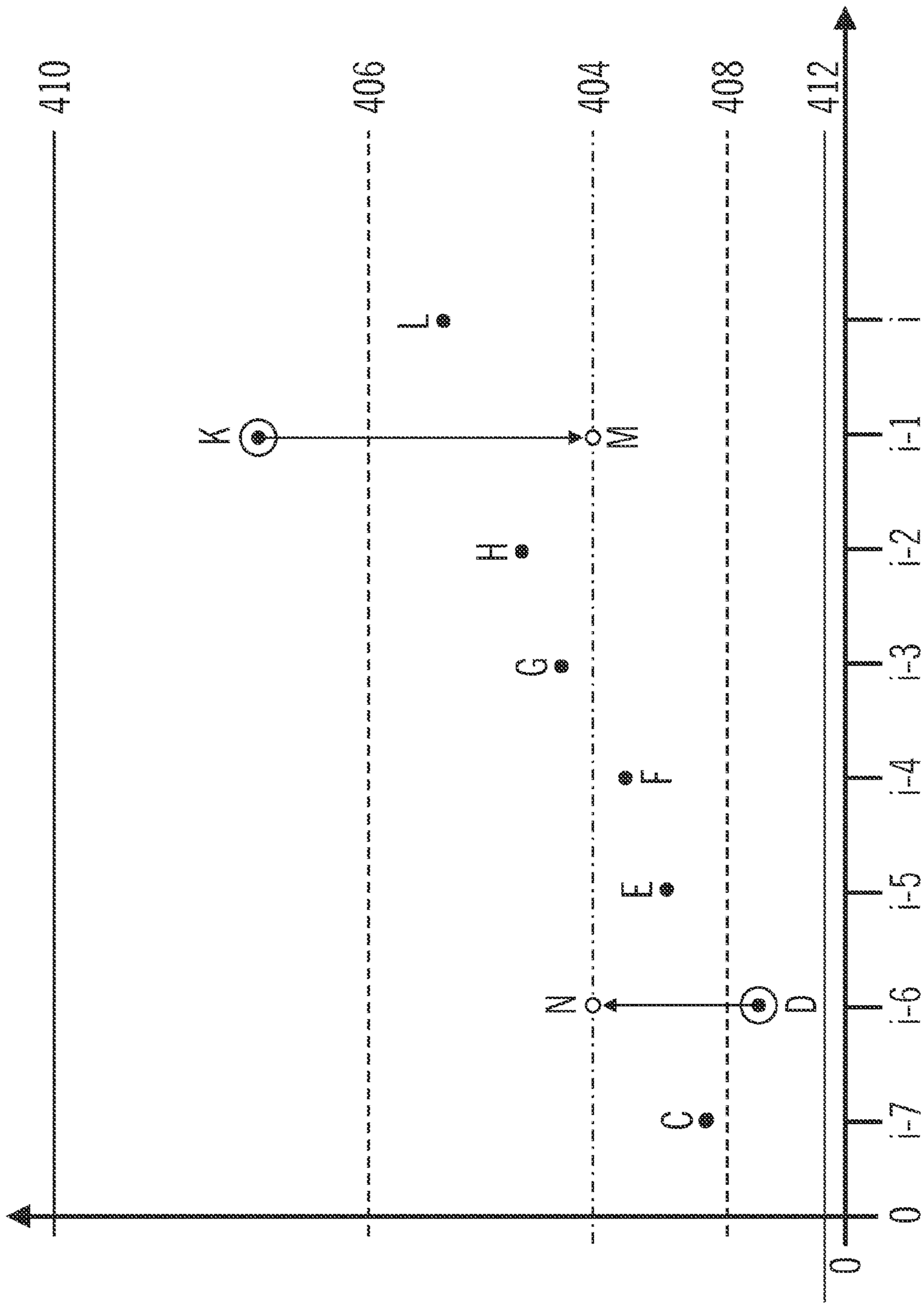

FIG. 17

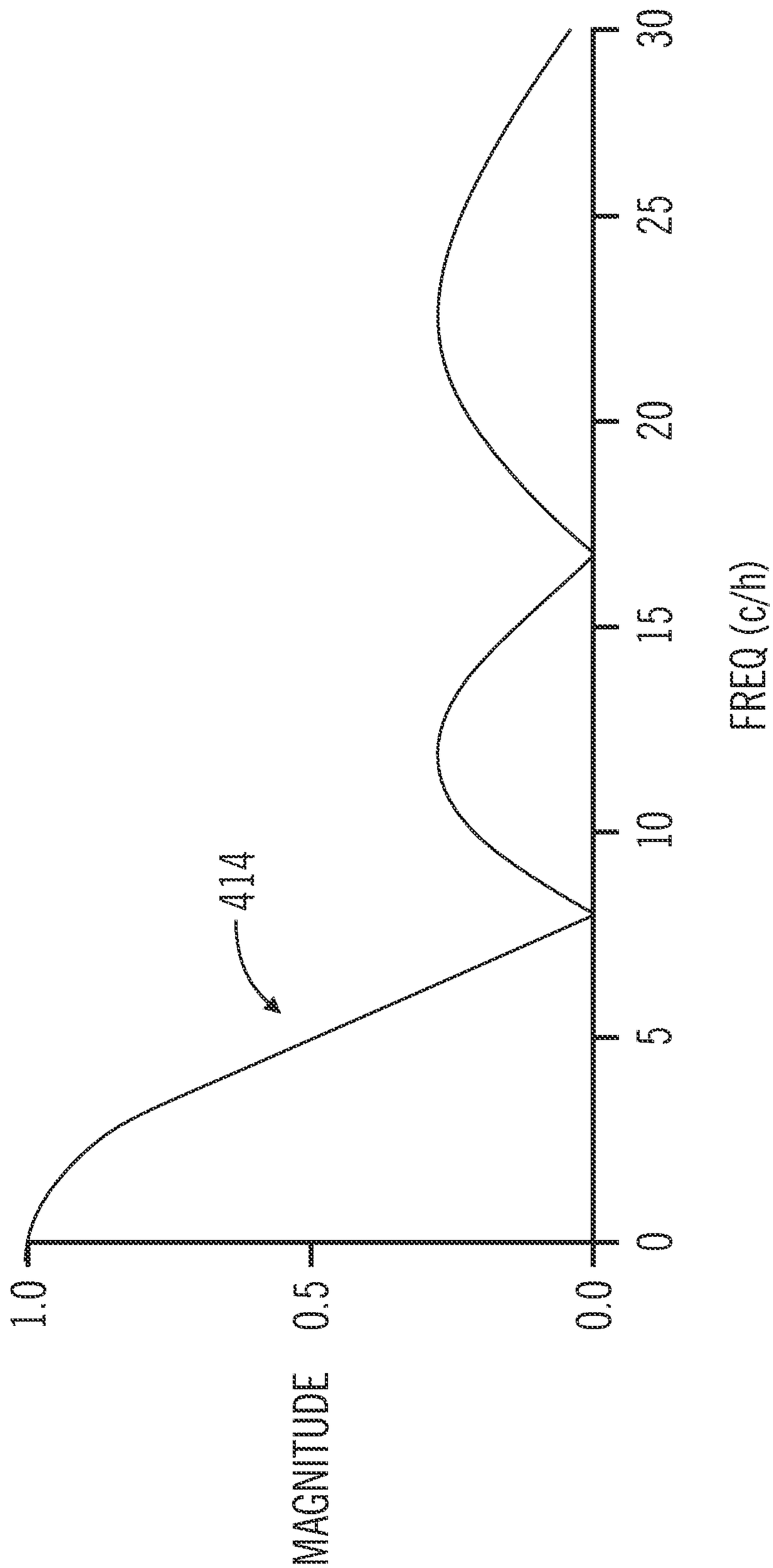

FIG. 18

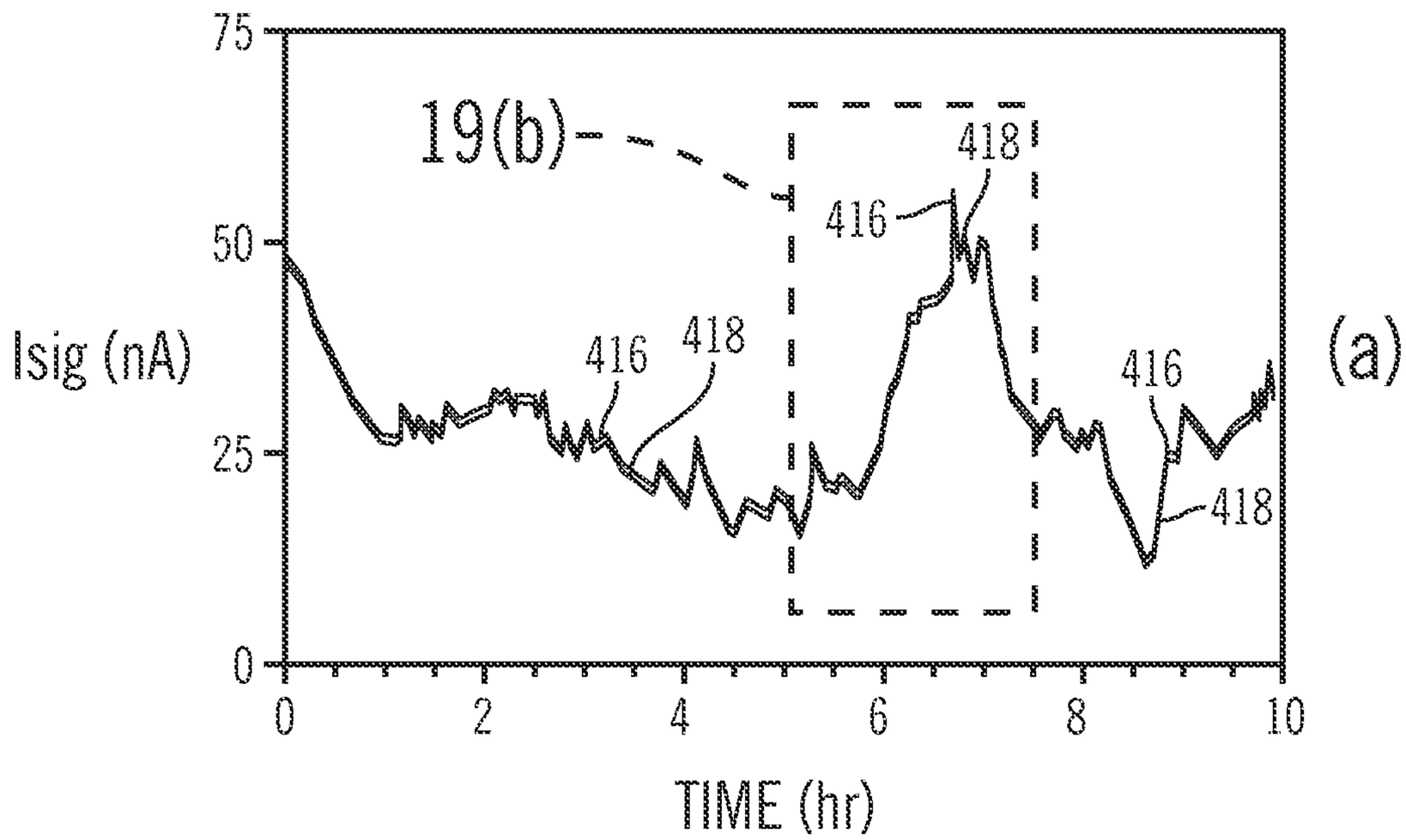
75
50
25
0
Isig (nA)
19(b)
416
418
416
418
416
418
(a)
0
2
4
6
8
10
TIME (hr)

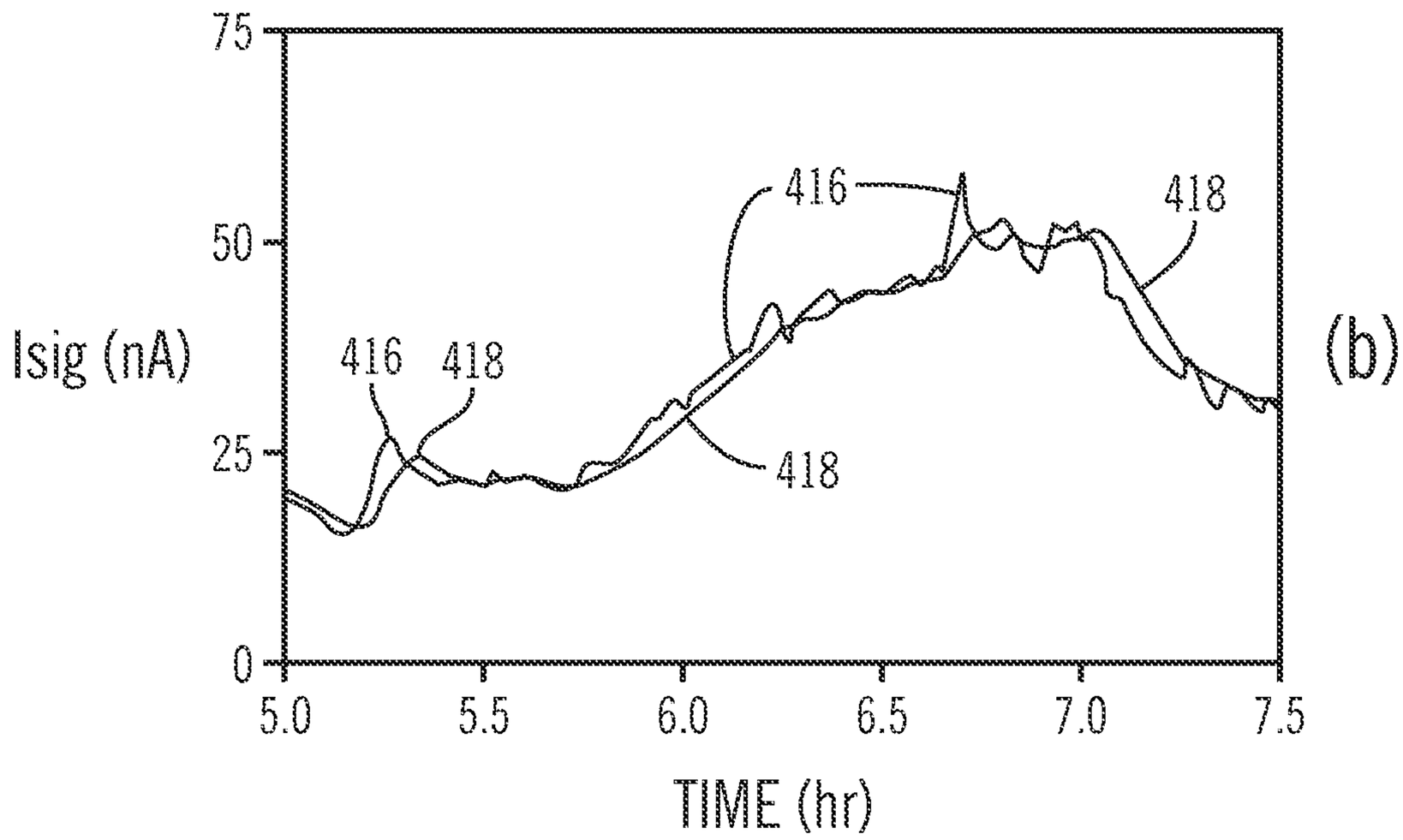
75
50
25
0
Isig (nA)
416
418
416
418
(b)
5.0
5.5
6.0
6.5
7.0
7.5
TIME (hr)

FIG. 19

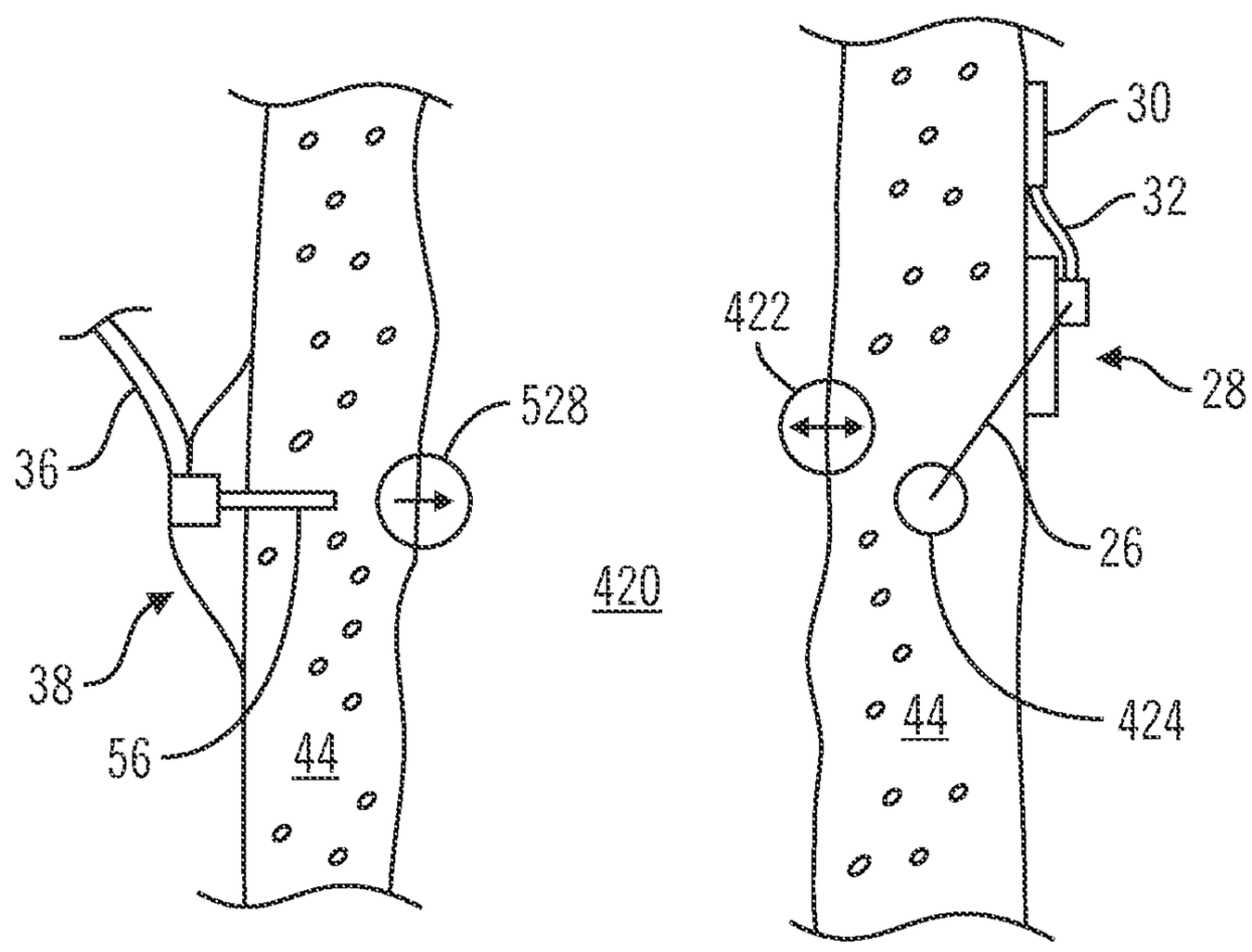

FIG. 20

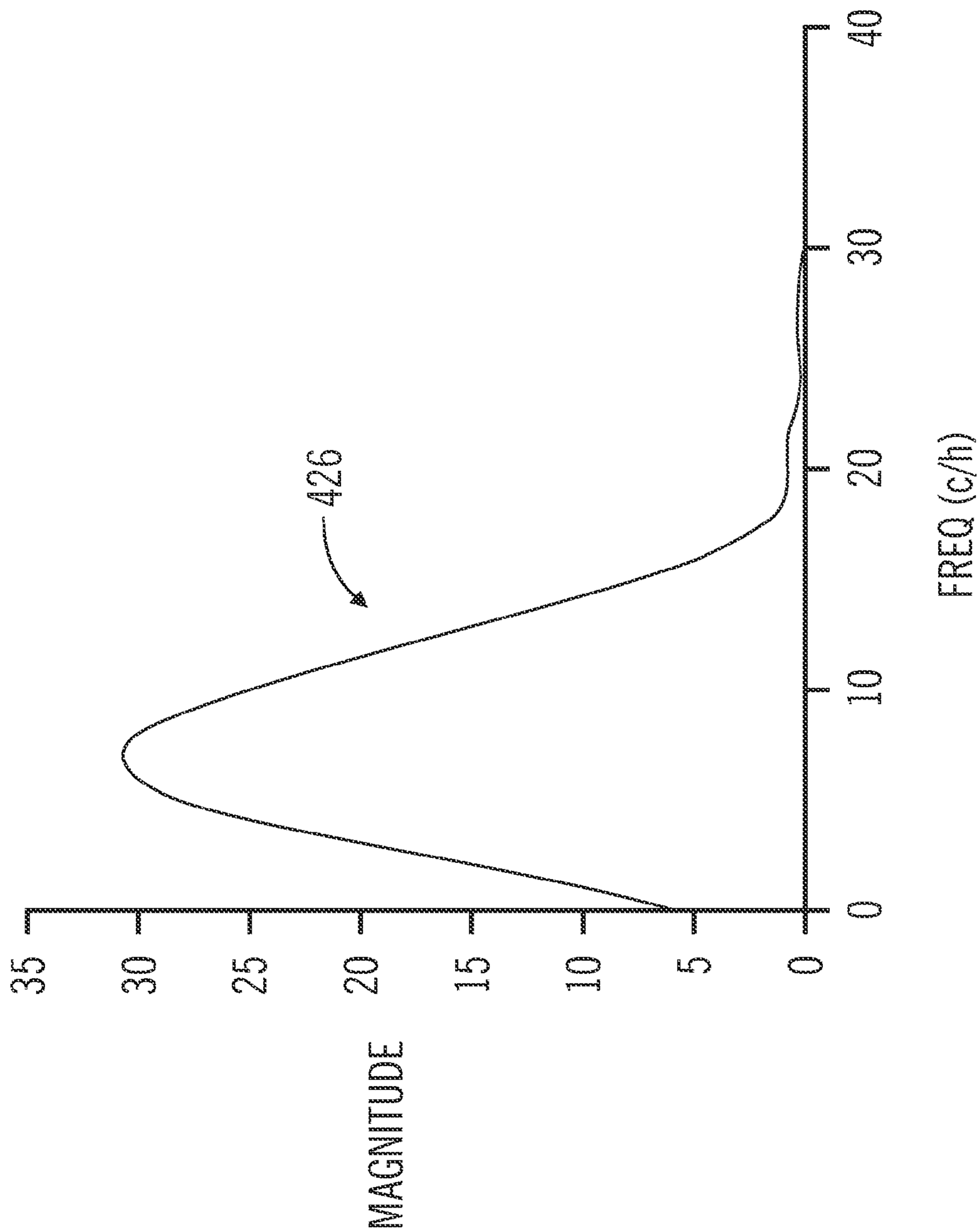

FIG. 21

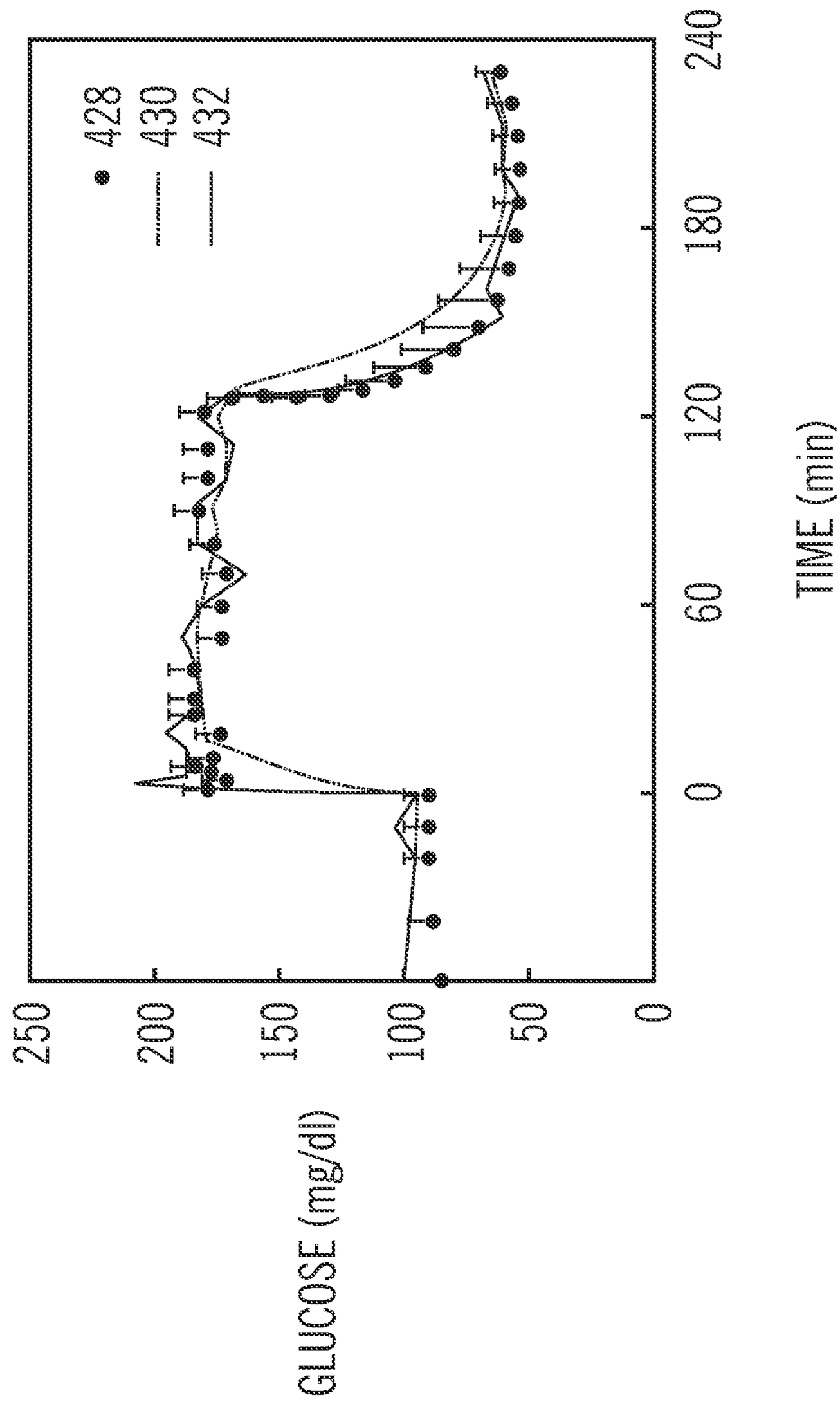
428
430
432
250
200
150
100
50
0
GLUCOSE (mg/dl)
0
60
120
180
240
TIME (min)

FIG. 22

(a)

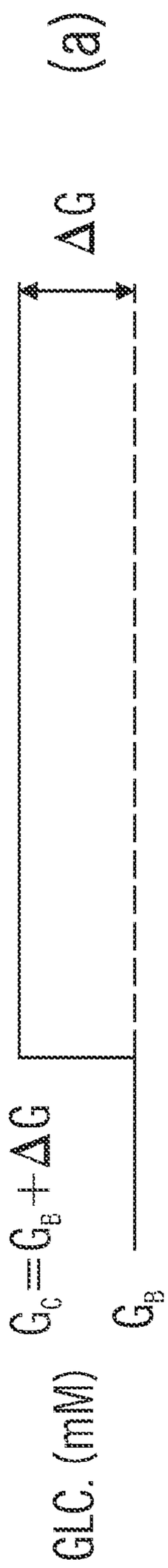

$$G_C = G_B + \Delta G$$

$$G_B$$

(b)

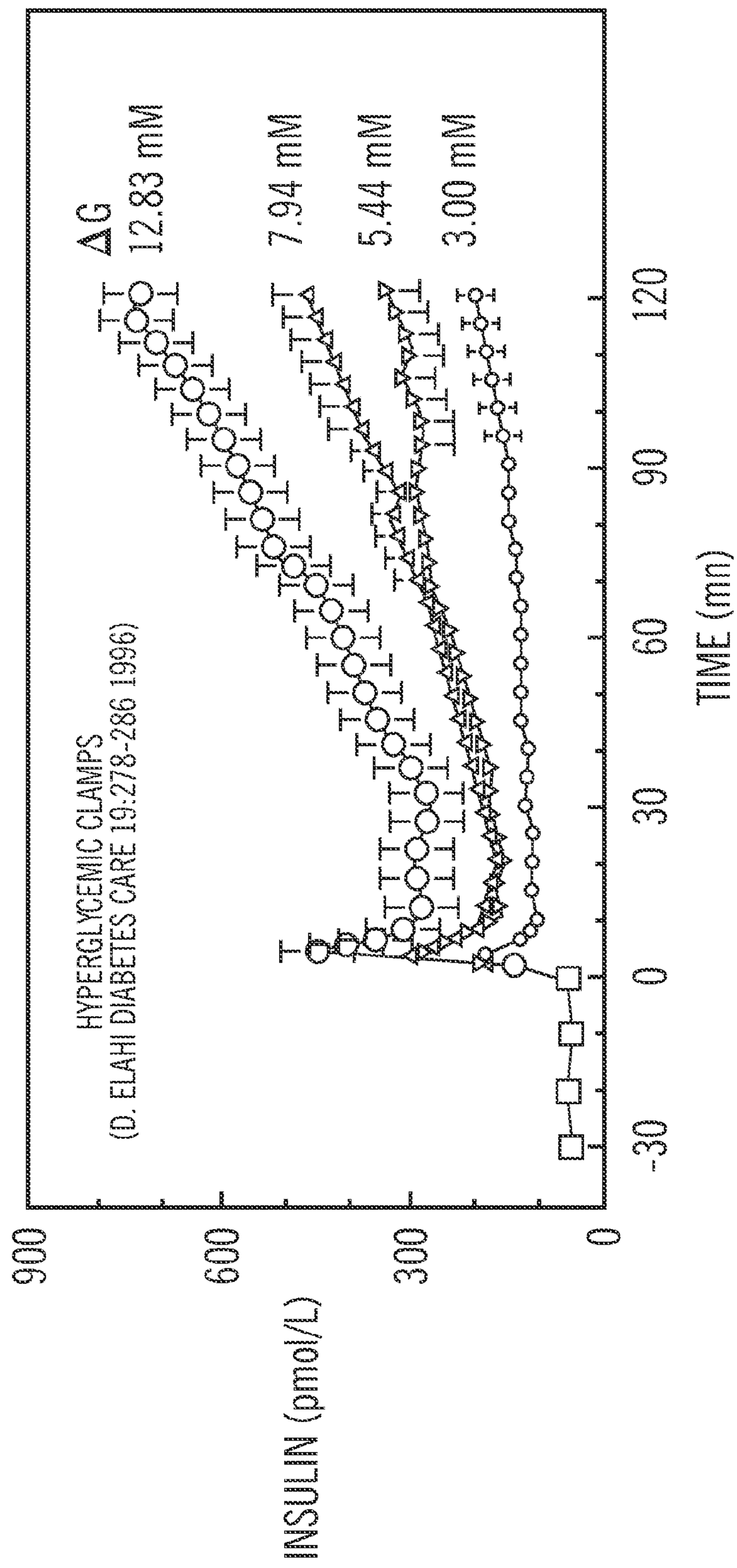

FIG. 23

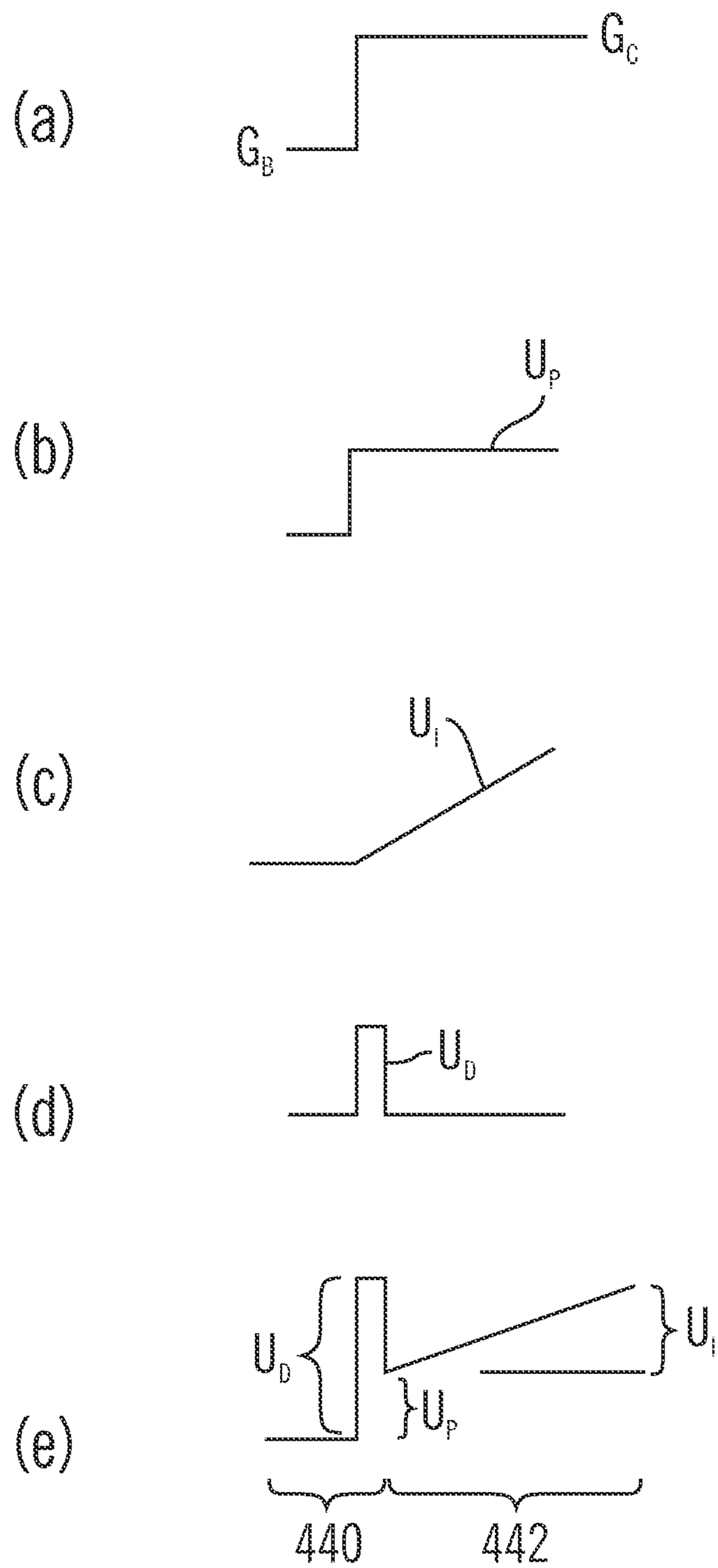

FIG. 24

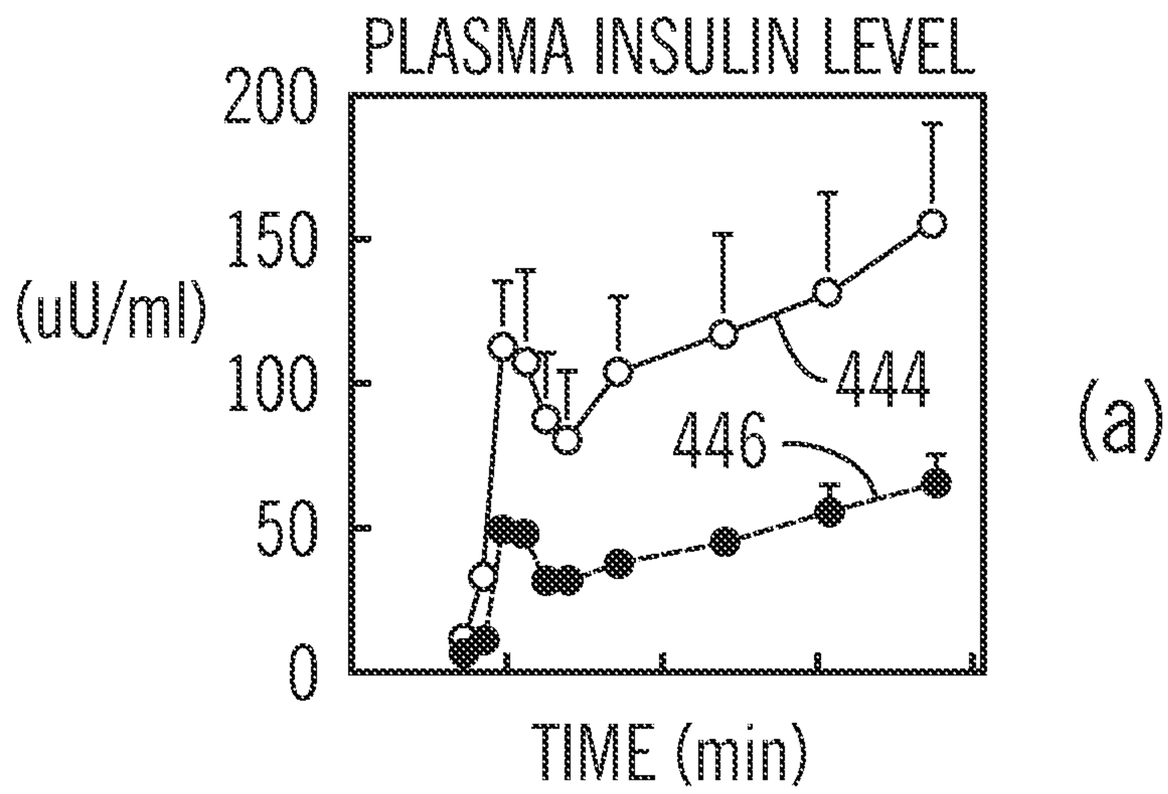
PLASMA INSULIN LEVEL
200
150
100
50
0
(uU/ml)
444
446
TIME (min)
(a)

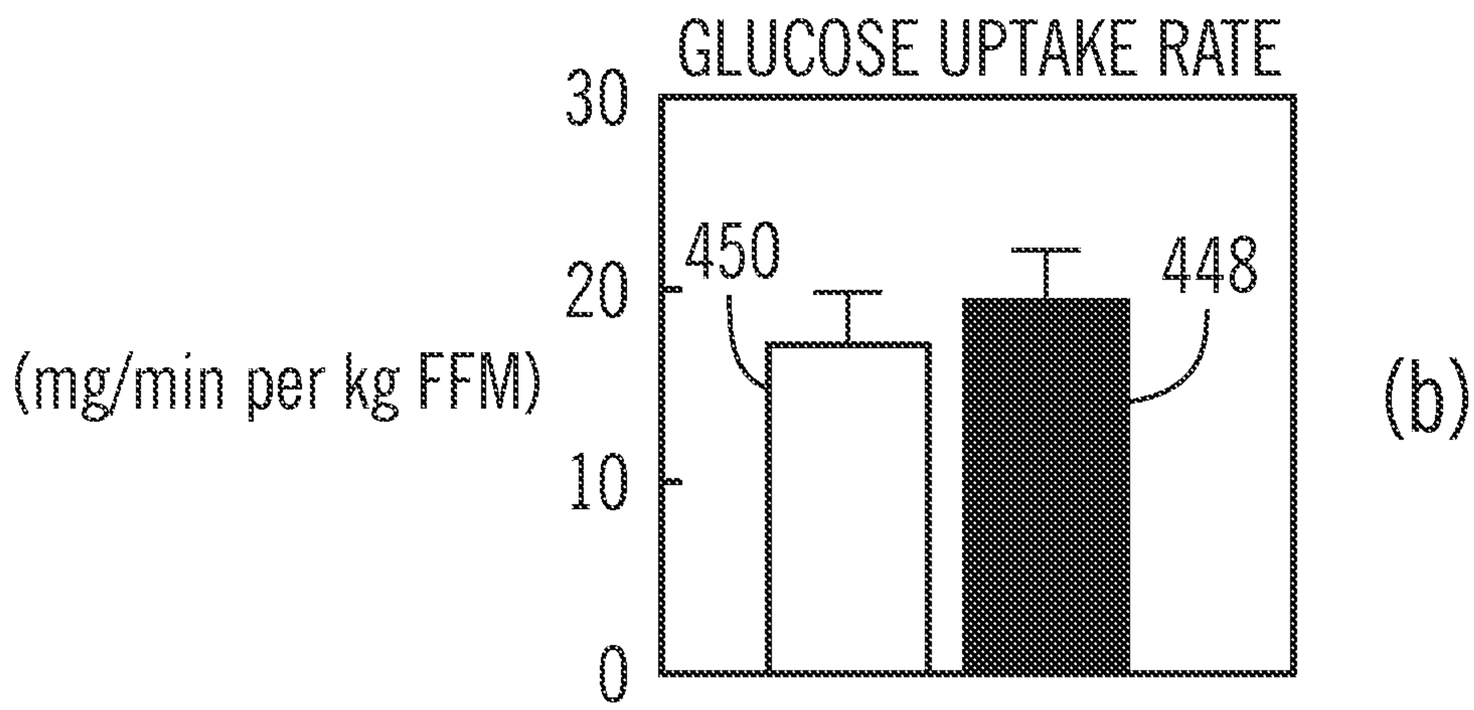
GLUCOSE UPTAKE RATE
30
20
10
0
(mg/min per kg FFM)
450
448
(b)

FIG. 25

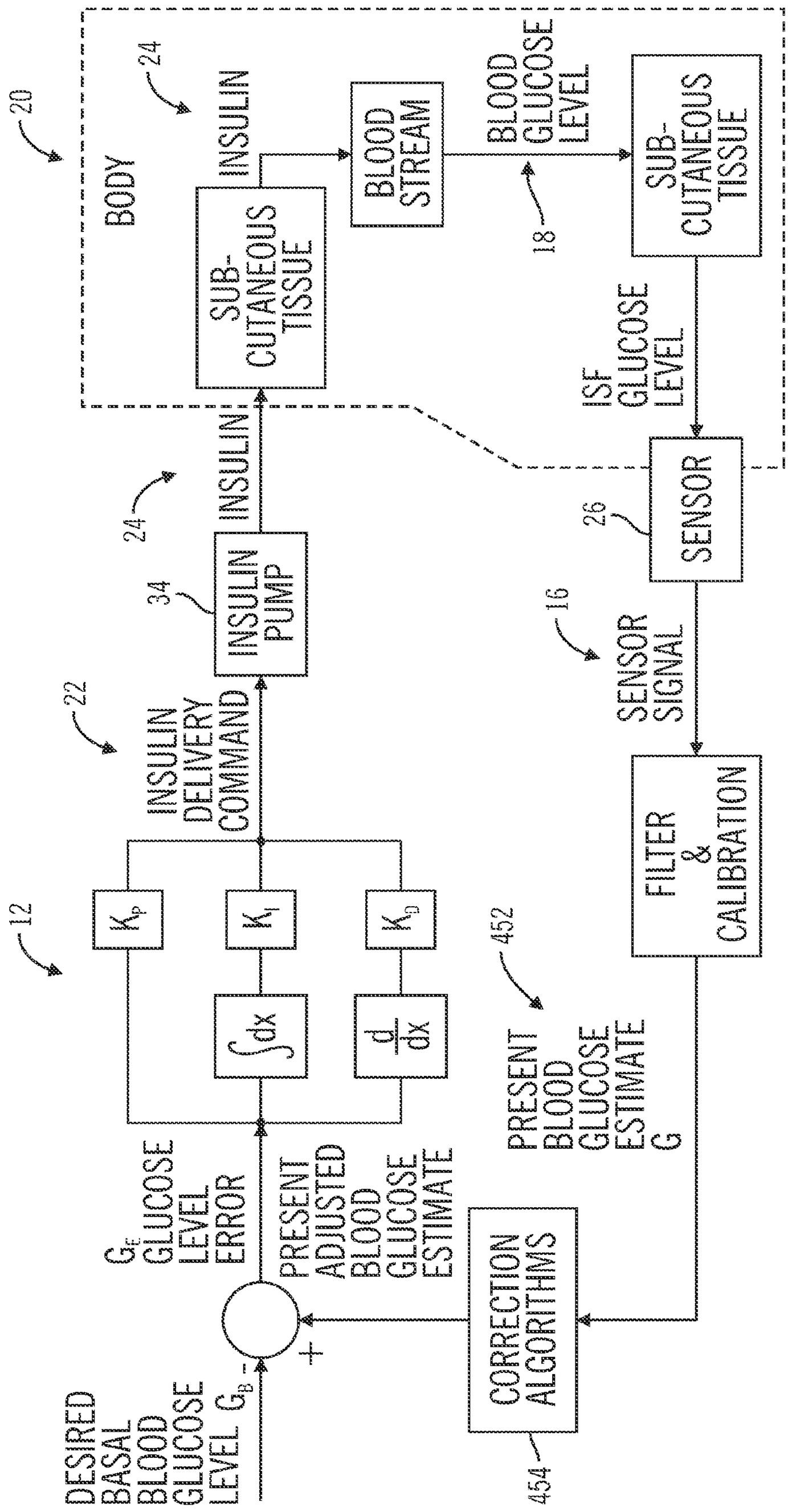
20
BODY
24
INSULIN
SUB-CUTANEOUS TISSUE
BLOOD STREAM
BLOOD GLUCOSE LEVEL
18
SUB-CUTANEOUS TISSUE
ISF GLUCOSE LEVEL
24
INSULIN
34
INSULIN PUMP
26
SENSOR
16
SENSOR SIGNAL
22
INSULIN DELIVERY COMMAND
FILTER & CALIBRATION
12
K_P
K_I
K_D
$\int dx$
$\frac{d}{dx}$
452
PRESENT BLOOD GLUCOSE ESTIMATE G
G_E GLUCOSE LEVEL ERROR
PRESENT ADJUSTED BLOOD GLUCOSE ESTIMATE
+
-
DESIRED BASAL BLOOD GLUCOSE LEVEL G_B
CORRECTION ALGORITHMS
454

FIG. 26

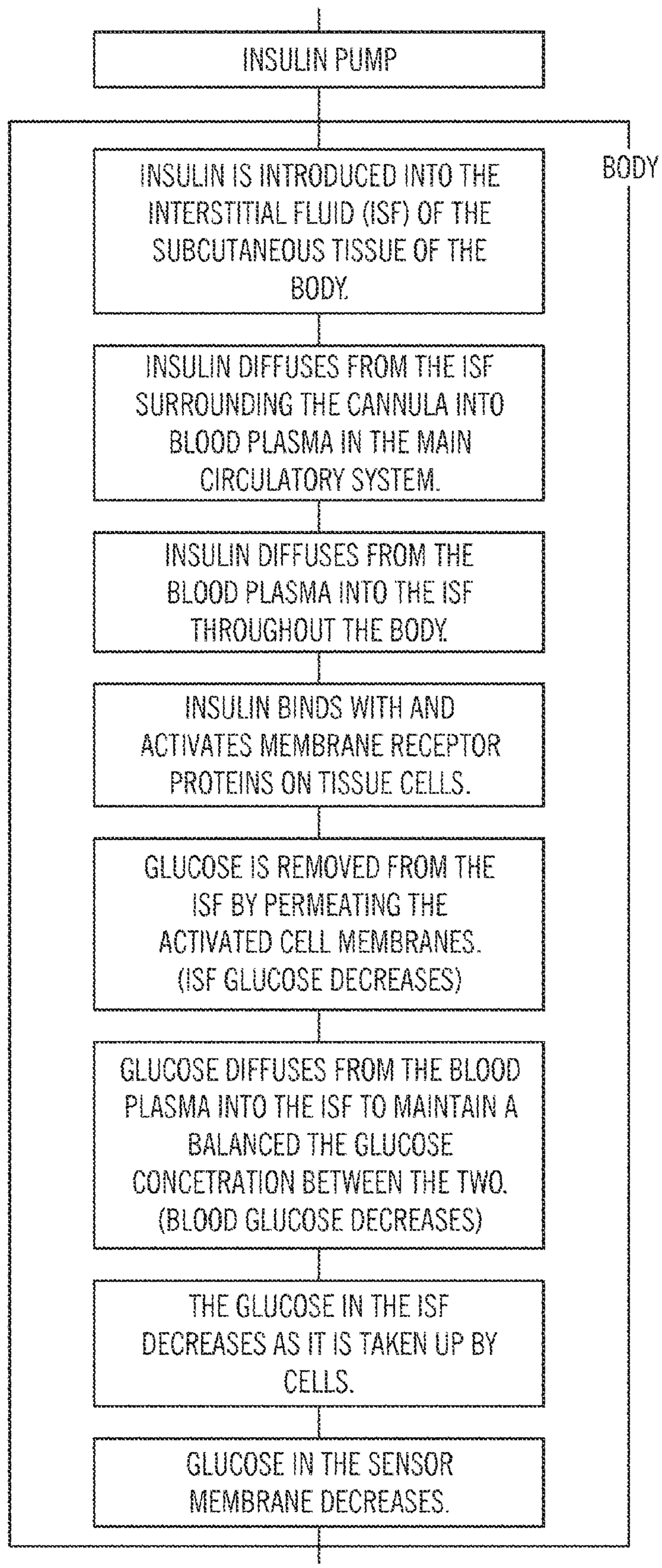
INSULIN PUMP
BODY
INSULIN IS INTRODUCED INTO THE INTERSTITIAL FLUID (ISF) OF THE SUBCUTANEOUS TISSUE OF THE BODY.
INSULIN DIFFUSES FROM THE ISF SURROUNDING THE CANNULA INTO BLOOD PLASMA IN THE MAIN CIRCULATORY SYSTEM.
INSULIN DIFFUSES FROM THE BLOOD PLASMA INTO THE ISF THROUGHOUT THE BODY.
INSULIN BINDS WITH AND ACTIVATES MEMBRANE RECEPTOR PROTEINS ON TISSUE CELLS.
GLUCOSE IS REMOVED FROM THE ISF BY PERMEATING THE ACTIVATED CELL MEMBRANES. (ISF GLUCOSE DECREASES)
GLUCOSE DIFFUSES FROM THE BLOOD PLASMA INTO THE ISF TO MAINTAIN A BALANCED THE GLUCOSE CONCETRATION BETWEEN THE TWO. (BLOOD GLUCOSE DECREASES)
THE GLUCOSE IN THE ISF DECREASES AS IT IS TAKEN UP BY CELLS.
GLUCOSE IN THE SENSOR MEMBRANE DECREASES.

FIG. 27

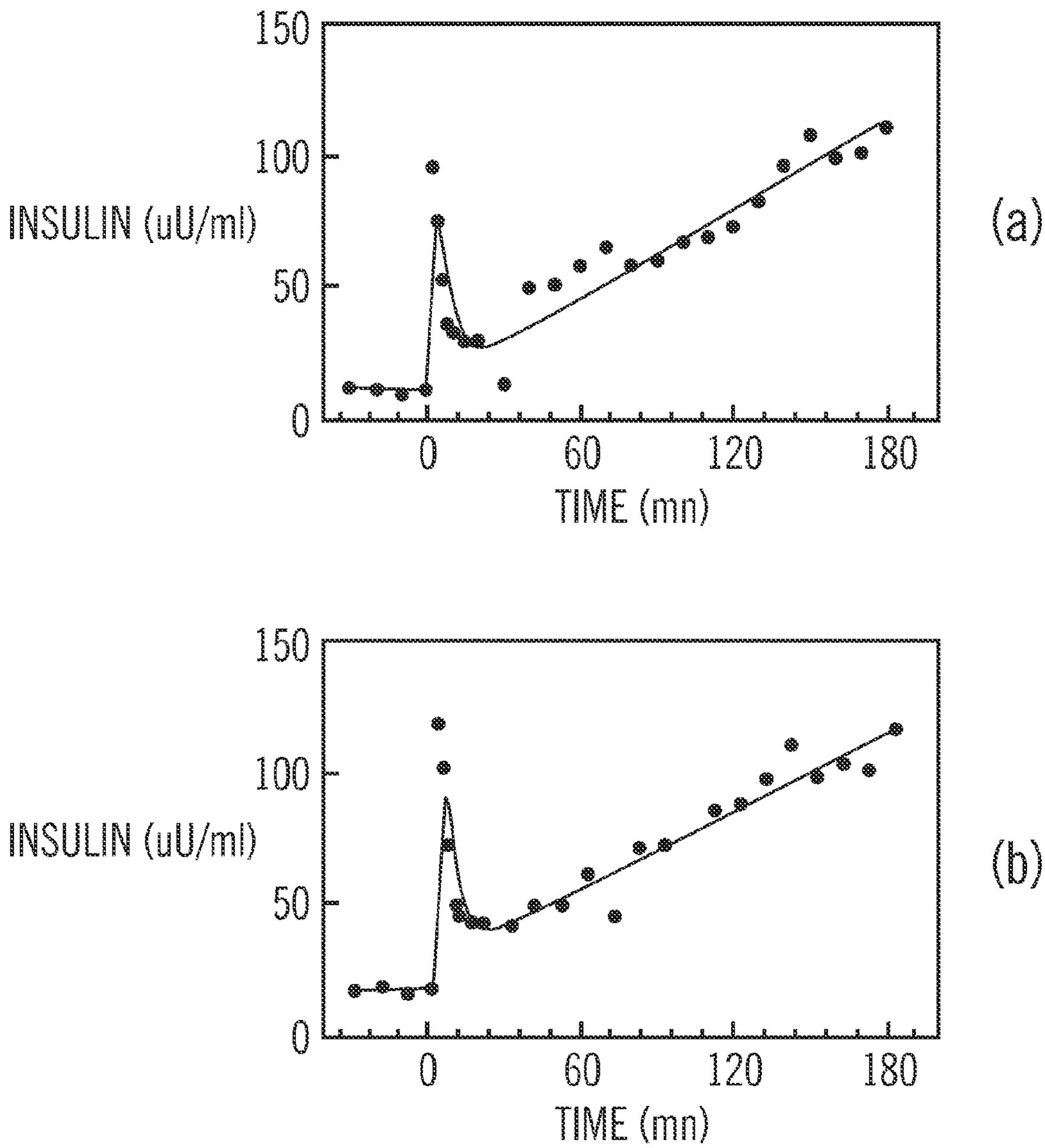
150
100
50
0
INSULIN (uU/ml)
0
60
120
180
TIME (mn)
(a)
150
100
50
0
INSULIN (uU/ml)
0
60
120
180
TIME (mn)
(b)

FIG. 28

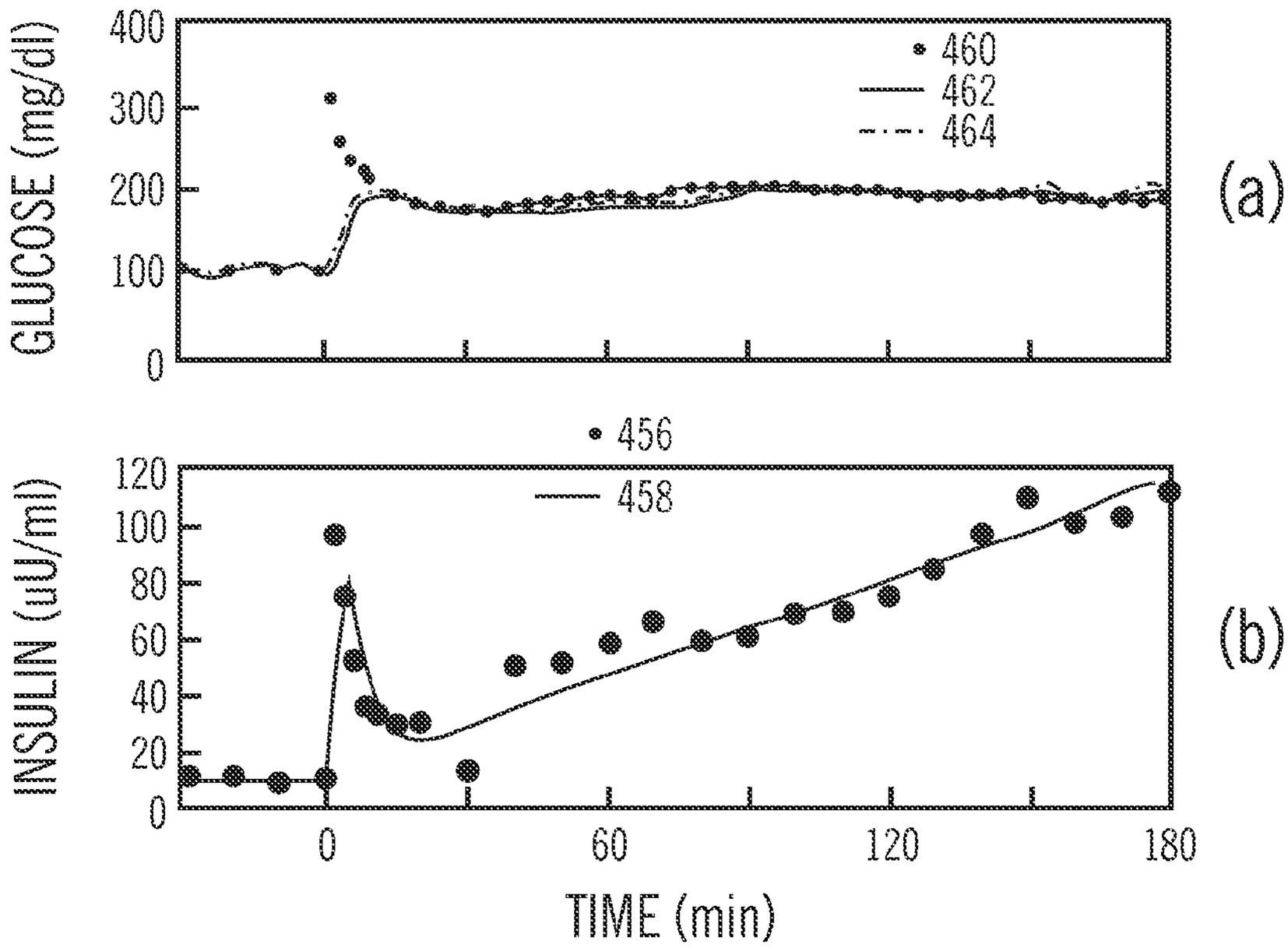
GLUCOSE (mg/dl)
400
300
200
100
0
460
462
464
(a)
456
INSULIN (uU/ml)
120
100
80
60
40
20
0
458
(b)
0
60
120
180
TIME (min)

FIG. 29

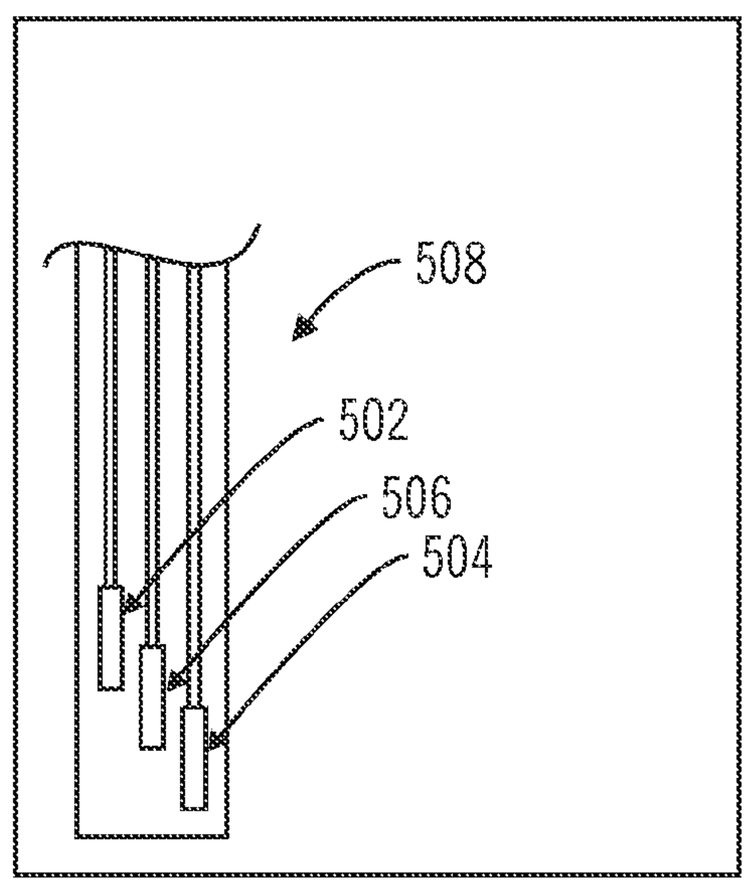
508
502
506
504

FIG. 30

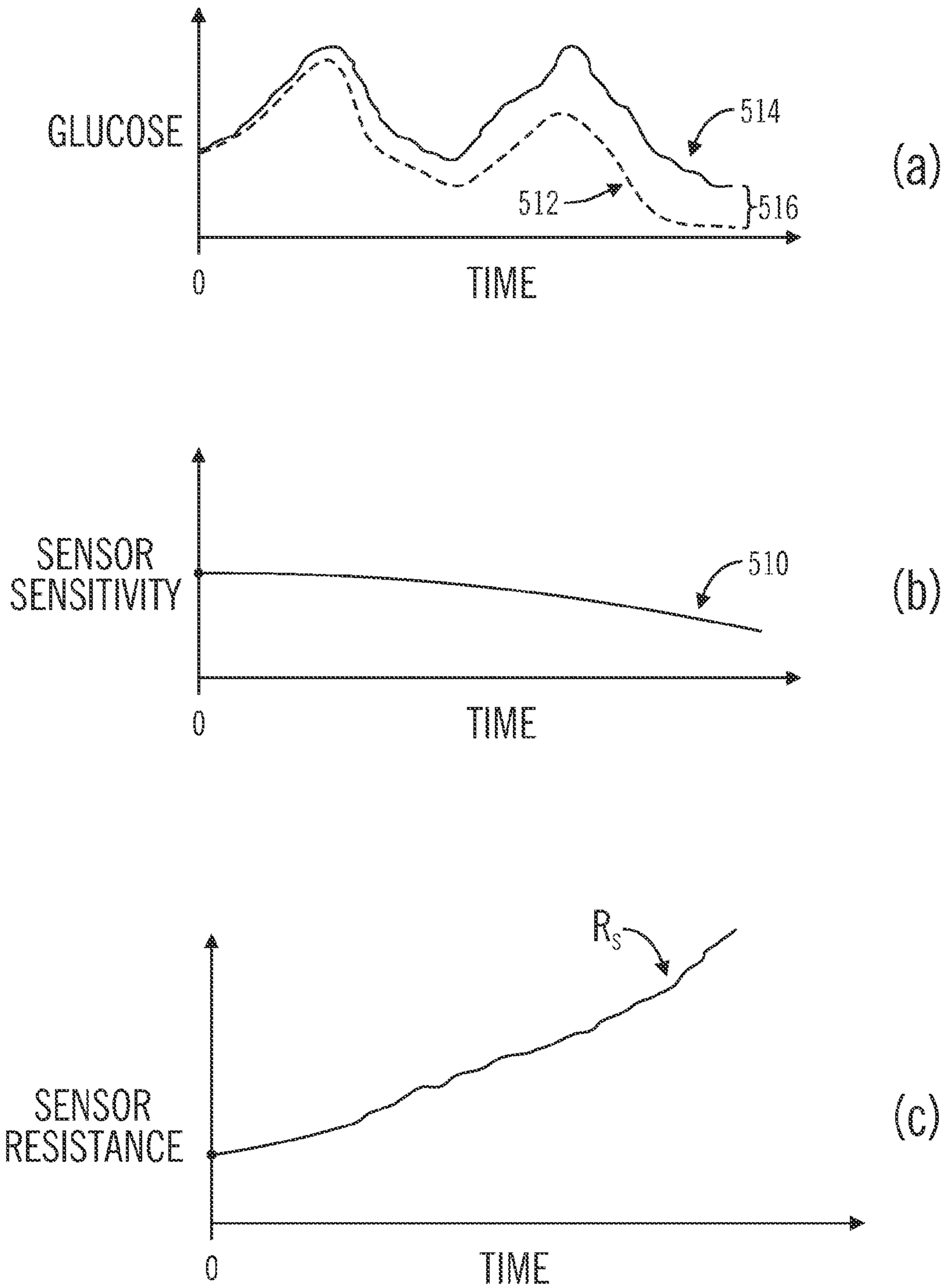
GLUCOSE
514
512
516
0
TIME
(a)
SENSOR SENSITIVITY
510
0
TIME
(b)
R_S
SENSOR RESISTANCE
0
TIME
(c)

FIG. 31

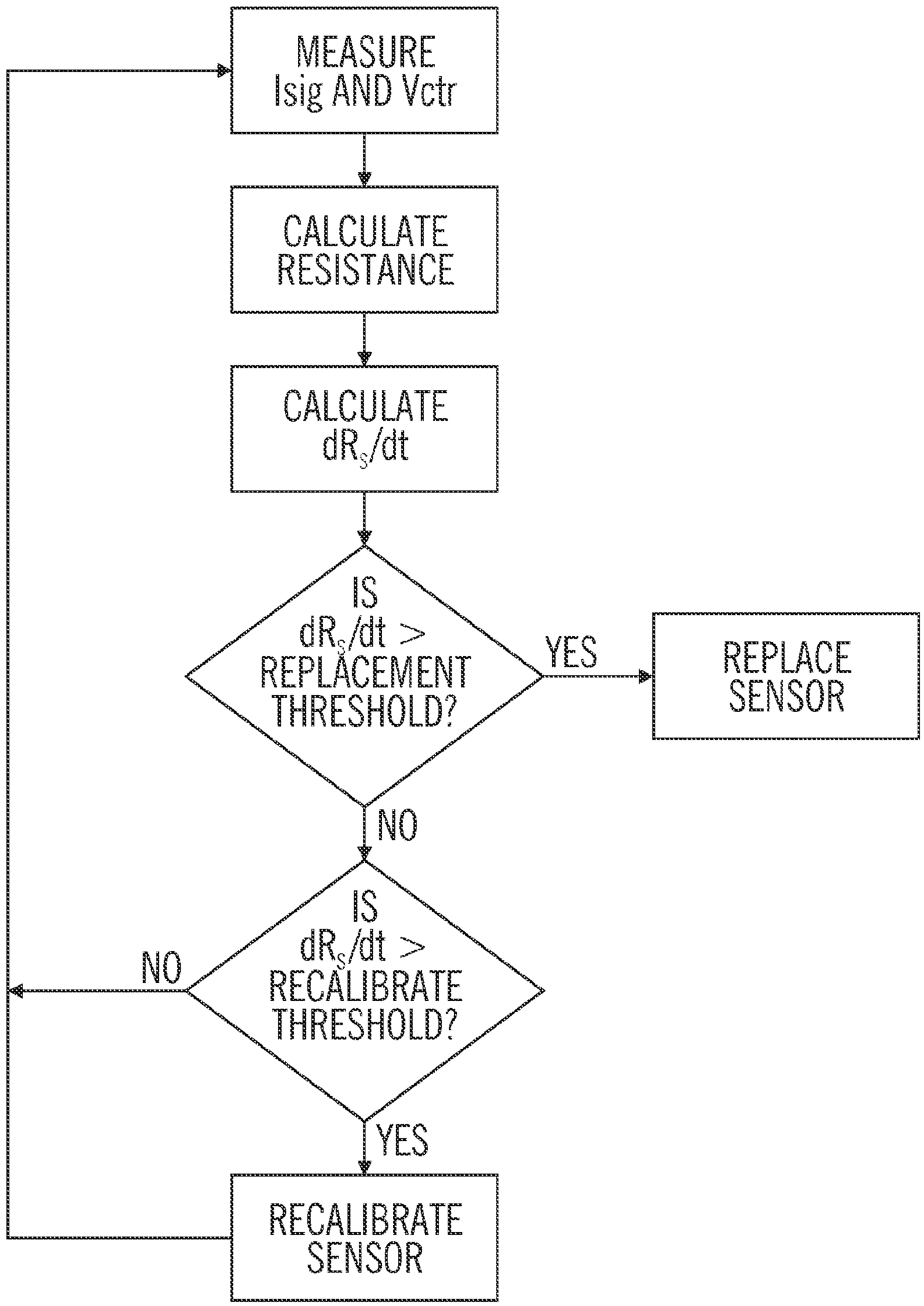
MEASURE
Isig AND Vctr
CALCULATE
RESISTANCE
CALCULATE
dRs/dt
IS
dRs/dt >
REPLACEMENT
THRESHOLD?
YES
REPLACE
SENSOR
NO
IS
dRs/dt >
RECALIBRATE
THRESHOLD?
NO
YES
RECALIBRATE
SENSOR

FIG. 32

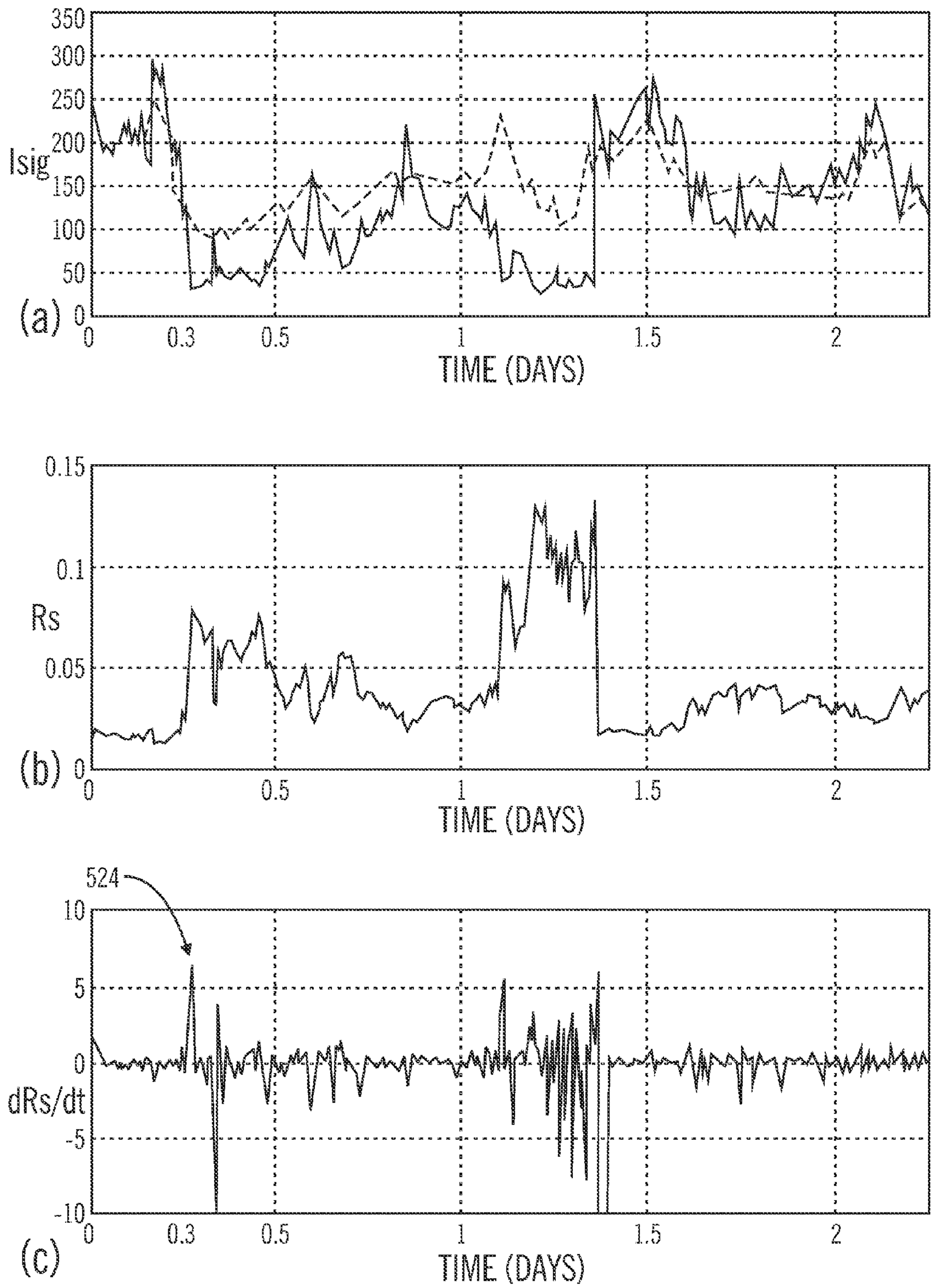
350
300
250
200
150
100
50
0
Isig
(a)
0
0.3
0.5
1
1.5
2
TIME (DAYS)
0.15
0.1
0.05
0
Rs
(b)
0
0.5
1
1.5
2
TIME (DAYS)
524
10
5
0
-5
-10
dRs/dt
(c)
0
0.3
0.5
1
1.5
2
TIME (DAYS)

FIG. 33

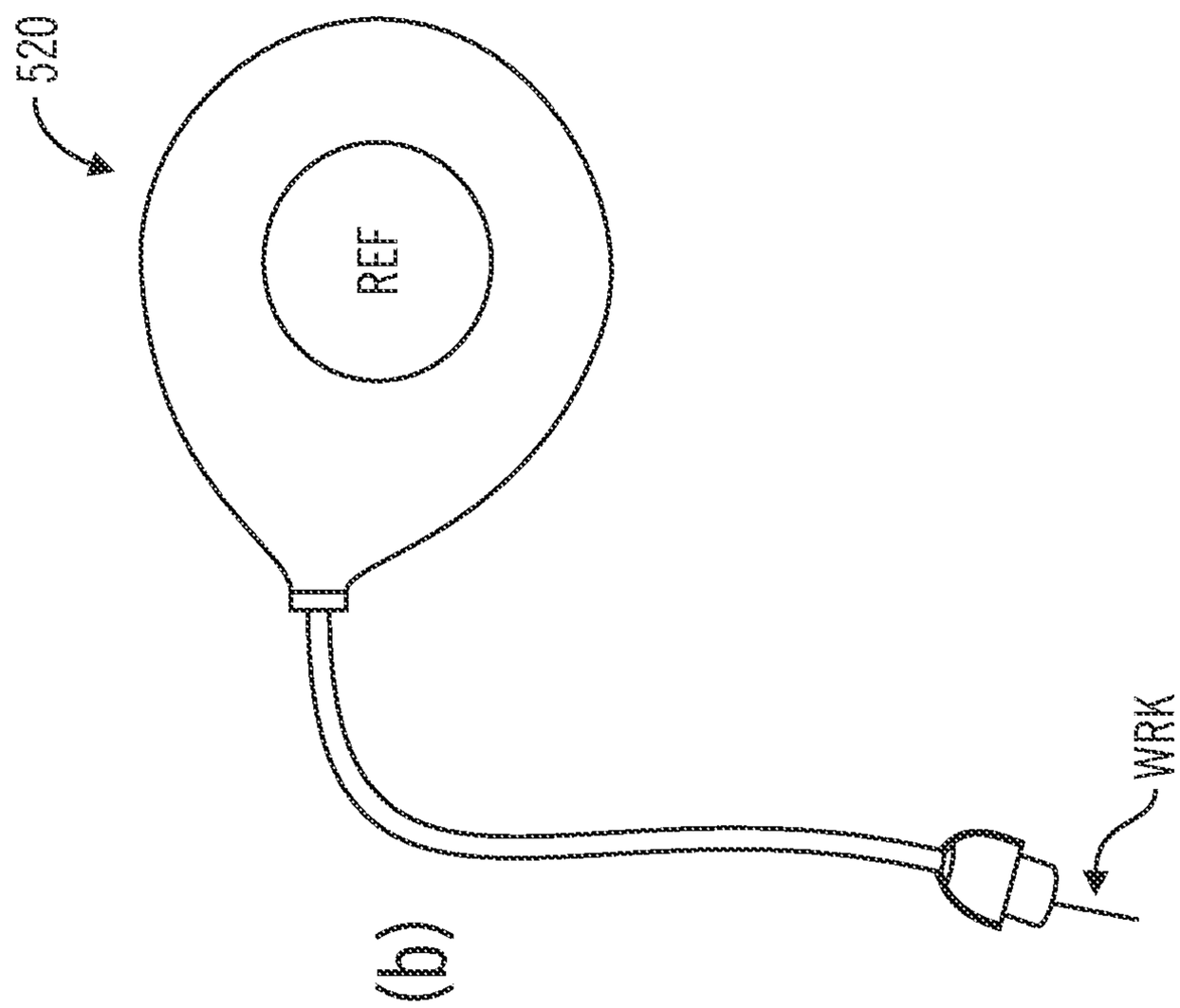

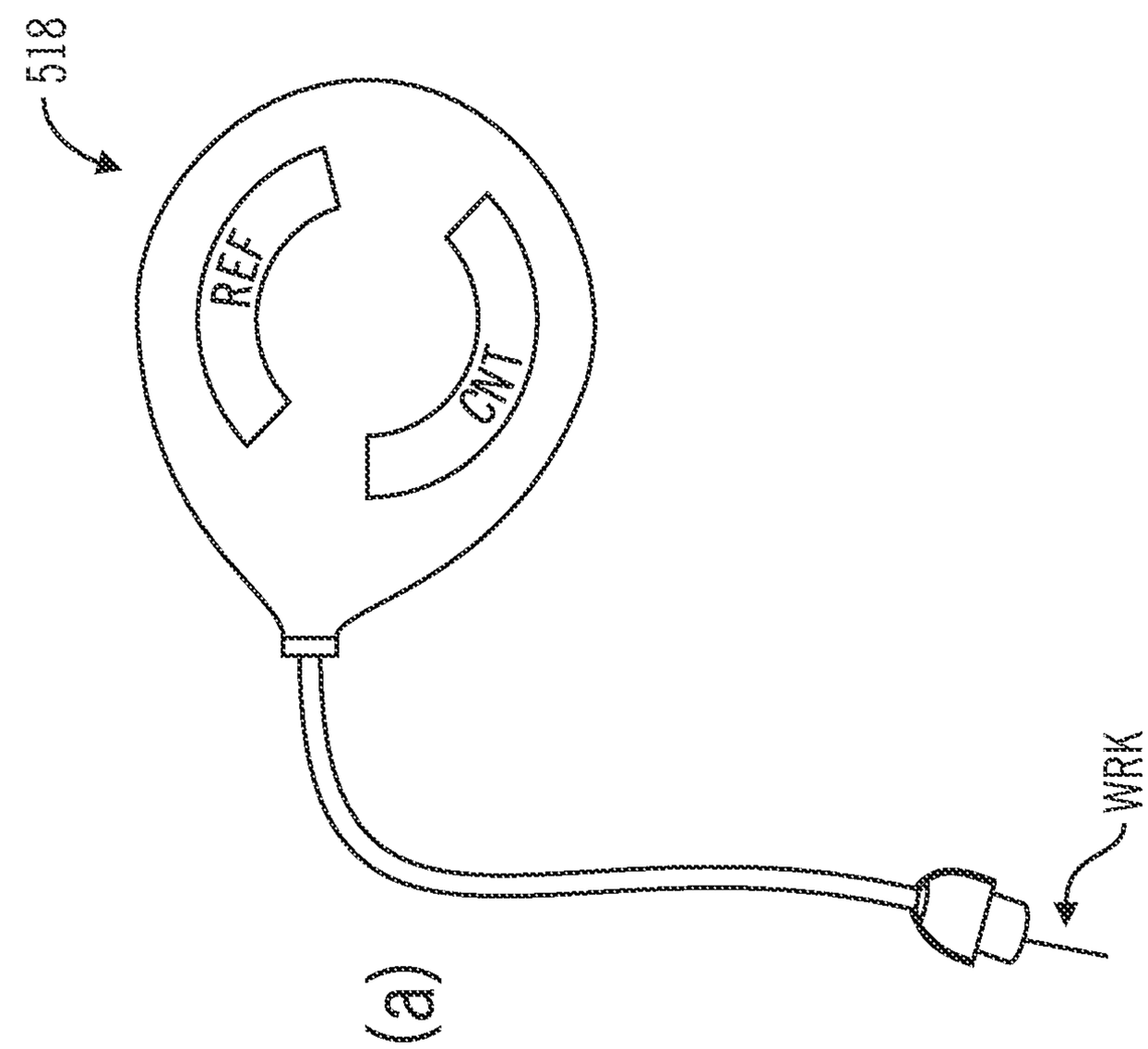

FIG. 34

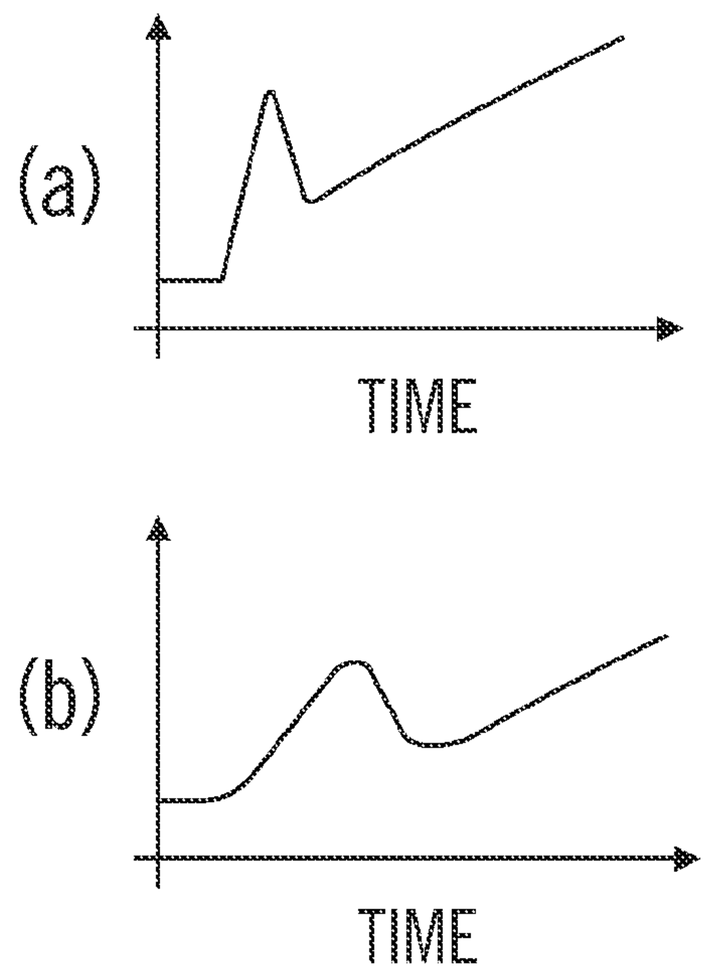

FIG. 35

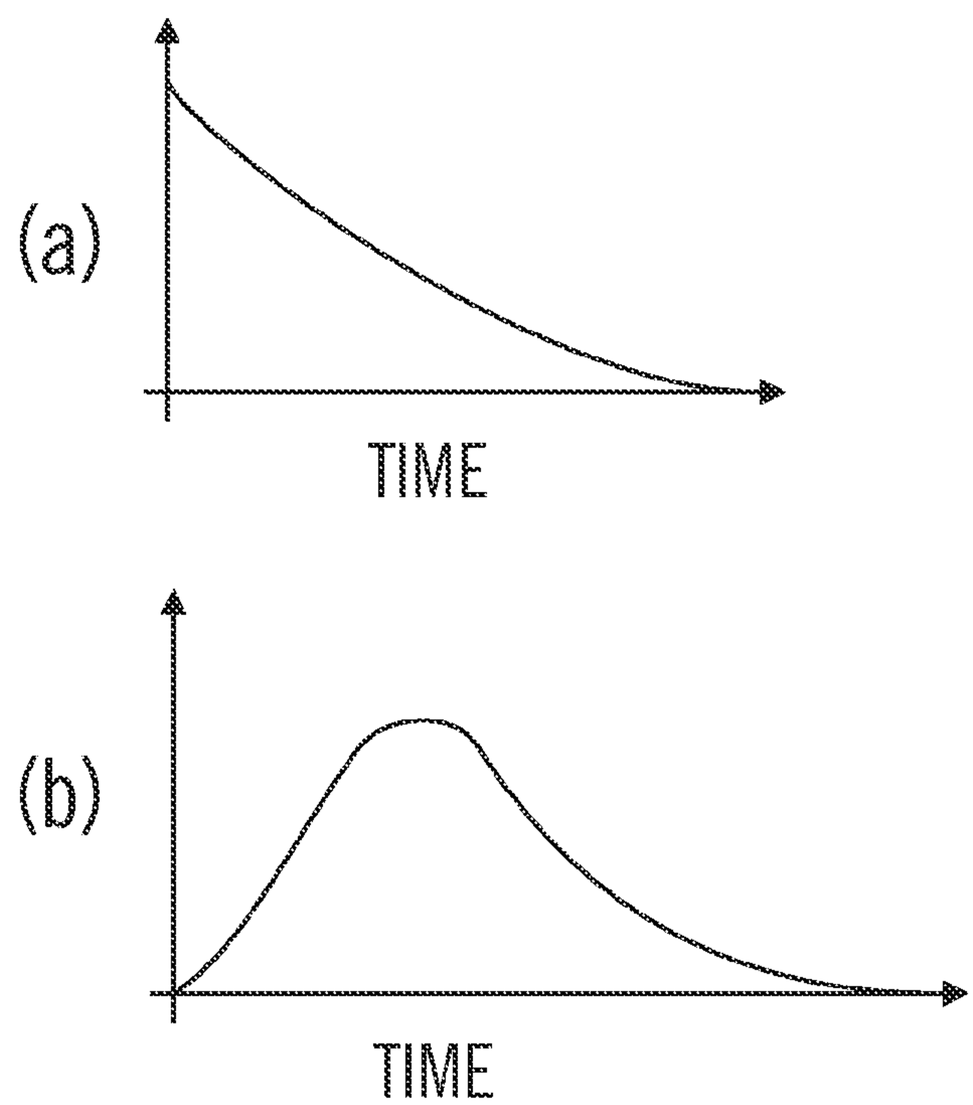

FIG. 36

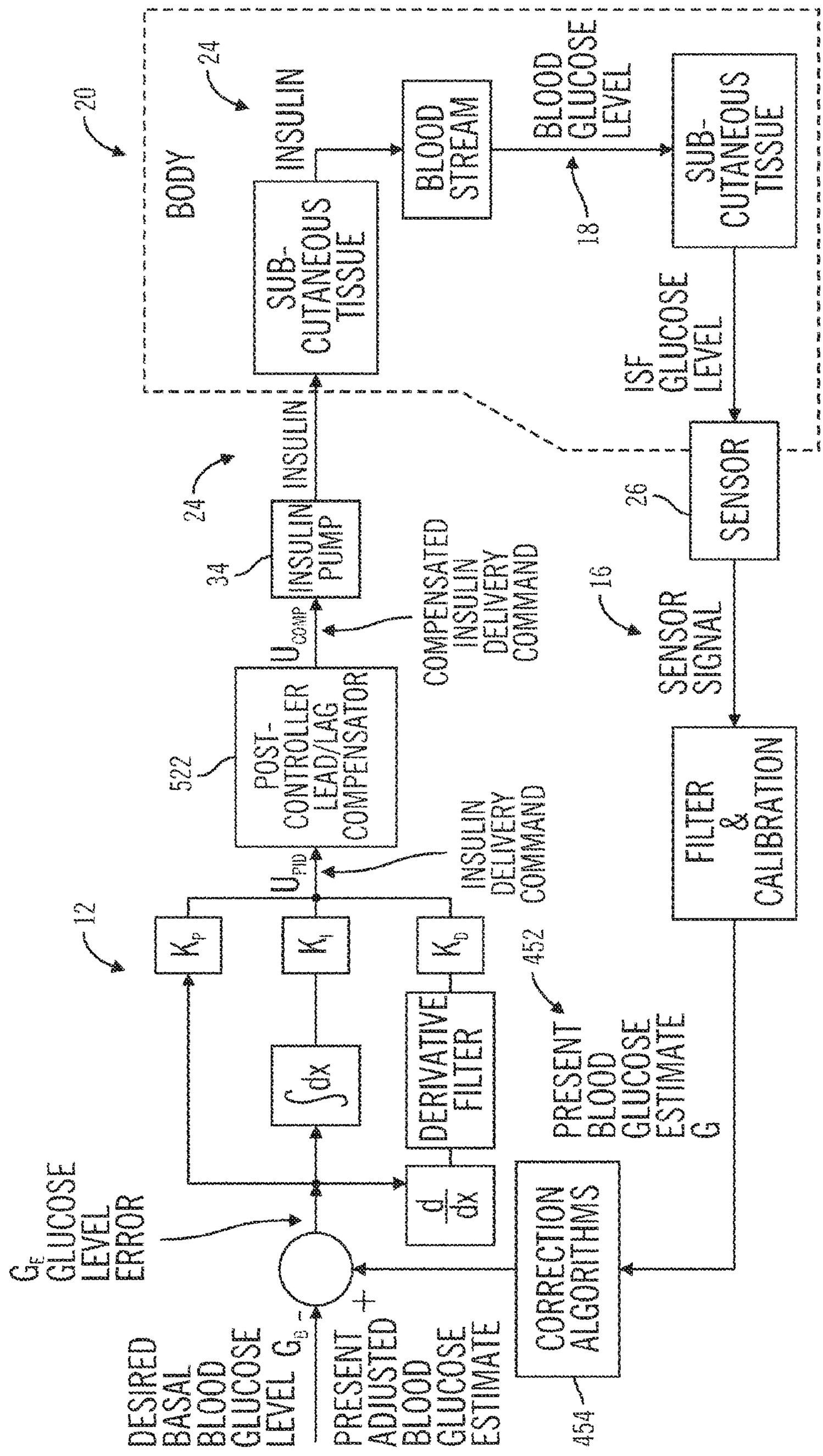
20
BODY
24
INSULIN
SUB-CUTANEOUS TISSUE
BLOOD STREAM
BLOOD GLUCOSE LEVEL
18
SUB-CUTANEOUS TISSUE
ISF GLUCOSE LEVEL
INSULIN
24
34
INSULIN PUMP
26
SENSOR
16
SENSOR SIGNAL
U_{COMP}
COMPENSATED INSULIN DELIVERY COMMAND
522
POST-CONTROLLER LEAD/LAG COMPENSATOR
FILTER & CALIBRATION
U_{PID}
INSULIN DELIVERY COMMAND
12
K_p
K_I
K_D
452
$\int dx$
DERIVATIVE FILTER
PRESENT BLOOD GLUCOSE ESTIMATE G
$\frac{d}{dx}$
CORRECTION ALGORITHMS
G_E GLUCOSE LEVEL ERROR
DESIRED BASAL BLOOD GLUCOSE LEVEL G_B
PRESENT ADJUSTED BLOOD GLUCOSE ESTIMATE
454

FIG. 37

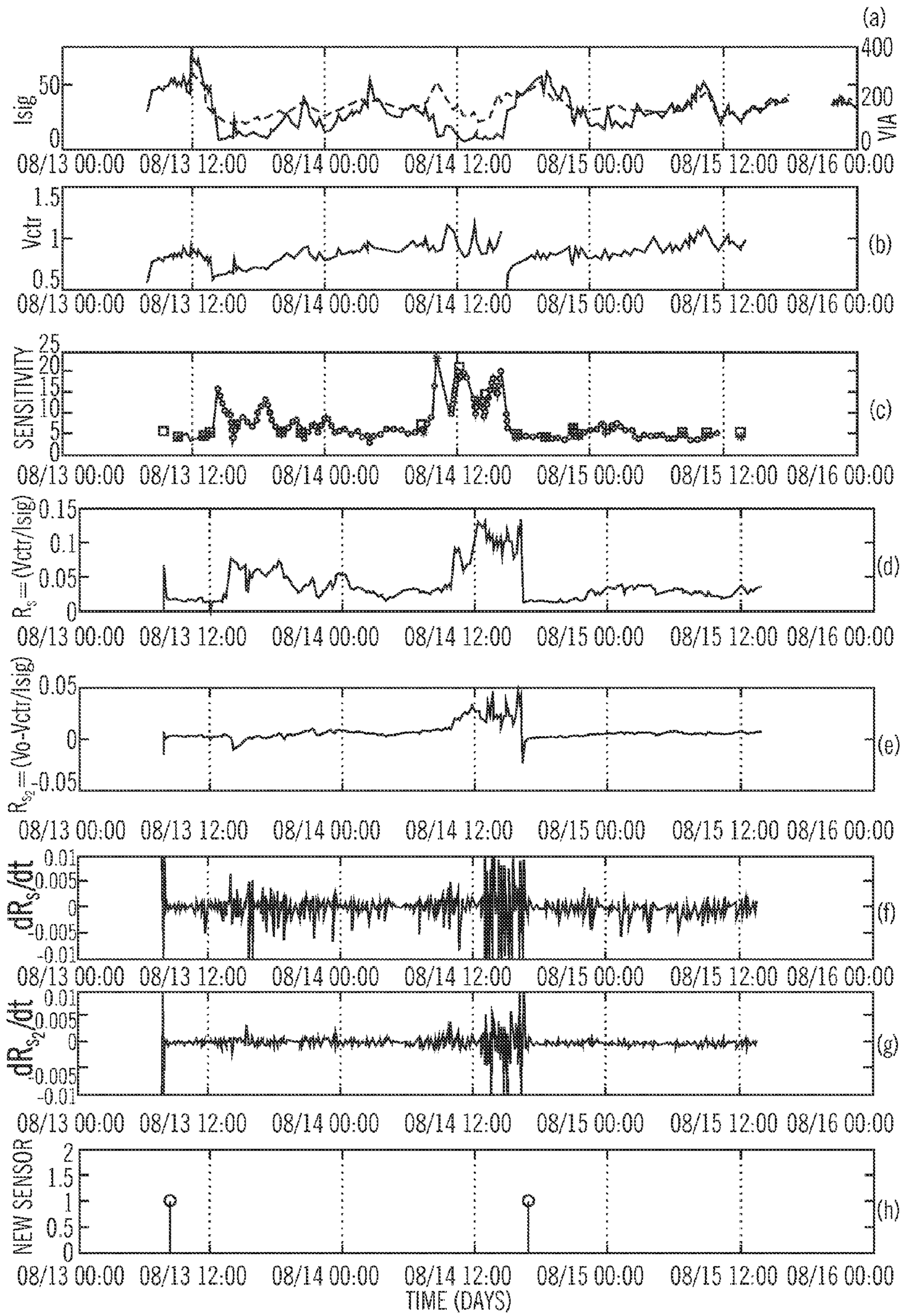
(a)
Isig
50
0
400
200
0
V/A
08/13 00:00 08/13 12:00 08/14 00:00 08/14 12:00 08/15 00:00 08/15 12:00 08/16 00:00
Vctr
1.5
1
0.5
(b)
SENSITIVITY
25
20
15
10
5
0
(c)
R_s=(Vctr/Isig)
0.15
0.1
0.05
0
(d)
R_{s_2}=(Vo-Vctr/Isig)
0.05
0
-0.05
(e)
dR_s/dt
0.01
0.005
0
-0.005
-0.01
(f)
dR_{s_2}/dt
0.01
0.005
0
-0.005
-0.01
(g)
NEW SENSOR
2
1.5
1
0.5
0
(h)
TIME (DAYS)

FIG. 38

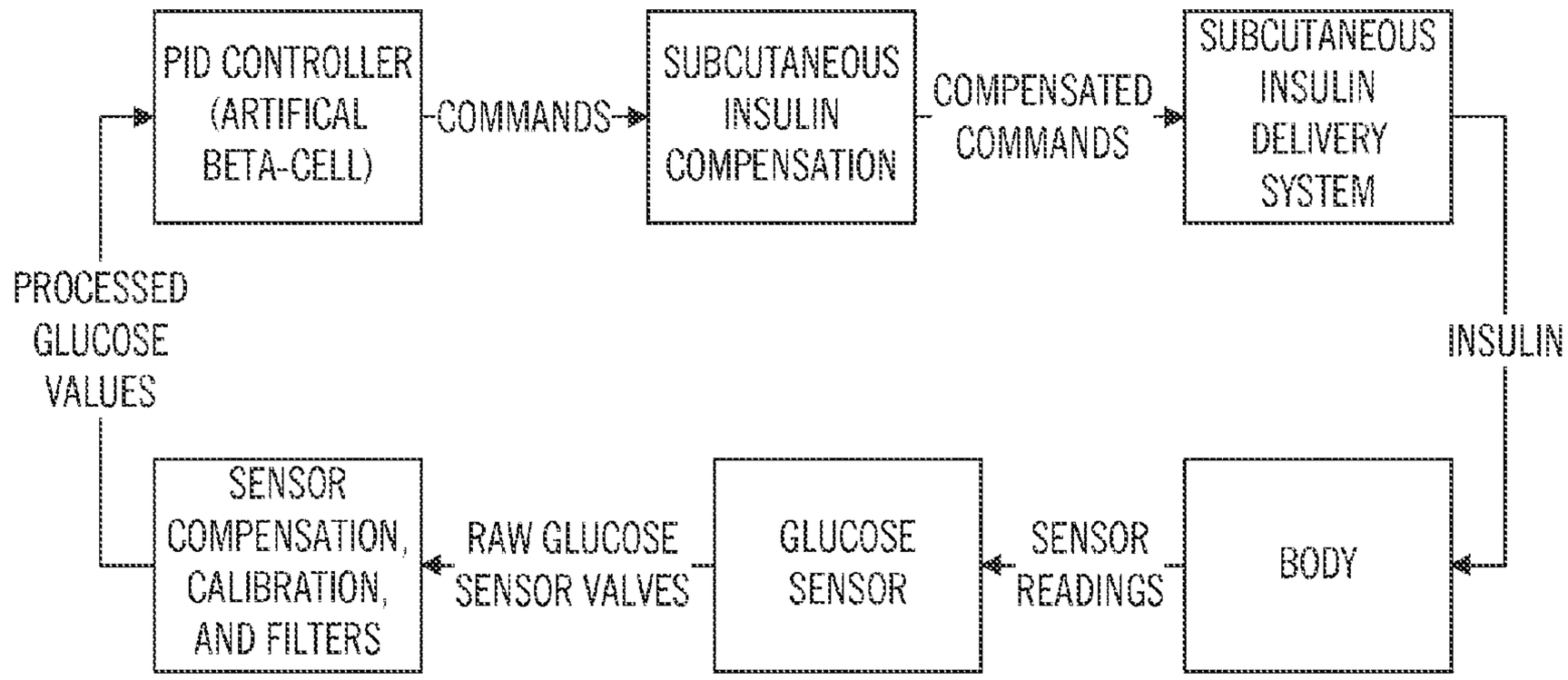

FIG. 39A

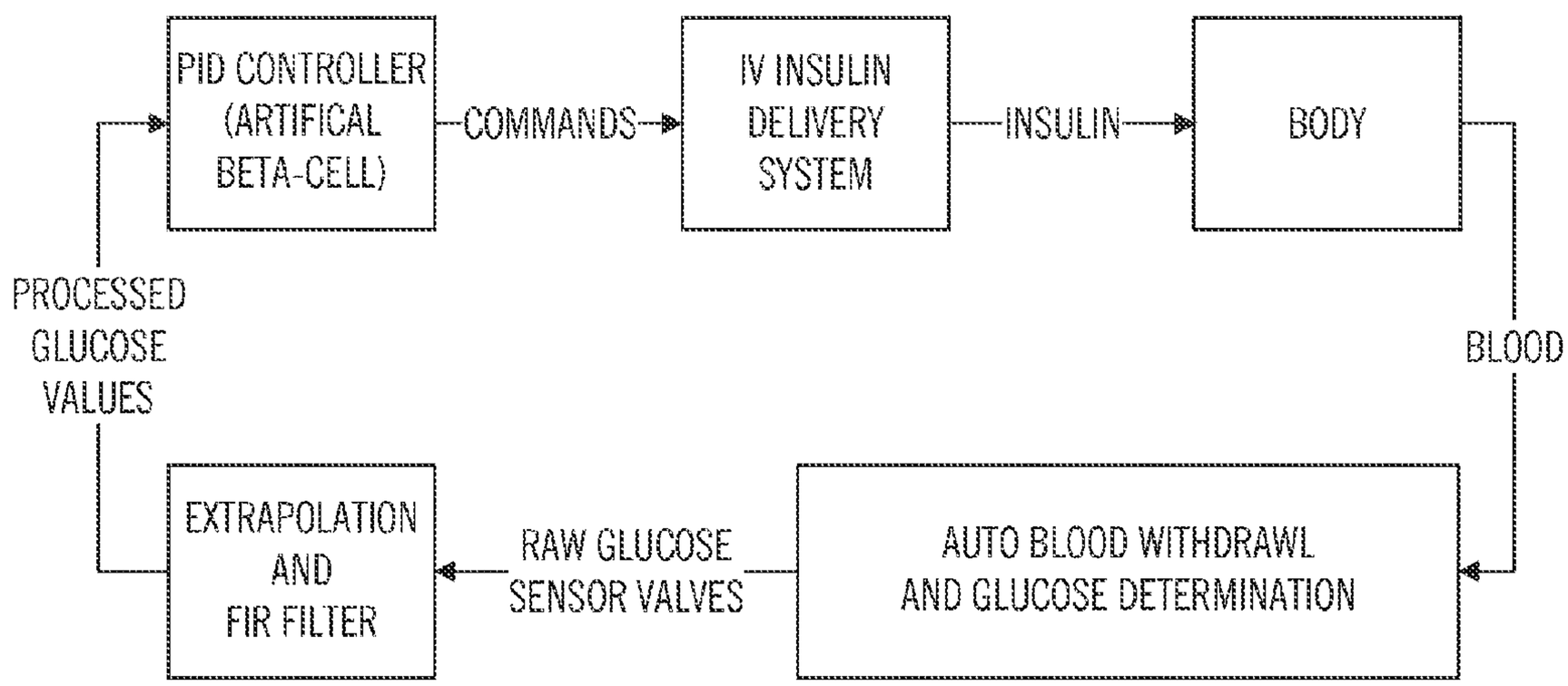

FIG. 39B

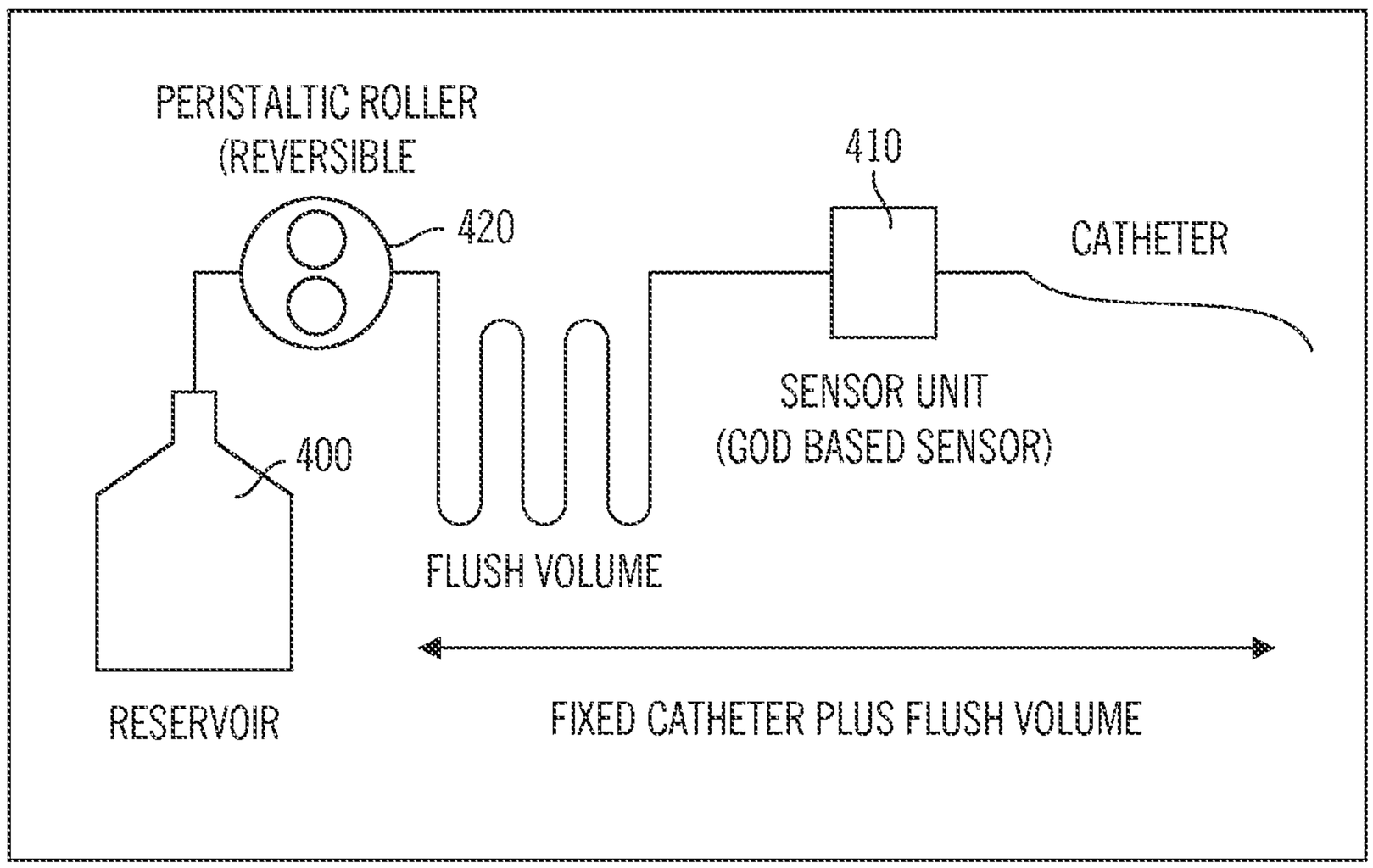
PERISTALTIC ROLLER
(REVERSIBLE
420
410
CATHETER
SENSOR UNIT
(GOD BASED SENSOR)
400
FLUSH VOLUME
RESERVOIR
FIXED CATHETER PLUS FLUSH VOLUME

FIG. 40

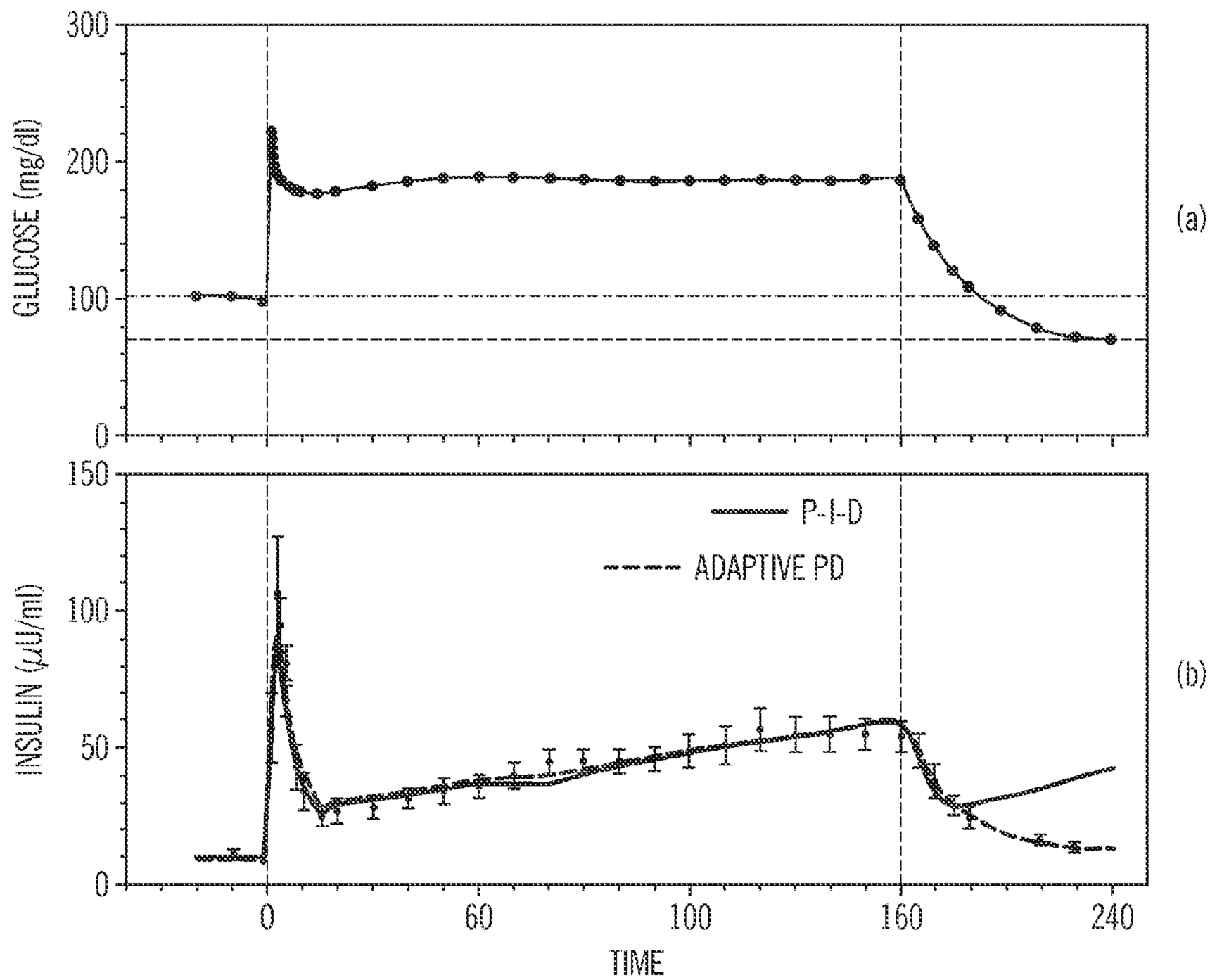
300
200
100
0
GLUCOSE (mg/dl)
(a)
150
100
50
0
INSULIN (μU/ml)
P-I-D
ADAPTIVE PD
(b)
0
60
100
160
240
TIME

FIG. 41

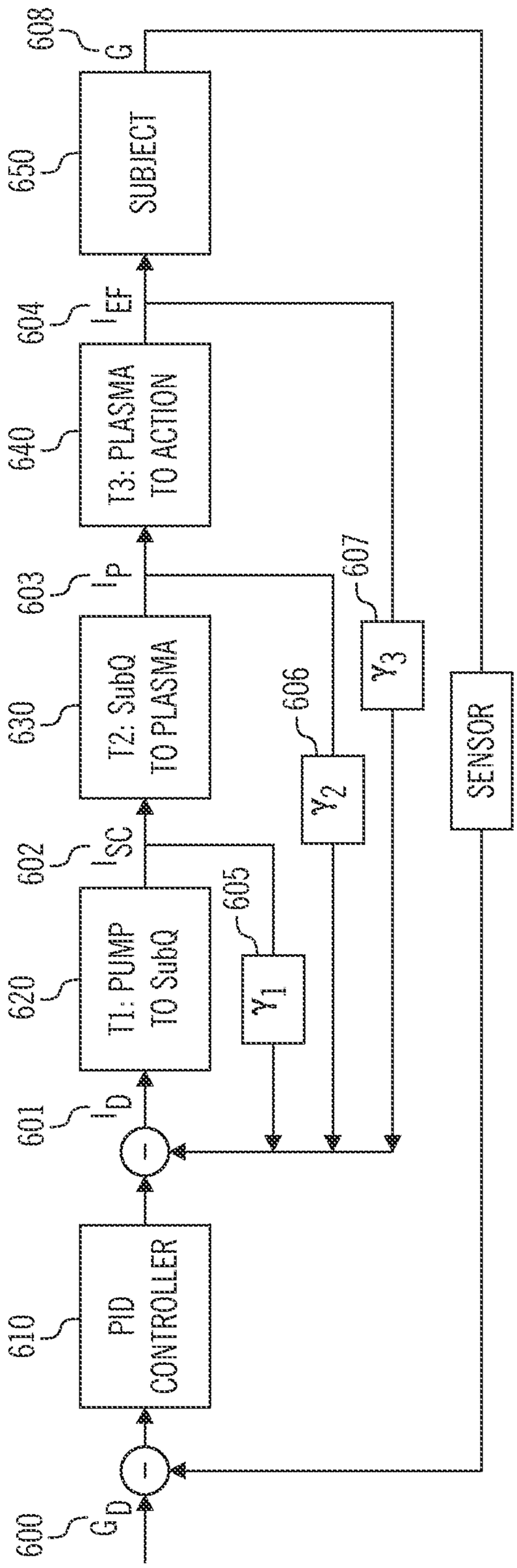
600
G_D
610
PID CONTROLLER
601
I_D
620
T1: PUMP TO SubQ
602
I_{SC}
630
T2: SubQ TO PLASMA
603
I_P
640
T3: PLASMA TO ACTION
604
I_{EF}
650
SUBJECT
608
G
605
γ_1
606
γ_2
607
γ_3
SENSOR

FIG. 42

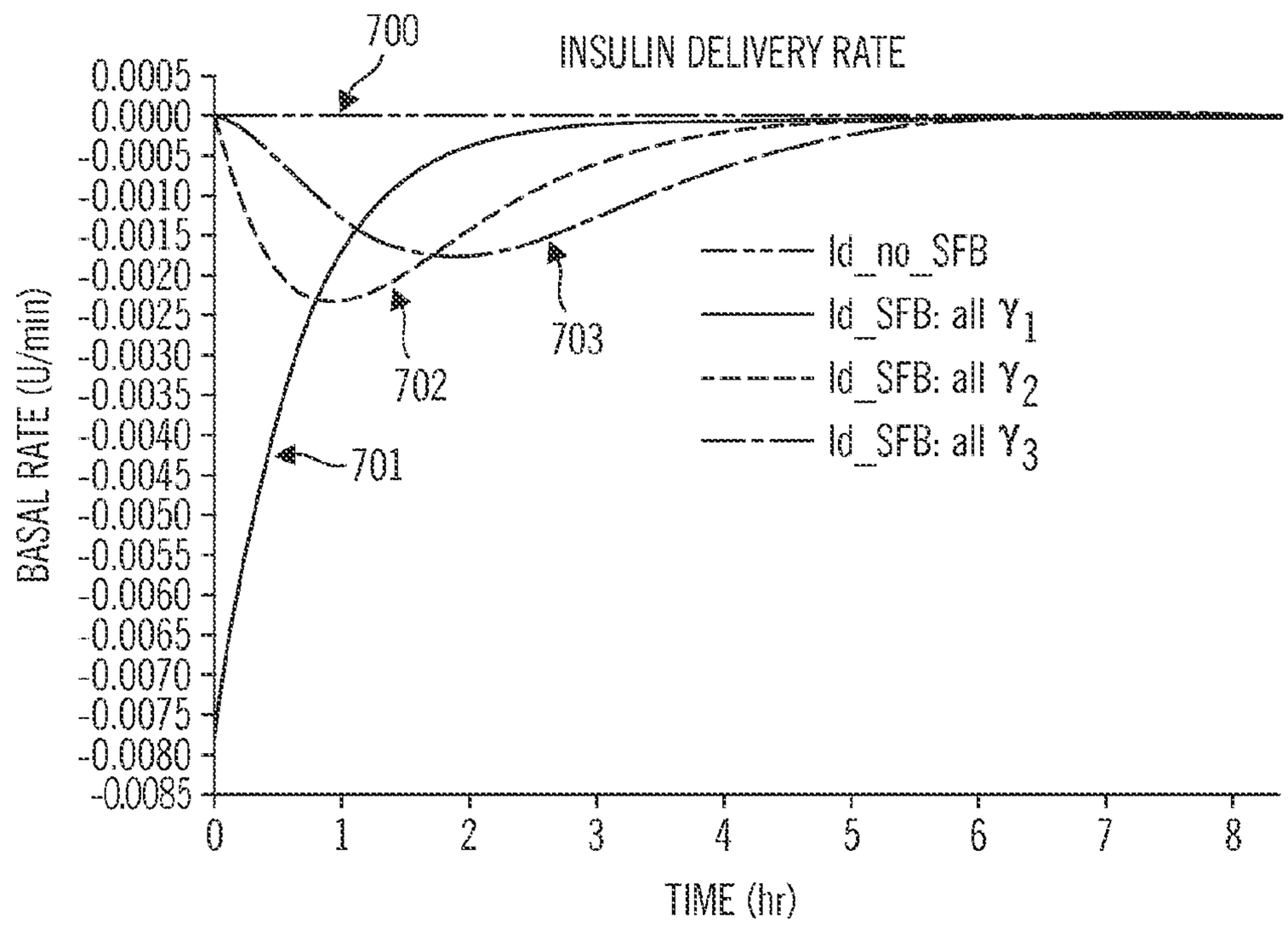
700
INSULIN DELIVERY RATE
BASAL RATE (U/min)
0.0005
0.0000
-0.0005
-0.0010
-0.0015
-0.0020
-0.0025
-0.0030
-0.0035
-0.0040
-0.0045
-0.0050
-0.0055
-0.0060
-0.0065
-0.0070
-0.0075
-0.0080
-0.0085
0
1
2
3
4
5
6
7
8
TIME (hr)
701
702
703
Id_no_SFB
Id_SFB: all Y1
Id_SFB: all Y2
Id_SFB: all Y3

FIG. 43

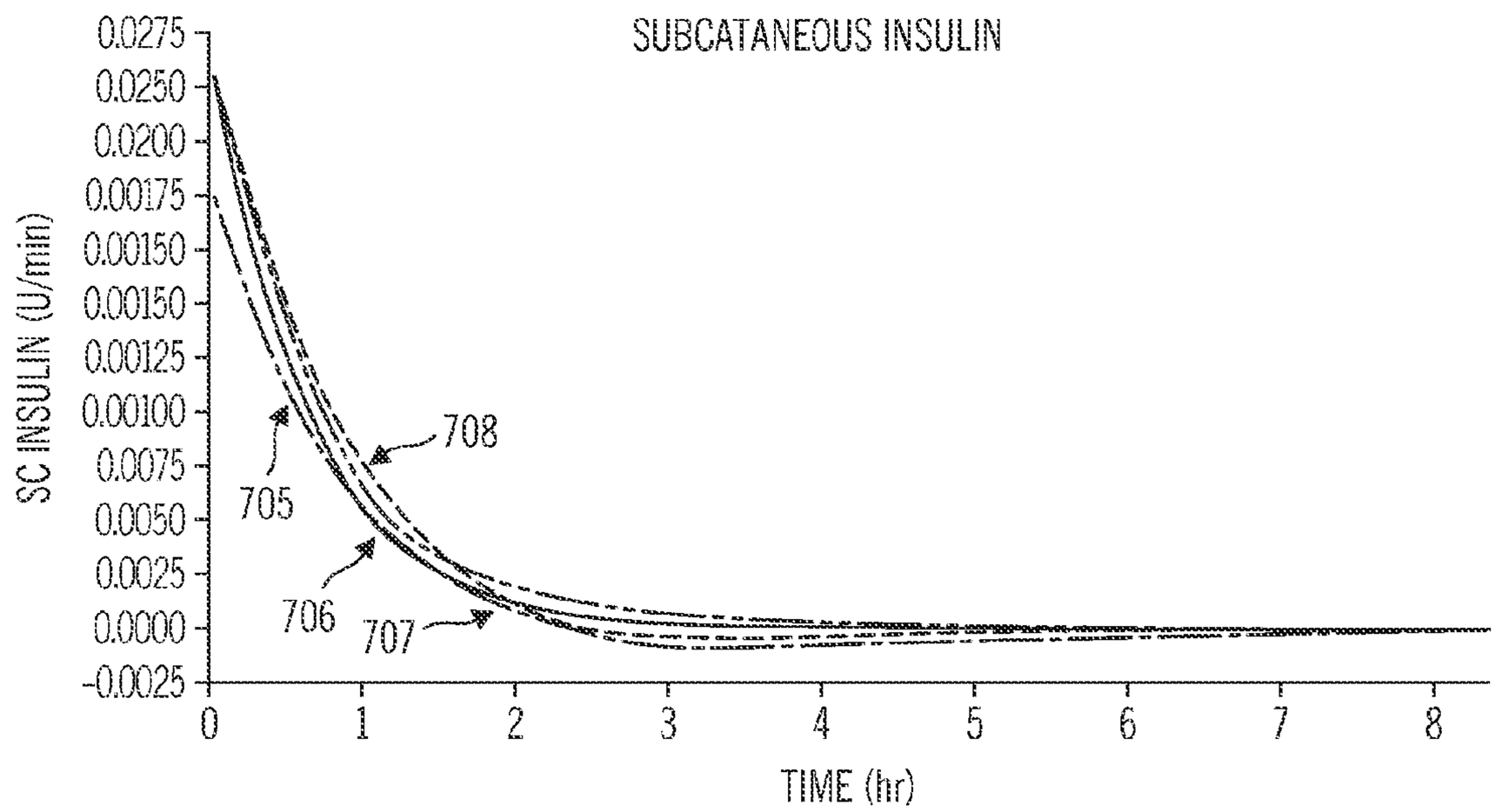
SUBCATANEOUS INSULIN
SC INSULIN (U/min)
0.0275
0.0250
0.0200
0.00175
0.00150
0.00150
0.00125
0.00100
0.0075
0.0050
0.0025
0.0000
-0.0025
0
1
2
3
4
5
6
7
8
TIME (hr)
705
706
707
708

FIG. 44

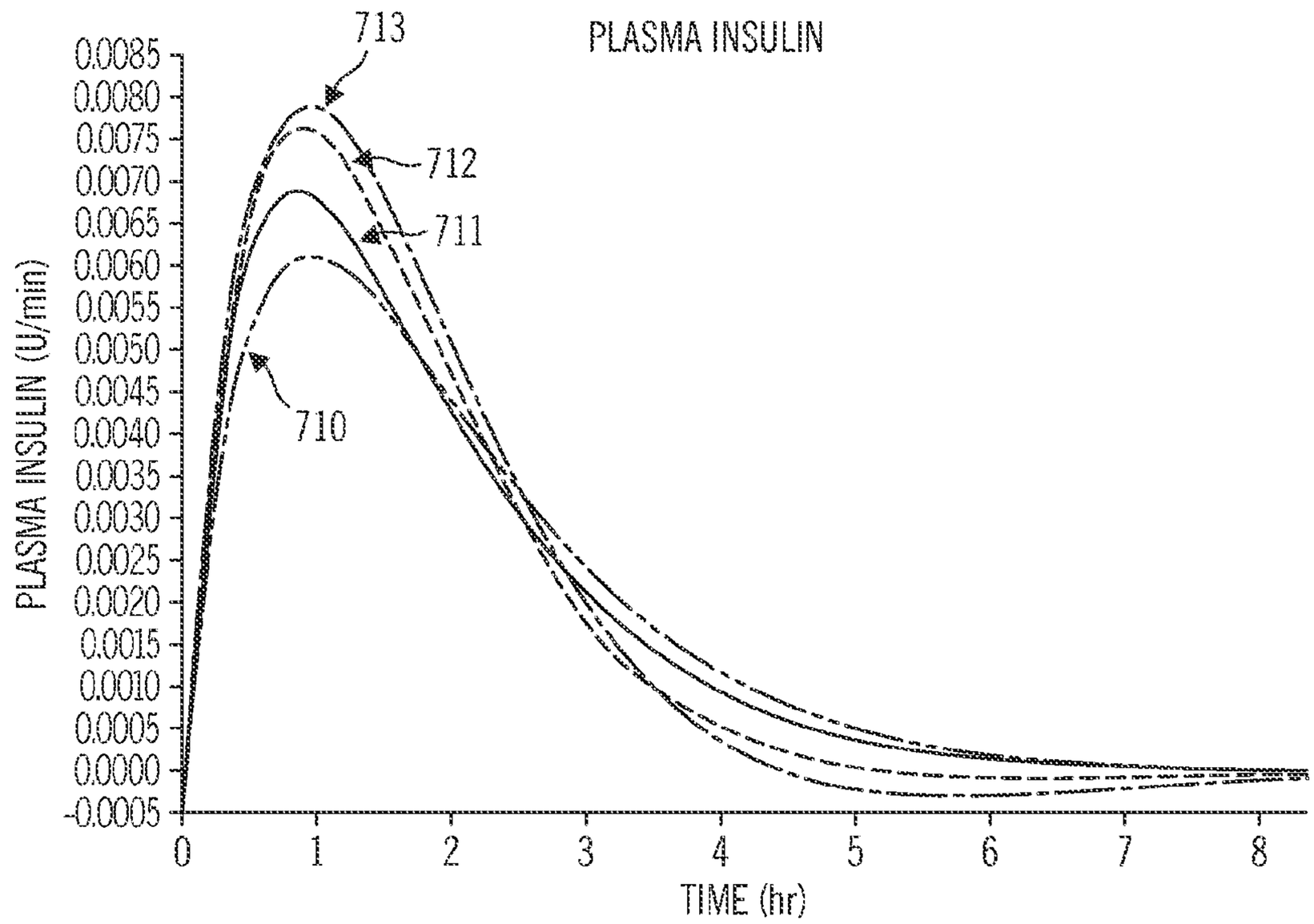
PLASMA INSULIN
713
712
711
710
PLASMA INSULIN (U/min)
0.0085
0.0080
0.0075
0.0070
0.0065
0.0060
0.0055
0.0050
0.0045
0.0040
0.0035
0.0030
0.0025
0.0020
0.0015
0.0010
0.0005
0.0000
-0.0005
0
1
2
3
4
5
6
7
8
TIME (hr)

FIG. 45

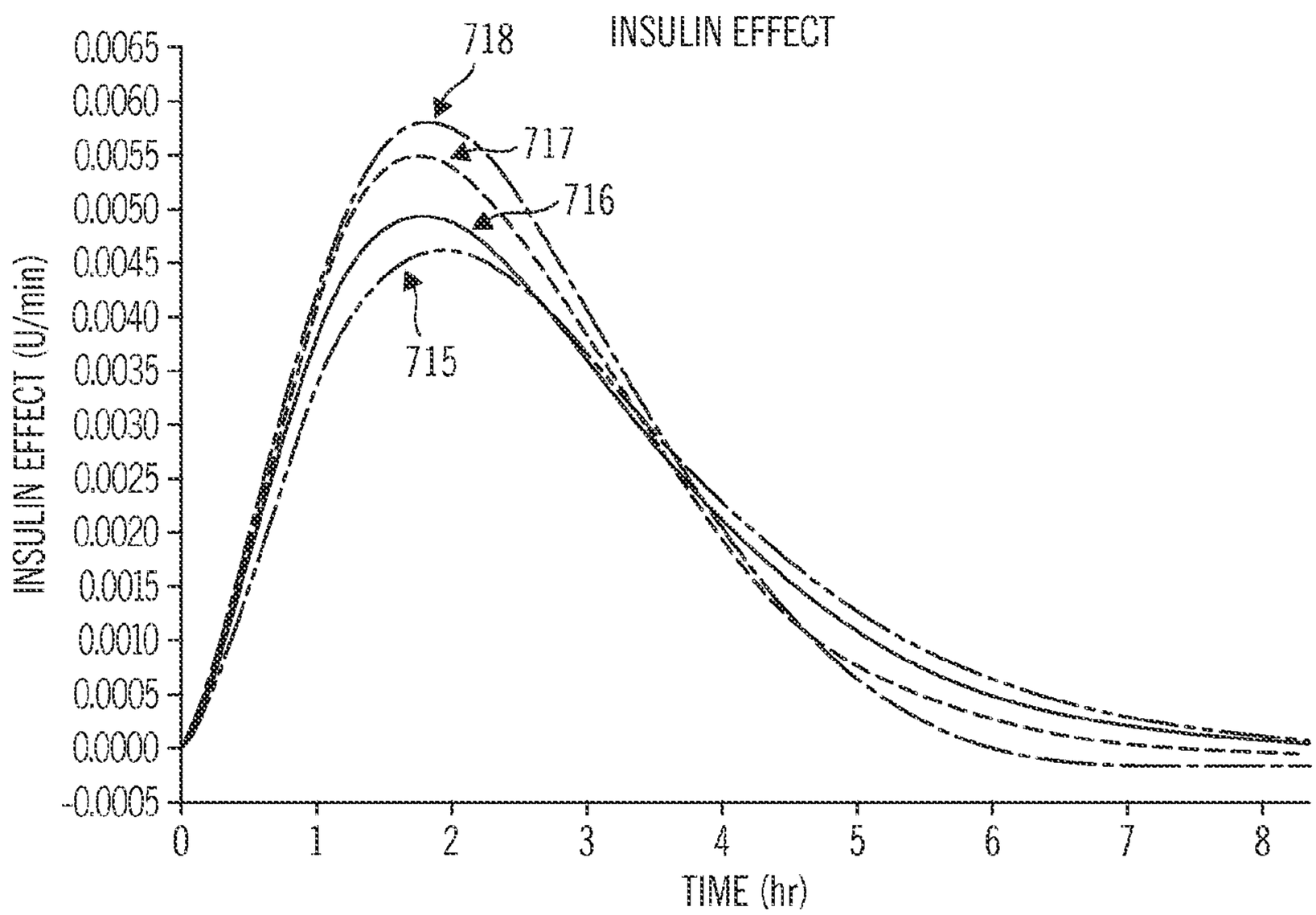
INSULIN EFFECT
718
717
716
715
INSULIN EFFECT (U/min)
0.0065
0.0060
0.0055
0.0050
0.0045
0.0040
0.0035
0.0030
0.0025
0.0020
0.0015
0.0010
0.0005
0.0000
-0.0005
0
1
2
3
4
5
6
7
8
TIME (hr)

FIG. 46

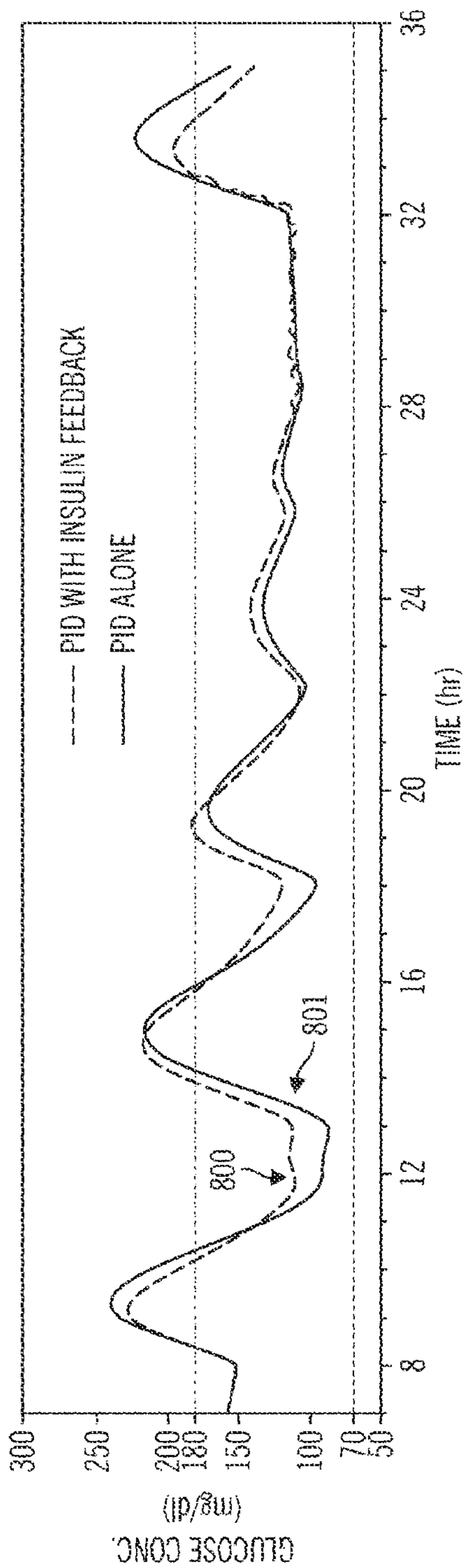
PID WITH INSULIN FEEDBACK
PID ALONE
GLUCOSE CONC.
(mg/dl)
300
250
200
180
150
100
70
50
800
801
8
12
16
20
24
28
32
36
TIME (hr)

FIG. 47

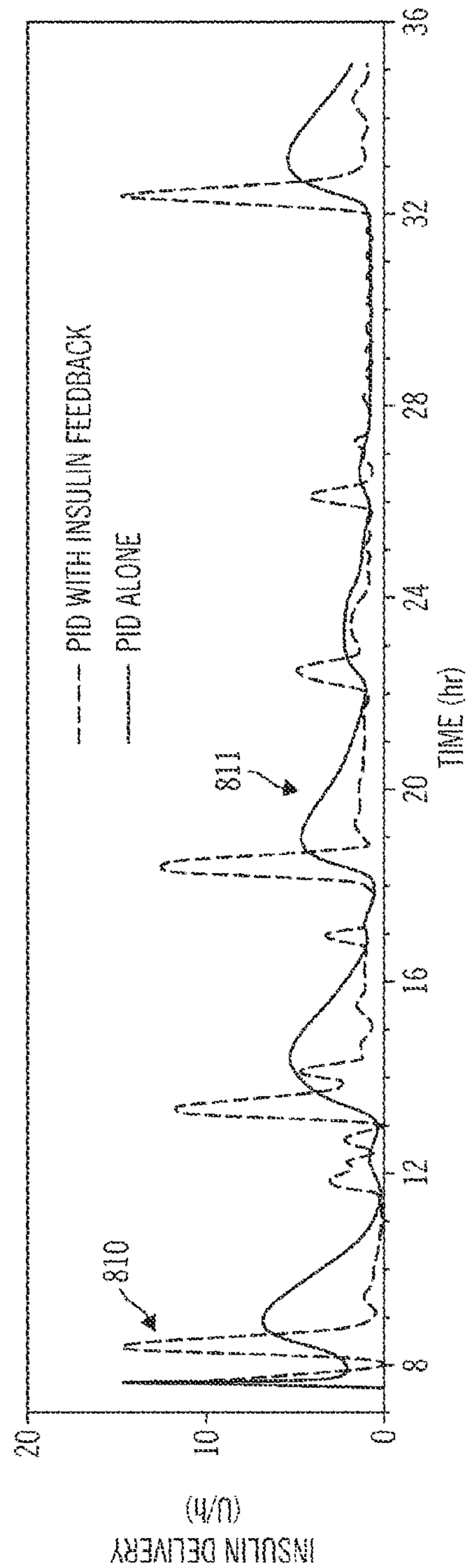
PID WITH INSULIN FEEDBACK
PID ALONE
INSULIN DELIVERY
(U/h)
20
10
0
810
811
8
12
16
20
24
28
32
36
TIME (hr)

FIG. 48

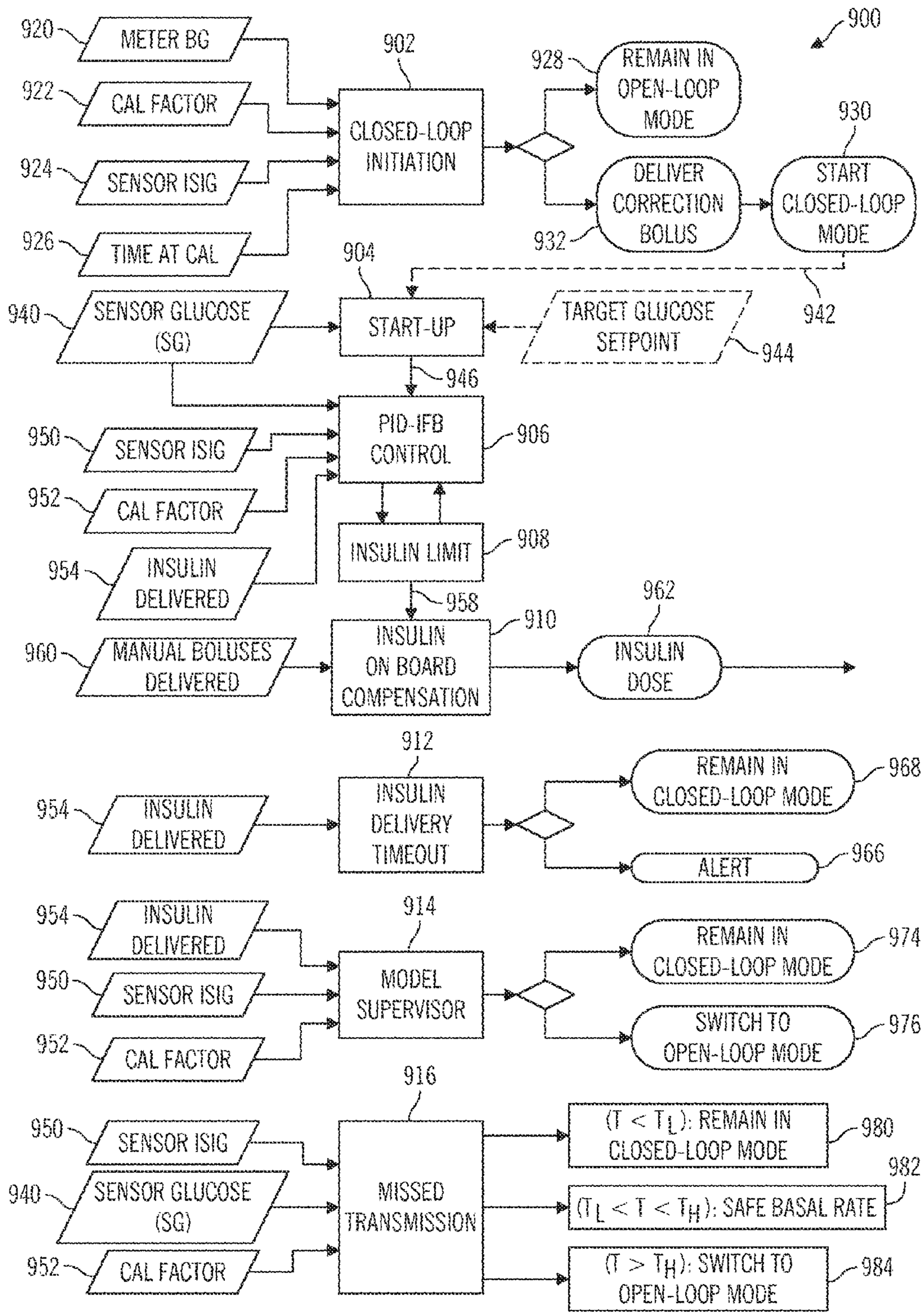
900
920
METER BG
922
CAL FACTOR
924
SENSOR ISIG
926
TIME AT CAL
902
CLOSED-LOOP INITIATION
928
REMAIN IN OPEN-LOOP MODE
930
DELIVER CORRECTION BOLUS
932
START CLOSED-LOOP MODE
904
942
940
SENSOR GLUCOSE (SG)
START-UP
TARGET GLUCOSE SETPOINT
944
946
PID-IFB CONTROL
906
950
SENSOR ISIG
952
CAL FACTOR
954
INSULIN DELIVERED
INSULIN LIMIT
908
958
910
962
960
MANUAL BOLUSES DELIVERED
INSULIN ON BOARD COMPENSATION
INSULIN DOSE
912
954
INSULIN DELIVERED
INSULIN DELIVERY TIMEOUT
REMAIN IN CLOSED-LOOP MODE
968
ALERT
966
954
INSULIN DELIVERED
914
950
SENSOR ISIG
952
CAL FACTOR
MODEL SUPERVISOR
REMAIN IN CLOSED-LOOP MODE
974
SWITCH TO OPEN-LOOP MODE
976
916
950
SENSOR ISIG
940
SENSOR GLUCOSE (SG)
952
CAL FACTOR
MISSED TRANSMISSION
(T < TL): REMAIN IN CLOSED-LOOP MODE
980
982
(TL < T < TH): SAFE BASAL RATE
(T > TH): SWITCH TO OPEN-LOOP MODE
984

FIG. 49

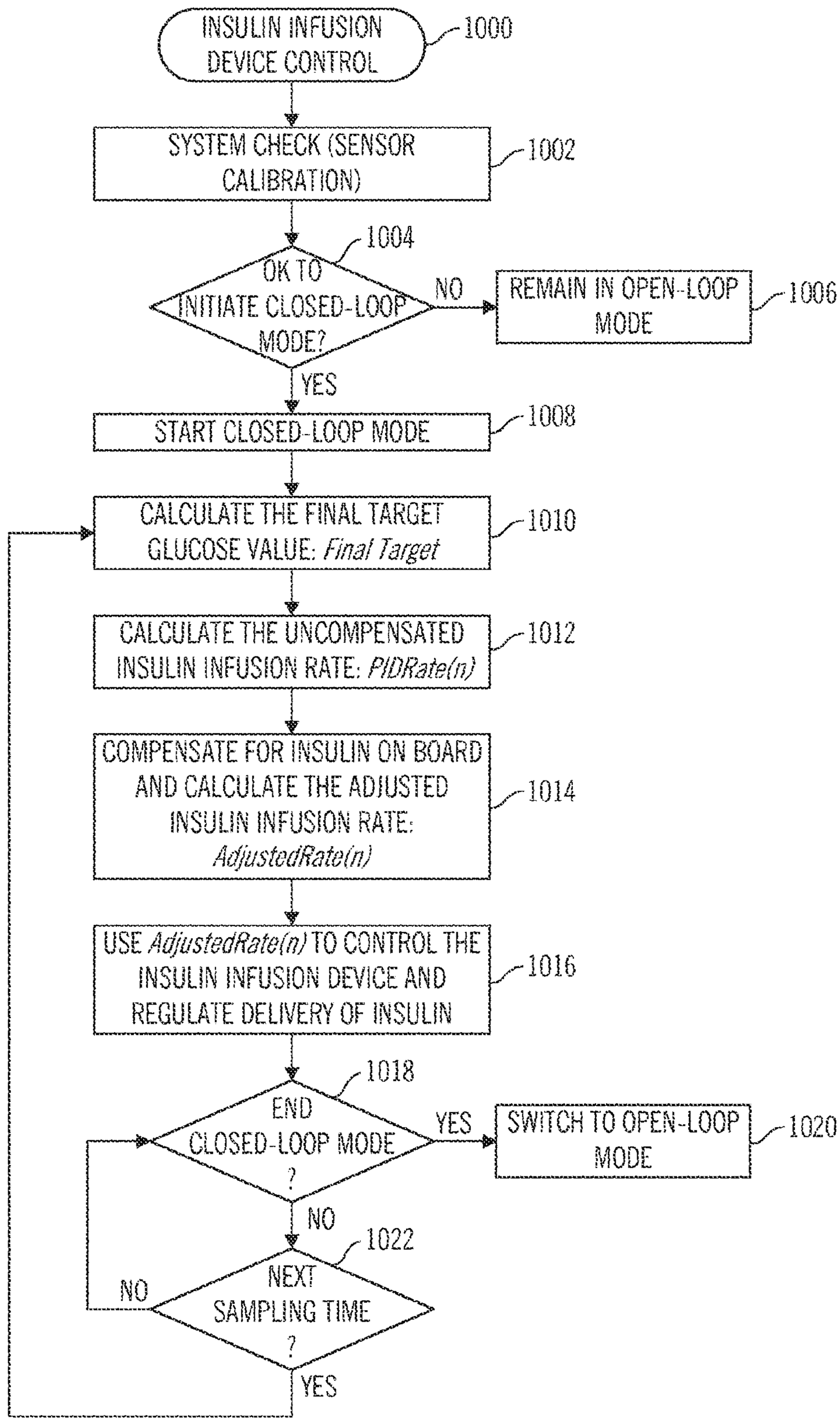
INSULIN INFUSION DEVICE CONTROL
1000
SYSTEM CHECK (SENSOR CALIBRATION)
1002
1004
OK TO INITIATE CLOSED-LOOP MODE?
NO
REMAIN IN OPEN-LOOP MODE
1006
YES
START CLOSED-LOOP MODE
1008
CALCULATE THE FINAL TARGET GLUCOSE VALUE: Final Target
1010
CALCULATE THE UNCOMPENSATED INSULIN INFUSION RATE: PIDRate(n)
1012
COMPENSATE FOR INSULIN ON BOARD AND CALCULATE THE ADJUSTED INSULIN INFUSION RATE: AdjustedRate(n)
1014
USE AdjustedRate(n) TO CONTROL THE INSULIN INFUSION DEVICE AND REGULATE DELIVERY OF INSULIN
1016
1018
END CLOSED-LOOP MODE ?
YES
SWITCH TO OPEN-LOOP MODE
1020
NO
1022
NEXT SAMPLING TIME ?
NO
YES

FIG. 50

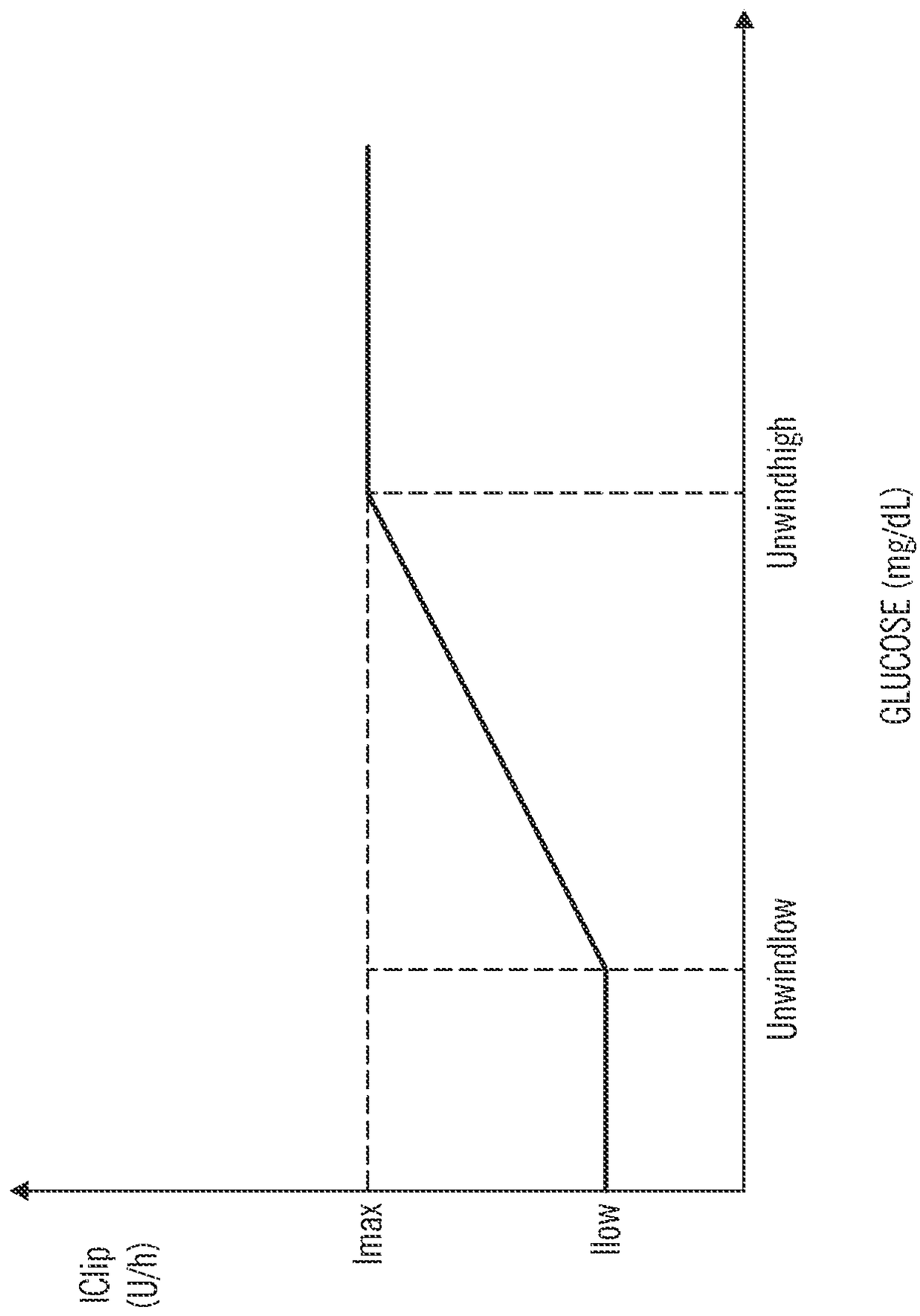

FIG. 51

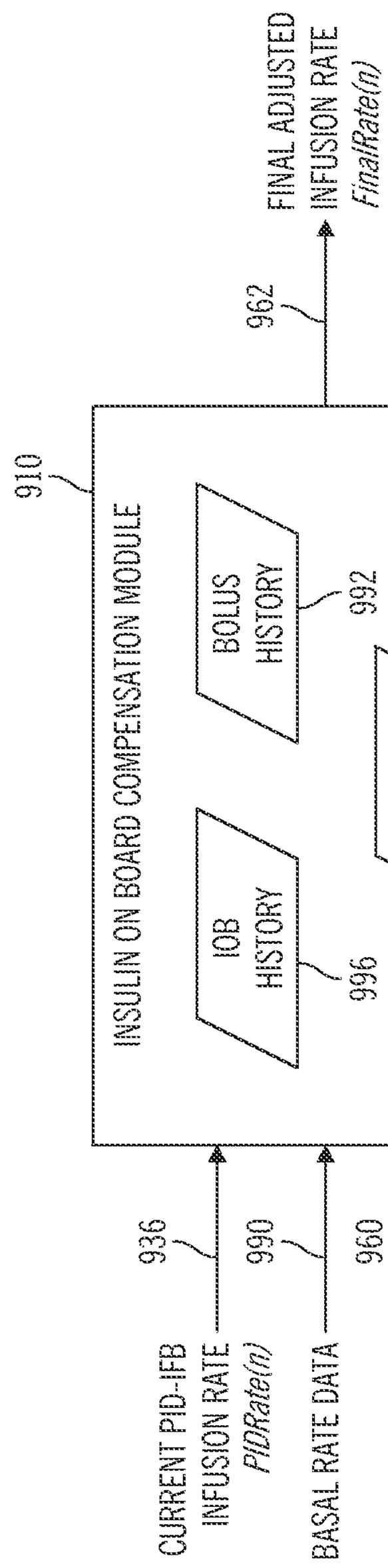
FINAL ADJUSTED INFUSION RATE FinalRate(n)
962
910
INSULIN ON BOARD COMPENSATION MODULE
BOLUS HISTORY
992
CONSTANTS
994
IOB HISTORY
996
936
990
960
CURRENT PID-IFB INFUSION RATE PIDRate(n)
BASAL RATE DATA
MANUAL BOLUSES DELIVERED

FIG. 52

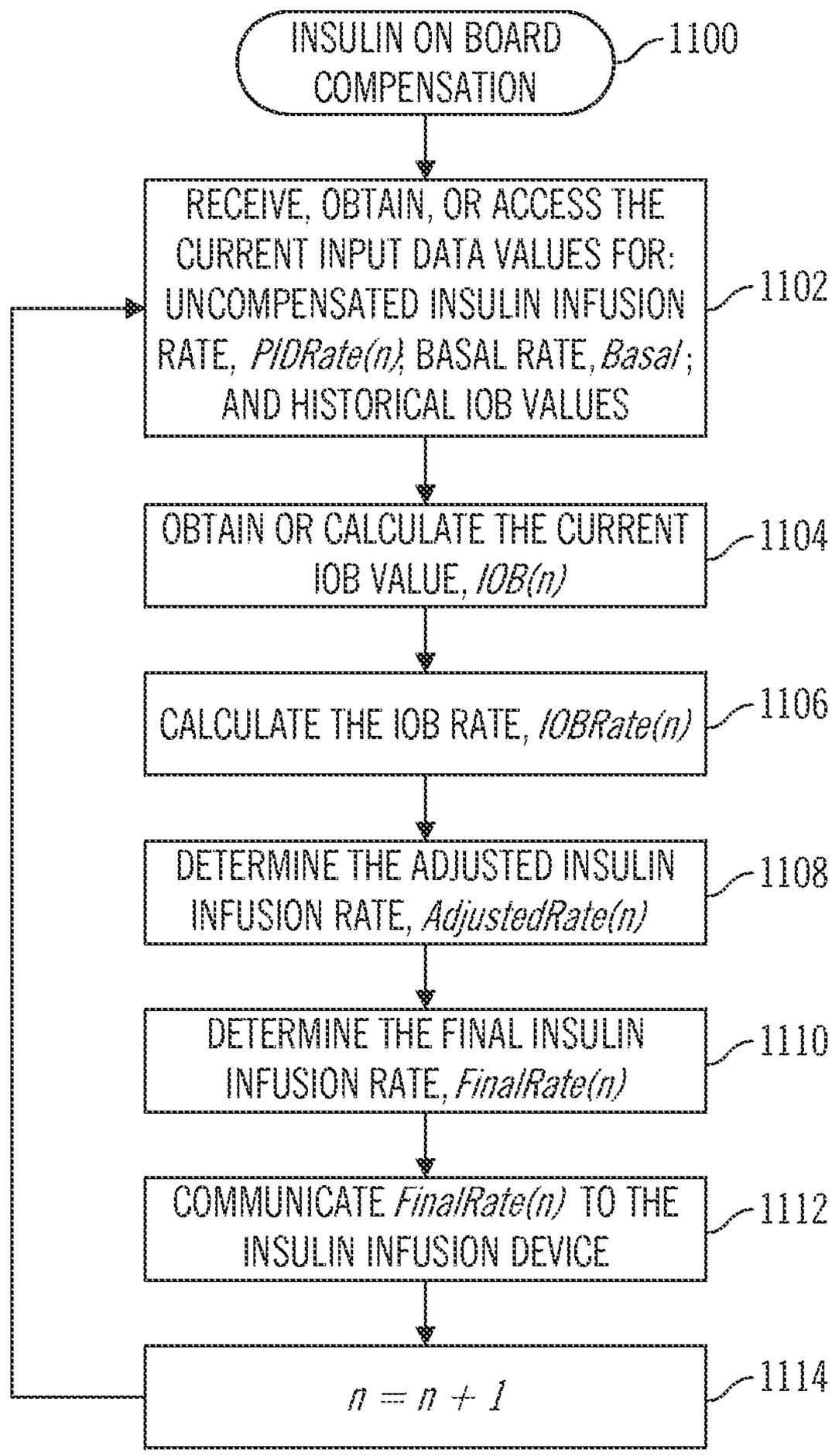
INSULIN ON BOARD COMPENSATION
1100
RECEIVE, OBTAIN, OR ACCESS THE CURRENT INPUT DATA VALUES FOR: UNCOMPENSATED INSULIN INFUSION RATE, PIDRate(n); BASAL RATE, Basal; AND HISTORICAL IOB VALUES
1102
OBTAIN OR CALCULATE THE CURRENT IOB VALUE, IOB(n)
1104
CALCULATE THE IOB RATE, IOBRate(n)
1106
DETERMINE THE ADJUSTED INSULIN INFUSION RATE, AdjustedRate(n)
1108
DETERMINE THE FINAL INSULIN INFUSION RATE, FinalRate(n)
1110
COMMUNICATE FinalRate(n) TO THE INSULIN INFUSION DEVICE
1112
n = n + 1
1114

FIG. 53

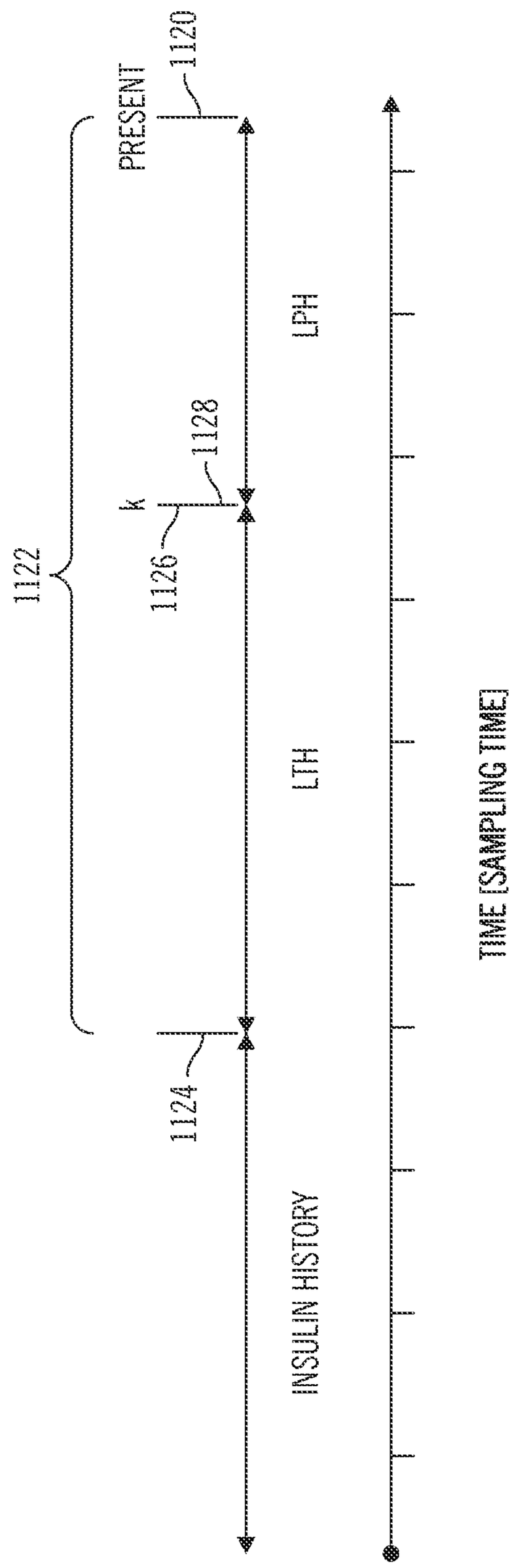
PRESENT
1120
1122
k
1126
1128
1124
LPH
LTH
INSULIN HISTORY
TIME [SAMPLING TIME]

FIG. 54

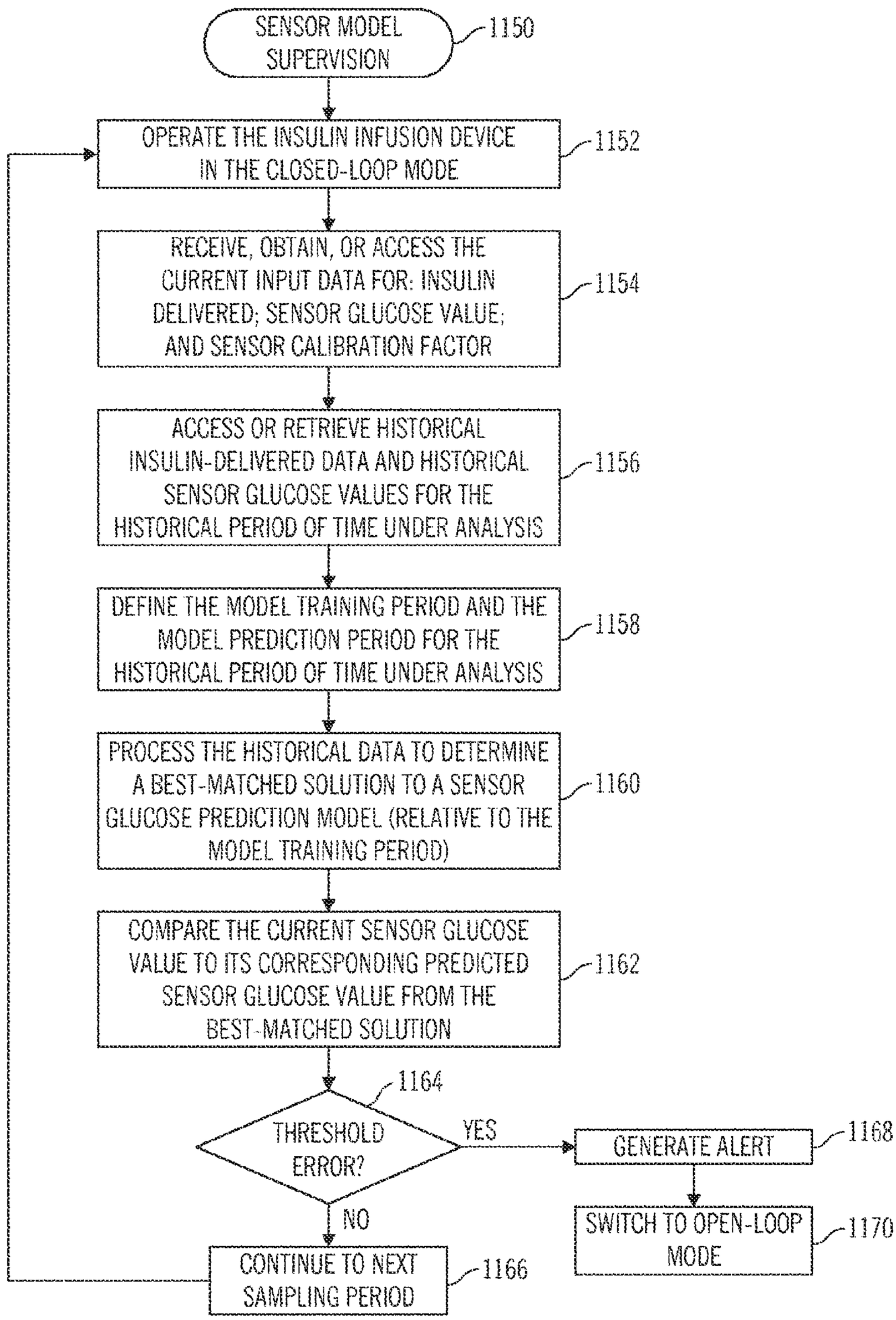
SENSOR MODEL SUPERVISION
1150
OPERATE THE INSULIN INFUSION DEVICE IN THE CLOSED-LOOP MODE
1152
RECEIVE, OBTAIN, OR ACCESS THE CURRENT INPUT DATA FOR: INSULIN DELIVERED; SENSOR GLUCOSE VALUE; AND SENSOR CALIBRATION FACTOR
1154
ACCESS OR RETRIEVE HISTORICAL INSULIN-DELIVERED DATA AND HISTORICAL SENSOR GLUCOSE VALUES FOR THE HISTORICAL PERIOD OF TIME UNDER ANALYSIS
1156
DEFINE THE MODEL TRAINING PERIOD AND THE MODEL PREDICTION PERIOD FOR THE HISTORICAL PERIOD OF TIME UNDER ANALYSIS
1158
PROCESS THE HISTORICAL DATA TO DETERMINE A BEST-MATCHED SOLUTION TO A SENSOR GLUCOSE PREDICTION MODEL (RELATIVE TO THE MODEL TRAINING PERIOD)
1160
COMPARE THE CURRENT SENSOR GLUCOSE VALUE TO ITS CORRESPONDING PREDICTED SENSOR GLUCOSE VALUE FROM THE BEST-MATCHED SOLUTION
1162
1164
THRESHOLD ERROR?
YES
GENERATE ALERT
1168
SWITCH TO OPEN-LOOP MODE
1170
NO
CONTINUE TO NEXT SAMPLING PERIOD
1166

FIG. 55

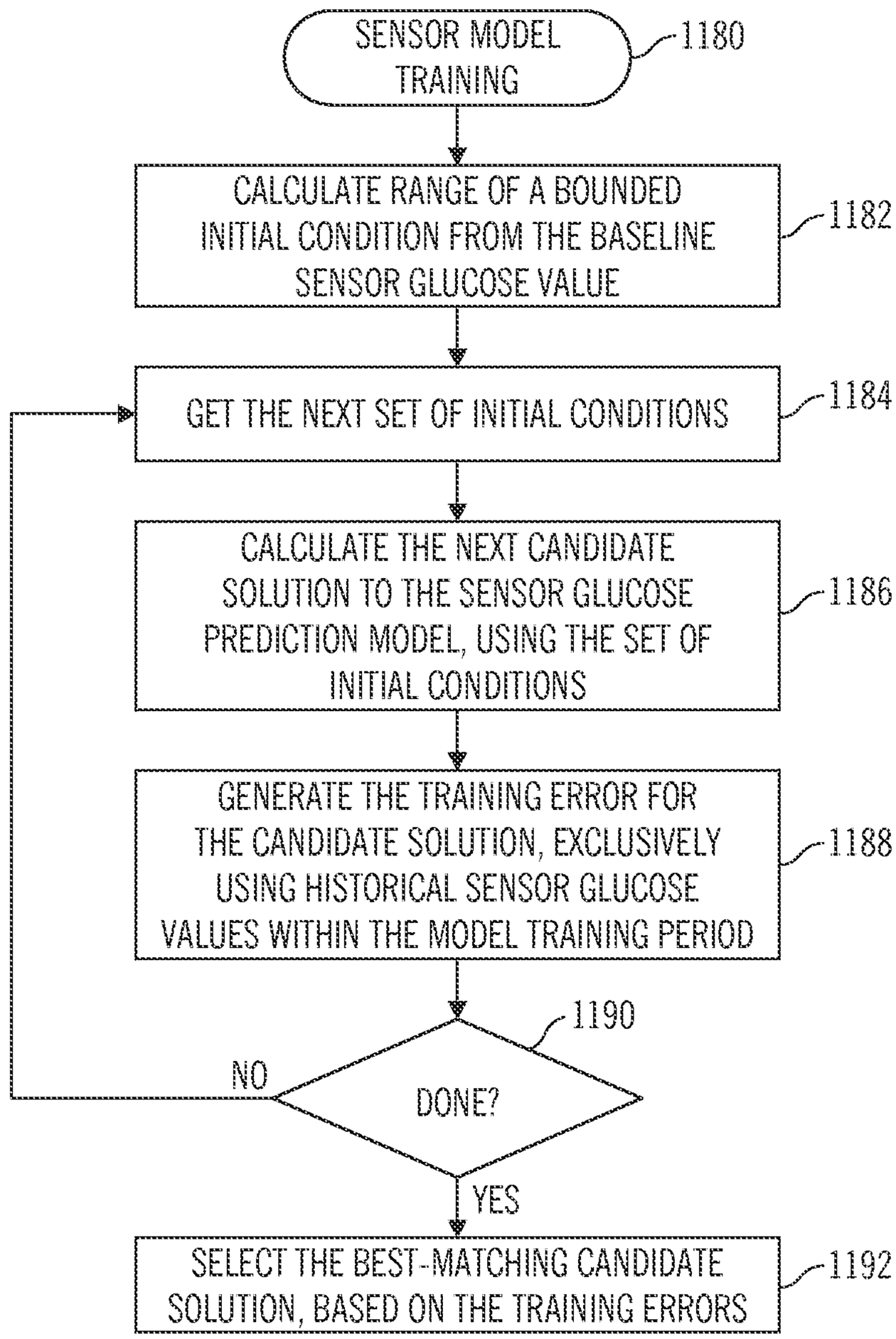
SENSOR MODEL TRAINING
1180
CALCULATE RANGE OF A BOUNDED INITIAL CONDITION FROM THE BASELINE SENSOR GLUCOSE VALUE
1182
GET THE NEXT SET OF INITIAL CONDITIONS
1184
CALCULATE THE NEXT CANDIDATE SOLUTION TO THE SENSOR GLUCOSE PREDICTION MODEL, USING THE SET OF INITIAL CONDITIONS
1186
GENERATE THE TRAINING ERROR FOR THE CANDIDATE SOLUTION, EXCLUSIVELY USING HISTORICAL SENSOR GLUCOSE VALUES WITHIN THE MODEL TRAINING PERIOD
1188
1190
NO
DONE?
YES
SELECT THE BEST-MATCHING CANDIDATE SOLUTION, BASED ON THE TRAINING ERRORS
1192

FIG. 56

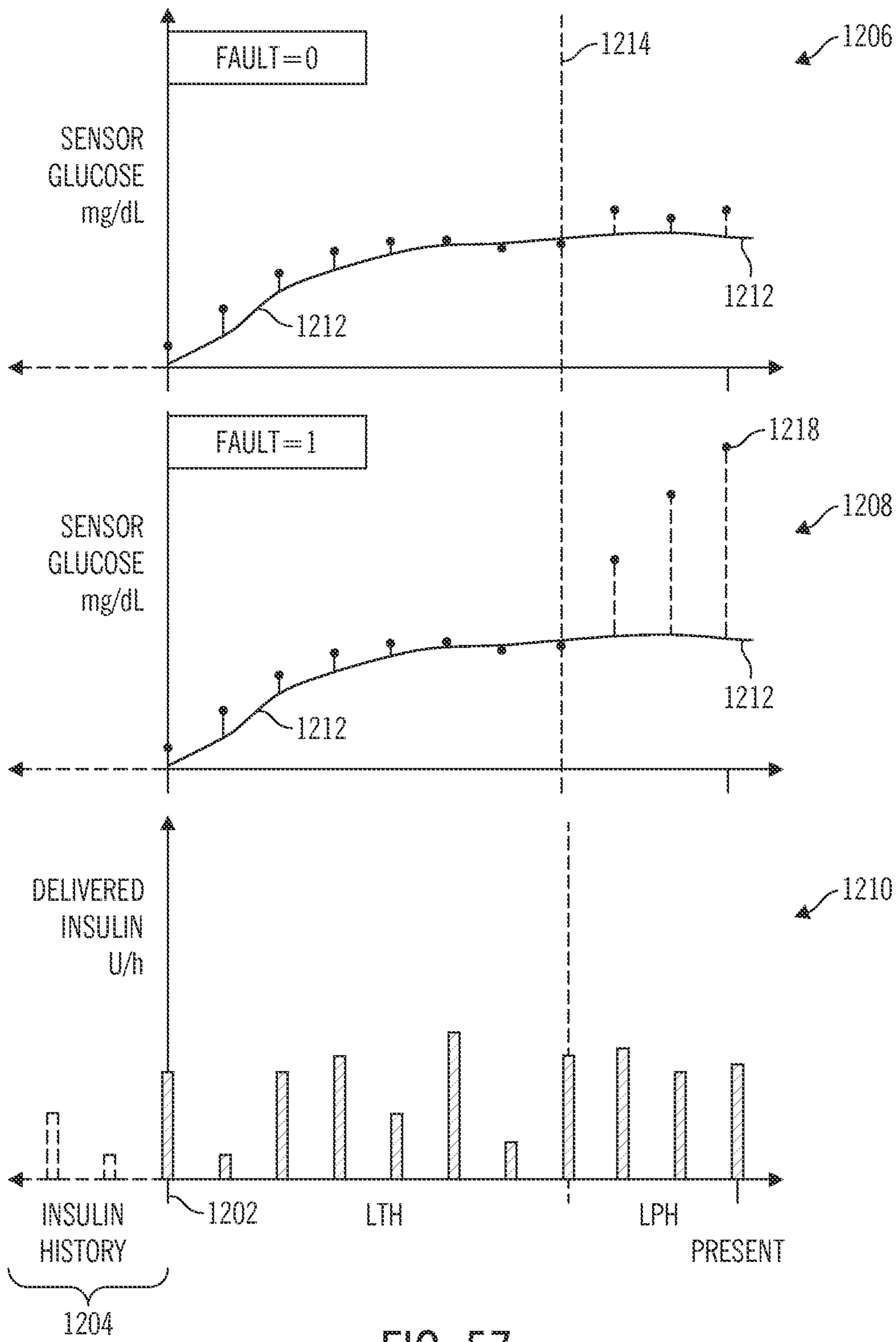
FAULT=0
1214
1206
SENSOR
GLUCOSE
mg/dL
1212
1212
FAULT=1
1218
1208
SENSOR
GLUCOSE
mg/dL
1212
1212
DELIVERED
INSULIN
U/h
1210
INSULIN
HISTORY
1202
LTH
LPH
PRESENT
1204

FIG. 57

INSULIN ON BOARD COMPENSATION FOR A CLOSED-LOOP INSULIN INFUSION SYSTEM

CROSS-REFERENCE TO RELATED APPLICATIONS

This application claims the benefit of U.S. provisional patent application Ser. No. 61/694,950, filed Aug. 30, 2012 (titled "Closed Loop System"). This application also claims the benefit of U.S. provisional patent application Ser. No. 61/694,961, filed Aug. 30, 2012 (titled "Closed Loop Mobile System"). This application also claims the benefit of U.S. provisional patent application Ser. No. 61/812,874, filed Apr. 17, 2013 (titled "Closed Loop System"). The content of the provisional applications cited above is incorporated by reference herein.

TECHNICAL FIELD

Embodiments of the subject matter described herein relate generally to drug delivery systems and more specifically to systems for controlling the infusion rate of insulin based on state variable feedback.

BACKGROUND

The pancreas of a normal healthy person produces and releases insulin into the blood stream in response to elevated blood plasma glucose levels. Beta cells (β-cells), which reside in the pancreas, produce and secrete the insulin into the blood stream, as it is needed. If β-cells become incapacitated or die, a condition known as Type I diabetes mellitus (or in some cases if β-cells produce insufficient quantities of insulin, Type II diabetes), then insulin must be provided to the body from another source.

Traditionally, since insulin cannot be taken orally, insulin has been injected with a syringe. More recently, use of infusion pump therapy has been increasing, especially for delivering insulin for diabetics. For example, external infusion pumps are worn on a belt, in a pocket, or the like, and deliver insulin into the body via an infusion tube with a percutaneous needle or a cannula placed in the subcutaneous tissue. As of 1995, less than 5% of Type I diabetics in the United States were using infusion pump therapy. Presently, over 7% of the more than 900,000 Type I diabetics in the United States are using infusion pump therapy, and the percentage of Type I diabetics that use an infusion pump is growing at an absolute rate of over 2% each year. Moreover, the number of Type I diabetics is growing at 3% or more per year. In addition, growing numbers of insulin-using Type II diabetics are also using infusion pumps. Physicians have recognized that continuous infusion provides greater control of a diabetic's condition, and are also increasingly prescribing it for patients. Although offering control, pump therapy can suffer from several complications that make use of traditional external infusion pumps less desirable for the user.

In insulin pumps, it is common to use fast acting insulin as opposed to the slower acting insulin that is used for injections, because pumps allow changing of insulin profiles. As insulin companies develop faster acting insulin, the faster acting insulin is often adopted quickly. However, current pumps are still limited by the speed of the insulin they are using.

BRIEF SUMMARY

A processor-implemented method is presented here. The method can be used to control an insulin infusion device for a

user. Certain embodiments of the method involve the operation of a processor architecture having at least one processor device to obtain a current insulin on board (IOB) value that represents an estimate of active insulin in the body of the user. The method continues by calculating, by the processor architecture, an IOB rate based at least in part on the obtained current IOB value. The method continues by determining, by the processor architecture, an adjusted insulin infusion rate based at least in part on the calculated IOB rate and an uncompensated insulin infusion rate. The processor architecture selects a final insulin infusion rate for the insulin infusion device, wherein either the determined adjusted insulin infusion rate, the uncompensated insulin infusion rate, or a current basal rate is selected as the final insulin infusion rate.

Also presented here is a processor-implemented method of controlling an insulin infusion device for a user. Certain embodiments of the method begin by generating a current IOB value that represents an estimate of active insulin in the body of the user. The method continues by calculating an IOB rate based at least in part on the generated current IOB value, obtaining an uncompensated insulin infusion rate, and determining an adjusted insulin infusion rate in accordance with the expression AdjustedRate(n)=max(0; PIDRate(n)−IOBRate(n)). The method continues by selecting a final insulin infusion rate in accordance with the expression

$$FinalRate(n) = \begin{cases} \max(\text{Basal}; AdjustedRate(n)), & PIDRate > \text{Basal} \\ PIDRate(n), & PIDRate \leq \text{Basal} \end{cases}.$$

In this expression: AdjustedRate(n) is the determined adjusted insulin infusion rate; PIDRate(n) is the obtained uncompensated insulin infusion rate; IOBRate(n) is the calculated IOB rate; FinalRate(n) is the selected final insulin infusion rate; and Basal is a current basal rate maintained by the insulin infusion device for the user.

Also presented here is a tangible and non-transitory electronic storage medium having processor-executable instructions that, when executed by a processor architecture comprising at least one processor device, perform a method of controlling an insulin infusion device for a user. In certain embodiments, the method begins by estimating a current IOB value that indicates an amount of active insulin in the body of the user. The method continues by calculating an IOB rate based at least in part on the estimated current IOB value, determining an adjusted insulin infusion rate based at least in part on the calculated IOB rate and an uncompensated insulin infusion rate, and selecting a final insulin infusion rate for the insulin infusion device, wherein either the determined adjusted insulin infusion rate, the uncompensated insulin infusion rate, or a current basal rate is selected as the final insulin infusion rate. The method then provides the selected final insulin infusion rate to regulate delivery of insulin by the insulin infusion device.

An electronic device is also presented here. Certain embodiments of the electronic device include a processor architecture and at least one memory element associated with the processor architecture. The at least one memory element stores processor-executable instructions that, when executed by the processor architecture, perform a method of controlling an insulin infusion device for a user. The method involves: computing a current IOB value that indicates an amount of active insulin in the body of the user; calculating an IOB rate based at least in part on the computed IOB value; determining an adjusted insulin infusion rate based at least in part on the calculated IOB rate and an uncompensated insulin

infusion rate; and selecting a final insulin infusion rate for the insulin infusion device. The selecting step selects either the determined adjusted insulin infusion rate, the uncompensated insulin infusion rate, or a current basal rate as the final insulin infusion rate.

An electronic controller for an insulin infusion device is also presented here. The electronic controller includes a processor architecture comprising at least one processor device, and at least one memory element associated with the processor architecture. The at least one memory element stores processor-executable instructions that, when executed by the processor architecture, provide an IOB compensation module that estimates a current IOB value that indicates an amount of active insulin in the body of the user, calculates an IOB rate based at least in part on the estimated current IOB value, and determines an adjusted insulin infusion rate based at least in part on the calculated IOB rate and an uncompensated insulin infusion rate. The IOB compensation module selects a final insulin infusion rate for the insulin infusion device, wherein the final insulin infusion rate is selected as either the determined adjusted insulin infusion rate, the uncompensated insulin infusion rate, or a current basal rate. The IOB compensation module then provides the selected final insulin infusion rate to regulate delivery of insulin by the insulin infusion device.

An exemplary embodiment of an electronic device is also provided here. The electronic device includes a processor architecture having at least one processor device, and at least one memory element associated with the processor architecture. The at least one memory element stores processor-executable instructions that, when executed by the processor architecture, perform a method of controlling an insulin infusion device for a user. The method operates the insulin infusion device in a closed-loop mode to deliver insulin to the body of the user, obtains current insulin-delivered data that indicates an amount of insulin delivered by the insulin infusion device during a most recent sampling period, obtains current sensor data that indicates a current sensor glucose value for the user corresponding to the most recent sampling period, and processes historical insulin-delivered data and historical sensor data, for a plurality of historical sampling periods prior to the most recent sampling period, to obtain predicted sensor glucose values for a historical time period. The method continues by calculating a difference between the current sensor glucose value and a predicted current sensor glucose value for the most recent sampling period, wherein the predicted sensor glucose values for the historical time period include the predicted current sensor glucose value. The method continues by generating an alert when the difference exceeds a threshold error amount.

The following detailed description also relates to a tangible and non-transitory electronic storage medium having processor executable instructions that, when executed by a processor architecture comprising at least one processor device, perform a method of controlling an insulin infusion device for a user. The method involves operation of the insulin infusion device in a closed-loop mode to deliver insulin to the body of the user. The method continues by identifying, from historical sensor glucose values for the user, a baseline historical sensor glucose value obtained during a begin-training sampling period. The method calculates a plurality of candidate solutions to a sensor glucose prediction model, wherein each of the plurality of candidate solutions is calculated as a function of a bounded initial condition and historical insulin delivered data for the user, and wherein the bounded initial condition is influenced by the baseline sensor glucose value. The method continues by selecting a best-matched solution from the calculated plurality of candidate solutions, based on a comparison of predicted sensor glucose values from the calculated plurality of candidate solutions to a first portion of the historical sensor glucose values. The predicted sensor glucose values from the best-matched solution are compared to a second portion of the historical sensor glucose values, wherein the first portion of the historical sensor glucose values corresponds to a distant history period, the second portion of the historical sensor glucose values corresponds to a recent history period, and the distant history period occurred before the recent history period that data samples. The method continues by generating an alert, in response to the comparing, when the second portion of the historical sensor glucose values deviates from the best-matched solution by at least a threshold error amount.

Also presented here is an embodiment of an electronic controller for an insulin infusion device. The electronic controller includes a processor architecture comprising at least one processor device, and at least one memory element associated with the processor architecture. The at least one memory element stores processor-executable instructions that, when executed by the processor architecture, provide a model supervisor module to obtain, during closed-loop operation of the insulin infusion device, insulin-delivered data that indicates an amount of insulin delivered by the insulin infusion device during a most recent sampling period, and current sensor data that indicates a current sensor glucose value for the user corresponding to the most recent sampling period. The model supervisor module defines a model training period and a model prediction period for a historical period of time, and finds a best-matched solution to a sensor glucose prediction model, relative to historical sensor glucose values obtained during the model training period, wherein the best-matched solution is a function of a baseline sensor glucose value obtained during the model training period, and is a function of historical insulin-delivered data for the user obtained during the historical period of time. The model supervisor module compares at least one predicted sensor glucose value from the best-matched solution to at least one historical sensor glucose value corresponding only to the model prediction period, and generates an alert, in response to the comparing, when the at least one historical sensor glucose value deviates from the at least one predicted sensor glucose value by at least a threshold error amount.

Also included below is a detailed description of a processor-implemented method of controlling an insulin infusion device for a user. The method may begin by operating the insulin infusion device in a closed-loop mode to deliver insulin to the body of the user. The method continues by obtaining current insulin-delivered data that indicates an amount of insulin delivered by the insulin infusion device during a most recent sampling period, obtaining current sensor data that indicates a current sensor glucose value for the user corresponding to the most recent sampling period, and processing historical insulin-delivered data and historical sensor data, for a plurality of historical sampling periods prior to the most recent sampling period, to obtain predicted sensor glucose values for a historical time period. The method then calculates a difference between the current sensor glucose value and a predicted current sensor glucose value for the most recent sampling period, wherein the predicted sensor glucose values for the historical time period include the predicted current sensor glucose value. An alert is generated when the difference exceeds a threshold error amount.

Also included below is a detailed description of a processor-implemented method of controlling an insulin infusion device for a user. The method may begin by operating the

insulin infusion device in a closed-loop mode to deliver insulin to the body of the user. The method continues by identifying, from historical sensor glucose values for the user, a baseline historical sensor glucose value obtained during a begin-training sampling period. Next, a plurality of candidate solutions to a sensor glucose prediction model is calculated, wherein each of the plurality of candidate solutions is calculated as a function of a bounded initial condition and historical insulin delivered data for the user, and wherein the bounded initial condition is influenced by the baseline sensor glucose value. The method continues by selecting a best-matched solution from the calculated plurality of candidate solutions, based on a comparison of predicted sensor glucose values from the calculated plurality of candidate solutions to a first portion of the historical sensor glucose values. At least one predicted sensor glucose value from the best-matched solution is compared to a second portion of the historical sensor glucose values, wherein the first portion of the historical sensor glucose values corresponds to a distant history period, the second portion of the historical sensor glucose values corresponds to a recent history period, and the distant history period occurred before the recent history period that data samples. An alert is generated, in response to the comparing, when the second portion of the historical sensor glucose values deviates from the best-matched solution by at least a threshold error amount.

Another embodiment of a processor-implemented method of controlling an insulin infusion device for a user is also presented below. The method involves operating the insulin infusion device in a closed-loop mode to deliver insulin to the body of the user, defining a model training period and a model prediction period for a historical period of time, and finding a best-matched solution to a sensor glucose prediction model, relative to historical sensor glucose values obtained during the model training period, wherein the best-matched solution is a function of a baseline sensor glucose value obtained during the model training period, and is a function of historical insulin-delivered data for the user obtained during the historical period of time. The method continues by comparing at least one predicted sensor glucose value from the best-matched solution to at least one historical sensor glucose value corresponding only to the model prediction period. An alert is generated, in response to the comparing, when the at least one historical sensor glucose value deviates from the at least one predicted sensor glucose value by at least a threshold error amount.

This summary is provided to introduce a selection of concepts in a simplified form that are further described below in the detailed description. This summary is not intended to identify key features or essential features of the claimed subject matter, nor is it intended to be used as an aid in determining the scope of the claimed subject matter.

BRIEF DESCRIPTION OF THE DRAWINGS

A more complete understanding of the subject matter may be derived by referring to the detailed description and claims when considered in conjunction with the following figures, wherein like reference numbers refer to similar elements throughout the figures.

FIG. **1** is a block diagram of a closed loop glucose control system in accordance with an embodiment of the present invention.

FIG. **2** is a front view of closed loop hardware located on a body in accordance with an embodiment of the present invention.

FIG. **3**A is a perspective view of a glucose sensor system for use in an embodiment of the present invention.

FIG. **3**B is a side cross-sectional view of the glucose sensor system of FIG. **3**A.

FIG. **3**C is a perspective view of a sensor set of the glucose sensor system of FIG. **3**A for use in an embodiment of the present invention.

FIG. **3**D is a side cross-sectional view of the sensor set of FIG. **3**C.

FIG. **4** is a cross sectional view of a sensing end of the sensor of FIG. **3**D.

FIG. **5** is a top view of an infusion device with a reservoir door in the open position, for use in an embodiment of the present invention.

FIG. **6** is a side view of an infusion set with the insertion needle pulled out, for use in an embodiment of the present invention.

FIG. **7** is a circuit diagram of a sensor and its power supply in accordance with an embodiment of the present invention.

FIG. **8**A is a diagram of a single device and its components in accordance with an embodiment of the present invention.

FIG. **8**B is a diagram of two devices and their components in accordance with an embodiment of the present invention.

FIG. **8**C is another diagram of two devices and their components in accordance with an embodiment of the present invention.

FIG. **8**D is a diagram of three devices and their components in accordance with an embodiment of the present invention.

FIG. **9** is a table listing the devices of FIGS. **8**A-D and their components.

FIG. **10** is a block diagram of the glucose sensor system of FIG. **3**A.

FIG. **11**A is a detailed block diagram of an A/D converter for the glucose sensor system of FIG. **10** in accordance with an embodiment of the present invention.

FIG. **11**B is a detailed block diagram of the A/D converter for the glucose sensor system of FIG. **10** with a pulse duration output selection option in accordance with an embodiment of the present invention.

FIG. **12** is a circuit diagram of an I-F A/D converter of FIG. **10** accompanied by charts of node signals in accordance with an embodiment of the present invention.

FIG. **13** is another circuit diagram of an I-F A/D converter of FIG. **10** accompanied by charts of node signals in accordance with an embodiment of the present invention.

FIG. **14** is still another circuit diagram of an I-F A/D converter of FIG. **10** accompanied by charts of node signals in accordance with an embodiment of the present invention.

FIG. **15** is a circuit diagram of an I-V A/D converter of FIG. **10** in accordance with an embodiment of the present invention.

FIG. **16** is a block diagram of the glucose sensor system of FIG. **10** with a pre-filter and a filter in accordance with an embodiment of the present invention.

FIG. **17** is a chart of an example of a pre-filter of FIG. **16** and its effects on digital sensor values Dsig in accordance with an embodiment of the present invention.

FIG. **18** is frequency response chart for a filter of FIG. **16** in accordance with an embodiment of the present invention.

FIG. **19**A is a plot of a filtered and an unfiltered sensor signal over time in accordance with an embodiment of the present invention.

FIG. **19**B is close up of a section of the plot of FIG. **19**A in accordance with an embodiment of the present invention.

FIG. **20** is a cross-sectional view of a sensor set and an infusion set attached to the body in accordance with an embodiment of the present invention.

FIG. **21** is a frequency response chart of a time delay correcting Weiner filter in accordance with an embodiment of the present invention.

FIG. **22** is a plot of a digital sensor values Dsig before and after time delay correction compared to actual glucose measurements over time in accordance with an embodiment of the present invention.

FIG. **23**A is a diagram of a glucose clamp (glucose level with respect to time).

FIG. **23**B is a plot of insulin concentration in a normal glucose tolerant (NGT) individual in response to various magnitudes of glucose clamps of FIG. **23**A.

FIG. **24**A is a diagram of a glucose clamp.

FIG. **24**B is a diagram of a proportional insulin response to the glucose clamp of FIG. **24**A in accordance with an embodiment of the present invention.

FIG. **24**C is a diagram of an integral insulin response to the glucose clamp of FIG. **24**A in accordance with an embodiment of the present invention.

FIG. **24**D is a diagram of a derivative insulin response to the glucose clamp of FIG. **24**A in accordance with an embodiment of the present invention.

FIG. **24**E is a diagram of a combined proportional, integral, and derivative insulin response to the glucose clamp of FIG. **24**A in accordance with an embodiment of the present invention.

FIG. **25**A is a plot of insulin responses to a glucose clamp for exercise trained and normal individuals.

FIG. **25**B is a bar chart of glucose uptake rates for exercise trained and normal individuals.

FIG. **26** is a block diagram of a closed loop system to control blood glucose levels through insulin infusion based on glucose level feedback in accordance with an embodiment of the present invention.

FIG. **27** is a detailed block diagram of the portion of the control loop of FIG. **26** that is in the body in accordance with an embodiment of the present invention.

FIGS. **28**A and **28**B are plots of measured insulin responses of two different normal glucose tolerant (NGT) individuals to a glucose clamp for use with an embodiment of the present invention.

FIG. **29**A is a plot of two different glucose sensor outputs compared to glucose meter readings during a glucose clamp in accordance with an embodiment of the present invention.

FIG. **29**B is a plot of actual insulin concentration in blood compared to a controller commanded insulin concentration in response to the glucose clamp of FIG. **29**A in accordance with an embodiment of the present invention.

FIG. **30** is a top view of an end of a multi-sensor for measuring both glucose concentration and pH in accordance with an embodiment of the present invention.

FIG. **31**A is a representative drawing of blood glucose compared to sensor measured blood glucose over time in accordance with an embodiment of the present invention.

FIG. **31**B is a representative drawing of sensor sensitivity over the same period of time as FIG. **31**A in accordance with an embodiment of the present invention.

FIG. **31**C is a representative drawing of sensor resistance over the same period of time as FIG. **31**A in accordance with an embodiment of the present invention.

FIG. **32** is a block diagram using the derivative of sensor resistance to determine when to recalibrate or replace the sensor in accordance with an embodiment of the present invention.

FIG. **33**A is a plot of an analog sensor signal Isig over time in accordance with an embodiment of the present invention.

FIG. **33**B is a plot of sensor resistance over the same period of time as FIG. **32**A in accordance with an embodiment of the present invention.

FIG. **33**C is a plot of the derivative of the sensor resistance of FIG. **32**B in accordance with an embodiment of the present invention.

FIG. **34**A is a bottom view of a telemetered characteristic monitor in accordance with an embodiment of the present invention.

FIG. **34**B is a bottom view of a different telemetered characteristic monitor in accordance with an embodiment of the present invention.

FIG. **35**A is a drawing of a blood plasma insulin response to a glucose clamp in a normal glucose tolerant (NGT) individual in accordance with an embodiment of the present invention.

FIG. **35**B is a drawing of the blood plasma insulin response of FIG. **35**A when delayed due to insulin being delivered to the subcutaneous tissue instead of directly into the blood stream in accordance with an embodiment of the present invention.

FIG. **36**A is a drawing of blood plasma insulin concentration over time after an insulin bolus is delivered directly into the blood stream in accordance with an embodiment of the present invention.

FIG. **36**B is a drawing of a blood plasma insulin concentration over time after an insulin bolus is delivered into the subcutaneous tissue in accordance with an embodiment of the present invention.

FIG. **37** is a block diagram of the closed loop system of FIG. **26** with the addition of a post-controller compensator and a derivative filter in accordance with an embodiment of the present invention.

FIG. **38**A is a plot of sensor signal measurements and Via measurements with respect to time in accordance with an embodiment of the present invention.

FIG. **38**B is a plot of a measured counter electrode voltage Vcnt with respect to time in accordance with an embodiment of the present invention.

FIG. **38**C is a plot of calculated sensor sensitivity with respect to time in accordance with an embodiment of the present invention.

FIG. **38**D is a plot of a calculation of sensor resistance Rs_1 with respect to time in accordance with an embodiment of the present invention.

FIG. **38**E is a plot of another calculation of sensor resistance Rs_2 with respect to time in accordance with an embodiment of the present invention.

FIG. **38**F is a plot of the derivative of sensor resistance Rs_1 of FIG. **38**D with respect to time in accordance with an embodiment of the present invention.

FIG. **38**G is a plot of the derivative of the sensor resistance Rs_2 of FIG. **38**E with respect to time in accordance with an embodiment of the present invention.

FIG. **38**H is a plot of when sensors were replaced with respect to time in accordance with an embodiment of the present invention.

FIGS. **39**A and **39**B are a block diagrams of a closed loop glucose control system in accordance with embodiments of the present invention.

FIG. **40** is a block diagram of auto blood withdrawal and return in accordance with an embodiment of the present invention.

FIG. **41**A is a plot actual blood glucose concentration in accordance with an embodiment of the present invention.

FIG. **41**B is a plot of actual insulin concentration in blood compared to a controller commanded insulin concentration in

response to the blood glucose in FIG. **41**A in accordance with an embodiment of the present invention.

FIG. **42** illustrates a control feedback block diagram of state variable feedback and in accordance with an embodiment of the present invention.

FIG. **43** is a plot of basal insulin delivery rate over time using different control gains in accordance with embodiments of the present invention.

FIG. **44** is a plot of subcutaneous insulin over time using different control gains in accordance with embodiments of the present invention.

FIG. **45** is a plot of plasma insulin over time using different control gains in accordance with embodiments of the present invention.

FIG. **46** is a plot of insulin effect over time using different control gains in accordance with embodiments of the present invention.

FIG. **47** is a plot of simulated glucose concentration over time using a PID controller with state variable feedback and a PID controller without state variable feedback in accordance with embodiments of the present invention.

FIG. **48** is a plot of simulated insulin delivery over time using a PID controller with state variable feedback and a PID controller without state variable feedback in accordance with embodiments of the present invention.

FIG. **49** is a block diagram that illustrates processing modules and algorithms of an exemplary embodiment of a closed-loop system controller.

FIG. **50** is a flow chart that illustrates an exemplary embodiment of a control process for an insulin infusion device.

FIG. **51** is a graph of integral clip value versus sensor glucose levels.

FIG. **52** is a block diagram that schematically illustrates an exemplary embodiment of an insulin on board (IOB) compensation module.

FIG. **53** is a flow chart that illustrates an exemplary embodiment of an IOB compensation process.

FIG. **54** is a diagram that depicts certain time events associated with the operation of a model supervisor module.

FIG. **55** is a flow chart that illustrates an exemplary embodiment of a sensor model supervision process.

FIG. **56** is a flow chart that illustrates an exemplary embodiment of a sensor model training process, which may be performed in conjunction with the sensor model supervision process depicted in FIG. **55**.

FIG. **57** is a diagram that illustrates two exemplary fault conditions that can be detected by the model supervisor module.

DETAILED DESCRIPTION

The following detailed description is merely illustrative in nature and is not intended to limit the embodiments of the subject matter or the application and uses of such embodiments. As used herein, the word "exemplary" means "serving as an example, instance, or illustration." Any implementation described herein as exemplary is not necessarily to be construed as preferred or advantageous over other implementations. Furthermore, there is no intention to be bound by any expressed or implied theory presented in the preceding technical field, background, brief summary or the following detailed description.

Techniques and technologies may be described herein in terms of functional and/or logical block components, and with reference to symbolic representations of operations, processing tasks, and functions that may be performed by various computing components or devices. Such operations, tasks, and functions are sometimes referred to as being computer-executed, computerized, software-implemented, or computer-implemented. It should be appreciated that the various block components shown in the figures may be realized by any number of hardware, software, and/or firmware components configured to perform the specified functions. For example, an embodiment of a system or a component may employ various integrated circuit components, e.g., memory elements, digital signal processing elements, logic elements, look-up tables, or the like, which may carry out a variety of functions under the control of one or more microprocessors or other control devices.

When implemented in software or firmware, various elements of the systems described herein are essentially the code segments or instructions that perform the various tasks. The program or code segments can be stored in any tangible and non-transitory processor-readable medium. The "processor-readable medium" or "machine-readable medium" may include any medium that can store or transfer information. Examples of the processor-readable medium include an electronic circuit, a semiconductor memory device, a ROM, a flash memory, an erasable ROM (EROM), a floppy diskette, a CD-ROM, an optical disk, a hard disk, or the like.

The various tasks performed in connection with a process described herein may be performed by software, hardware, firmware, or any combination thereof. It should be appreciated that a described process may include any number of additional or alternative tasks, the tasks shown in a particular figure need not be performed in the illustrated order, and a described process may be incorporated into a more comprehensive procedure or process having additional functionality not described in detail herein. Moreover, one or more of the tasks shown in the figures could be omitted from an embodiment of a described process as long as the intended overall functionality remains intact.

As shown in the drawings for purposes of illustration, the invention is embodied in a closed loop infusion system for regulating the rate of fluid infusion into a body of a user based on feedback from an analyte concentration measurement taken from the body. In particular embodiments, the invention is embodied in a control system for regulating the rate of insulin infusion into the body of a user based on a glucose concentration measurement taken from the body. In preferred embodiments, the system is designed to model a pancreatic beta cell (β-cell). In other words, the system controls an infusion device to release insulin into a body of a user in a similar concentration profile as would be created by fully functioning human β-cells when responding to changes in blood glucose concentrations in the body.

Thus, the system simulates the body's natural insulin response to blood glucose levels and not only makes efficient use of insulin, but also accounts for other bodily functions as well since insulin has both metabolic and mitogenic effects. However, the algorithms must model the β-cells closely, since algorithms that are designed to minimize glucose excursions in the body, without regard for how much insulin is delivered, may cause excessive weight gain, hypertension, and atherosclerosis. In preferred embodiments of the present invention, the system is intended to emulate the in vivo insulin secretion pattern and to adjust this pattern consistent with the in vivo β-cell adaptation experienced by normal healthy individuals. The in vivo β-cell response in subjects with normal glucose tolerance (NGT), with widely varying insulin sensitivity (S_I), is the optimal insulin response for the maintenance of glucose homeostasis.

Preferred embodiments include a glucose sensor system **10**, a controller **12** and an insulin delivery system **14**, as shown in FIG. **1**. The glucose sensor system **10** generates a sensor signal **16** representative of blood glucose levels **18** in the body **20**, and provides the sensor signal **16** to the controller **12**. The controller **12** receives the sensor signal **16** and generates commands **22** that are communicated to the insulin delivery system **14**. The insulin delivery system **14** receives the commands **22** and infuses insulin **24** into the body **20** in response to the commands **22**.

Generally, the glucose sensor system **10** includes a glucose sensor, sensor electrical components to provide power to the sensor and generate the sensor signal **16**, a sensor communication system to carry the sensor signal **16** to the controller **12**, and a sensor system housing for the electrical components and the sensor communication system.

Typically, the controller **12** includes controller electrical components and software to generate commands for the insulin delivery system **14** based on the sensor signal **16**, and a controller communication system to receive the sensor signal **16** and carry commands to the insulin delivery system **14**.

Generally, the insulin delivery system **14** includes an infusion device and an infusion tube to infuse insulin **24** into the body **20**. In particular embodiments, the infusion device includes infusion electrical components to activate an infusion motor according to the commands **22**, an infusion communication system to receive the commands **22** from the controller **12**, and an infusion device housing to hold the infusion device.

In preferred embodiments, the controller **12** is housed in the infusion device housing and the infusion communication system is an electrical trace or a wire that carries the commands **22** from the controller **12** to the infusion device. In alternative embodiments, the controller **12** is housed in the sensor system housing and the sensor communication system is an electrical trace or a wire that carries the sensor signal **16** from the sensor electrical components to the controller electrical components. In other alternative embodiments, the controller **12** has its own housing or is included in a supplemental device. In another alternative embodiment, the controller is located with the infusion device and the sensor system all within one housing. In further alternative embodiments, the sensor, controller, and/or infusion communication systems may utilize a cable, a wire, fiber optic lines, RF, IR, or ultrasonic transmitters and receivers, or the like instead of the electrical traces.

System Overview

Preferred embodiments of the invention include a sensor **26**, a sensor set **28**, a telemetered characteristic monitor **30**, a sensor cable **32**, an infusion device **34**, an infusion tube **36**, and an infusion set **38**, all worn on the body **20** of a user, as shown in FIG. **2**. The telemetered characteristic monitor **30** includes a monitor housing **31** that supports a printed circuit board **33**, batteries **35**, antenna (not shown), and a sensor cable connector (not shown), as seen in FIGS. **3**A and **3**B. A sensing end **40** of the sensor **26** has exposed electrodes **42** and is inserted through skin **46** into a subcutaneous tissue **44** of a user's body **20**, as shown in FIGS. **3**D and **4**. The electrodes **42** are in contact with interstitial fluid (ISF) that is present throughout the subcutaneous tissue **44**. The sensor **26** is held in place by the sensor set **28**, which is adhesively secured to the user's skin **46**, as shown in FIGS. **3**C and **3**D. The sensor set **28** provides for a connector end **27** of the sensor **26** to connect to a first end **29** of the sensor cable **32**. A second end **37** of the sensor cable **32** connects to the monitor housing **31**. The batteries **35** included in the monitor housing **31** provide power for the sensor **26** and electrical components **39** on the printed circuit board **33**. The electrical components **39** sample the sensor signal **16** and store digital sensor values (Dsig) in a memory and then periodically transmit the digital sensor values Dsig from the memory to the controller **12**, which is included in the infusion device.

The controller **12** processes the digital sensor values Dsig and generates commands **22** for the infusion device **34**. Preferably, the infusion device **34** responds to the commands **22** and actuates a plunger **48** that forces insulin **24** out of a reservoir **50** located inside the infusion device **34**, as shown in FIG. **5**. In particular embodiments, a connector tip **54** of the reservoir **50** extends through the infusion device housing **52** and a first end **51** of the infusion tube **36** is attached to the connector tip **54**. A second end **53** of the infusion tube **36** connects to the infusion set **38**. Insulin **24** is forced through the infusion tube **36** into the infusion set **38** and into the body **20**. The infusion set **38** is adhesively attached to the user's skin **46**, as shown in FIG. **6**. As part of the infusion set **38**, a cannula **56** extends through the skin **46** and terminates in the subcutaneous tissue **44** completing fluid communication between the reservoir **50** and the subcutaneous tissue **44** of the user's body **20**.

In alternative embodiments, the closed-loop system can be a part of a hospital-based glucose management system. Given that insulin therapy during intensive care has been shown to dramatically improve wound healing, reduce blood stream infections, renal failure, and polyneuropathy mortality, irrespective of whether subjects previously had diabetes (See Van den Berghe G. et al., NEJM 345: 1359-67, 2001, which is incorporated by reference herein), the present invention can be used in this hospital setting to control the blood glucose level of a patient in intensive care. In these alternative embodiments, since an intravenous (IV) hookup is typically implanted into a patient's arm while the patient is in an intensive care setting (e.g., ICU), a closed loop glucose control can be established which piggy-backs off the existing IV connection. Thus, in a hospital based system, IV catheters which are directly connected to a patient vascular system for purposes of quickly delivering IV fluids, can also be used to facilitate blood sampling and direct infusion of substances (e.g., insulin, anticoagulants) into the intra-vascular space. Moreover, glucose sensors may be inserted through the IV line to give real-time glucose levels from the blood stream. Therefore, depending on the type of hospital based system, the alternative embodiments would not necessarily need the described system components such as the sensor **26**, the sensor set **28**, the telemetered characteristic monitor **30**, the sensor cable **32**, the infusion tube **36**, and the infusion set **38** as described in the preferred embodiments. Instead, standard blood glucose meters or vascular glucose sensors as described in provisional application entitled "Multi-lumen Catheter," filed Sep. 27, 2002, Ser. No. 60/414,248, which is incorporated herein in its entirety by reference, can be used to provide the blood glucose values to the infusion pump control and the existing IV connection can be used to administer the insulin to the patient.

It is important to appreciate that numerous combinations of devices in the hospital-based system can be used with the closed loop controller of the present invention. For example, as described in FIG. **39**B compared to the preferred system in FIG. **39**A, an auto blood glucose/intravenous insulin infusion system can automatically withdraw and analyze blood for glucose concentration at fixed intervals (preferably 5-20 minutes), extrapolate the blood glucose values at a more frequent interval (preferably 1 minute), and use the extrapolated signal for calculating an IV-insulin infusion according to the controller described below. The modified auto blood glucose/intravenous insulin infusion system would eliminate the need for subcutaneous sensor compensation and subcutaneous insulin compensation (as described with regards to the lead-

lag compensator below). The automatic withdrawal of blood, and subsequent glucose determination can be accomplished with existing technology (e.g. VIA or Biostator like blood glucose analyzer) or by the system described in FIG. **40**. The system in FIG. **40** uses a peristaltic pump **420** to withdraw blood across an amperometric sensor **410** (the same technology as used in sensor **26**) and then return the blood with added flush (0.5 to 1.0 ml) from the reservoir **400**. The flush can consist of any makeup of saline, heparin, glucose solution and/or the like. If the blood samples are obtained at intervals longer than 1 minute but less than 20 minutes, the blood glucose determinations can be extrapolated on a minute-to-minute basis with extrapolation based on the present (n) and previous values (n−1) to work with the logic of the controller as described in detail below. For blood samples obtained at intervals greater than 20 minutes, a zero-order-hold would be used for the extrapolation. Based on these blood glucose values, the infusion device can administer insulin based on the closed loop controller described in greater detail below.

In other modifications to the system, a manual blood glucose/intravenous insulin infusion system can be used where frequent manual entry of blood glucose values from a standard blood glucose meter (e.g., YSI, Beckman, etc.) and extrapolate the values at more frequent intervals (preferably 1 min) to create a surrogate signal for calculating IV-insulin infusion. Alternatively, a sensor blood glucose/intravenous insulin infusion system can use a continuous glucose sensor (e.g., vascular, subcutaneous, etc.) for frequent blood glucose determination. Moreover, the insulin infusion can be administered subcutaneously rather than intravenously in any one of the previous examples according to the controller described below.

In still further alternative embodiments, the system components may be combined in a smaller or greater number of devices and/or the functions of each device may be allocated differently to suit the needs of the user.

Controller

Once the hardware for a closed loop system is configured, such as in the preferred embodiments described above, the effects of the hardware on a human body are determined by the controller. In preferred embodiments, the controller **12** is designed to model a pancreatic beta cell (β-cell). In other words, the controller **12** commands the infusion device **34** to release insulin **24** into the body **20** at a rate that causes the insulin concentration in the blood to follow a similar concentration profile as would be caused by fully functioning human β-cells responding to blood glucose concentrations in the body **20**. In further embodiments, a "semi-closed-loop" system may be used, in which the user is prompted to confirm insulin delivery before any insulin is actually delivered.

A controller that simulates the body's natural insulin response to blood glucose levels not only makes efficient use of insulin but also accounts for other bodily functions as well since insulin has both metabolic and mitogenic effects. Controller algorithms that are designed to minimize glucose excursions in the body without regard for how much insulin is delivered may cause excessive weight gain, hypertension, and atherosclerosis. In preferred embodiments, of the present invention, the controller **12** is intended to emulate the in vivo insulin secretion pattern and to adjust this pattern to be consistent with in vivo 3-cell adaptation. The in vivo 3-cell response in subjects with normal glucose tolerance (NGT), with widely varying insulin sensitivity (S_I), is the optimal insulin response for the maintenance of glucose homeostasis.

The β-Cell and PID Control

Generally, the in vivo 3-cell response to changes in glucose is characterized by "first" and "second" phase insulin responses. This biphasic insulin response is clearly seen during hyperglycemic clamps applied to NGT subjects, as shown in FIG. **23**B. During a hyperglycemic clamp the glucose level is rapidly increased from a basal level G_B to a new higher level G_C and then held constant at the higher-level G_C as shown in FIG. **23**A. The magnitude of the increase in glucose (ΔG) affects the insulin response. Four insulin response curves are shown for four different glucose clamp levels in FIG. **23**B.

The biphasic insulin response of a β-cell can be modeled using components of a proportional, plus integral, plus derivative (PID) controller. A PID controller is selected since PID algorithms are stable for a wide variety of non-medical dynamic systems, and PID algorithms have been found to be stable over widely varying disturbances and changes in system dynamics.

The insulin response of β-cells during a hyperglycemic clamp is diagrammed in FIGS. **24**A-E using the components of a PID controller to model the β-cell. A proportional component U_P and a derivative component U_D of the PID controller may be combined to represent a first phase insulin response **440**, which lasts several minutes. An integral component U_I of the PID controller represents a second phase insulin response **442**, which is a steady increase in insulin release under hyperglycemic clamp conditions. The magnitude of each component's contribution to the insulin response is described by the following equations:

$$\text{Proportional Component Response: } U_P = K_P(G - G_B)$$

$$\text{Integral Component Response: } U_I = K_I \int_{t_0}^{t} (G - G_B)\,dt + I_B, \text{ and}$$

$$\text{Derivative Component Response: } U_D = K_D \frac{dG}{dt},$$

Where

U_P is the proportional component of the command sent to the insulin delivery system,

U_I is the integral component of the command sent to the insulin delivery system,

U_D is the derivative component of the command sent to the insulin delivery system,

K_P is a proportional gain coefficient,

K_I is an integral gain coefficient,

K_D is a derivative gain coefficient,

G_B is a present blood glucose level,

G_B is a desired basal glucose level,

t is the time that has passed since the last sensor calibration,

t_0 is the time of the last sensor calibration, and

I_B is a basal insulin concentration at t_0, or can also be described as $U_I(t_0)$.

The combination of the PID components that model the two phases of insulin response by a β-cell is shown in FIG. **24**E as it responds to the hyperglycemic clamp of FIG. **24**A. FIG. **24**E shows that the magnitude of the first phase response **440** is driven by the derivative and proportional gains, K_D and K_P. And the magnitude of the second phase response **442** is driven by the integral gain K_I.

The components of the PID controller can also be expressed in its discrete form:

$$\text{Proportional Component Response: } P_{con}^{n} = K_p(SG_f^n - G_{sp})$$

$$\text{Integral Component Response: } I_{con}^{n} = I_{con}^{n-1} + K_I(SG_f^n - G_{sp}); I_{con}^{0} = I_b$$

$$\text{Derivative Component Response: } D_{con}^{n} = K_D dGdt_f^n$$

Where K_P, K_I, and K_D are the proportional, integral, and derivative gain coefficients, SG_f and $dGdt_f$ are the filtered sensor glucose and derivative respectively, and the superscript n refers to discrete time.

An acute insulin response is essential for preventing wide postprandial glycemic excursions. Generally, an early insulin response to a sudden increase in glucose level results in less total insulin being needed to bring the glucose level back to a desired basal glucose level. This is because the infusion of insulin increases the percentage of glucose that is taken up by the body. Infusing a large amount of insulin to increase the percentage of glucose uptake while the glucose concentration is high results in an efficient use of insulin. Conversely, infusing a large amount of insulin while the glucose concentration is low results in using a large amount of insulin to remove a relatively small amount of glucose. In other words, a larger percentage of a big number is more than a larger percentage of a small number. The infusion of less total insulin helps to avoid development of insulin resistance in the user. As well, first-phase insulin is thought to result in an early suppression of hepatic glucose output.

Insulin sensitivity is not fixed and can change dramatically in a body depending on the amount of exercise by the body. In one study, for example, insulin responses in highly exercise-trained individuals (individuals who trained more than 5 days a week) were compared to the insulin responses in subjects with normal glucose tolerance (NGT) during a hyperglycemic clamp. The insulin response in exercise-trained individuals **444** was about one-half of the insulin response of the NGT subjects **446**, as shown in FIG. **25**A. But the glucose uptake rate for each of the individuals (exercise-trained **448** or normal **450**) was virtually identical, as shown in FIG. **25**B. Thus, it can be speculated that the exercise-trained individuals have twice the insulin sensitivity and half of the insulin response leading to the same glucose uptake as the NGT individuals. Not only is the first phase insulin response **440** reduced due to the effects of exercise, but the second phase insulin response **442** has also been shown to adjust to insulin sensitivity, as can be seen in FIG. **25**A.

In preferred embodiments, a closed loop control system may be used for delivering insulin to a body to compensate for β-cells that perform inadequately. There is a desired basal blood glucose level G_B for each body. The difference between the desired basal blood glucose level G_B and an estimate of the present blood glucose level G is the glucose level error G_E that must be corrected. The glucose level error G_E is provided as an input to the controller **12**, as shown in FIG. **26**.

If the glucose level error G_E is positive (meaning that the present estimate of the blood glucose level G is higher than the desired basal blood glucose level G_B) then the controller **12** generates an insulin delivery command **22** to drive the infusion device **34** to provide insulin **24** to the body **20**. In terms of the control loop, glucose is considered to be positive, and therefore insulin is negative. The sensor **26** senses the ISF glucose level and generates a sensor signal **16**. The sensor signal **16** is filtered and calibrated to create an estimate of the present blood glucose level **452**. In particular embodiments, the estimate of the present blood glucose level G is adjusted with correction algorithms **454** before it is compared to the desired basal blood glucose level G_B to calculate a new glucose level error G_E to start the loop again.

If the glucose level error G_E is negative (meaning that the present estimate of the blood glucose level is lower than the desired basal blood glucose level G_B) then the controller **12** reduces or stops the insulin delivery depending on whether the integral component response of the glucose error G_E is still positive.

If the glucose level error G_E is zero, (meaning that the present estimate of the blood glucose level is equal to the desired basal blood glucose level G_B) then the controller **12** may or may not issue commands to infuse insulin depending on the derivative component (whether the glucose level is raising or falling) and the integral component (how long and by how much glucose level has been above or below the basal blood glucose level G_B). In "semi-closed loop" embodiments, the user is prompted before the controller **12** issues the commands to infuse insulin. The prompts may be displayed to the user on a display, sounded to the user, or otherwise provide an indication to the user that the system is ready to deliver insulin, for example a vibration or other tactile indication. In addition, the amount of insulin to be delivered may be displayed, with or without other information, such as the total amount infused for the day or the potential effect on the user's blood glucose level by the insulin delivery. In response, the user may indicate that the insulin should or should not be delivered, for example by selecting a button, key, or other input. In further embodiments, there must be at least two keystrokes so that insulin is not delivered by accident.

To more clearly understand the effects that the body has on the control loop, a more detailed description of the physiological effects that insulin has on the glucose concentration in the interstitial fluid (ISF) is needed. In preferred embodiments, the infusion device **34** delivers insulin through the cannula **56** of the infusion set **38** into the ISF of the subcutaneous tissue **44** of the body **20**. And the insulin **24** diffuses from the local ISF surrounding the cannula into the blood plasma and then spreads throughout the body **20** in the main circulatory system, as described in the block diagram of FIG. **27**. The insulin then diffuses from the blood plasma into the interstitial fluid ISF substantially throughout the entire body. The insulin **24** binds with and activates membrane receptor proteins on cells of body tissues. This facilitates glucose permeation into the activated cells. In this way, the tissues of the body **20** take up the glucose from the ISF. As the ISF glucose level decreases, glucose diffuses from the blood plasma into the ISF to maintain glucose concentration equilibrium. Finally, the glucose in the ISF permeates the sensor membrane and affects the sensor signal **16**.

In addition, insulin has direct and indirect effects on liver glucose production. Increased insulin concentration decreases liver glucose production. Therefore, acute and immediate insulin response not only helps the body to efficiently take up glucose but also substantially stops the liver from adding to the glucose in the blood stream. In alternative embodiments, insulin is delivered more directly into the blood stream instead of into the interstitial fluid, such as delivery into veins, arteries, the peritoneal cavity, or the like. And therefore, any time delay associated with moving the insulin from the interstitial fluid into the blood plasma is diminished. In other alternative embodiments, the glucose sensor is in contact with blood or body fluids other than interstitial fluid, or the glucose sensor is outside of the body and measures glucose through a non-invasive means. The embodiments that use alternative glucose sensors may have shorter or longer delays between the blood glucose level and the measured blood glucose level.

Selecting Controller Gains

In preferred embodiments, the controller gains K_P, K_I, and K_D, are selected so that the commands from the controller **12** cause the infusion device **34** to release insulin **24** into the body **20** at a rate, that causes the insulin concentration in the blood to follow a similar concentration profile, as would be caused by fully functioning human β-cells responding to blood glucose concentrations in the body. In preferred embodiments, the gains may be selected by observing the insulin response of several normal glucose tolerant (NGT) individuals, with healthy normally functioning β-cells. The first step in determining a set of controller gains is to take

periodic measurements of blood glucose and blood insulin concentrations from the group of NGT individuals. Second, each individual in the group is subjected to a hyperglycemic clamp, while continuing to periodically measure and record the blood glucose and blood insulin concentrations. Third, a least squares curve fit is applied to the recorded blood insulin concentrations measured over time for each individual. The result is a set of curves representing the insulin responses to the hyperglycemic clamp for each individual of the group. Fourth, the curves are used to calculate the controller gains K_P, K_I, and K_D, for each individual. And finally, the proportional gains from each of the individuals are averaged together to obtain an average proportional gain, K_P, to be used in a controller **12**. Similarly, the integral gains, K_I, and the derivative gains, K_D, are averaged to obtain an average integral gain, K_I, and an average derivative gain, K_D, for the controller **12**. Alternatively, other statistical values may be used instead of averages such as, maximums, minimums, the high or low one, two or three sigma standard deviation values, or the like. The gains calculated for various individuals in a group may be filtered to remove anomalous data points before statistically calculating the gains to be used in a controller.

In an example, a least squares curve-fitting method is used to generate representative insulin response curves from two fasted individuals in a group, as shown in FIGS. **28**A and B. Then the controller gains were calculated from the insulin response curves of the two representative individuals and are shown in Table 1. When calculating the controller gains, the insulin clearance rate (k), was assumed to be 10 (ml of insulin)/min/(kg. of body weight). The insulin clearance rate k is the rate that insulin is taken out of the blood stream in a body. Finally, the average value for each type of gain is calculated using the measurements from the group, as shown in Table 1.

TABLE 1

PID Controller Gains Calculated From The Insulin Response Curves Of Two NGT Individuals

Individuals	Proportional Gain, K_P	Integral Gain, K_I	Derivative Gain, K_D
a	0.000406	0.005650	0.052672
b	0.000723	0.003397	0.040403
Average	0.000564	0.004523	0.046537

The controller gains may be expressed in various units and/or may be modified by conversion factors depending on preferences for British or S. I. Units, floating-point or integer software implementation, the software memory available, or the like. The set of units for the controller gains in Table 1 is:

K_P: (mU of insulin)/min/(Kg of body weight) per (mg of glucose)/(dl of plasma);

K_I: (mU of insulin)/min/(Kg of body weight) per (mg of glucose)/(dl of plasma) min.; and

K_D: (mU of insulin)/min/(Kg of body weight) per (mg of glucose)/(dl of plasma)/min.

In alternative embodiments, other curve fitting methods are used to generate the insulin response curves from the measurements of blood insulin concentrations.

An estimate of an insulin clearance rate (k), the individual's body weight (W), and the insulin sensitivity S_I are needed to calculate the controller gains from the insulin response curves for each NGT individual. The insulin clearance rate (k) is generally proportional to body weight and is well documented in literature. The individual's insulin sensitivity S_I may be measured using an intravenous glucose tolerance test, a hyperinsulinemic clamp, or in the case of a diabetic, comparing the individual's daily insulin requirement to their daily carbohydrate intake.

In particular embodiments, two parameters, the insulin sensitivity S_I and the insulin clearance rate k, are measured for each individual. In other embodiments, the insulin clearance rate k is estimated from literature given the individual's body weight. In other particular embodiments, longer or shorter insulin clearance times are used. In still other embodiments, all of the parameters are estimated. In additional embodiments, one or more parameters are measured, while at least one parameter is estimated from literature.

In other alternative embodiments, the controller gains are calculated using a group of individuals with similar body types. For example, the insulin response to a hyperglycemic clamp may be measured for several tall, thin, NGT, males in order to calculate the controller insulin response gains for each individual in the group. Then the gains are statistically combined to generate a set of representative controller gains for tall, thin, NGT, males. The same could be done for other groups such as, but not limited to, short, heavy, NGT, females; medium height, medium weight, highly exercised trained, females; average height and weight 10 year olds; or the like. Then the controller gains are selected for each individual user based on the group that best represents them. In further alternative embodiments, controller gains are uniquely selected for each individual user. In particular embodiments, the controller gains for a user are selected based on measurements of insulin sensitivity, insulin clearing time, insulin appearance time, insulin concentration, body weight, body fat percentage, body metabolism, or other body characteristics such as pregnancy, age, heart conditions, or the like.

In other alternative embodiments, the controller gains are estimated as a function of a user's body weight W and insulin sensitivity S_I. A series of observations are used to justify this method. The first observation is that the controller gains are proportional to each other. In other words, small changes in glucose concentration cause a small derivative response U_D, a small proportional response U_P and a small integral response U_I. And larger changes in glucose concentration cause a proportionally larger derivative response U_D, a proportionally larger proportional U_P response and a proportionally larger integral response U_I, as shown in FIG. **23**B. Changes in the glucose concentration proportionally affect all three components of the controller response U_{PID}. The second observation is that the first phase insulin response ($\phi 1$) is proportional to the derivative gain K_D. And the third observation is that two constants may be readily obtained from information in published literature or may be measured from a cross-section of the general population. The two constants are the insulin clearance rate (k) for a human given a body weight and the disposition index (DI) for a human given a change in glucose concentration.

While there are multiple sources for the information needed to calculate the insulin clearance rate k, one source is the article "Insulin clearance during hypoglycemia in patients with insulin-dependent diabetes mellitus", written by Kollind M et al., published in Horm Metab Res, 1991 July; 23(7):333-5. The insulin clearance rate k is obtained from the insulin infused divided by the steady state plasma insulin concentration. An insulin clearance constant A_k, which is independent of an individual's body weight, may be obtained by dividing the insulin clearance rate k (measured from a particular individual) by the individual's body weight. The insulin clearance constant A_k is generally the same for all humans, except

under extenuating circumstances such as after an individual has contracted HIV, other metabolic affecting diseases, or the like.

The disposition index (DI) for a human given a change in glucose concentration is available from information presented in the article "Quantification of the relationship between insulin sensitivity and beta-cell function in human subjects. Evidence for a hyperbolic function", written by Khan S E et al., published in Diabetes, 1993 November; 42(11):1663-72.

Both the disposition index DI and the insulin clearance rate k may be measured directly from tests. The disposition index DI may be calculated given the first phase insulin response measured form a glucose clamp test and the individual's insulin sensitivity measured from an insulin sensitivity test. The insulin clearance rate k may be measured from an insulin clearance test. The glucose clamp test and the insulin clearance test are described in the above-mentioned articles and are well known in the art. The insulin sensitivity S_I may be measured using an intravenous glucose tolerance test or a hyperinsulinemic clamp test.

Given these observations, then the following parameters may be measured from an NGT individual's insulin response to a glucose clamp: a desired first phase insulin response $\phi 1$, the ratio of K_D to K_p, and the ratio of K_D to K_I. Then the derivative gain K_D may be calculated from the first phase insulin response $\phi 1$ using the constants k and DI. And finally K_p and K_I may be calculated using the ratios of K_D to K_p and K_D to K_I.

The first phase insulin response $\phi 1$ may be observed in a NGT individual as the area under the insulin response curve during approximately the first 10 minutes of a glucose clamp. The increase in the glucose concentration during the glucose clamp is $\Delta G=(G-GB)$, where G is equal to Gc, the glucose concentration during the clamp, and G_B is the basal glucose concentration before the clamp.

The importance of the first phase insulin response $\phi 1$ has been emphasized by studies indicating that, in subjects with normal glucose tolerance (NGT), the product of first phase insulin response $\phi 1$ and insulin sensitivity (S_I) is a constant known as the disposition index, $DI=\phi 1\ S_I$. Therefore,

$$\phi 1 = \frac{DI}{S_I}.$$

For a different ΔG there is a different $\phi 1$ and therefore a different DI. But, the ratio $DI/\Delta G$ is substantially constant even for different individuals with different insulin sensitivities.

The insulin sensitivity S_I is defined as the percentage of the glucose concentration that the body tissues will take up for a given amount of insulin. The β-cell naturally adapts to changes in insulin sensitivity by adjusting the amount of insulin it secretes during the first phase insulin response $\phi 1$. This suggests that the body naturally seeks an optimal level of glucose tolerance. A controller that mimics this characteristic of the β-cell more accurately simulates the body's natural insulin response.

The instantaneous insulin response (RI) may be calculated given the insulin clearance rate (k) and the first phase insulin response $\phi 1$, $RI=k\phi 1$.

The insulin clearance rate k is proportional to body weight (W), therefore substituting a proportional constant A_k and the user's body weight W for k and replacing $\phi 1$ with the ratio of DI over S_I yields the following equation:

$$R_I = A_k W \frac{DI}{S_I}.$$

The instantaneous insulin response R_I may also be expressed as the product of the derivative gain K_D and the change in glucose concentration ΔG, $R_I=K_D\Delta G$.

Setting the two equations for R_I equal to each other and solving for K_D yields,

$$K_D = \frac{W}{S_I}\frac{A_k DI}{\Delta G}.$$

As mentioned above, $DI/\Delta G$ and A_k are constants available or calculated from data in published literature. Combining the constants into a single constant, Q,

$$Q = \frac{A_k DI}{\Delta G},$$

yields an equation for the derivative gain K_D that is a function of the user's body weight W and the user's insulin sensitivity S_I,

$$K_D = \frac{W}{S_I}Q.$$

Once the derivative gain K_D is calculated, the proportional and integral gains are calculated using ratios. The ratio of K_D/K_P can be set to the dominant time constant for insulin action, ranging from 10-60 minutes, but more typically 20-40 minutes and preferably 30 minutes. For example, calculating K_P given K_D using a time constant of 30 minutes, yields the following relationship:

$$\frac{K_D}{K_P} = 30 \Rightarrow K_P = \frac{K_D}{30}.$$

In a similar fashion, the ratio of K_D/K_I can be set to the average ratio measured from a population of NGT individuals. And K_I can be calculated from K_D.

In particular embodiments, the user enters their body weight W and insulin sensitivity S_I into the device that contains the controller. Then the controller gains are automatically calculated and used by the controller. In alternative embodiments, an individual enters the user's body weight W and insulin sensitivity S_I into a device and the device provides the information to the controller to calculate the gains.

A study was conducted to confirm that the insulin response for an individual could be reproduced using the glucose sensor as an input. In the study, glucose and insulin measurements were taken while a hyperglycemic clamp was applied to a NGT individual. The glucose level measurements, shown in FIG. **29**A, were used as the inputs to a mathematical model created to simulate a PID insulin response controller. The insulin dosing commanded by the controller in response to the glucose clamp very closely approximates the actual insulin appearance in the NGT individual, as shown in FIG. **29**B. The insulin concentration measured from periodic blood samples **456** taken from the individual during the test are represented by dots in FIG. **29**B. The output from the math-

ematical model simulating the insulin response commanded by the controller is shown as a solid line **458** in FIG. **29**B.

Three different devices were used to measure the individual's blood glucose during the study. Blood glucose meter readings **460** from periodic blood samples taken from the individual are represented by the dots in FIG. **29**A. Two MiniMed sensors (such as those described in the section entitled "sensor", below) were placed in the individual's subcutaneous tissue, and the sensor readings **462**, **464** are shown as lines in FIG. **29**A. The sensor readings **462**, **464** are slightly delayed compared to the meter readings **460**. The delay is most likely due to the delay between blood glucose and interstitial fluid (ISF) glucose and can be substantially corrected through the use of a filter if needed. In this study, the delay was not corrected by a filter and did not significantly affect the controller's ability to command an insulin response that matches the natural response of the NGT individual. This study indicates that the PID insulin response controller model is a good minimal model of insulin secretion that captures the biphasic response of healthy β-cells. Correction of the delay is only expected to increase the accuracy of the model.

Fuzzy Logic to Select Between Multiple Sets of Controller Gains

In preferred embodiments, one set of controller gains is used for a particular individual. In alternative embodiments, more than one set of controller gains is used, and fuzzy logic is used to select between sets of controller gains and to determine when to change from one set of controller gains to another. In particular alternative embodiments, the controller gains are different if the glucose level is above or below the desired glucose basal level. In other alternative embodiments, the controller gains are different if the glucose level is increasing or decreasing. A justification for different sets of gains comes from physiological studies that indicate that β-cells turn off faster than they turn on. In still other alternative embodiments, the controller gains are different depending on whether the glucose level is above or below the desired glucose basal level and whether the glucose level is increasing or decreasing, which results in four sets of controller gains. In additional alternative embodiments, the controller gains change depending on the magnitude of the hypoglycemic excursion. In other words, the controller gains for small changes in glucose are different than those for large changes in glucose.

Self-Tuning Controller Gains

Further embodiments may include a controller that self-tunes one or more the gains, K_P, K_I, K_D to accommodate changes in insulin sensitivity. In particular embodiments, previous measurements of glucose levels are compared to the desired basal glucose level G_B. For example, the desired basal glucose level G_B is subtracted from the previous glucose level measurements. Then any negative values, within a predefined time window, are summed (in essence integrating the glucose level measurements that were below the basal glucose level G_B). If the resulting sum is greater than a pre-selected hypoglycemic integral threshold, then the controller gains are increased by a factor $(1+\alpha)$. Conversely, if the integral of the glucose level measurements that were measured above the basal glucose level G_B within the predefined time window is greater than a pre-selected hyperglycemic integral threshold, then the controller gains are decreased by a factor $(1-\alpha)$.

In particular embodiments, the predefined time window over which the glucose concentration integrals are evaluated is generally 24 hours, and the controller gains are adjusted if needed at the end of each predefined time window. In alternative embodiments, the integrals of the glucose level measurements are continuously calculated over a moving window of time, and if either integral exceeds a threshold, the gains are immediately adjusted. In particular embodiments, the moving time window is one hour, and the time window may be restarted whenever the gains are adjusted. In other alternative embodiments, the time window is longer or shorter depending on the sensor accuracy, the rate at which an individual's insulin sensitivity changes, the computational capabilities of the hardware, or the like.

In particular embodiments, the adjustment amount (α) is 0.01. In alternative embodiments, the adjustment amount α is greater or smaller depending on the sensor accuracy, the rate at which an individual's insulin sensitivity changes, the rate at which the sensor sensitivity S_I changes, or the like. In still other alternative embodiments, the adjustment amount α is made larger or smaller depending on the amount that the integral of the measured glucose levels exceeds a threshold. In this way, the gains are adjusted by greater amounts if the measured glucose level G is significantly deviating from the desired blood glucose level G_B and less if the measured glucose level G is closer to the desired blood glucose level G_B. In additional alternative embodiments, the controller employs a Kalman filter.

State Variable Feedback

While the primary signal determining the β-cell's insulin response is glucose, there also exists a putative effect of insulin per se to inhibit insulin secretion. This effect may be directly related to the concentration of insulin in plasma (IP(t)), or mediated through some signal proportional to insulin effect (IEFF(t)). The β-cell can likely directly sense these signals (i.e., directly sense insulin concentration and secondary signals proportional to insulin effect such as free fatty acid). Feedback from these intermediary signals is analogous to what is known as state variable feedback; that is feedback, whereby the variable being controlled (glucose in this case) is used together with feedback of each intermediary signal that affects the variable (insulin concentration in plasma and interstitial fluid). With this type of feedback, undesirable slow kinetic process can be made to appear much faster than they are. For example, if β-cell insulin secretion were inhibited by a signal proportional to insulin concentration in the interstitial fluid where it acts, the delay between plasma and interstitial insulin could be made to appear to be shorter. For the artificial closed-loop algorithm, or for "semi-closed-loop" algorithms, this beneficial effect can be achieved by using "state observers" (mathematical equations that predict the insulin concentration in various parts of the body knowing the history of past insulin delivery). In "semi-closed loop" algorithms, the algorithms are the same as for closed loop algorithms but there is a user confirmation step before any insulin is actually administered. By using state variable feedback, it is possible to make the insulin in an insulin pump act faster than the insulin actually is.

To estimate subcutaneous insulin concentration, plasma insulin concentration, and insulin effect, the following equations may be used:

$$\frac{dI_{SC}}{dt} = \alpha_1(I_D - I_{SC})$$

$$\frac{dI_P}{dt} = \alpha_2(I_{SC} - I_P)$$

$$\frac{dI_{EF}}{dt} = \alpha_3(I_P - I_{EF})$$

Wherein I_{SC} is the estimate of normalized insulin concentration in the subcutaneous space, I_P is the estimate of nor-

malized insulin concentration in the plasma, I_{EF} is the estimate of insulin effect on glucose, α_1 is the rate constant between insulin delivery and the subcutaneous insulin compartment, α_2 is the rate constant between subcutaneous insulin and plasma compartments, α_3 is the rate constant between the plasma compartment and the insulin effect. I_D is the delivered insulin, which can be a function of the three state variables (I_{SC}, I_P, and I_{EF}).

In particular embodiments, an open loop fixed base rate plus user requested bolus would result in the bolus being increased a certain amount and the basal rate subsequently decreased the same amount in accordance to the following formula:

$$I_D'=(1+\gamma_1+\gamma_2+\gamma_3)I_D-\gamma_1 I_{SC}-\gamma_2 I_P-\gamma_3 I_{EF}$$

Wherein I_D is the user requested basal (U/h) plus bolus (U) profile and I_D' is the state feedback adjusted profiles. Note that for a given kinetic excursion the total amount of insulin requested (area under curve of I_D) and delivered (area under curve of I_D') is identical. Here, γ_1, γ_2, and γ_3 are state-feedback gains (scalars). Careful choice of these gains the pump to correct its delivery rate to compensate for delays associated with the dispersion of insulin from the bolus injection into the subcutaneous layer of the patient, to the plasma, and to its actual insulin effect/action on the body. Thus, by estimating how much insulin from a bolus is in the subcutaneous layer, the plasma, or is actually acting on the patient's glucose level (state variables I_{SC}, I_P and I_{EF}), it is possible to optimize delivery of insulin over time to the patient. Using state feedback the bolus is increased by an amount $(1+\gamma_1+\gamma_2+\gamma_3)$ that is gradually taken away from future insulin delivery $(-\gamma_1 I_{SC}-\gamma_2 I_P-\gamma_3 I_{EF})$. As a result, the apparent insulin pharmokinetic curve appears faster. This is akin to developing a faster acting insulin, but it is achieved algorithmically by rearranging the distribution of the insulin delivery per unit bolus by delivering more upfront and removing the extra amount at a later time. The three gains can be chosen to move the time delays ($1/\alpha_1$, $1/\alpha_2$, and $1/\alpha_3$) to any arbitrary locations. In control theory, this is known as pole placement.

State feedback can be used in open loop and closed loop insulin delivery algorithms and with "semi-closed-loop" delivery algorithms. State feedback can be used in conjunction with a Proportional-Integral-Derivative (PID) or any other type of closed loop controller. γ_1 is the feedback gain multiplied to I_{SG}, γ_2 is the feedback gain multiplied to I_p, and γ_3 is the feedback gain multiplied to I_{EF}.

The physical state space form directly taken from the equations above is:

$$\begin{cases} \begin{bmatrix} \dot{I}_{SC} \\ \dot{I}_P \\ \dot{I}_{EF} \end{bmatrix} = \begin{bmatrix} -\alpha_1 & 0 & 0 \\ \alpha_2 & -\alpha_2 & 0 \\ 0 & \alpha_3 & -\alpha_3 \end{bmatrix} \cdot \begin{bmatrix} I_{SC} \\ I_P \\ I_{EF} \end{bmatrix} + \begin{bmatrix} \alpha_1 \\ 0 \\ 0 \end{bmatrix} \cdot I_D \\ I_D = [0 \quad 0 \quad 0] \cdot \begin{bmatrix} I_{SC} \\ I_P \\ I_{EF} \end{bmatrix} + \begin{bmatrix} 1 \\ 0 \\ 0 \end{bmatrix} \cdot I_D \end{cases} \text{ or } \begin{cases} \dot{x} = Ax + Bu \\ y = Cx + du \end{cases}$$

The finite difference form is calculated as follows (wherein e^X indicates an exponential function):

Define: $k_1=e^{-\alpha_1 T}$, $k_2=e^{-\alpha_2 T}$, $k_3=e^{-\alpha_1 T}$

$$I_{SC}(i)=(1-k_1)(I_D(i-1))+k_1 I_{SC}(i-1) \quad \text{(eq 1b)}$$

$$I_P(i)=(1-k_2)(I_{SC}(i))+k_2 I_P(i-1) \quad \text{(eq 2b)}$$

$$I_{EF}(i)=(1-k_3)(I_P(i))+k_3 I_{EF}(i-1) \quad \text{(eq 3b)}$$

The Laplace Form is as follows, wherein s represents the Stackel determinant used in Laplace equations:

$$\frac{I_{SC}}{I_D} = \frac{\alpha_1}{s+\alpha_1} \quad \text{(eq 1c)}$$

$$\frac{I_P}{I_{SC}} = \frac{\alpha_2}{s+\alpha_2} \quad \text{(eq 2c)}$$

$$\frac{I_{EFF}}{I_P} = \frac{\alpha_3}{s+\alpha_3} \quad \text{(eq 3c)}$$

$$\frac{I_P}{I_D} = \frac{\alpha_1\alpha_2}{(s+\alpha_1)(s+\alpha_2)} \quad \text{(eq 4)}$$

$$\frac{I_{EFF}}{I_D} = \frac{\alpha_1\alpha_2\alpha_3}{(s+\alpha_1)(s+\alpha_2)(s+\alpha_3)} \quad \text{(eq 5)}$$

To obtain the transfer function of insulin delivery with state feedback, the control equation is as follows, wherein E represents the error between the actual glucose concentration and the desired glucose concentration ($G-G_D$):

$$I_D=\text{PID}\cdot E-\gamma_1 I_{SC}-\gamma_2 I_P-\gamma_3 I_{EFF} \quad \text{(eq 6)}$$

Substituting equations (eq 1c), (eq 4) and (eq 5) into (eq 6) and rearranging, the following transfer functions are obtained, wherein GM is a gain multiplier:

$$\frac{I_D}{E} = \frac{(GM)(PID)(s+\alpha_1)(s+\alpha_2)(s+\alpha_3)}{(s+\alpha_1)(s+\alpha_2)(s+\alpha_3)+\alpha_1\gamma_1(s+\alpha_2)(s+\alpha_3)+\alpha_1\alpha_2\gamma_2(s+\alpha_3)+\alpha_1\alpha_2\alpha_3\gamma_3} \quad \text{(eq 7)}$$

$$\frac{I_{SC}}{E} = \frac{(GM)(PID)\alpha_1(s+\alpha_2)(s+\alpha_3)}{(s+\alpha_1)(s+\alpha_2)(s+\alpha_3)+\alpha_1\gamma_1(s+\alpha_2)(s+\alpha_3)+\alpha_1\alpha_2\gamma_2(s+\alpha_3)+\alpha_1\alpha_2\alpha_3\gamma_3} \quad \text{(eq 8)}$$

$$\frac{I_P}{E} = \frac{(GM)(PID)\alpha_1\alpha_2(s+\alpha_3)}{(s+\alpha_1)(s+\alpha_2)(s+\alpha_3)+\alpha_1\gamma_1(s+\alpha_2)(s+\alpha_3)+\alpha_1\alpha_2\gamma_2(s+\alpha_3)+\alpha_1\alpha_2\alpha_3\gamma_3} \quad \text{(eq 9)}$$

$$\frac{I_{EFF}}{E} = \frac{(GM)(PID)\alpha_1\alpha_2\alpha_3}{(s+\alpha_1)(s+\alpha_2)(s+\alpha_3)+\alpha_1\gamma_1(s+\alpha_2)(s+\alpha_3)+\alpha_1\alpha_2\gamma_2(s+\alpha_3)+\alpha_1\alpha_2\alpha_3\gamma_3} \quad \text{(eq 10)}$$

The computation of the gain multiplier is also obtained in the state variable feedback method. When state variable feedback is used, the gain multiplier (GM) is a scalar that forces a step response to reach the same steady value whether state feedback is used or not. In other words, GM ensures that the total amount given per unit of bolus will be the same in both cases. In the case of state feedback, more insulin is given up front, but this extra insulin is taken away later. To calculate GM in particular embodiments, the "final value theorem" from control systems is used. The final value theorem states that to evaluate the steady state of any transfer function T(s) given any input X(s), the steady state output response to the input is given by:

$$y_{SS}(t\rightarrow\infty)=lim_{s\rightarrow 0}(sT(s)X(s))$$

The Laplace form of a step input is given by

$$X(s) = \frac{1}{s}$$

and the steady state solution of the final value theorem simplifies to:

$$y_{SS}(t\rightarrow\infty))=lim_{S\rightarrow 0}(T(s)).$$

In the case when there is no state feedback, (γ_1, γ_2 and γ_3=0), the steady state solution may be obtained from equation (eq 7) to be as follows:

$$I_D(t\rightarrow\infty)=1 \quad \text{(eq 11)}$$

With state feedback without the gain correction factor, the steady state solution is:

$$I_D(t \rightarrow \infty) = \frac{1}{1+\gamma_1+\gamma_2+\gamma_3} \quad \text{(eq 12)}$$

GM is then evaluated as the ratio of equation (eq 12) to equation (eq 11) to obtain the following: $GM=1+\gamma_1+\gamma_2+\gamma_3$.

Using state variable feedback, a closed loop control equation and state feedback gain are determined for pole placement. Specifically, the gains are calculated for the insulin delivery equation shown above. In particular embodiments, they are determined as follows: First, with state feedback, the denominator of equations (eq 7), (eq 8), (eq 9), and (eq 10) is:

$$D=s^3+(\alpha_1+\alpha_2+\alpha_3+\gamma_1\alpha_1)s^2+(\alpha_1\alpha_2+(\alpha_1+\alpha_2)\alpha_3+\gamma_2\alpha_1\alpha_2+(\alpha_2+\alpha_3)\gamma_1\alpha_1)s+(\alpha_1\alpha_2\alpha_3+\gamma_3\alpha_1\alpha_2\alpha_3+\gamma_2\alpha_1\alpha_2\alpha_3+\gamma_1\alpha_1\alpha_2\alpha_3) \quad \text{(eq 14)}$$

To get the poles of the system in the equations (eq 7), (eq 8), (eq 9), or (eq 10), D may be set equal to zero yield the characteristic equation:

$$s^3+(\alpha_1+\alpha_2+\alpha_3+\gamma_1\alpha_1)s^2+(\alpha_1\alpha_2+(\alpha_1+\alpha_2)\alpha_3+\gamma_2\alpha_1\alpha_2+(\alpha_2+\alpha_3)\gamma_1\alpha_1)s+(\alpha_1\alpha_2\alpha_3+\gamma_3\alpha_1\alpha_2\alpha_3+\gamma_2\alpha_1\alpha_2\alpha_3+\gamma_1\alpha_1\alpha_2\alpha_3)=0 \quad \text{(eq 16)}$$

If the desired system poles or roots of (eq 16) are defined by eigenvalues λ_1, λ_2 and λ_3, then the characteristic equation can be written as:

$$(s-\lambda_1)(s-\lambda_2)(s-\lambda_3)=0$$

Expanding and collecting like powers of s, (eq 16) can be written as:

$$s^3-(\lambda_1+\lambda_2+\lambda_3)s^2+(\lambda_1\lambda_2+\lambda_1\lambda_3+\lambda_2\lambda_3)S-\lambda_1\lambda_2\lambda_3=0 \quad \text{(eq 17)}$$

Setting the coefficients of like powers of s equal to each other we have the system of equations:

$$\alpha_1+\alpha_2+\alpha_3+\gamma_1\alpha_1=-(\lambda_1+\lambda_2+\lambda_3) \quad \text{(eq 18)}$$

$$\alpha_1\alpha_2+\alpha_1\alpha_3+\alpha_2\alpha_3+\gamma_2\alpha_1\alpha_2+\gamma_1\alpha_1(\alpha_2+\alpha_3)=\lambda_1\lambda_2+\lambda_1\lambda_3+\lambda_2\lambda_3 \quad \text{(eq 19)}$$

$$\alpha_1\alpha_2\alpha_3+\gamma_3\alpha_1\alpha_2\alpha_3+\gamma_2\alpha_1\alpha_2\alpha_3+\gamma_1\alpha_1\alpha_2\alpha_3=\lambda_1\lambda_2\lambda_3 \quad \text{(eq 20)}$$

This results in three equations and three unknowns, γ_1, γ_2 and γ_3. Therefore, the unknown gains can be solved for in terms of the desired poles λ_1, λ_2, λ_3, and system time constants, α_1, α_2 and α_3. These formulas enable us to control the desired pharmacokinetics of insulin as it appears in the different compartments:

$$\gamma_1 = \frac{-(\lambda_1+\lambda_2+\lambda_3+\alpha_1+\alpha_2+\alpha_3)}{\alpha_1}$$

$$\gamma_2 = \frac{\lambda_1\lambda_2+\lambda_1\lambda_3+\lambda_2\lambda_3-\alpha_1\alpha_2-\alpha_1\alpha_3-\alpha_2\alpha_3+(\lambda_1+\lambda_2+\lambda_3+\alpha_1+\alpha_2+\alpha_3)(\alpha_2+\alpha_3)}{\alpha_1\alpha_2}$$

$$\gamma_3 = \frac{-\lambda_1\lambda_2\lambda_3}{\alpha_1\alpha_2\alpha_3} - \frac{\lambda_1\lambda_2+\lambda_1\lambda_3+\lambda_2\lambda_3-\alpha_1\alpha_2-\alpha_1\alpha_3-\alpha_2\alpha_3+(\lambda_1+\lambda_2+\lambda_3+\alpha_1+\alpha_2+\alpha_3)(\alpha_2+\alpha_3)}{\alpha_1\alpha_2} + \frac{(\lambda_1+\lambda_2+\lambda_3+\alpha_1+\alpha_2+\alpha_3)}{\alpha_1} - 1$$

Thus, through the above calculations, the gains can be calculated and used in the control equation for insulin delivery of:

$$I_D=\text{PID}\cdot E-\gamma_1 I_{SC}-\gamma_2 I_P-\gamma_3 I_{EF}$$

PID is the output of a PID controller of any other closed loop (or "semi-closed-loop") controller. The gains are generally calculated just once, but could be calculated more often if desired. The control equation may be calculated on a repeated basis, after predetermined periods of time or continuously. For example, and without limitation, it may be calculated every five, ten, thirty or sixty minutes. Just the state variable portion ($\gamma_1 I_{SC}-\gamma_2 I_P-\gamma_3 I_{EF}$) may be updated or the entire equation may be updated. By updating the control equation, it is possible to continually improve the delivery of insulin to the patient.

A control feedback block diagram of an embodiment of a pump using state variable feedback is shown in FIG. **42**. As shown, the desired glucose G_D **600** of the patient is entered into the PID Controller **610**. The output of the PID controller is an insulin delivery value I_D **601**. The block then calculates how much insulin should actually be delivered to the patient as a bolus in addition to the insulin delivery value and how much should be taken away from the basal rate, as discussed above. At each discrete time interval, Ti, (T1 **620**, T2 **630**, and T3 **640**), the amount of insulin that has entered into the subcutaneous layer from the pump is calculated to provide I_{SC} **602**. That value will be multiplied (or otherwise factored by) γ_1 **605** and subtracted from the output of the PID controller to provide an improved desired insulin value based on the subcutaneous insulin concentration (with the other calculations following). At each discrete time interval Ti, the amount of insulin that has entered into the plasma from the subcutaneous compartment is calculated to provide I_P **603**. That value will be multiplied (or otherwise factored by) γ_2 **606** and subtracted from the output of the PID controller to determine an improved desired insulin value based on the plasma insulin concentration. At each discrete time interval Ti, the amount of insulin actually going into action or the effective insulin compartment from the insulin in the plasma is calculated to provide I_{EF} **604**. That value will be multiplied (or otherwise factored by) γ_3 **607** and subtracted from the output of the PID controller to determine an improved desired insulin value based on the effective insulin. The insulin actually delivered to the subject **650** will then change the blood glucose G of the user **608**, which will then be measured by the sensor **660** and compared to the desired glucose **600**.

FIGS. **43-46** show graphs with the effect of state feedback. FIG. **43** shows the effect on the basal insulin delivery rate achieved using the algorithm described above. A bolus is given at time zero. Line **700** shows the insulin delivery when no state feedback is used. This line would be the same as a regular delivery of an insulin bolus and is indicated as 0.0000, because it does not change the amount of basal rate being delivered. The other three lines illustrate the change in insulin delivery rate over time when all of the state feedback is placed in one of the gains γ_1, γ_2, or γ_3. As can be seen, if all the state feedback is placed in the gain γ_1 (for the subcutaneous layer), the basal insulin delivery rate **701** (in relation to the standard basal rate) starts out low and gradually moves to a limit of zero, or the rate without state feedback, as steady state is reached. If all of the state feedback is placed in the gain γ_2 (for the plasma layer), the basal insulin delivery rate **702** starts at zero, dips lower, and then gradually returns up to a limit of zero as steady state is reached. If all of the state feedback is placed in the gain γ_3 (for the insulin action/effect), the basal insulin delivery rate **703** starts at zero, dips lower, but more

slowly than for the all γ_2 delivery rate, and then gradually returns up to a limit of zero as steady state is reached. In all cases, the total delivery of insulin is the same.

FIG. **44** shows the effect of state feedback per unit bolus on the subcutaneous insulin. In other words, a bolus of insulin is given to a patient at time zero and the figure shows the rate in which the amount of insulin in the subcutaneous layer, from that bolus, decreases to zero. Line **705** shows the amount of insulin in the subcutaneous layer over time with no state feedback. Line **706** shows the amount of insulin in the subcutaneous layer over time when all of the state feedback is placed in gain γ_1. Line **707** shows the amount of insulin in the subcutaneous layer over time when all of the state feedback is placed in gain γ_2. Line **708** shows the amount of insulin in the subcutaneous layer over time when all of the state feedback is placed in gain γ_3.

FIG. **45** shows the effect of state feedback per unit bolus on the plasma insulin. In other words, a bolus of insulin is given to a patient at time zero and the figure shows the rate in which the amount of insulin in the plasma layer, from that bolus, increases from zero (there is a slight delay from injecting insulin to when the insulin moves into the plasma from the subcutaneous layer), reaches its peak and then returns to zero. Line **710** shows the amount of insulin in the plasma over time with no state feedback. Line **711** shows the amount of insulin in the plasma over time when all of the state feedback is placed in gain γ_1. Line **712** shows the amount of insulin in the plasma over time when all of the state feedback is placed in gain γ_2. Line **713** shows the amount of insulin in the plasma over time when all of the state feedback is placed in gain γ_3.

FIG. **46** shows the effect of state feedback per unit bolus on the insulin effect. In other words, a bolus of insulin is given to a patient at time zero and the figure shows the rate in which the amount of insulin from that bolus creates the insulin effect on the body, starting at zero (there is a delay from the injection of insulin into the subcutaneous layer and through the plasma to the insulin effect), rising to its maximum point, and decreasing to zero. Line **715** shows the insulin effect over time with no state feedback. Line **716** shows the insulin effect over time when all of the state feedback is placed in gain γ_1. Line **717** shows the insulin effect over time when all of the state feedback is placed in gain γ_2. Line **718** shows the insulin effect over time when all of the state feedback is placed in gain γ_3.

FIGS. **47** and **48** compare insulin state variable feedback used in conjunction with a PID closed loop controller as opposed to use of a PID closed loop controller alone (with no insulin state variable feedback). FIG. **47** shows the simulated glucose concentration of a patient over time. Meals are given at 8, 13, 18, 22, and 32 hours. The glucose concentration using the PID with insulin state feedback is shown as line **800**. The glucose concentration using the PID without insulin state feedback is shown as line **801**. With glucose concentrations, it is always preferable to keep a patient's concentrations from being too high or too low, so the more that the closed loop program can avoid high and low values, the better. As can be seen in FIG. **47**, as time goes on, the glucose concentration using the PID with insulin state feedback improves over time (versus the glucose concentration using the PID without insulin state feedback) in that it varies less as time goes on, keeping the patient with a more steady glucose level that will greatly reduce hyper- and hypoglycemic events. FIG. **48** shows average simulated insulin delivery profiles from the same system as FIG. **47**. Line **810** represents the insulin delivery using the PID with insulin state feedback. Line **811** represents the insulin delivery using the PID without insulin state feedback. As can be seen, the insulin delivery using the PID with insulin state feedback contains more spikes and dips, resulting from the state feedback.

Modifying the PID Controller to Incorporate an Integrator Leak In preferred embodiments, the PID control response was described with constant gain components, K_P, K_I, K_D. Although the preferred control response guarantees zero steady-state error (i.e., steady state glucose minus a desired basal glucose (G_B)=0), inherently, the integral component $U_I=K_I\int_{t_0}^{t}(G-G_B)dt+U_I(t_0)$ destabilizes feedback control because there is no temporal wind down of the insulin response while the integral component models the increase in the insulin response. Without any correction, the integral component has a tendency to over-estimate the increase in the insulin response. Since a small difference between steady-state glucose and G_B is typically acceptable in insulin response control, an alternative modeling of the integral component can incorporate an integrator leak to reduce the magnitude of the destabilizing effect. Specifically, changes in $U_I(t)$ can be described by a term proportional to the error in glucose and a term that leaks in proportion to the magnitude of U_I. This can be expressed in the formula:

$$\frac{dU_I}{dt}K_I(G-G_B)-K_{LEAK}U_I;$$

with initial condition $U_I(t_0)$.

The parameter K_{LEAK} is the reciprocal time constant of the rate of leaking (τ_{LEAK} in min=$1/K_{LEAK}$), where τ_{LEAK} is a tuning parameter that can be set based on empirical data, and be tied with the other gain components K_P, K_I, K_D. However, the current realization of the artificial β-cell has τ_{LEAK} as a user input. U_I can also be expressed in discrete form by standard methods.

Post-Controller (Lead/Lag) Compensator

In preferred embodiments, commands are issued from the controller without regard to where in the body the insulin delivery system will infuse the insulin. In essence, the assumption is that the insulin is either delivered directly into the blood stream for immediate use by the body, or that any time delays caused by delivering the insulin somewhere in the body other than the blood stream can be compensated for by adjusting K_P, K_I, and K_D. In this case, the commands generally model a β-cell insulin secretion profile, an example of which is shown in FIG. **35**A. And since the β-cells secrete insulin directly into the blood stream, the β-cell insulin secretion profile is the intended blood plasma insulin concentration profile. However, an insulin delivery delay may distort the intended blood plasma insulin concentration profile, as shown in FIG. **35**B. The insulin delivery delay is the amount of time between the instant that the command is given to the insulin delivery system to infuse insulin and the time that insulin reaches the blood plasma. An insulin delivery delay may be caused by a diffusion delay, represented by a circle with an arrow **528** in FIG. **20**, which is the time required for insulin that has been infused into a tissue to diffuse into the blood stream. Other contributors to insulin delivery delay may include, time for the delivery system to deliver the insulin to the body after receiving a command to infuse insulin, time for the insulin to spread throughout the circulatory system once it has entered the blood stream, and/or by other mechanical or physiological causes. In addition, the body clears insulin even while an insulin dose is being delivered from the insulin delivery system into the body. Since insulin is continuously cleared from the blood plasma by the body, an insulin dose that is delivered to the blood plasma too slowly or

is delayed is at least partially, if not significantly, cleared before the entire insulin dose fully reaches the blood plasma. And therefore, the insulin concentration profile in the blood plasma never achieves the same peak (nor follows the same profile) it would have achieved if there were no delay. Given an insulin dose delivered all at once into the blood plasma at time zero, the insulin concentration in the blood plasma is raised virtually instantaneously (not shown) and then would decrease exponentially over time as the body clears (uses or filters out) the insulin, as shown in FIG. **36**A per equation:

$$C_P = \frac{I_0}{V_p} e^{-P_1 t},$$

where:

C_P is the concentration of insulin in the blood plasma,

I_0 is a mass of the insulin dose delivered directly to the blood plasma at time zero,

V_p is a volume of the blood plasma in the body,

P_1 is a reciprocal time constant for insulin clearance, and

t is the time that has passed since the delivery of the insulin dose directly into the blood plasma.

The time constant for insulin clearance P_1 may be calculated using the following equation:

$$P_1 = -\frac{k}{V_p},$$

where:

k is the volume insulin clearance rate, and

V_p is a volume of the blood plasma in the body.

Or the time constant for insulin clearance P_1 may be obtained by providing insulin to an individual that does not generate his own insulin, and then periodically testing blood samples from the individual for insulin concentration. Then, using an exponential curve fitting routine, generate a mathematical expression for a best-fit curve for the insulin concentration measurements, and observe the time constant in the mathematical expression.

Given the same insulin dose (delivered at time zero all at once) into the subcutaneous tissue, instead of directly into the blood plasma, the concentration of insulin in the blood plasma would begin to rise slowly as insulin diffuses from the interstitial fluid ISF into the blood plasma, as shown in FIG. **36**B. At the same time that insulin is entering the blood plasma, the body is clearing insulin from the blood. While the rate at which insulin is entering the blood plasma exceeds the insulin clearance rate, the insulin concentration in the blood plasma continues to increase. When the insulin clearance rate exceeds the rate at which insulin is entering the blood plasma from the interstitial fluid ISF, the insulin concentration in the blood plasma begins to decrease. So, the result of delivering insulin into the interstitial fluid ISF instead of directly into the blood stream is that the insulin concentration in the blood plasma is spread over time rather than increased virtually instantaneously to a peak followed by a decay.

A bi-exponential equation may be used to model the insulin concentration in blood plasma given an insulin dose delivered to the subcutaneous tissue:

$$C_P = \frac{I_0 D}{V_p V_{ISF}(P_3 - P_2)}(e^{-P_2 t} - e^{-P_3 t}),$$

where:

C_P is the concentration of insulin in the blood plasma,

I_0 is the mass of the insulin dose delivered to the subcutaneous tissue at time zero,

D is a diffusion coefficient (the rate at which insulin diffuses from the interstitial fluid ISF into the blood glucose)

V_p is a volume of the blood plasma in the body,

V_{ISF} is a volume of interstitial fluid ISF that the insulin is delivered to,

P_2 is a time constant,

P_3 is a time constant greater than or equal to P_2, and

t is time since the delivery of the insulin dose into the interstitial fluid ISF.

The time constants may be calculated using the quadratic formula:

$$P_2, P_3 = -\frac{a_1 \pm \sqrt{a_1^2 - 4a_0}}{2}, \text{ where:}$$

$$a_1 = \frac{D+K}{V_p} + \frac{D}{V_{ISF}}, \text{ and}$$

$$a_0 = \left(\frac{D+K}{V_P}\right)\left(\frac{D}{V_{ISF}}\right) - \frac{D^2}{V_{ISF} V_P}.$$

In alternative embodiments, a post-controller lead-lag compensator **522** is used to modify the commands (U_{PID}) to compensate for the insulin delivery delay and/or the insulin clearance rate k, as shown in FIG. **37**. The post-controller lead-lag compensator **522** is of the form

$$\frac{U_{COMP}}{U_{PID}} = \frac{s+\alpha}{s+\gamma}$$

where $1/\alpha$ and $1/\gamma$ are the lead and lag constants respectively, s is the Laplace variable, and U_{COMP} is the compensated commands calculated by the lead-lag compensator **522**.

The PID controller generates commands (U_{PID}) for a desired insulin delivery rate into the blood plasma. The commands U_{PID} are calculated and issued periodically depending on the update rate for the control loop, which is selected based on a maximum anticipated rate of change of the blood glucose level, an insulin delivery system minimum insulin dosage, insulin sensitivity, a maximum and a minimum acceptable glucose concentration, or the like. The commands U_{PID} are used as inputs to the post-controller lead-lag compensator **522**.

In particular embodiments, the compensated commands (U_{COMP}) issued from the post-controller lead-lag compensator **522** uses more than one value from the controller. In particular embodiments, post-controller lead-lag compensator **522** uses the present command (U_{PID}^n) and the previous command (U_{PID}^{n-1}) to calculate a compensated command U_{COMP} per a compensation equation:

$$U_{COMP}^n = (1-\gamma)U_{COMP}^{n-1} + U_{PID}^n + (1-\alpha)U_{PID}^{n-1},$$

where:

U_{PID}^n is the present command,

U_{PID}^{n-1} is the previous command,

U_{COMP}^{n-1} is the previous compensated control output,

α is the reciprocal lead time constant in min^{-1}, and

γ is the reciprocal lag time constant in min^{-1}.

This is a first forward difference equation. However, other forms can be used alternatively (e.g., first backward or bilinear), but all result in a compensated control output (U_{COMP}) that is comprised of a weighted history of both past PID outputs (U_{PID}), and past compensated outputs (U_{COMP}).

An alternative method of modifying the commands (U_{PID}) to compensate for the insulin delivery delay and/or the insulin clearance can be performed based on a weighted history of past insulin delivery. By giving the most recent delivery history more weight, the weighted history of the previous insulin delivered can then be subtracted from the present PID control output to yield a compensated control output. Expressed in Laplace domain this results in:

$$U_{COMP} = PID\ E - \frac{\lambda}{s+\alpha} U_{COMP},$$

where E is the Laplace transformed error signal ($G-G_B$), λ determines how much the PID output is reduce in proportion to the weighted history of past control outputs, and α is the reciprocal time constant determining how long a history is weighted (the preferred value of α would be equal to the reciprocal dominant time constant or subcutaneous insulin appearance, P_2). Solving the compensated signals as a function of the error results in:

$$\frac{U(s)}{E(s)} = PID\frac{s+\alpha_w}{s+(\alpha+\lambda)} = PID\frac{s+\alpha_w}{s+\gamma},$$

which is identical to the previously described lead-lag compensation.

In other alternative embodiments, additional previous command values may be used. In still other alternative embodiments, the compensation equation compensates for both time constants P_2 and P_3.

In still more alternative embodiments, the controller gains are modified to include the effects of the post-controller lead/lag compensator so that the post-controller lead/lag compensator is not needed to modify the commands to account for the insulin delivery delay.

In particular embodiments, the insulin delivery system provides finite insulin doses into the body in response to commands from the controller. The smallest amount of insulin that the insulin delivery system can deliver is the minimum finite insulin dose. The controller may generate commands for a dose of insulin to be delivered that is not a whole number multiple of the minimum finite insulin dose. Therefore, either too much or too little insulin is delivered by the insulin delivery system in response to the commands. In particular alternative embodiments, the post-controller lead-lag compensator truncates the command to the nearest whole number multiple of the minimum finite insulin dose and adds the remaining commanded volume of insulin to the next command. In other alternative embodiments, a compensator rounds the command to the nearest whole number multiple of the minimum finite insulin dose. In still other alternative embodiments, other methods are used to compensate for the difference between the commands and the nearest whole number multiple of the minimum finite insulin dose. In other embodiments, no compensation is needed.

Eliminating the Lead-Lag Compensator with Feedback of Predicted Plasma Insulin

Yet in another alternative embodiment, the PID control commands may be modified to emulate the effect of plasma insulin on a β-cell to determine optimal insulin administration by feeding back a predicted plasma insulin based on the subcutaneous insulin infusion. The net effect of such feedback is to replace an undesired dynamic with a more desirable one and achieve a plasma insulin profile that a β-cell would achieve. This can be seen as follows (using Laplace transformed variables). Assume the relation between glucose above basal ($G-G_B$) and insulin delivery (ID) is described by a linear transfer function $ID(s)=C(s)(G(s)-G_B)$, where C(s) may be, but is not necessarily, described by the PID controller transfer function. If the β-cell is using peripheral insulin ($I_p(s)$) levels to suppress insulin secretion the predicted rate of insulin delivery would be modified as: $ID(s)=C(s)(G(s)-G_B)-kI_p(s)$.

For portal insulin delivery the relation between ID(s) and plasma insulin $I_P(s)$ is known to be approximated by a single time delay:

$$I_p(s) = \frac{k_1}{s+\alpha} ID(s).$$

Substituting $I_p(s)$ value into the previous formula and making k large results in:

$$ID(s) = \frac{C(s)(G(s)-G_B)}{1+\frac{kk_1}{s+\alpha}} \approx C(s)\frac{s+\alpha}{kk_1}(G(s)-G_B);\ 1 \ll \frac{kk_1}{s+\alpha},$$

which would completely cancel the undesirable time constant $1/\alpha$. In practice a lower value of k would be used resulting in:

$$ID(s) = C(s)(G(s)-G_B) - \frac{kk_1}{s+\alpha} ID(s) = C(s)\frac{s+\alpha}{s+\gamma}(G(s)-G_B).$$

where $\gamma=\alpha+kk_1$ (i.e., something greater than α). Thus, the effect for the β-cell, of adding a plasma insulin feedback is to replace the portal insulin delivery time constant (α) with a faster time constant ($\gamma=\alpha+kk_1$; $\gamma>\alpha$). In block diagram form:

$$G-G_B \rightarrow \boxed{C(s)\cdot\frac{s+a}{s+\gamma}} \xrightarrow{ID} \boxed{\frac{k_1}{s+\alpha}} \xrightarrow{I_p}$$

which is equivalent to:

$$G-G_B \rightarrow \boxed{C(s)\cdot\frac{1}{s+\gamma}} \xrightarrow{I_p}$$

To apply this mechanism to subcutaneous insulin delivery all that is needed is the transfer function between sc insulin delivery and plasma insulin. This transfer function is well approximated by a bi-exponential time course (bolus response) or:

$$\frac{I_p(s)}{ID_{SC}(s)} = \frac{k_2}{(s+\alpha_1)(s+\alpha_2)}$$

thus,

$$ID(s) = C(s)(G(s)-G_B) - \frac{kk_2}{(s+\alpha_1)(s+\alpha_2)} ID(s)$$
$$= C(s)\frac{1}{1+\frac{kk_2}{(s+\alpha)(s+\alpha_2)}}(G(s)-G_B)$$

in the limiting case as $kk_2/(s+\alpha_1)(s+\alpha_2)>>1$ this is approximately equal to

$$ID(s) = C(s)\frac{(s+\alpha_1)(s+\alpha_2)}{kk_2}(G(s)-G_B)$$

where again, the undesirable time constants associated with subcutaneous insulin delivery have been eliminated. In practice they would just be replaced with more desirable rate constants (i.e., faster time constants).

Correction of Hypoglycemic Excursion Around ~200 Minutes (Wind-Down)

Previous modeling of β-cells using a PID controller gave excellent predictability of the "first" and "second" phase

insulin responses during prolonged periods of increased glucose appearance. However, if the periods of increased glucose appearance is followed by a rapid decrease in glucose appearance, the PID controller would not be able to correctly predict the wind down of the insulin response to lower glucose levels. FIG. **41**B illustrates the insulin response to the blood glucose level of FIG. **41**A based on the clinical data (shown as data points), the PID modeling (shown as a solid line), and correction of the PID for the hypoglycemic excursion (shown as a dashed line).

In preferred embodiments, the hypoglycemic excursion is corrected by modifying the PID controller to a PD control with Adaptive Proportional Gain (or Bilinear PID controller), which is modified form of the original PID equations. As described previously, the discrete PID algorithm is as follows:

Proportional Component Response:

$$P_{con}^{n}=K_p(SG_f^n-G_{sp}),$$

Integral Component Response:

$$I_{con}^{n}=I_{con}^{n-1}+K_I(SG_f^n-G_{sp});I_{con}^{0}=I_b, \text{ and}$$

Derivative Component Response:

$$D_{con}^{n}=K_D dGdt_f^n,$$

where K_P, K_I and K_D are the proportional, integral, and derivative gain coefficients, SG_f and $dGdt_f$ are the filtered sensor glucose and derivative respectively, and the superscript n refers to discrete time.

In the Bilinear PID controller, the proportional gain K_P is based on the integrated error term. The magnitude of each component's contribution to the insulin response is described by the following equations:

$$P_{con}^{n}=K_P^n(SG_f^n-\text{INT})$$

$$D_{con}^{n}=K_D dGdt_f^n$$

$$K_P^n=K_P^{n-1}+K_I(SG_f^n-G_{sp}), \text{ where } K_P^0=K_{P0}$$

Where the proportional gain now integrates at rate K_I (initial value K_{P0}) and the proportional component is related to an intercept value (INT) where (INT<G_{sp}). The modified formulation can be seen to fit the hypoglycemic glucose excursion without systematic error as the adaptive PD line shown as a dashed line in FIG. **39**.

In additional embodiments, the Bilinear PID controller can also incorporate an integrator leak by modifying the formula to multiply the previous K_P with a value such as a as follows:

$$K_P^n=\alpha K_P^{n-1}+K_I(SG_f^n-G_{sp}), \text{ where } \alpha\approx 0.99$$

An alternative method of correcting the hypoglycemic glucose excursion can be performed by integrator clip into the PID control. PID controllers generally have integrator-reset rules that prevent excessive "winding" and such a rule can be used to correct the hypoglycemic glucose excursion. For example, the integrator can be clipped as follows:

$$\text{If } (SG\leq 60 \text{ mg/dl AND } I_{con}^{n-1}>K_P(SP-60)) \text{ then } I_{con}^{n-1}=K_P(SP-60)$$

This equation resets the integrator such that if the sensor glucose falls below 60 mg/dl the insulin delivery is zero for all stable or falling sensor glucose signals. The clipping limit represents an absolute threshold, similar to the human counter regulatory response.

However, other approaches that may emulate the β-cell more accurately include the use of piecewise continuous functions. For example, the following function allows for progressive clipping to be tuned:

$$\gamma(SG)=\gamma_0+(1-\gamma_0)\left[\frac{T_{1-SG}}{T_{1-60}}\right]$$

$$\text{if } (SG\leq T_1 \text{mg/dl AND } I_{con}^{n-1}>\gamma K_p(SP-60))$$

$$\text{then}$$

$$I_{con}^{n-1}=\gamma K_P(SP-60)$$

This equation introduces two additional tuning parameters (γ_0 and T_1) and starts to check the integrator output at a higher threshold. For example, if γ_0=5 and T_1=100 mg/dl, the integrator output would be clipped to 4 K_P60 if glucose fell to 90 mg/dl, 3 K_P60 if glucose fell to 80 mg/dl and so forth until glucose reached 60 where it would be clipped at K_P60. Other functions than that proposed in the above equation (e.g. functions based on the rate of fall of glucose, or percent decrease in I_{con}) may alternatively be used.

System Configurations

The following sections provide exemplary, but not limiting, illustrations of components that can be utilized with the controller described above. Various changes in components, layout of various components, combinations of elements, or the like may be made without departing from the scope of the embodiments of the invention.

Before it is provided as an input to the controller **12**, the sensor signal **16** is generally subjected to signal conditioning such as pre-filtering, filtering, calibrating, or the like. Components such as a pre-filter, one or more filters, a calibrator and the controller **12** may be split up or physically located together, and may be included with a telemetered characteristic monitor transmitter **30**, the infusion device **34**, or a supplemental device. In preferred embodiments, the pre-filter, filters and the calibrator are included as part of the telemetered characteristic monitor transmitter **30**, and the controller **12** is included with the infusion device **34**, as shown in FIG. **8**B. In alternative embodiments, the pre-filter is included with the telemetered characteristic monitor transmitter **30** and the filter and calibrator are included with the controller **12** in the infusion device, as shown in FIG. **8**C. In other alternative embodiments, the pre-filter may be included with the telemetered characteristic monitor transmitter **30**, while the filter and calibrator are included in the supplemental device **41**, and the controller is included in the infusion device, as shown in FIG. **8**D. To illustrate the various embodiments in another way, FIG. **9** shows a table of the groupings of components (pre-filter, filters, calibrator, and controller) in various devices (telemetered characteristic monitor transmitter, supplemental device, and infusion device) from FIGS. **8**A-D. In other alternative embodiments, a supplemental device contains some of (or all of) the components.

In preferred embodiments, the sensor system generates a message that includes information based on the sensor signal such as digital sensor values, pre-filtered digital sensor values, filtered digital sensor values, calibrated digital sensor values, commands, or the like. The message may include other types of information as well such as a serial number, an ID code, a check value, values for other sensed parameters, diagnostic signals, other signals, or the like. In particular embodiments, the digital sensor values Dsig may be filtered in the telemetered characteristic monitor transmitter **30**, and then the filtered digital sensor values may be included in the

message sent to the infusion device **34** where the filtered digital sensor values are calibrated and used in the controller. In other embodiments, the digital sensor values Dsig may be filtered and calibrated before being sent to the controller **12** in the infusion device **34**. Alternatively, the digital sensor values Dsig may be filtered, and calibrated and used in the controller to generate commands **22** that are then sent from the telemetered characteristic monitor transmitter **30** to the infusion device **34**.

In further embodiments, additional optional components, such as a post-calibration filter, a display, a recorder, and a blood glucose meter may be included in the devices with any of the other components or they may stand-alone. Generally, if a blood glucose meter is built into one of the devices, it will be co-located in the device that contains the calibrator. In alternative embodiments, one or more of the components are not used.

In preferred embodiments, RF telemetry is used to communicate between devices, such as the telemetered characteristic monitor transmitter **30** and the infusion device **34**, which contain groups of components. In alternative embodiments, other communication mediums may be employed between devices such as wires, cables, IR signals, laser signals, fiber optics, ultrasonic signals, or the like.

Filtering

In preferred embodiments, the digital sensor values Dsig and/or the derivative of the digital sensor values are processed, filtered, modified, analyzed, smoothed, combined, averaged, clipped, scaled, calibrated, or the like, to minimize the effects of anomalous data points before they are provided as an input to the controller. In particular embodiments, the digital sensor values Dsig are passed through a pre-filter **400** and then a filter **402** before they are passed to the transmitter **70**, as shown in FIG. **16**. The filters are used to detect and minimize the effects of anomalous digital sensor values Dsig. Some causes of anomalous digital sensor values Dsig may include temporary signal transients caused by sensor separation from the subcutaneous tissue, sensor noise, power supply noise, temporary disconnects or shorts, and the like. In particular embodiments, each individual digital sensor value Dsig is compared to maximum and minimum value-thresholds. In other particular embodiments, the differences between consecutive pairs of digital sensor values Dsig are compared with rate-of-change-thresholds for increasing or decreasing values.

Pre-Filter

In particular embodiments, the pre-filter **400** uses fuzzy logic to determine if individual digital sensor values Dsig need to be adjusted. The pre-filter **400** uses a subset of a group of digital sensor values Dsig to calculate a parameter and then uses the parameter to determine if individual digital sensor values Dsig need to be adjusted in comparison to the group as a whole. For example, the average of a subset of a group of digital sensor values Dsig may be calculated, and then noise thresholds may be placed above and below the average. Then individual digital sensor values Dsig within the group are compared to noise thresholds and eliminated or modified if they are outside of the noise thresholds.

A more detailed example is provided below to more clearly illustrate, but not limit, an embodiment of a pre-filter. A group of eight digital sensor values Dsig are shown in FIG. **17** including a most recently sampled value, labeled L, sampled from the analog sensor signal Isig at time i, and the seven previous values K, H, G, F, E, D, and C sampled at times (i−1) through (i−7). An average value is calculated using the four temporally middle values in the group, H, G, F, and E sampled at times (i−2) through (i−5). The calculated average value is represented as a dashed/dotted average line **404**. A high noise threshold **406** is established at 100% above the average line **404**. In other words, the magnitude of the high noise threshold **406** is two times the magnitude of the average line **404**. A negative noise threshold **408** is established at 50% below the average line **404**. In other words, the magnitude of the negative noise threshold **408** is one half of the magnitude of the average line **404**. The individual magnitudes of each of the eight values, L, K, H, G, F, E, D, and C are compared to the high and negative noise thresholds **406** and **408**. If a value is above the high noise threshold **406** or below the negative noise threshold **408** then the value is considered anomalous and the anomalous value is replaced with the magnitude of the average line **404**. In the example shown in FIG. **17**, the value K is above the high noise threshold **406** so it is replaced with the average value M. Also, the value D is below the negative noise threshold **408** so it is replaced with the average value N. In this way noisy signal spikes are reduced. Therefore, in the example, values L, K, H, G, F, E, D, and C are inputs to the pre-filter **400** and values L, M, H, G, F, E, N, and C are outputs from the pre-filter **400**. In alternative embodiments, other noise threshold levels (or percentages) may be used. In other alternative embodiments, values outside of the thresholds may be replaced with values other than the average value, such as the previous value, the value of the closest threshold, a value calculated by extrapolating a trend line through previous data, a value that is calculated by interpolation between other values that are inside the thresholds, or the like.

In preferred embodiments, when any of a group's values are outside of the noise thresholds **406** or **408** then a warning flag is set. If one to three values are outside of the noise thresholds **406** or **408**, a "noise" flag is set. If more than three values are outside of the noise thresholds **406** or **408**, a "discard" flag is set which indicates that the whole group of values should be ignored and not used. In alternative embodiments, more or less values need be outside of the thresholds **406** or **408** to trigger the "noise" flag or the "discard" flag.

In preferred embodiments, each digital sensor value Dsig is checked for saturation and disconnection. To continue with the example of FIG. **17**, each individual value is compared to a saturation threshold **410**. If a value is equal to or above the saturation threshold **410** then a "saturation" flag is set. In particular embodiments, when the "saturation" flag is set, a warning is provided to the user that the sensor **26** may need calibration or replacement. In further particular embodiments, if an individual digital sensor value Dsig is at or above the saturation threshold **410**, the individual digital sensor value Dsig may be ignored, changed to a value equal to the average line **404**, or the entire group of values associated with the individual digital sensor value Dsig may be ignored. In preferred embodiments, the saturation threshold **410** is set at about 16% below the maximum value of the range of digital sensor values that may be generated. In preferred embodiments, the maximum digital sensor value represents a glucose concentration greater than 150 mg/dl. In alternative embodiments, the maximum digital sensor value may represent larger or smaller a glucose concentrations depending on the range of expected glucose concentrations to be measured, the sensor accuracy, the sensor system resolution needed for closed loop control, or the like. The full range of values is the difference between the maximum and the minimum digital sensor value that may be generated. Higher or lower saturation threshold levels may be used depending on an expected signal range of the sensor, sensor noise, sensor gains, or the like.

Similarly, in preferred embodiments, if a digital signal value Dsig is below a disconnect threshold **412**, then a "dis-

connect" flag is set indicating to a user that the sensor is not properly connected to the power supply and that the power supply or sensor may need replacement or recalibration. In further particular embodiments, if a digital sensor value Dsig is below the disconnect threshold **412**, the individual value may be ignored, changed to a value equal to the average line **404**, or the entire group of values associated with the individual digital sensor value Dsig may be ignored. In preferred embodiments, the disconnect threshold **410** is set at about 20% of the full range of values. Higher or lower disconnect threshold levels may be used depending on an expected signal range of the sensor, sensor system noise, sensor gains, or the like.

In alternative embodiments, other methods are used to pre-filter the digital sensor values Dsig such as rate-of-change thresholds, rate-of-change squared thresholds, noise thresholds about a least squares fit line rather than about the average of a subset of a group's values, higher or lower noise threshold lines, or the like.

Noise Filter

After the digital sensor values Dsig are evaluated, and if necessary, modified by the pre-filter **400**, the digital sensor values Dsig are passed to the filter **402**. The filter **402** may be used to reduce noise in particular frequency bands. Generally the body's blood glucose level **18** changes relatively slowly compared to a rate at which digital sensor values Dsig are collected. Therefore, high frequency signal components are typically noise, and a low pass filter may be used to improve the signal to noise ratio.

In preferred embodiments, the filter **402** is a finite impulse response (FIR) filter used to reduce noise. In particular embodiments, the FIR filter is a 7th order filter tuned with a pass band for frequencies from zero to 3 cycles per hour (c/hr) and a stop band for frequencies greater than about 6 c/hr, as shown in an example frequency response curve **414** in FIG. **18**. However, typically FIR filters tuned with a pass band for frequencies from zero up to between about 2 c/hr and 5 c/hr and a stop band beginning at 1.2 to three times the selected pass band frequency will sufficiently reduce noise while passing the sensor signal. In particular embodiments, FIR filters tuned with a pass band for frequencies from zero up to between about 2 c/hr and 10 c/hr and a stop band beginning at 1.2 to three times the selected pass band frequency will sufficiently reduce noise. In the 7th order filter, unique weighting factors are applied to each of eight digital sensor values Dsig. The digital sensor values Dsig include the most recently sampled value and the seven previous values. The effects of a low pass filter on a digital sensor values collected at one minute intervals is shown in FIGS. **19**A and B. An unfiltered sensor signal curve **416** of digital sensor values is contrasted with a curve of the same signal after the effects of a 7th order FIR filter **418**. The filtered signal curve **418** is delayed and the peaks are smoother compared to the unfiltered sensor signal curve **416**. In other particular embodiments, higher or lower order filters may be used. In still other particular embodiments, filter weighting coefficients may be applied to digital sensor values Dsig collected at time intervals shorter or longer than one minute depending on the desired sensor sample rate based on the body's physiology, the computational capabilities of the telemetered characteristic monitor transmitter **30**, the sensor's response time, or the like. In alternative embodiments, filters with other frequency responses may be used to eliminate other noise frequencies depending on the type of sensor, noise from the power supply or other electronics, the sensor's interaction with the body, the effects of body motion on the sensor signal, or the like. In still other alternative embodiments, the filter is an infinite impulse response (IIR) filter.

In alternative embodiments, other methods are used to pre-filter the digital sensor values Dsig such as rate-of-change thresholds, rate-of-change squared thresholds, noise thresholds about a least squares fit line rather than about the average of a subset of a group's values, higher or lower noise threshold lines, or the like.

Delay Compensation Filter

Aside from noise reduction, a filter may be used to compensate for time delays. Ideally, a sensor would provide a real time, noise-free measurement of a parameter that a control system is intended to control, such as a blood glucose measurement. However, realistically there are physiological, chemical, electrical, and algorithmic sources of time delays that cause the sensor measurement to lag behind the present value of blood glucose.

A physiological delay **422** is due to the time required for glucose to move between blood plasma **420** and interstitial fluid (ISF). The delay is represented by the circled double headed arrow **422** in FIG. **20**. Generally, as discussed above, the sensor **26** is inserted into the subcutaneous tissue **44** of the body **20** and the electrodes **42** near the tip of the sensor **40** are in contact with interstitial fluid (ISF). But the desired parameter to be measured is the concentration of blood glucose. Glucose is carried throughout the body in blood plasma **420**. Through the process of diffusion, glucose moves from the blood plasma **420** into the ISF of the subcutaneous tissue **44** and vice versa. As the blood glucose level **18** changes so does the glucose level in the ISF. But the glucose level in the ISF lags behind the blood glucose level **18** due to the time required for the body to achieve glucose concentration equilibrium between the blood plasma **420** and the ISF. Studies show the glucose lag times between blood plasma **420** and ISF vary between 0 to 30 minutes. Some parameters that may affect the glucose lag time between blood plasma **420** and ISF are the individual's metabolism, the current blood glucose level, whether the glucose level is rising, or falling, or the like.

A chemical reaction delay **424** is introduced by the sensor response time, represented by the circle **424** surrounding the tip of the sensor **26** in FIG. **20**. The sensor electrodes **42** are coated with protective membranes that keep the electrodes **42** wetted with ISF, attenuate the glucose concentration, and reduce glucose concentration fluctuations on the electrode surface. As glucose levels change, the protective membranes slow the rate of glucose exchange between the ISF and the electrode surface. In addition, there is a chemical reaction delay simply due to the reaction time for glucose to react with glucose oxidase GOX to generate hydrogen peroxide, and the reaction time for a secondary reaction, the reduction of hydrogen peroxide to water, oxygen and free electrons.

There is also a processing delay as the analog sensor signal Isig is converted to digital sensor values Dsig. In preferred embodiments, the analog sensor signal Isig is integrated over one-minute intervals and then converted to a number of counts. In essence an A/D conversion time results in an average delay of 30 seconds. In particular embodiments, the one-minute values are averaged into 5-minute values before they are sent to the controller. The resulting average delay is two and one half minutes. In alternative embodiments, longer or shorter integration times are used resulting in longer or shorter delay times. In other embodiments the analog sensor signal current Isig is continuously converted to an analog voltage Vsig and a A/D converter samples the voltage Vsig every 10 seconds. Then six 10-second values are pre-filtered and averaged to create a one-minute value. Finally, five

1-minute values are filtered and then averaged creating a five-minute value resulting in an average delay of two and one half minutes. Other embodiments use other electrical components or other sampling rates and result in other delay periods.

Filters also introduce a delay due to the time required to acquire a sufficient number of digital sensor values Dsig to operate the filter. Higher order filters, by definition, require more digital sensor values Dsig. Aside from the most recent digital sensor value Dsig, FIR filters use a number of previous values equal to the order of the filter. For example, a 7th order filter uses 8 digital sensor values Dsig. There is a time interval between each digital sensor value Dsig. To continue with the example, if the time interval between digital sensor values Dsig is one minute, then the oldest digital sensor value Dsig used in a 7th order FIR filter would be seven minutes old. Therefore, the average time delay for all of the values used in the filter is three and a half minutes. However, if the weighting factors associated with each of the values are not equal then the time delay may be longer or shorter than three and one half minutes depending on the effects of the coefficients.

Preferred embodiments of the invention include a FIR filter that compensates for both the various time delays, of up to about 30 minutes as discussed above, and high frequency noise, greater than about 10 c/hr also discussed above. Particular embodiments employ a 7th order Weiner type FIR filter. The coefficients for the filter are selected to correct for time lags while simultaneously reducing high frequency noise. An example of a frequency response curve **426** is shown in FIG. **21**. The example frequency response curve **416** is generated for a Weiner filter with a pass band for frequencies from zero up to about 8 c/hr and a stop band for frequencies greater than about 15 c/hr for a sensor with a sensitivity of about 20 μA/100 mg/dl. A study conducted with sensors in dogs demonstrates that a FIR filter may be used to compensate for time delays. During the study a filter was used to compensate for a time delay of about 12 minutes. The results, presented in FIG. **22**, show dots **428** representing actual blood plasma glucose levels measured with a blood glucose meter, a broken line **430** representing sensor measurements without delay compensation, and a solid line **432** representing sensor measurements with delay compensation. The sensor in the test was abnormally low in sensitivity. Studies with average sensitivity sensors in humans are indicating a time delay of about 3 to 10 minutes is more normal. Other filter coefficients and other orders of filters may be used to compensate for the time delay and/or noise.

In alternative embodiments, other types of filters may be used as long as they remove a sufficient portion of the noise from the sensor signal. In other alternative embodiments, no time compensation is used if the rate of change in the blood glucose level is slow compared to the time delay. For example, a five-minute delay between blood plasma glucose and a sensor measurement does not have to be corrected for a closed loop glucose control system to function.

Derivative Filter

Further embodiments may include a filter to remove noise from the derivative of the sensor signal before the controller uses it. A derivative is taken from the digital sensor values Dsig, which results in digital derivative sensor values (dDsig/dt). The digital derivative sensor values dDsig/dt are passed through a FIR filter. In particular embodiments, the derivative filter is at least a 7th order FIR filter tuned to remove high frequency noise. In alternative embodiments, higher or lower order filters may be used and the filters may be tuned to remove various frequencies of noise. In other alternative embodiments, a derivative is taken from the glucose level error G_E values and then passed through a derivative filter **526**, as shown in FIG. **37**. In further alternative embodiments, a derivative is taken of an analog sensor signal Isig and a hardware filter is used to remove noise.

Calibration

In preferred embodiments, after filtering, the digital sensor values Dsig are calibrated with respect to one or more glucose reference values. The glucose reference values are entered into the calibrator and compared to the digital sensor values Dsig. The calibrator applies a calibration algorithm to convert the digital sensor values Dsig, which are typically in counts into blood glucose values. In particular embodiments, the calibration method is of the type described in U.S. patent application Ser. No. 09/511,580, filed on Feb. 23, 2000, entitled "GLUCOSE MONITOR CALIBRATION METHODS", which is incorporated by reference herein. In particular embodiments, the calibrator is included as part of the infusion device **34** and the glucose reference values are entered by the user into the infusion device **34**. In other embodiments, the glucose reference values are entered into the telemetered characteristic monitor transmitter **30** and the calibrator calibrates the digital sensor values Dsig and transmits calibrated digital sensor values to the infusion device **34**. In further embodiments, the glucose reference values are entered into a supplemental device where the calibration is executed. In alternative embodiments, a blood glucose meter is in communication with the infusion device **34**, telemetered characteristic monitor transmitter **30** or supplemental device so that glucose reference values may be transmitted directly into the device that the blood glucose meter is in communication with. In additional alternative embodiments, the blood glucose meter is part of the infusion device **34**, telemetered characteristic monitor transmitter **30** or supplemental device such as that shown in U.S. patent application Ser. No. 09/334,996, filed on Jun. 17, 1999, entitled "CHARACTERISTIC MONITOR WITH A CHARACTERISTIC METER AND METHOD OF USING THE SAME", which is incorporated by reference herein.

In preferred embodiments, to obtain blood glucose reference values, one or more blood samples are extracted from the body **20**, and a common, over-the-counter, blood glucose meter is used to measure the blood plasma glucose concentration of the samples. Then a digital sensor value Dsig is compared to the blood glucose measurement from the meter and a mathematical correction is applied to convert the digital sensor values Dsig to blood glucose values. In alternative embodiments, a solution of a known glucose concentration is introduced into the subcutaneous tissue surrounding the sensor **26** by using methods and apparatus such as described in U.S. patent application Ser. No. 09/395,530, filed on Sep. 14, 1999, entitled "METHOD AND KIT FOR SUPPLYING A FLUID TO A SUBCUTANEOUS PLACEMENT SITE", which is incorporated by reference herein, or by using injection, infusion, jet pressure, introduction through a lumen, or the like. A digital sensor value Dsig is collected while the sensor **26** is bathed in the solution of known glucose concentration. A mathematical formula such as a factor, an offset, an equation, or the like, is derived to convert the digital sensor value Dsig to the known glucose concentration. The mathematical formula is then applied to subsequent digital sensors values Dsig to obtain blood glucose values. In alternative embodiments, the digital sensor values Dsig are calibrated before filtering. In additional alternative embodiments, the digital sensor values Dsig are calibrated after pre-filtering and before filtering. In other alternative embodiments, the sensors are calibrated before they are used in the body or do not require calibration at all.

Sensor Signal Processing Systems

Before filtering and calibrating, generally the sensor signal is processed to convert the sensor signal from a raw form into a form acceptable for use in the filters and/or calibrator. In preferred embodiments, as shown in FIG. **10**, an analog sensor signal Isig is digitally quantified through an A/D converter **68** resulting in digital sensor values Dsig that are transmitted by a transmitter **70** from the telemetered characteristic monitor transmitter **30** to another device. In particular embodiments, the analog sensor signal Isig is an analog current value that is converted to a digital sensor value Dsig in the form of a digital frequency measurement, as shown in FIG. **11** (*a*). The general circuit includes an integrator **72**, a comparator **74**, a counter **76**, a buffer **78**, a clock **80** and the transmitter **70**. The integrator **72** generates a substantially ramped voltage signal (A), and the instantaneous slope of the ramped voltage signal is proportional to the magnitude of the instantaneous analog sensor signal Isig. The comparator **74** converts the ramped voltage signal (A) from the integrator **72** into square wave pulses (B). Each pulse from the comparator **74** increments the counter **76** and also resets the integrator **72**. The clock **80** periodically triggers the buffer **78** to store the present value from the counter **76** and then resets the counter **76**. The values stored in the buffer **78** are the digital sensor values Dsig. The clock **80** may also periodically signal the transmitter **70** to send a value from the buffer **78**. In preferred embodiments, the clock period is one minute. However, in alternative embodiments, the clock period may be adjusted based on how often measurements are needed, sensor signal noise, sensor sensitivity, required measurement resolution, the type of signal to be transmitted, or the like. In alternative embodiments, a buffer is not used.

A/D Converters

Various A/D converter designs may be used in embodiments of the present invention. The following examples are illustrative, and not limiting, since other A/D converters may be used.

I to F (Current to Frequency (Counts)), Single Capacitor, Quick Discharge

In preferred embodiments, the integrator **72** consists of a first Op-Amp **92** and a capacitor **82**, shown in FIG. **12**. The integrator **72** sums the analog sensor signal Isig current by charging the capacitor **82** until the capacitor voltage (A') achieves a high reference voltage (VrefH). The capacitor voltage (A') is measured at the output of the first Op-Amp **92**. A second Op-Amp **94** is used as a comparator. When the capacitor voltage (A') reaches VrefH, the comparator output (B') changes from low to high. The high comparator output (B') closes a reset switch **84** that discharges the capacitor **82** through a voltage source (V+). The high comparator output (B') also triggers a reference voltage switch **88** to close, while substantially simultaneously an inverter **86** inverts the comparator output (B'). And the inverter output (C') triggers a reference voltage switch **90** to open. The result is that the reference voltage of the comparator is changed from VrefH to the low reference voltage (VrefL).

When the capacitor voltage (A') is discharged to VrefL, the comparator output (B') returns to low, thus forming a pulse. The low comparator output (B') opens the reset switch **84** allowing the capacitor **82** to begin charging again.

Virtually simultaneously, the low comparator output (B') also triggers the reference voltage switch **88** to open and the inverter output (C') triggers reference voltage switch **90** to close resulting in changing the comparator reference voltage from VrefL back to VrefH.

I to F, Single Reversible Capacitor

In alternative embodiments, two or more integrator switches are used to control the polarity of one or more capacitors. A particular embodiment is shown in FIG. **13**. Generally, only one of the two integrator-switches **110** and **112** is closed and the other integrator switch is open. When the first integrator switch **110** is closed, the second integrator switch **112** is open and an integrator Op-Amp **114** sums the analog sensor signal Isig current by charging a capacitor **116** until the capacitor voltage (A") achieves a high reference voltage (VrefH). The comparator **120** compares the integrator output (A") to the reference voltage VrefH. And when the capacitor voltage (A") reaches VrefH, the comparator output (B") shifts from low to high, initiating a pulse.

The high comparator output (B") pulse causes the capacitor polarity to reverse using the following method. The high comparator output (B") triggers the second integrator switch **112** to close while virtually simultaneously the inverter **118** inverts the comparator output (B"). And the low inverter output (C") pulse triggers the first integrator switch **110** to open. Once the capacitor's polarity is reversed, the capacitor **116** discharges at a rate proportional to the analog sensor signal Isig. The high comparator output (B") pulse also triggers the reference voltage of the comparator to change form VrefH the low reference voltage (VrefL). When the capacitor voltage (A") is discharged to VrefL, the comparator output (B") returns to low. The low comparator output (B") opens the second integrator switch **112** and virtually simultaneously the high inverter output (C") closes the first integrator switch **110** allowing the capacitor **116** to begin charging again. The low comparator output (B") also triggers the comparator reference voltage to change from VrefL back to VrefH.

An advantage of this embodiment is that sensor signal errors, which may be created due to capacitor discharge time, are reduced since the magnitude of the analog sensor signal Isig drives both the charging and the discharging rates of the capacitor **116**.

I to F, Dual Capacitor

In further alternative embodiments, more than one capacitor is used such that as one capacitor is charging, at a rate proportional to the magnitude of the analog sensor signal Isig, another capacitor is discharging. An example of this embodiment is shown in FIG. **14**. A series of three switches are used for each capacitor. A first group of switches **210** is controlled by a latch voltage C", and a second group of switches **212** are controlled by voltage D", which is the inverse of C". Substantially, only one group of switches is closed at a time. When the first group of switches **210** is closed, the voltage across a first capacitor **216** increases at a rate proportional to the analog sensor signal Isig until the integrator voltage (A") at the output of Op-Amp **214** achieves a reference voltage (Vref). At the same time one of the switches shorts the circuit across a second capacitor **222** causing it to discharge. A comparator **220** compares the integrator output (A") to the reference voltage Vref. And when the integrator output (A") reaches Vref, the comparator output (B") generates a pulse. The comparator output pulse increments a counter **76**, and triggers the latch output voltage C" from a latch **221** to toggle from a low voltage to a high voltage. The change in the latch voltage C" causes the second group of switches **212** to close and the first group of switches **210** to open. One of the switches from the second group of switches **212** shorts the circuit across the first capacitor **216** causing it to discharge. At the same time the voltage across the second capacitor **222** increases at a rate proportional to the analog sensor signal Isig until the integrator voltage (A"') at the output of Op-Amp **214** achieves a reference voltage (Vref). Again, the comparator **220** com-

pares the integrator output (A''') to the reference voltage Vref. And when the integrator output (A''') reaches Vref, the comparator output (B''') generates a pulse. The comparator output pulse increments the counter **76**, and triggers the latch output voltage C''' to toggle from a high voltage to a low voltage, which causes the switches to return to their initial position with the first group of switches **210** closed and the second group of switches **212** to open.

In summary, as the blood glucose level **18** increases, the analog sensor signal Isig increases, which causes the voltage coming out of the integrator **72** to ramp up faster to the high reference voltage VrefH, which causes the comparator **74** to generate pulses more often, which adds counts to the counter **76** faster. Therefore, higher blood glucose levels generate more counts per minute.

The charge storage capacity for the capacitors used in the integrator **72**, and the reference voltages VrefH, and VrefL are selected such that the count resolution for counts collected in a one-minute period at a glucose level of 200 mg/dl represents a blood glucose measurement error of less than 1 mg/dl. In particular embodiments, VrefH is 1.1 volts and VrefL is 0.1 volts. Higher or lower reference voltages may be selected based on the magnitude of the analog sensor signal Isig, the capacity of the capacitors, and the desired measurement resolution. The source voltage V+ is set to a voltage sufficiently high to discharge one or more capacitors quickly enough that the discharge times do not significantly reduce the number of counts per minute at a blood glucose level of 200 mg/dl.

Pulse Duration Output Feature

In preferred embodiments, the transmitter **70** transmits the digital sensor values Dsig from the buffer **78** whenever triggered by the clock **80**. However, in particular embodiments, the user or another individual may use a selector **96** to choose other outputs to be transmitted from the transmitter **70**, as shown in FIG. **11**B. In preferred embodiments, the selector **96** is in the form of a menu displayed on a screen that is accessed by the user or another individual by using buttons on the surface of the telemetered characteristic monitor transmitter **30**. In other embodiments, a dial selector, dedicated buttons, a touch screen, a signal transmitted to the telemetered characteristic monitor transmitter **30**, or the like, may be used. Signals that may be selected to be transmitted, other than the digital sensor values Dsig, include, but are not limited to, a single pulse duration, digital sensor values before pre-filtering, digital sensor values after pre-filtering but before filtering, digital sensor values after filtering, or the like.

In particular embodiments, a pulse duration counter **98** counts clock pulses from a pulse duration clock **100** until the pulse duration counter **98** is reset by a rising or falling edge of a pulse from the comparator **74**, as shown in FIG. **11**B. The accumulated count at the time that the pulse duration counter **98** is reset represents the pulse duration for a portion of a single pulse from the comparator **74**. The accumulated count from the pulse duration counter **98** is stored in the single pulse buffer **102** when triggered by the reset signal. When an individual selects the single pulse output, the transmitter **70** transmits the values from the single pulse buffer **102**. The pulse duration clock **100** period must be sufficiently shorter than the period between individual pulse edges from the comparator **74** given a high analog sensor signal Isig to have sufficient resolution to quantify different pulse durations from the comparator **74**.

I to V (Current to Voltage), Voltage A/D

Alternative methods may be used to convert the analog sensor signal Isig from an analog current signal to a digital voltage signal. The analog sensor signal Isig is converted to an analog voltage Vsig using an Op Amp **302** and a resistor **304**, as shown in FIG. **15**. And then periodically a clock **308** triggers an A/D converter **306** to take a sample value from the analog voltage Vsig and convert it to a digital signal representing the magnitude of the voltage. The output values of the A/D converter **306** are digital sensor values Dsig. The digital sensor values Dsig are sent to a buffer **310** and then to the transmitter **70**. In particular embodiments, the resistor **304** may be adjusted to scale the Vsig to use a significant portion of the range of the voltage A/D converter **306** depending on the sensor sensitivity, the maximum glucose concentration to be measured, the desired resolution from the voltage A/D converter **306**, or the like.

In alternative embodiments, a buffer **310** is not needed and the digital sensor values Dsig are sent from the A/D converter directly to the transmitter **70**. In other alternative embodiments, the digital sensor values Dsig are processed, filtered, modified, analyzed, smoothed, combined, averaged, clipped, scaled, calibrated, or the like, before being sent to the transmitter **70**. In preferred embodiments, the clock **308** triggers a measurement every 10 seconds. In alternative embodiments, the clock **308** runs faster or slower triggering measurements more or less frequently depending on how quickly the blood glucose level can change, the sensor sensitivity, how often new measurements are needed to control the delivery system **14**, or the like.

Finally, in other alternative embodiments, other sensor signals from other types of sensors, as discussed in the section "Sensor and Sensor Set" below, are converted to digital sensor values Dsig if necessary before transmitting the digital sensor values Dsig to another device.

Additional Controller Inputs

Generally, the proportional plus, integral plus, derivative (PID) insulin response controller uses only glucose (digital sensor values Dsig) as an input. Conversely, in a normally glucose tolerant human body, healthy β-cells benefit from additional inputs such as neural stimulation, gut hormone stimulation, changes in free fatty acid (FFA) and protein stimulation etc. Thus in other alternative embodiments, the PID controller, as discussed above, can be augmented with one or more additional inputs. In particular alternative embodiments, the user may manually input supplemental information such as a start of a meal, an anticipated carbohydrate content of the meal, a start of a sleep cycle, an anticipated sleep duration, a start of an exercise period, an anticipated exercise duration, an exercise intensity estimation, or the like. Then, a model predictive control feature assists the controller to use the supplemental information to anticipate changes in glucose concentration and modify the output commands accordingly. For example, in a NGT individual, neural stimulation triggers the β-cells to begin to secrete insulin into the blood stream before a meal begins, which is well before the blood glucose concentration begins to rise. So, in alternative embodiments, the user can tell the controller that a meal is beginning and the controller will begin to secrete insulin in anticipation of the meal.

In other alternative embodiments, the user or another individual may manually override the control system or select a different controller algorithm. For instance, in particular alternative embodiments, an individual may select to normalize to a basal glucose level immediately, and instead of using the β-cell emulating PID controller another controller would take over such as a PID controller with different gains, a PD controller for rapid glucose adjustment, or the like. Additional alternative embodiments allow an individual to turn off the integral component of the PID controller once the glucose level is normalized and no meals are anticipated. In other particular alternative embodiments, the user may select to

turn off the controller entirely, therefore disengaging the closed loop system. Once the closed loop system is not controlling insulin dosing, the user may program the infusion device with a basal rate, variable basal rates, boluses, or the like, or the user may manually enter each individual dosage when it is needed.

In still other alternative embodiments, more than one body characteristic is measured, and the measurements are provided as inputs to a controller. Measured body characteristics that may be used by the controller include, but are not limited to, the blood glucose level, blood and/or ISF pH, body temperature, the concentration of amino acids in blood (including arginine and/or lysine, and the like), the concentration of gastrointestinal hormones in blood or ISF (including gastrin, secretin, cholecystokinin, and/or gastro inhibitory peptide, and the like), the concentration of other hormones in blood or ISF (including glucagons, growth hormone, cortisol, progesterone and/or estrogen, and the like), blood pressure, body motion, respiratory rate, heart rate, and other parameters.

In NGT individuals, the glucose-induced secretion of insulin by healthy β-cells may be as much as doubled in the presence of excess amino acids. Yet, the presence of excess amino acids alone, without elevated blood glucose, only mildly increases insulin secretions according to the Textbook of Medical Physiology, Eighth Edition, written by Arthur C. Guyton, published by W.B. Saunders Company, 1991, Ch. 78, pg. 861, section "Other Factors That Stimulate Insulin Secretion". In particular alternative embodiments, amino acid concentrations are estimated or measured, and the controller's insulin response increases when amino acid concentrations are sufficiently high.

In NGT individuals, the presence of sufficient quantities of gastrointestinal hormones in the blood causes an anticipatory increase in blood insulin, which suggests that β-cells release insulin before increases in blood glucose due to an individual's anticipation of a meal. In particular alternative embodiments, the concentration of gastrointestinal hormones is measured or estimated, and when concentrations are high enough to indicate that a meal is anticipated, the controller commands are adjusted to cause insulin introduction into the body even before the blood glucose level changes. In other alternative embodiments, the controller uses measurements or estimates of other hormones to modify the rate of insulin secretion.

In NGT individuals, the body's cells take up glucose during periods of heavy exercise with significantly lower levels of insulin. In alternative embodiments, physiologic parameters such as body motion, blood pressure, pulse rate, respiratory rate, or the like, are used to detect periods of heavy exercise by the body and therefore provide inputs to the controller that decreases (or eliminates) the amount of insulin infused into the body to compensate for glucose concentrations.

Sensor Compensation and End-of-Life Detection

In particular embodiments, the sensor sensitivity **510** may degrade over time, as shown in FIG. **31**B. As the sensor sensitivity **510** changes the sensor signal accuracy degrades. If the sensor sensitivity **510** changes significantly then the sensor must be recalibrated or replaced. A diagnostic signal may be used to evaluate whether sensor signal accuracy has changed and/or may be used to adjust the signal or to indicate when to recalibrate or replace the sensor. As the sensor sensitivity **510** decreases, the measured glucose level **512** using the sensor signal underestimates the actual blood glucose level **514**, and the measurement error **516** between the measured glucose level **512** and the actual blood glucose level **514** becomes greater over time, as shown in FIG. **31**A. The sensor sensitivity **510** decreases due to increases in sensor resistance Rs, as shown in FIG. **31**C. The sensor resistance Rs is the resistance provided by the body between the working electrode WRK and the counter electrode CNT, shown as the sum or R1 and R2 in the circuit diagram of FIG. **7**. The sensor resistance Rs can be obtained indirectly by measuring the analog sensor signal Isig and the counter electrode voltage Vcnt and then calculating the resistance, Rs=Vcnt/Isig.

As the sensor resistance Rs increases, the analog sensor signal Isig response to a given glucose concentration decreases. In preferred embodiments, the decrease in the analog sensor signal Isig may be compensated for by identifying the amount that the sensor resistance Rs has changed since the last calibration and then using the change in resistance in a correction algorithm **454** to adjust the analog sensor signal value. A compensation value calculated by the correction algorithm **454** is used to increase the sensor analog signal value. The compensation value increases over time as the sensor resistance Rs increases. The correction algorithm **454** includes at least one value that varies with changes in sensor resistance Rs. In particular embodiments, a low pass filter is applied to the sensor resistance Rs measurement to decrease high frequency noise before evaluating how much the sensor resistance Rs has changed since the last calibration.

In alternative embodiments, the sensor resistance Rs may be calculated using different equations. For instance, a sensor resistance Rs_2 may be calculated as:

$$Rs_2=(V_0-Vcnt/Isig)$$

In particular embodiments, V_0 is the same voltage as Vset. An advantage of this approach is that it accounts for the voltage level Vset, which can vary from sensor to sensor and/or monitor to monitor, and/or as the analog sensor signal changes. This removes the noise and/or offset associated with variations in Vset, and can provide a more accurate indication of sensor resistance. In other particular embodiments, V_0 is set at −0.535 volts, which is a commonly used voltage for Vset. In further embodiments, V_0 is calculated from paired measurements of Vcnt and Isig. Using least squares or another curve fitting method, a mathematical equation representing the curve (typically a straight line equation) is derived from the relationship between Vcnt and Isig. Then, V_0 is obtained by extrapolating the curve to find the value for Vcnt when Isig is zero.

FIGS. **38**A-H show a comparison between calculating the sensor resistance with V_0 and without V_0. The plot of the derivative of Rs_2 shown in FIG. **38**G is cleaner and indicates the sensor failure more clearly than the plot of the derivative of Rs shown in FIG. **38**F. Hence sensor resistance Rs_2 may be used instead of, or in conjunction with, sensor resistance Rs described above.

In preferred embodiments, the sensor is recalibrated or replaced when the change in the sensor resistance Rs since the last calibration exceeds a threshold, or the rate of change of the sensor resistance dRs/dt exceeds another threshold. In particular embodiments, the rate of change of the sensor resistance dRs/dt may be compared to two thresholds as shown in FIG. **32**. If dRs/dt exceeds a "replacement" threshold then a warning is provided to the user to replace the sensor. If dRs/dt exceeds a "recalibrate" threshold then a warning is provided to the user to recalibrate the sensor.

In an example shown in FIGS. **33**A-C, the analog sensor signal Isig decreases dramatically at approximately 0.3 days, as seen in FIG. **33**A. Given only the analog sensor signal Isig, the user would believe that the decrease in the analog sensor signal Isig is due to a decrease in blood glucose. But in reality the drop in the analog sensor signal Isig is due to a sudden change in sensor sensitivity. The sensor resistance Rs, shown

in FIG. **33**A increases as the analog sensor signal Isig drops at about 0.3 days. The derivative of the sensor resistance dRs/dt, shown in FIG. **33**C, clearly shows a spike **522** at about 0.3 days when the analog sensor signal Isig dropped. The spike **522** in the change in sensor resistance dRs/dt indicates a sensor anomaly rather than a realistic drop in blood glucose. If a threshold were placed at +/−4 on the dRs/dt, the user would have received a warning to replace the sensor at about 0.3 days. As seen in FIG. **33**A, the sensor was not replaced until about 1.4 days. The analog sensor signal Isig was under estimating the true glucose level from about 0.3 days until the sensor was replaced at about 1.4 days.

In particular embodiments, the amount of time dt over which the derivative of the sensor resistance Rs is taken is the entire time since the last calibration. In other embodiments, the amount of time dt over which the derivative is taken is fixed, for example over the last hour, 90 minutes, 2 hours, or the like.

In alternative embodiments, the sensor is recalibrated or replaced when the integral of the sensor resistance Rs over a predetermined time window (∫Rs d/dt) exceeds a predetermined resistance integral threshold. An advantage to this approach is that it tends to filter out potential noise that could be encountered from a signal that includes occasional spikes, sudden variations in voltage levels, or the like. Preferably, the integral of the sensor resistance Rs is calculated over a time window (such as 15 minutes, or the like) based on Rs measurements obtained at set rates (such as 1 minute, 5 minutes, or the like) during the time window. In alternative embodiments, the time windows may be longer or shorter and different sampling rates may be used, with the selection being dependent on noise, response of the system, sampling rate used in the controller, or the like. In further embodiments, the time windows and sampling rates may change over time, such as when approaching the end of the expected sensor life, or as the equations indicate that the sensor is degrading, or the like.

Like above, multiple thresholds may be used. For instance, if ∫Rs d/dt exceeds a "replacement" threshold then a warning is provided to the user to replace the sensor. And if ∫Rs d/dt exceeds a "recalibrate" threshold then a warning is provided to the user to recalibrate the sensor. In further alternative embodiments, the counter electrode voltage Vcnt is used to evaluate other characteristics such as, sensor accuracy, sensor bio-fouling, sensor function, sensor voltage operating range, sensor attachment, or the like.

pH Controller Input

In alternative embodiments, the controller uses measurements of both the interstitial fluid (ISF) glucose level and a local pH in the ISF surrounding the sensor to generate commands for the infusion device. In particular alternative embodiments, a single multi-sensor **508** located in the subcutaneous tissue is used to measure both the glucose level and the pH. The tip of the multi-sensor **508** that is placed into the subcutaneous tissue with three electrodes is shown in FIG. **30**. The working electrode **502** is plated with platinum black and coated with glucose oxidase (GOX). The reference electrode **506** is coated with silver-silver chloride. And the counter electrode **504** is coated with iridium oxide (Ir Ox). The analog sensor signal Isig is generated at the working electrode **502** due to the reaction between glucose oxidase GOX and the ISF glucose as described with the preferred sensor embodiment. In this alternative embodiment however, as glucose in the ISF reacts with the glucose oxidase GOX on the working electrode and gluconic acid is generated, the local pH in the ISF surrounding the sensor decreases, which changes the potential of the iridium oxide on the counter electrode **504**, with respect to the reference electrode REF. So, as the pH decreases, the voltage at the counter electrode **504** increases. Therefore, as the glucose concentration increases, the local pH decreases, which causes the counter electrode voltage to increase. So, the glucose concentration may be estimated based on the counter electrode voltage. The counter electrode voltage estimate of glucose concentration can be compared to the estimate of glucose level from the analog sensor signal Isig. The two estimates of the glucose level may be combined by a weighted average or one estimate may simply be used as a check to verify that the other sensing method is functioning properly. For example, if the difference between the two estimates is 10% for a period of time and then suddenly the difference increased to 50%, a warning would be issued indicating to the user that the sensor may need to be replaced or recalibrated.

In additional alternative embodiments, the pH level near the sensor may be used to detect infection. By tracking trends in the pH over time, a dramatic change in pH may be used to identify that an infection has developed in proximity to the sensor. A warning is used to notify the user to replace the sensor.

The pH sensor may be used in other embodiments. When insulin is not available to assist the body to use glucose, the body shifts to consuming fat for energy. As the body shifts from using glucose to using almost exclusively fat for energy, concentrations of keto acids (acetoacetic acid and β-hydroxybutyric acid) increase from about 1 mEq/liter to as high as 10 mEq/liter. In particular alternative embodiments, the pH level is measured to detect increases in keto acids in the body. In embodiments of the present invention, a warning is provided to the user when the ISF pH level is too low.

A side effect of the increased of keto acid concentrations is that sodium is drawn from the body's extra cellular fluid to combine with the acids so that the body can excrete the acids. This leads to increased quantities of hydrogen ions, which greatly increases the acidosis. Severe cases lead to rapid deep breathing, acidotic coma and even death. In other alternative embodiments, an ion-selective electrode (ISE) is used to detect changes in sodium concentration. A special membrane is used to coat the ISE so that it only senses changes in sodium concentration. In particular alternative embodiments, the ISE is a fourth electrode added to the glucose sensor. In another alternative embodiment, a three-electrode system is used with a silver-silver chloride reference electrode REF, an Ir Ox counter electrode CNT, and a sodium ion-selective (Na ISE) working electrode WRK.

While pH measurements, end-of-life measurements, hormone measurements, or the like, add inputs to the controller that can significantly affect the accuracy of insulin delivery, the basic input to the controller is generally a glucose measurement. The glucose measurement is provided by the sensor system. And once the controller uses the glucose measurement to generate commands, the delivery system executes the commands. The following is a detailed description of several apparatus embodiments for the sensor system and the delivery system.

Sensor System

The sensor system provides the glucose measurements used by the controller. The sensor system includes a sensor, a sensor set to hold the sensor if needed, a telemetered characteristic monitor transmitter, and a cable if needed to carry power and/or the sensor signal between the sensor and the telemetered characteristic monitor transmitter.

Sensor and Sensor Set

In preferred embodiments, the glucose sensor system **10** includes a thin film electrochemical sensor such as the type disclosed in U.S. Pat. No. 5,391,250, entitled "METHOD OF

FABRICATING THIN FILM SENSORS"; U.S. patent application Ser. No. 09/502,204, filed on Feb. 10, 2000, entitled "IMPROVED ANALYTE SENSOR AND METHOD OF MAKING THE SAME"; or other typical thin film sensors such as described in commonly assigned U.S. Pat. Nos. 5,390,671; 5,482,473; and 5,586,553 which are incorporated by reference herein. See also U.S. Pat. No. 5,299,571.

The glucose sensor system **10** also includes a sensor set **28** to support the sensor **26** such as described in U.S. Pat. No. 5,586,553, entitled "TRANSCUTANEOUS SENSOR INSERTION SET" (published as PCT Application WO 96/25088); and U.S. Pat. No. 5,954,643, entitled "INSERTION SET FOR A TRANSCUTANEOUS SENSOR" (published as PCT Application WO 98/56293); and U.S. Pat. No. 5,951,521, entitled "A SUBCUTANEOUS IMPLANTABLE SENSOR SET HAVING. THE CAPABILITY TO REMOVE OR DELIVER FLUIDS TO AN INSERTION SITE", which are incorporated by reference herein.

In preferred embodiments, the sensor **26** is inserted through the user's skin **46** using an insertion needle **58**, which is removed and disposed of once the sensor is positioned in the subcutaneous tissue **44**. The insertion needle **58** has a sharpened tip **59** and an open slot **60** to hold the sensor during insertion into the skin **46**, as shown in FIGS. **3**C and D and FIG. **4**. Further description of the needle **58** and the sensor set **28** are found in U.S. Pat. No. 5,586,553, entitled "TRANSCUTANEOUS SENSOR INSERTION SET" (published as PCT Application WO 96/25088); and U.S. Pat. No. 5,954,643, entitled "INSERTION SET FOR A TRANSCUTANEOUS SENSOR" (published as PCT Application WO 98/5629), which are incorporated by reference herein.

In preferred embodiments, the sensor **26** has three electrodes **42** that are exposed to the interstitial fluid (ISF) in the subcutaneous tissue **44** as shown in FIGS. **3**D and **4**. A working electrode WRK, a reference electrode REF and a counter electrode CNT are used to form a circuit, as shown in FIG. **7**. When an appropriate voltage is supplied across the working electrode WRK and the reference electrode REF, the ISF provides impedance (R1 and R2) between the electrodes **42**. And an analog current signal Isig flows from the working electrode WRK through the body (R1 and R2, which sum to Rs) and to the counter electrode CNT. Preferably, the working electrode WRK is plated with platinum black and coated with glucose oxidase (GOX), the reference electrode REF is coated with silver-silver chloride, and the counter electrode is plated with platinum black. The voltage at the working electrode WRK is generally held to ground, and the voltage at the reference electrode REF is substantially held at a set voltage Vset. Vset is between 300 and 700 mV, and preferably to about 535 mV.

The most prominent reaction stimulated by the voltage difference between the electrodes is the reduction of glucose as it first reacts with GOX to generate gluconic acid and hydrogen peroxide (H_2O_2). Then the H_2O_2 is reduced to water (H_2O) and (O^-) at the surface of the working electrode WRK. The O^- draws a positive charge from the sensor electrical components, thus repelling an electron and causing an electrical current flow. This results in the analog current signal Isig being proportional to the concentration of glucose in the ISF that is in contact with the sensor electrodes **42**. The analog current signal Isig flows from the working electrode WRK, to the counter electrode CNT, typically through a filter and back to the low rail of an op-amp **66**. An input to the op-amp **66** is the set voltage Vset. The output of the op-amp **66** adjusts the counter voltage Vcnt at the counter electrode CNT as Isig changes with glucose concentration. The voltage at the working electrode WRK is generally held to ground, the voltage at the reference electrode REF is generally equal to Vset, and the voltage Vcnt at the counter electrode CNT varies as needed.

In alternative embodiments, more than one sensor is used to measure blood glucose. In particular embodiments, redundant sensors are used. The user is notified when a sensor fails by the telemetered characteristic monitor transmitter electronics. An indicator may also inform the user of which sensors are still functioning and/or the number of sensors still functioning. In other particular embodiments, sensor signals are combined through averaging or other means. If the difference between the sensor signals exceeds a threshold then the user is warned to recalibrate or replace at least one sensor. In other alternative embodiments, more than one glucose sensor is used, and the glucose sensors are not of the same design. For example, an internal glucose sensor and an external glucose sensor may be used to measure blood glucose at the same time.

In alternative embodiments, other continuous blood glucose sensors and sensor sets may be used. In particular alternative embodiments, the sensor system is a micro needle analyte sampling device such as described in U.S. patent application Ser. No. 09/460,121, filed on Dec. 13, 1999, entitled "INSERTION SET WITH MICROPIERCING MEMBERS AND METHODS OF USING THE SAME", incorporated by reference herein, or an internal glucose sensor as described in U.S. Pat. Nos. 5,497,772; 5,660,163; 5,791,344; and 5,569,186, and/or a glucose sensor that uses florescence such as described in U.S. Pat. No. 6,011,984 all of which are incorporated by reference herein. In other alternative embodiments, the sensor system uses other sensing technologies such as described in Patent Cooperation Treaty publication No. WO 99/29230, light beams, conductivity, jet sampling, micro dialysis, micro-poration, ultra sonic sampling, reverse iontophoresis, or the like. In still other alternative embodiments, only the working electrode WRK is located in the subcutaneous tissue and in contact with the ISF, and the counter CNT and reference REF electrodes are located external to the body and in contact with the skin. In particular embodiments, the counter electrode CNT and the reference electrode REF are located on the surface of a monitor housing **518** and are held to the skin as part of the telemetered characteristic monitor, as shown in FIG. **34**A. In other particular embodiments, the counter electrode CNT and the reference electrode REF are held to the skin using other devices such as running a wire to the electrodes and taping the electrodes to the skin, incorporating the electrodes on the underside of a watch touching the skin, or the like. In more alternative embodiments, more than one working electrode WRK is placed into the subcutaneous tissue for redundancy. In additional alternative embodiments, a counter electrode is not used, a reference electrode REF is located outside of the body in contact with the skin, and one or more working electrodes WRK are located in the ISF. An example of this embodiment implemented by locating the reference electrode REF on a monitor housing **520** is shown in FIG. **34**B. In other embodiments, ISF is harvested from the body of an individual and flowed over an external sensor that is not implanted in the body.

Sensor Cable

In preferred embodiments, the sensor cable **32** is of the type described in U.S. patent application Ser. No. 60/121,656, filed on Feb. 25, 1999, entitled "TEST PLUG AND CABLE FOR A GLUCOSE MONITOR", which is incorporated by reference herein. In other embodiments, other cables may be used such as shielded, low noise cables for carrying nA currents, fiber optic cables, or the like. In alternative embodi-

ments, a short cable may be used or the sensor may be directly connected to a device without the need of a cable.

Telemetered Characteristic Monitor Transmitter

In preferred embodiments, the telemetered characteristic monitor transmitter **30** is of the type described in U.S. patent application Ser. No. 09/465,715, filed on Dec. 17, 1999, entitled "TELEMETERED CHARACTERISTIC MONITOR SYSTEM AND METHOD OF USING THE SAME" (published as PCT Application WO 00/19887 and entitled, "TELEMETERED CHARACTERISTIC MONITOR SYSTEM"), which is incorporated by reference herein, and is connected to the sensor set **28** as shown in FIGS. **3**A and B.

In alternative embodiments, the sensor cable **32** is connected directly to the infusion device housing, as shown in FIG. **8**A, which eliminates the need for a telemetered characteristic monitor transmitter **30**. The infusion device contains a power supply and electrical components to operate the sensor **26** and store sensor signal values.

In other alternative embodiments, the telemetered characteristic monitor transmitter includes a receiver to receive updates or requests for additional sensor data or to receive a confirmation (a hand-shake signal) indicating that information has been received correctly. Specifically, if the telemetered characteristic monitor transmitter does not receive a confirmation signal from the infusion device, then it re-sends the information. In particular alternative embodiments, the infusion device anticipates receiving blood glucose values or other information on a periodic basis. If the expected information is not supplied when required, the infusion device sends a "wake-up" signal to the telemetered characteristic monitor transmitter to cause it to re-send the information.

Insulin Delivery System

Infusion Device

Once a sensor signal **16** is received and processed through the controller **12**, commands **22** are generated to operate the infusion device **34**. In preferred embodiments, semi-automated medication infusion devices of the external type are used, as generally described in U.S. Pat. Nos. 4,562,751; 4,678,408; 4,685,903; and U.S. patent application Ser. No. 09/334,858, filed on Jun. 17, 1999, entitled "EXTERNAL INFUSION DEVICE WITH REMOTE PROGRAMMING, BOLUS ESTIMATOR AND/OR VIBRATION CAPABILITIES" (published as PCT application WO 00/10628), which are herein incorporated by reference. In alternative embodiments, automated implantable medication infusion devices, as generally described in U.S. Pat. Nos. 4,373,527 and 4,573,994, are used, which are incorporated by reference herein.

Insulin

In preferred embodiments, the infusion device reservoir **50** contains HUMALOG® lispro insulin to be infused into the body **20**. Alternatively, other forms of insulin may be used such as HUMALIN®, human insulin, bovine insulin, porcine insulin, analogs, or other insulins such as insulin types described in U.S. Pat. No. 5,807,315, entitled "METHOD AND COMPOSITIONS FOR THE DELIVERY OF MONOMERIC PROTEINS", and U.S. Patent Application Ser. No. 60/177,897, filed on Jan. 24, 2000, entitled "MIXED BUFFER SYSTEM FOR STABILIZING POLYPEPTIDE FORMULATIONS", which are incorporated by reference herein, or the like. In further alternative embodiments, other components are added to the insulin such as polypeptides described in U.S. patent application Ser. No. 09/334,676, filed on Jun. 25, 1999, entitled "MULTIPLE AGENT DIABETES THERAPY", small molecule insulin mimetic materials such as described in U.S. patent application Ser. No. 09/566,877, filed on May 8, 2000, entitled "DEVICE AND METHOD FOR INFUSION OF SMALL MOLECULE INSULIN MIMETIC MATERIALS", both of which are incorporated by reference herein, or the like.

Infusion Tube

In preferred embodiments, an infusion tube **36** is used to carry the insulin **24** from the infusion device **34** to the infusion set **38**. In alternative embodiments, the infusion tube carries the insulin **24** from infusion device **34** directly into the body **20**. In further alternative embodiments, no infusion tube is needed, for example if the infusion device is attached directly to the skin and the insulin **24** flows from the infusion device, through a cannula or needle directly into the body. In other alternative embodiments, the infusion device is internal to the body and an infusion tube may or may not be used to carry insulin away from the infusion device location.

Infusion Set

In preferred embodiments, the infusion set **38** is of the type described in U.S. Pat. No. 4,755,173, entitled "SOFT CANNULA SUBCUTANEOUS INJECTION SET", which is incorporated by reference herein. In alternative embodiments, other infusion sets, such described in U.S. Pat. Nos. 4,373,527 and 4,573,994, are used, which are incorporated by reference herein. In alternative embodiments, other infusion sets, such as the Rapid set from Disetronic, the Silhouette from MiniMed, or the like, may be used. In further alternative embodiments, no infusion set is required, for example if the infusion device is an internal infusion device or if the infusion device is attached directly to the skin.

Configurations With Supplemental Devices

In further alternative embodiments, the pre-filter, filters, calibrator and/or controller **12** are located in a supplemental device that is in communication with both the telemetered characteristic monitor transmitter **30** and the infusion device **34**. Examples of supplemental devices include, a hand held personal digital assistant such as described in U.S. patent application Ser. No. 09/487,423, filed on Jan. 20, 2000, entitled "HANDHELD PERSONAL DATA ASSISTANT (PDA) WITH A MEDICAL DEVICE AND METHOD OF USING THE SAME", which is incorporated by reference herein, a computer, a module that may be attached to the telemetered characteristic monitor transmitter **30**, a module that may be attached to the infusion device **34**, a RF programmer such as described in U.S. patent application Ser. No. 09/334,858, filed on Jun. 17, 1999, entitled EXTERNAL INFUSION DEVICE WITH REMOTE PROGRAMMING, BOLUS ESTIMATOR AND/OR VIBRATION CAPABILITIES (published as PCT application WO 00/10628), which is incorporated by reference herein, or the like. In particular embodiments, the supplemental device includes a post-calibration filter, a display, a recorder, and/or a blood glucose meter. In further alternative embodiments, the supplemental device includes a method for a user to add or modify information to be communicated to the infusion device **34** and/or the telemetered characteristic monitor transmitter **30** such as buttons, a keyboard, a touch screen, and the like.

In particular alternative embodiments, the supplemental device is a computer in combination with an analyte monitor and a RF programmer. The analyte monitor receives RF signals from the telemetered characteristic monitor transmitter **30**, stores the signals and down loads them to a computer when needed. The RF programmer sends control signals to the infusion device **34** to reprogram the rate of insulin infusion. Both the analyte monitor and the RF programmer are placed into separate communication stations. The communication stations include IR transmitters and IR receivers to communicate with the analyte monitor and the RF programmer. The sensor signal values are transmitted via the telemetered characteristic monitor transmitter **30** to the analyte

monitor located in one of the communication stations. Then the sensor signal values are communicated through the IR receiver in a first communication station and to the computer. The computer processes the sensor signal values through one or more filters, calibrators, and controllers to generate commands **22**. The commands are sent to a second communication station and sent to an RF programmer by the IR transmitter in the communication station. Finally the RF programmer transmits the commands **22** to the infusion device **34**. The communication station, analyte monitor and infusion device **34** may be of the type described in U.S. patent application Ser. No. 09/409,014, filed on Sep. 29, 1999 entitled COMMUNICATION STATION FOR INTERFACING WITH AN INFUSION PUMP, ANALYTE MONITOR, ANALYTE METER OR THE LIKE (published as a PCT application WO 00/18449), which is incorporated by reference herein. Alternatively, the RF programmer may be omitted and the infusion device may be placed in a communication station, or the infusion device may receive the commands without the use of an RF programmer and/or a communication station.

Overnight Closed-Loop System

A closed-loop insulin delivery system of the type described herein may utilize a variety of control algorithms to regulate the delivery of insulin to the body of the patient in a safe and predictable manner. Overnight operation of a closed-loop insulin infusion system should be carefully controlled in an automated way that need not depend on patient, user, or caregiver interaction. In this regard, a number of safeguards can be implemented with the system. These safeguards are intended to provide actionable sensor glucose readings, assess the accuracy of sensor readings, and constrain insulin delivery based upon possible sensor over-read conditions. These safeguards will alert the user and allow the patient to take appropriate actions. Therefore, these safeguards will mitigate the potential risks of overnight closed-loop control.

The control algorithm utilized by the system may be considered to be one type of safeguard in that it emulates the effect of insulin inhibiting insulin secretion. The system may also implement sensor performance safeguards. For example, a closed-loop initiation algorithm determines if the system can enter the closed-loop mode by calculating a recent calibration factor. The initiation algorithm checks the time between recent and prior calibration factors and determines the relative sensor error between the readings. As another example of a sensor safeguard, the system may employ a model supervisor during the closed-loop mode. The model supervisor checks that the sensor glucose readings are adequate for use during overnight closed-loop mode by comparing model-predicted sensor glucose values in real-time against actual sensor glucose values. If the model-predicted glucose values and the actual values differ significantly, the system triggers a fail-safe alert indicating a faulty sensor. This fail-safe alert can be generated in response to a number of sensor issues, such as sensor drift, sensor dislodgement, sensor compression artifact, etc.

The system may also implement a target glucose level safeguard. In this regard, a start-up algorithm can be deployed to provide a smooth transition between the open-loop mode and the closed-loop mode by gradually adjusting the target glucose level while in the closed-loop mode. The adjusted target glucose is used by the closed-loop control algorithm until the adjusted target glucose converges to a particular setpoint. At that time, the setpoint can be used for future dosing calculations during the closed-loop mode.

The system may also utilize at least one insulin limit as an insulin delivery and sensor performance safeguard. In this context, the insulin limit constrains the maximum amount of insulin delivered to the patient at any time in order to avoid over-delivery of insulin by the closed-loop control system due to potential sensor faults. In practice, the insulin limit is a value that is specific to each patient and is calculated based on the patient's basal rate, fasting blood glucose, and insulin sensitivity.

The system may also employ one or more insulin delivery safeguards. For example, an insulin delivery timeout continuously monitors (during closed-loop operation) if the patient is receiving insulin at the insulin limit for a prolonged period of time and, if so, triggers a fail-safe alert. This safeguard also monitors if the system is not delivering insulin for a prolonged period of time and, if so, triggers a fail-safe alert. A correction bolus is another insulin delivery safeguard. The system calculates an insulin bolus dosage for mitigating hyperglycemia at the commencement of closed-loop mode if the patient is above a designated blood glucose threshold. The determination can be achieved by acquiring a blood glucose meter reading at the initiation of closed-loop mode. The correction bolus is calculated based on the patient's insulin sensitivity, the amount of insulin on board, and a glucose target. Insulin on board (IOB) compensation is yet another insulin delivery safeguard. IOB compensation estimates the amount of insulin on board based on manual boluses administered, such that the system can effectively account for the IOB. In this regard, the manual boluses may be subtracted from the insulin dose that is calculated by the PID-IFB control algorithm.

The system may also implement one or more communication safeguards. For example, a "missed sensor transmission" feature continuously monitors data being received by the controller. For missed data packets totaling less than 15 minutes of operating time, the system remains in closed-loop mode. During this time, however, the system continues to calculate the insulin dose using the closed loop control algorithm based on the last valid sensor glucose value. For missed data packets totaling 15-60 minutes, the safeguard will switch to a pre-programmed safe basal rate, defined as half the patient's night time basal rate. If the controller starts receiving data packets during the safe basal rate timeframe, the system will again switch to the closed-loop mode. For missed data packets totaling more than 60 minutes, the system will switch to the open-loop mode where it will deliver a pre-programmed basal rate (which may be set by a caregiver).

The exemplary closed-loop control algorithms, methodologies, and techniques described in more detail below may be based around a PID control algorithm of the type presented in the preceding sections of this disclosure. In certain embodiments, the closed-loop control algorithms utilize a PID insulin feedback (PID-IFB) control algorithm. More specifically, the PID-IFB control algorithm cooperates with other algorithms, processes, and controls that represent additional safeguards that may apply during overnight use (and/or during other periods of use). These additional safeguards may include, without limitation: the use of an "Insulin Limits" parameter; a closed-loop initiation circuit that is based on glucose sensor calibration; an insulin on board (IOB) compensation algorithm; monitoring missed transmissions; and monitoring sensor glucose against predicted sensor glucose.

In practice, optimal or desired settings for the Insulin Limits parameter should be determined. In this regard, the Insulin Limits parameter serves as an input to the controller logic for each patient, and it imposes an upper limit to the insulin delivery rate as an additional safety feature to avoid over-delivery of insulin by the controller due to potential sensor

error. In certain embodiments, the Insulin Limits parameter is calculated from the patient's basal rate, fasting blood glucose, and insulin sensitivity.

Referring again to FIG. **1**, a closed-loop system generally includes a glucose sensor system **10**, a controller **12**, and an insulin delivery system **14**. Although FIG. **1** depicts these primary elements as separate blocks, embodiments of the system may combine two or more of the illustrated blocks into a single physical component. For example, an investigational test configuration of the closed-loop system may include a traditional patient-worn infusion pump (corresponding to the insulin delivery system **14**), a conventional continuous glucose sensor/transmitter assembly (corresponding to the glucose sensor system **10**), and a mobile computing device with a suitably written software application installed thereon (corresponding to the controller **12**). The mobile computing device may be, for example: a smartphone; a tablet computer; a netbook computer; a digital media player; a handheld video game device; or the like. It should be appreciated that the desired closed-loop control functionality can be carried out by way of one or more computer-executable programs or applications designed to run on the mobile computing device. An investigational test configuration may also include a translator device that serves as a data communication interface between the mobile computing device (which may utilize standard wireless data communication technologies such as the Wi-Fi or BLUETOOTH data communication protocol) and the glucose sensor system **10** (which may use a proprietary data communication protocol that is usually incompatible with the mobile computing device).

In other embodiments, the functionality of the glucose sensor system **10** could be integrated into the insulin delivery system **14**, perhaps as an interchangeable disposable module that attaches to the housing of the insulin delivery system **14**. In yet other embodiments, the functionality of the controller **12** could be incorporated into the insulin delivery system **14** such that a separate and distinct controller device need not be carried by the patient. Indeed, the control software utilized by the controller **12** can be ported for installation in an insulin infusion pump, a pump monitor device, or the like to implement the functionality of the controller **12** in those devices if so desired. In further embodiments, a single hardware device platform could be suitably designed to accommodate the functionality of the insulin delivery system **14**, the glucose sensor system **10**, and the controller **12**. These and other possible implementations are contemplated by this disclosure, and the particular manner in which the closed-loop system is configured and deployed is not intended to limit or otherwise restrict the scope or application of the closed-loop control techniques described herein.

Although not shown in FIG. **1**, the closed-loop system may include or cooperate with a conventional blood glucose meter (e.g., a finger stick device) that provides measured BG values to the controller **12** and/or to the insulin delivery system **14**, such that the glucose sensor system **10** can be calibrated. In certain embodiments, the measured BG values are sent to the insulin delivery system **14**, which in turn sends the BG value, sensor calibration factor, and calibration time to the controller **12**. The controller **12** can process and analyze the received information to determine whether or not the system can enter the closed-loop operating mode. In this regard, the controller **12** may check to ensure that the calibration of the glucose sensor system **10** is within an acceptable range before allowing the system to enter the closed-loop mode.

After entering the closed-loop mode, the insulin delivery system **14** sends sensor glucose (SG) values, sensor Isig values, calibration factors, "insulin delivered" values, and other data as needed to the controller **12** in accordance with a predetermined schedule, e.g., at five minute intervals. The controller **12** determines the desired insulin dose based on the closed-loop algorithm to maintain the patient at a target glucose setpoint, and communicates suitable control data and instructions to the insulin delivery system **14**. The insulin delivery system **14** responds to deliver the insulin dose specified by the controller **12** to the user.

FIG. **49** is a block diagram that illustrates processing modules and algorithms of an exemplary embodiment of a closed-loop system controller **900**, and FIG. **50** is a flow chart that illustrates an exemplary embodiment of a control process **1000** that may be performed at least in part by the controller **900** to control the insulin delivery system **14**. The controller **12** shown in FIG. **1** may be configured in accordance with that shown in FIG. **49**. FIG. **49** schematically depicts certain inputs and outputs of the controller **900**, where the parallelograms represent the inputs, the ovals represent the outputs, and the rectangles represent the various functional modules of the controller **900**. In the context of this description, a "functional module" may be any process, technique, method, algorithm, computer-executable program logic, or the like. In this regard, the controller **900** could be realized as any electronic device having a processor architecture with at least one processor device, and at least one memory element that is cooperatively associated with the processor architecture. The processor architecture is suitably configured to execute processor-executable instructions stored in the at least one memory element such that the controller **900** can perform the various control operations and methods described in detail herein.

The host electronic device that implements the controller **900** may be realized as a monitor device for an insulin infusion device, where the monitor device and the insulin infusion device are two physically distinct hardware devices. In another embodiment of the system, the host electronic device that implements the controller **900** may be realized as a portable wireless device, where the portable wireless device and the insulin infusion device are two physically distinct hardware devices. The portable wireless device in this context may be, without limitation: a mobile telephone device; a tablet computer device; a laptop computer device; a portable video game device; a digital media player device; a portable medical device; or the like. In yet other system embodiments, the host electronic device and the insulin infusion device are physically and functionally integrated into a single hardware device. In such embodiments, the insulin infusion device will include the functionality of the controller **900** as presented here.

Certain embodiments of the controller **900** include a plurality of cooperating functional modules that are designed and configured to determine the insulin dose to be delivered to keep the patient at the target glucose setpoint during an overnight closed-loop operating mode. In this regard, the illustrated embodiment of the controller **900** may include the following functional modules, without limitation: a closed-loop initiation module **902**; a start-up module **904**; a proportional integral derivative insulin feedback (PID-IFB) control module **906**; an insulin limit module **908**; an insulin on board (IOB) compensation module **910**; an insulin delivery timeout module **912**; a model supervisor module **914**; and a missed transmission module **916**.

Referring to FIG. **50**, the control process **1000** may begin at any time when it is desired to enter the closed-loop operating mode. Accordingly, the control process **1000** may begin in response to a user-initiated command, automatically in

response to the detection of operating conditions that are usually indicative of closed-loop operation (e.g., sleeping), or the like. Certain embodiments of the control process **1000** may begin with one or more system checks (task **1002**) to confirm whether or not the system is allowed to enter the closed-loop operating mode. This particular example employs a sensor calibration check before allowing the system to proceed to the closed-loop mode. Referring to FIG. **49**, the closed-loop initiation module **902** may be involved during task **1002**.

In some embodiments, the closed-loop initiation module **902** may consider certain sensor performance criteria that prevents closed-loop initiation. Such criteria may include, without limitation: (1) during start-up when the calibration is not stable; (2) when the sensor sensitivity changes significantly; (3) when sensors may be calibrated with a potentially invalid meter reading thereby changing the sensor sensitivity significantly; (4) any other situation that could cause a mismatch between the sensor and meter for a number of most recent calibrations spaced over a designated period of time (e.g., the two most recent calibrations).

The illustrated embodiment of the closed-loop initiation module **902** receives at least the following items as inputs: a meter (measured) BG value **920**; at least one sensor calibration factor **922** (i.e., calibration measurements, calibration data, etc.); the current sensor Isig value **924**; and timestamp data **926** that indicates the calibration time associated with the BG value **920** and the sensor calibration factor **922**. Some or all of this input data may be provided directly or indirectly by the insulin delivery system **14** (see FIG. **1**), a translator device, a monitor device, or any device in the closed-loop system. This description assumes that a new sensor calibration factor **922** and new timestamp data **926** is generated for each measured BG value **920**, wherein the sensor calibration factor **922** is associated with the calibration of the glucose sensor system **10** (see FIG. **1**) that is being used to monitor the patient. In particular, the sensor calibration factor may be based on the meter BG value **920** and the corresponding sensor Isig value **924**.

The closed-loop initiation module **902** analyzes the input data (both current values and historical values) to determine whether or not the system is allowed to enter into the closed-loop mode. For example, the closed-loop initiation module **902** may: check the period between two consecutive calibration timestamp values; compare recent and prior calibration factor values; and the like. The "outputs" of the closed-loop initiation module **902** correspond to two operating modes of the system. More specifically, the closed-loop initiation module **902** controls whether the system remains operating in the open-loop mode **928** or whether the system starts the closed-loop mode **930**.

Referring to FIG. **50**, if the closed-loop mode is not permitted (the "No" branch of query task **1004**), then the control process **1000** operates the system such that it remains in the open-loop mode (task **1006**). On the other hand, if the closed-loop mode is permitted (the "Yes" branch of query task **1004**), then the control process **1000** can initiate and start the closed-loop mode in an appropriate manner (task **1008**). Referring again to FIG. **49**, a correction bolus **932** can be calculated and delivered (if needed) to mitigate hyperglycemia at the commencement of the closed-loop mode. This correction bolus **932** serves as an additional safeguard to achieve a target blood glucose level if a measured meter reading is greater than a threshold value. If the control process **1000** determines that a correction bolus is required, then an appropriate insulin dose instruction is generated for execution by the insulin delivery system at the outset of the closed-loop mode.

Referring to FIG. **49**, the start-up module **904** may be called in response to a determination that the system can proceed to the closed-loop operating mode. Once the system is in the closed-loop mode, the controller retrieves historical data that can be processed and used as described in more detail below. In certain embodiments, for example, the controller obtains data for the last 24 hours (from the insulin delivery system, from a monitor, or the like). Thereafter, the controller retrieves data packets once every sampling period to obtain, without limitation: sensor glucose (SG) values; sensor Isig values; sensor calibration factors; information related to the amount of insulin delivered; information related to manual boluses delivered; and sensor calibration factors. As explained in more detail below, the received information can be used in the various safeguards, and to determine the final insulin dose.

The start-up module **904** receives sensor glucose (SG) values **940** as an input, and the functionality of the start-up module **904** may be initiated in response to the start of the closed-loop mode **930** (this trigger mechanism is represented by the dashed arrow **942** in FIG. **49**). The SG values **940** may be provided directly by the glucose sensor system **10** or indirectly via the insulin delivery system **14**, a translator device, or any device in the closed-loop system (see FIG. **1**). This description assumes that SG values **940** are received by the start-up module **904** in an ongoing manner as they become available. The start-up module **904** may also utilize a target glucose setpoint value **944**, which may be internally maintained, generated, and/or provided by the controller **900**. For the implementation presented here, the target glucose setpoint value **944** represents a fixed (constant) value that the user can specify (FIG. **49** depicts the target glucose setpoint value **944** in dashed lines to indicate that the value is a user-specified parameter rather than a functional module or data received by the system).

In certain embodiments, the start-up module **904** calculates a final target glucose value **946**, which serves as an input to the PID-IFB control module **906**. The final target glucose value **946** enables the system to make a smoother transition between open-loop and closed-loop modes (by gradually adjusting the final target glucose value **946**). The start-up module **904** may utilize the target glucose setpoint value **944** to calculate the final target glucose value **946**. In this regard, the start-up module **904** elevates the final target glucose value **946** to the same level as the sensor glucose value at the start of the closed-loop mode, provided the sensor glucose is above a certain threshold. As time progresses, the final target glucose value **946** gradually decreases back to the target glucose setpoint value **944** (usually in approximately two hours). Referring to FIG. **50**, the control process **1000** calculates the final target glucose value (task **1010**) and continues by calculating an uncompensated insulin infusion rate, PIDRate(n), based at least in part on the final target glucose value (task **1012**). For this example, the start-up module **904** may be involved during task **1010**, and the PID-IFB control module **906** may be involved during task **1012**.

As an additional safeguard, the insulin limit module **908** cooperates with the PID-IFB control module **906** to provide an upper insulin limit that is calculated based on the patient's basal rate, fasting blood glucose, and insulin sensitivity. This upper insulin limit imposes an upper limit to the insulin delivery rate to avoid over-delivery of insulin by the system due to potential sensor error.

The PID-IFB control module **906** may be configured to carry out the control processes described in more detail above with reference to FIGS. **1-48**. In some embodiments, the PID-IFB control module **906** receives at least the following

items as inputs: the SG value **940** (which may be used to calculate a rate of change value that indicates the rate of change of the SG value); the current sensor Isig value **950**; the current sensor calibration factor **952**; and an amount of insulin delivered **954**. The inputs to the PID-IFB control module **906** may be provided directly or indirectly by the insulin delivery system **14**, the glucose sensor system **10**, a translator device, a monitor device, and/or any device in the closed-loop system (see FIG. **1**). The PID-IFB control module **906** is suitably configured to calculate the insulin infusion rate based on the current and past SG values **940**, the SG rate of change, the sensor Isig value **950**, the sensor calibration factor **952**, the final target glucose value **946**, and the insulin delivered **954** in order to achieve euglycemia. These (and possibly other) values may be received by the PID-IFB control module **906** in an ongoing manner as they become available, e.g., in five minute intervals or in accordance with any desired schedule.

The insulin delivered **954** is a parameter or value that indicates the amount of insulin that has been delivered to the patient by the insulin delivery system. Thus, the insulin delivered **954** may indicate recent boluses (typically by Units) delivered over a period of time. In certain implementations, the insulin delivered **954** corresponds to the amount of insulin delivered in the last sampling time, which may be, without limitation: one minute; five minutes; thirty seconds; or any designated sampling time. The insulin delivered **954** may also indicate the amount of insulin delivered by the delivery system as basal or boluses in any defined period of time in the past (e.g., the last N hours) or the amount of insulin delivered by the system in the last sampling cycle. In practice, the PID-IFB control module **906** (and the IOB compensation module **910**) may be "initialized" to collect and save historical values for the insulin delivered **954** as needed. Thereafter, the insulin delivered **954** can simply indicate an amount of insulin administered by the system during the last sampling time period if by a bolus or basal channels.

As mentioned above, the PID-IFB control module **906** may utilize an upper insulin limit, which is a patient-specific parameter. In certain embodiments, the upper insulin limit may be entered by the user, a caregiver, or the like. Alternatively, the insulin limit module **908** may be responsible for calculating or otherwise managing the upper insulin limit if so desired. The upper insulin limit imposes an upper limit to the insulin delivery rate as an additional safety feature to avoid over-delivery of insulin by the controller **900** due to potential sensor error. Thus, if the PID-IFB control module **906** recommends a dose higher than the insulin limit, the insulin limit will constrain the insulin delivered to the insulin limit value. In addition, the insulin limit will "freeze" the integral component of the PID to its previous value to prevent integral windup, which can cause continuous integrating of the glucose error until it reaches maximum values. In certain embodiments, the upper insulin limit has a default value set at five times the patient's basal rate. Hence, if the maximum value is reached, the PID-IFB control algorithm will be fairly aggressive in calculating an insulin dose. Accordingly, to minimize integral windup, the insulin limit is fed back to the PID-IFB control module **906** (as depicted in FIG. **49**) for use in the next insulin dose calculation.

The PID-IFB control module **906** operates as described previously to calculate a current insulin dose **958** as an output value (the current insulin dose **958** is also referred to herein as the uncompensated insulin infusion rate, PIDRate(n)). In practice, the current insulin dose **958** is typically expressed as an infusion rate (Units/Hour). In the context of this description, the current insulin dose **958** represents a baseline closed-loop infusion rate, which may be subjected to further adjustment or compensation by the IOB compensation module **910**. Referring again to FIG. **50**, the control process **1000** may compensate for the insulin "on board" the patient by calculating an adjusted insulin infusion rate, AdjustedRate(n), based at least in part on the uncompensated insulin infusion rate (task **1014**). For this example, the IOB compensation module **910** may be involved during task **1014**.

The IOB compensation module **910** receives at least the following items as inputs: the current insulin dose **958**; and information regarding manual boluses delivered **960**. The manual boluses delivered **960** may be provided directly or indirectly by the insulin delivery system **14**, a translator device, a monitor device, and/or any device in the closed-loop system (see FIG. **1**). This description assumes that the manual boluses delivered **960** is received by the IOB compensation module **910** in an ongoing manner as it becomes available, e.g., in five minute intervals or in accordance with any desired schedule. The IOB compensation module **910** is suitably configured to estimate insulin on board based on manual boluses delivered, before or during closed-loop operation, in order to compensate the final infusion rate to help avoid over-delivery of insulin by the controller **900**. Accordingly, the output of the IOB compensation module **910** may be a final insulin dose **962** expressed as a final infusion rate (Units/Hour). The final insulin dose **962** is also referred to herein as the adjusted insulin infusion rate, AdjustedRate(n).

Referring to FIG. **50**, the control process **1000** uses the adjusted insulin infusion rate, AdjustedRate(n), to control the insulin infusion device, which in turn regulates the delivery of insulin to the body of the user (task **1016**). In certain embodiments, the adjusted insulin infusion rate is communicated to the insulin infusion device in an appropriate manner (such as wireless data communication). The control process **1000** may continue as described above in an iterative and ongoing manner to monitor the condition of the user and deliver insulin as needed without user involvement. That said, if the control process **1000** determines that the closed-loop operating mode should be terminated (the "Yes" branch of query task **1018**), then the control process **1000** causes the system to switch back to the open-loop mode (task **1020**). The closed-loop mode may be ended in response to a user-initiated command, automatically in response to the detection of operating conditions that are usually indicative of open-loop operation, or the like.

If query task **1018** determines that the closed-loop mode should continue (the "No" branch of query task **1018**), then the control process **1000** may check whether it is time to perform another iteration of the control routine. In other words, the control process **1000** may check for the next sampling time (query task **1022**). If it is time for the next iteration, then the control process **1000** may return to task **1010** and repeat the computations with the next set of data values. For example, the next iteration of the control routine may obtain and process the current values of some or all of the following parameters, without limitation: the SG value **940**; the SG rate of change; the sensor Isig value **924**; the amount of insulin delivered **954**; and the manual boluses delivered **960**. This allows the control process **1000** to adjust the final insulin infusion rate in an ongoing manner in accordance with a predetermined schedule, a designated sampling rate, or the like.

The insulin delivery timeout module **912** monitors if the patient is receiving continuous delivery of insulin at the maximum insulin limit or the minimum allowable infusion of zero Units/Hour for a time specified by the controller. Accordingly, the insulin delivery timeout module **912** may receive

the insulin delivered **954** as an input. If the specified time is exceeded, the system will trigger a fail-safe alert **966**. Otherwise, the system remains in the closed-loop operating mode **968**.

Referring back to FIG. **49**, the model supervisor module **914** receives at least the following as inputs: the insulin delivered **954**; sensor Isig values **950**; and one or more sensor calibration factors **952**. The inputs to the model supervisor module **914** may be provided directly or indirectly by the insulin delivery system **14**, the glucose sensor system **10**, a translator device, a monitor device, and/or any device in the closed-loop system (see FIG. **1**). The model supervisor module **914** is suitably designed and configured to estimate the user's glucose concentration in real time (or substantially real time) based on the insulin delivered **954**, the sensor Isig values **950**, and the sensor calibration factors **952**. The sensor calibration factors **952** used by the model supervisor module **914** are equal to the sensor calibration factors **922** used by the closed-loop initiation module **902**. That said, the closed-loop initiation module **902** utilizes the sensor calibration factors **922** at one particular time, whereas the model supervisor module **914** considers the sensor calibration factors **952** in an ongoing and continuous manner during operation in the closed-loop mode. Should the model-predicted glucose and the sensor glucose values differ significantly, the system will exit closed loop mode. Accordingly, the model supervisor module **914** regulates whether the system remains in the closed-loop mode **974** or switches to the open-loop mode **976**.

The missed transmission module **916** is suitably configured to monitor the following, without limitation: the sensor Isig values **950**; the SG values **940**; and the sensor calibration factors **952**. More particularly, the missed transmission module **916** continuously monitors to check whether the system is receiving data packets that convey the necessary information and input values. For missed data packets totaling less than a lower threshold of time (e.g., 15 minutes), the system remains in the closed-loop mode, as indicated by block **980** in FIG. **49**. During this time, the system will continue to calculate the insulin dose using the closed-loop control methodology based on the last valid sensor glucose value. For missed data packets totaling a time longer than the lower threshold and shorter than an upper threshold of time (e.g., 60 minutes), the missed transmission module **916** will switch the system to a pre-programmed safe basal rate, as indicated by block **982** in FIG. **49**. In certain embodiments, this safe basal rate is defined as half the patient's overnight basal rate, and this parameter may be programmed by a caregiver or physician. If the missed transmission module **916** starts receiving data packets while the safe basal rate is being administered, the system will switch back to the closed-loop mode. For missed data packets totaling more than the upper threshold of time, the system will switch to the open-loop mode, as indicated by block **984** in FIG. **49**. At this point, the system will be controlled to deliver a pre-programmed open-loop overnight basal rate.

To summarize, the controller **900** determines whether to enter into the closed-loop mode in response to at least the recent meter BG values **920**, the sensor calibration factors **922**, and the calibration timestamp data **926**. The controller **900** utilizes the closed-loop initiation module **902** to check if the sensor calibration time between the last two calibration values is within an acceptable range, and whether any change between the two calibration values (recent and prior value) is acceptable. If so, the controller **900** will switch the system into the closed-loop mode. Once the system is in the closed-loop mode, the controller **900** will periodically receive data packets (e.g., every five minutes) that include the current SG value **940**, the current sensor Isig values **950**, the insulin delivered **954**, the sensor calibration factors **952**, and manual boluses delivered **960**. In certain embodiments, each of the data packets received by the controller **900** includes data collected during the previous 24-hour period.

The start-up module **904** utilizes the SG values **940** and the target glucose setpoint value **944** to calculate the final target glucose value **946**. In some embodiments, the target glucose setpoint value **944** is set to 120 mg/dL, although other settings could be used if so desired (a typical range of settings may be, for example 70-300 mg/dL). This results in a smoother transition between open-loop and closed-loop modes by gradually adjusting the final target glucose value **946**. The final target glucose value **946** is sent to the PID-IFB control module **906** for use as one input to calculate the final insulin dose **962**.

The PID-IFB control module **906** utilizes the final target glucose value **946**, the current and past SG values **940**, the SG rate of change values, and the insulin delivered **954** to determine the insulin infusion rate (final insulin dose **962**) in order to achieve euglycemia. As an additional safeguard, the upper insulin limit (calculated based on the patient's basal rate, fasting blood glucose, and insulin sensitivity) from the insulin limit module **908** is input into the controller **900** for each patient to impose an upper limit to the insulin delivery rate to avoid over-delivery of insulin by the controller **900**. The PID-IFB control module **906** considers the upper insulin limit before sending the final insulin dose **962** to the IOB compensation module **910**, which estimates insulin on board from manual boluses, before or during closed-loop operation, in order to calculate the final insulin dose **962**. The final insulin dose **962** may be communicated from the controller **900** directly or indirectly to the insulin delivery system **14** such that the final insulin dose **962** can be delivered to the patient during closed-loop operation.

Additional safeguards could be implemented to monitor the system during closed-loop operation, such that the system exits the closed-loop mode when certain criteria are not met. For example, the controller **900** may cause the system to exit the closed-loop mode if more than a designated number of consecutive data packets are missed. This assumes that the controller **900** usually receives data packets (from the insulin delivery system **14**, from a monitor, from a translation device, or the like) in a continuous manner during closed-loop operation. Thus, if the controller **900** detects that more than a threshold number of consecutive data packets are not received as expected, the system will be commanded to exit the closed-loop mode. This functionality is associated with the missed transmission module **916**, as described previously.

Moreover, the model supervisor module **914** estimates the user's glucose concentration in an ongoing manner, based on the insulin delivered **954**, the sensor Isig values **950**, and the sensor calibration factors **952**. If the difference between the model-predicted glucose and the sensor glucose value is greater than a stated threshold, the controller **900** may cause the system to exit the closed-loop mode.

As summarized above, the controller **900** employs a number of modules or functions that cooperate to regulate the delivery of insulin during closed-loop operation: the closed-loop initiation module **902**; the start-up module **904**; the PID-IFB control module **906**; the insulin limit module **908**; and the IOB compensation module **910**. Moreover, the controller **900** may employ a number of modules that perform various safeguarding functions during closed-loop operation. These safeguarding modules may include: the insulin deliv-

ery timeout module **912**; the model supervisor module **914**; and the missed transmission module **916**.

Closed-Loop Initiation Module: First Representation

The closed-loop initiation module **902** checks for changes in sensor sensitivity and determines whether or not the system is allowed to enter the closed-loop mode. Referring again to FIG. **49**, the inputs to the closed-loop initiation module **902** include the meter BG value **920**, the sensor calibration factor **922**, and the calibration timestamp data **926**. The closed-loop initiation module **902** checks for a series of conditions pertaining to the sensor calibration factor values **922** and the times when the sensor calibration factor values **922** were obtained. If all the conditions are met, the controller **900** initiates the closed-loop operating mode. If this criteria is not met, the system remains in the open-loop operating mode and the controller **900** requests a new sensor calibration.

Certain embodiments of the closed-loop initiation module **902** execute one or more functions, algorithms, or methods to determine whether or not the system can proceed to the closed-loop mode. The following are the parameters and variables used by an exemplary embodiment of the closed-loop initiation module **902**:

t=time when attempting to enter the closed-loop mode;

Recent Calibration Factor (CFR)=the most recent sensor calibration factor (CF) value;

tR=the time when the CFR was obtained;

Prior Calibration Factor (CFP)=the last CF value before the CFR;

tP=the time when the CFP was obtained;

CFchange=percentage change in CF from a previous CF to a current CF, for any pair of CFs. The CFchange can be calculated according to the following equation:

$$CF\text{change}=(\text{abs}(CF\text{current}-CF\text{previous})/CF\text{previous})*100 \quad \text{(eq 50)}$$

tRecent=time window for the most recent calibration before attempting to start closed-loop mode (minutes)

tDiffmin=minimum time difference between the recent calibration and the calibration prior to the recent calibration (minutes)

tDiffmax=maximum time difference between the recent calibration and the prior calibration (minutes)

CFmin=minimum acceptable CF (mg/dL per nA)

CFmax=maximum acceptable CF (mg/dL per nA)

CFprevious=the CF value before CFcurrent in the pair of CF values

CFchangeTh=threshold for acceptable CFchange in % (mg/dL per nA)

In some embodiments, the closed-loop initiation module **902** is implemented in the form of a series of processing steps. Using the logic described below, the closed-loop initiation module **902** decides whether to let the system enter the closed-loop mode.

Case A

```
If (tP is not in the time window (tR−tDiffmin : tR)), the following
logic is checked.
If (CFmin ≤ CFR ≤ CFmax)
  If (t−tRecent ≤ tR ≤ t)
    If (tR−tDiffmax ≤ tP ≤ tR−tDiffmin)
      If (CFmax ≤ CFP ≤ CFmax)
        Calculate CFchange with CFR as the CFcurrent and
        with CFP as the CFprevious in Equation 50 stated
        above
        If (CFchange ≤ CFchangeTh)
          Enter Closed Loop
        Else Cannot enter closed loop at that time
```

-continued

Case A

```
        Else Cannot enter closed loop at that time
      Else Cannot enter closed loop at that time
    Else Cannot enter closed loop at that time
  Else Cannot Enter Closed Loop
```

If any of the above conditions is not met, the system remains in the open-loop mode. Thus, in order to enter the closed-loop mode, new calibration(s) that satisfy all of the conditions in Case A (or Case B as described below) will be required.

Case B

```
If (tP is in the time window (tR−tDiffmin : tR)),
CFV = most recent CF value in the time window of
tR−tDiffmax : tR−tDiffmin
tV = time when CFV was obtained
If (CFmin ≤ CFR ≤ CFmax)
  If there is a CFV available
      Calculate CFchange with CFR as the CFcurrent and with CFV
      as the CFprevious in Equation 50 stated above
      If (CFV, CFR and all CF values between times tV and tR lie in
      the range of (CFmin:CFmax) AND CFchange between CFV
      and CFR is ≤ CFchangeTh)
        Enter closed loop
      Else Cannot enter closed loop at that time
    Else Cannot enter closed loop at that time
  Else Cannot enter closed loop at that time
Else Cannot Enter Closed Loop
```

If any of the above conditions is not met, the system remains in the open-loop mode. Thus, in order to enter the closed-loop mode, new calibration(s) that satisfy all of the conditions in Case A or Case B will be required.

In accordance with certain variations of the closed-loop initiation module **902**, the system requests a meter BG and related calibration when entering the closed-loop mode. In such alternative embodiments, therefore, the closed-loop initiation module **902** uses the meter BG and Isig to calculate CFR. Thus, in such an implementation, the sensor current would also be an input to the closed-loop initiation module **902**. Accordingly, because CFR is now being calculated by the closed-loop initiation module **902** itself, the conditions in Case A and Case B (i.e., checking whether t−tRecent≤tR≤t) will always be met.

In particular implementations, some of the parameters mentioned above can be fixed. In this regard, the following values may be utilized in an exemplary embodiment. It should be appreciated that these values are provided here for illustrative purposes only, and that an implementation of the closed-loop initiation module **902** may utilize different values if so desired.

tRecent=120 minutes

tDiffmin=120 minutes

tDiffmax=480 minutes

CFmin=2.5 mg/dL per nA

CFmax=6 mg/dL per nA

Closed-Loop Initiation Module: Second Representation

In accordance with some embodiments, the functionality of the closed-loop initiation module **902** can be represented as follows. The closed-loop initiation module **902** may be implemented in the form of a series of case steps. In this regard, the closed-loop initiation module **902** first calculates the recent calibration factor value (CFR) using the most recent meter BG and Isig values as shown in the following Equation A1:

$$CFR=\text{meter}BG/(Isig-2) \quad \text{(eq A1)}$$

Here, CFR is the recent calibration factor value, meterBG is the meter BG value, and Isig is the sensor Isig value. The "−2" in Equation A1 represents a constant offset that is used by the calibration algorithm when calculating calibration factors and sensor glucose.

Using the logic described below for Case C or Case D, the closed-loop initiation module **902** decides whether to let the system enter the closed-loop mode. Each case condition is dependent upon the time at which the most recent prior calibration factor (CFP) was obtained.

Case C

Case C corresponds to a scenario where the time of prior calibration is greater than 120 minutes before the most recent calibration. In addition, the recent calibration factor (CFR) and the prior calibration factor (CFP) are within limits as shown in the following logical expressions.

$$CF\text{min} \leq \text{CFR} \leq CF\text{max} \quad \text{(eq A2)}$$

$$CF\text{min} \leq \text{CFP} \leq CF\text{max} \quad \text{(eq A3)}$$

Here, CFR is the recent calibration factor value, CFP is the prior calibration value, CFmin is the minimum value for the calibration factor that is set as 2.5 mg/dL per nA, and CFmax is the maximum value for the calibration factor that is set as 6 mg/dL per nA.

For Case C, the time of recent calibration (tR) is within two hours of the start of closed-loop initiation as shown in the following logical expression.

$$t - t\text{Recent} \leq tR \leq t \quad \text{(eq A4)}$$

Here, tR is the time of recent calibration, t is the time when attempting to enter the closed-loop mode, and tRecent is the time window for the most recent calibration before attempting to start the closed-loop mode (which is set to 120 minutes).

For Case C, the time of prior calibration (tP) occurs between two and eight hours before time of recent calibration factor as shown in the following logical expression.

$$tR - t\text{Diffmax} \leq tP \leq tR - t\text{Diffmin} \quad \text{(eq A5)}$$

Here, tP is the time of prior calibration, tR is the time when CFR was obtained, tDiffmax is the maximum time difference between the recent calibration and the prior calibration (which is set as 480 minutes (8 hours)), and tDiffmin is the minimum time difference between the recent calibration and the calibration prior to the recent calibration (which is set as 120 minutes (2 hours)).

For Case C, the calibration change (CFchange) is less than 35% as shown in the following logical expression, where CFchange is calculated according to Equation A6.

$$CF\text{change} = (\text{abs}(\text{CFR} - \text{CFP})/\text{CFP}) \times 100 \quad \text{(eq A6)}$$

$$CF\text{change} \leq CF\text{change}Th \quad \text{(eq A7)}$$

Here, CFchange is the percentage change in calibration factor from the previous calibration factor to a current calibration factor for any pair of calibration factors, CFchangeTh is the threshold for acceptable CFchange, (which is set to 35% for this example), CFR is the most recent calibration factor value, and CFP is the last calibration factor value before CFR.

If all of the foregoing conditions are met for Case C (Equations A2-A7), the closed-loop initiation module **902** can initiate the methodology for calculating the correction bolus (if needed). If, however, any condition is not met, the controller **900** remains in the open-loop mode. Thus, in order to enter the closed-loop mode, new calibration(s) that satisfy all of the conditions in Case C or Case D will be required.

Case D

Case D corresponds to a scenario where the time of prior calibration is less than 120 minutes before the most recent calibration. If the prior calibration is less than two hours before the recent calibration, an additional prior calibration factor (CFP2) is included in the analysis. This allows the closed-loop initiation module **902** to evaluate sensor sensitivity that has at least a two hour time span.

For Case D, the closed-loop initiation module **902** finds an earlier second prior calibration factor (CFP2) that occurs within two to eight hours before the time of the recent calibration factor (CFR) as shown in the following logical expression.

$$tR - t\text{Diffmax} \leq tP2 \leq tR - t\text{Diffmin} \quad \text{(eq A8)}$$

Here, tP2 is the time when the second prior calibration factor (CFP2) is obtained, tR is the time when CFR was obtained, tDiffmax is the maximum time difference between tP2 and tR (which is set as 480 minutes (8 hours) for this example), and tDiffmin is the minimum time difference between tP2 and tR (which is set as 120 minutes (2 hours) for this example).

For Case D, the closed-loop initiation module **902** also determines if more than one calibration factor (CF1 . . . CFn) is available between the time of the second prior calibration factor (CFP2) and the time of the recent calibration factor (CFR), as shown in the following logical expression.

$$tP2 \leq t1 \ldots tn \leq tR \quad \text{(eq A9)}$$

Here, t1 . . . tn is the time when more calibration factors (CF1 . . . CFn) are observed, tR is the time when CFR was obtained, and tP2 is the time when CFP2 is obtained.

For Case D, the time of recent calibration (tR) is within two hours of the start of closed-loop initiation, as shown in the following logical expression.

$$t - t\text{Recent} \leq tR \leq t \quad \text{(eq A10)}$$

Here, tR is the time of recent calibration, t is time when attempting to enter the closed-loop mode, and tRecent is the time window for the most recent calibration before attempting to start the closed-loop mode (which is set to 120 minutes for this example).

For Case D, all calibration factors including recent calibration factor (CFR), prior calibration factor (CFP), second prior calibration factor (CFP2) and CF1 . . . CFn are within limits as shown in the following logical expressions.

$$CF\text{min} \leq \text{CFR} \leq CF\text{max} \quad \text{(eq A11)}$$

$$CF\text{min} \leq \text{CFP} \leq CF\text{max} \quad \text{(eq A12)}$$

$$CF\text{min} \leq \text{CFP2} \leq CF\text{max} \quad \text{(eq A13)}$$

$$CF\text{min} \leq CF1 \ldots CFn \leq CF\text{max} \quad \text{(eq A14)}$$

Here, CFR is the recent calibration factor, CFP is the prior calibration factor, CFP2 is the second prior calibration factor, CF1 . . . CFn are calibration factors obtained between tP2 and tR, CFmin is the minimum value for the calibration factor (which is set as 2.5 mg/dL per nA for this example), and CFmax is the maximum value for the calibration factor (which is set as 6 mg/dL per nA for this example).

For Case D, the calibration change (CFchange) between CFR and CFP2 is less than 35%, as shown in the following logical expression where CFchange is calculated according to Equation A15.

$$CF\text{change} = (\text{abs}(\text{CFR} - \text{CFP2})/\text{CFP2}) \times 100 \quad \text{(eq A15)}$$

$$CF\text{change} \leq CF\text{change}Th \quad \text{(eq A16)}$$

Here, CFchange is the percentage change in calibration factor from the previous calibration factor to a current calibration factor for any pair of calibration factors, CFchangeTh is the threshold for acceptable CFchange (which is set to 35% for this example), CFR is the most recent calibration factor value, and CFP2 is the most recent calibration factor value in the time range described in Equation A8.

If all of the foregoing conditions are met for Case D (Equations A8-A16), the closed-loop initiation module **902** can initiate the methodology for calculating the correction bolus (if needed). If, however, any condition is not met, the controller **900** remains in the open-loop mode. Thus, in order to enter the closed-loop mode, new calibration(s) that satisfy all of the conditions in Case C or Case D will be required.

Correction Bolus With IOB Compensation

As described above, a correction bolus **932** may be commanded at the beginning of the closed-loop mode. The purpose of the correction bolus is to provide an insulin dose for mitigating hyperglycemia at the initiation of the closed-loop mode. This can be achieved by first acquiring a blood glucose meter reading value immediately prior to closed-loop initiation. If that BG meter reading value is above a certain correction threshold (CTH, which is 180 mg/dL for this example), the controller **900** will deliver an insulin dose based on the patient's insulin sensitivity (ISF, mg/dL/Units), insulin on board, and the desired target glucose level (TG, mg/dL) in order to bring the subject's glucose level to the target glucose level.

In accordance with certain implementations, the correction bolus (CB) is delivered based on the meter BG value (in mg/dL) acquired at the start of the closed-loop mode, as shown below:

$$CB = \begin{cases} \frac{BG - TG}{ISF} - IOB(n), & \text{if } (BG > CTH) \\ 0, & \text{if } (BG \le CTH) \end{cases} \quad \text{(eq A17)}$$

Here, CB is the correction bolus, BG is the blood glucose meter value (mg/dL), TG is the target glucose (mg/dL), ISF (see Equation A18) is the patient's adjusted insulin sensitivity factor (mg/dL/Units), CTH is the correction threshold for blood glucose beyond which a correction bolus will be delivered (mg/dL), and IOB(n) is the active insulin on board from manual boluses (Units) where n is the current sampling point as described previously.

$$ISF = ISFfactor \times ISF_0 \quad \text{(eq A18)}$$

Here, ISF is the patient's adjusted insulin sensitivity factor (mg/dL/Units), ISF_0 is the patient's established insulin sensitivity factor (mg/dL/Units) and ISFfactor is an ISF adjusting factor (unit less). The default value for ISFfactor is set to one, which makes $ISF = ISF_0$. However, for this particular example, ISFfactor has been assigned as an adjustable parameter with a range of 0.5 to 2 in order to provide greater flexibility for optimizing the patient's insulin sensitivity factor.

$$CB = \begin{cases} CB, & \text{if } (CB \ge 0) \\ 0, & \text{if } (CB < 0) \end{cases} \quad \text{(eq A19)}$$

Here, CB is the correction bolus expressed in Units. It should be appreciated that Equation A19 is utilized because the controller **900** can only deliver positive boluses.

Start-Up Module

The start-up module **904** processes sensor glucose (SG) values **940** and the target glucose setpoint value **944** (which is set to 120 mg/dL in certain embodiments) to calculate the final target glucose value **946**, which in turn serves as an input to the PID-IFB control module **906**. Accordingly, the final target glucose value **946** is sent to the PID-IFB control module **906** to calculate the final insulin dose **962**. Referring again to FIG. **49**, the start-up module **904** is "activated" or initiated in response to the starting of the closed-loop mode.

At the beginning of the closed-loop operating mode, the start-up module **904** calculates the difference between the current SG value **940** and the target glucose setpoint value **944**, as indicated by Equation 51 below.

$$DeltaGlu(n) = \begin{cases} SG(n) - Setpoint, & m = 1 \\ 0, & m > 1 \end{cases} \quad \text{(eq 51)}$$

In Equation 51, SG is the sensor glucose value, n is the current sampling point, Setpoint is the target glucose setpoint value defined by user, and m is the sampling time during closed-loop operation (m=1 indicates the start of the closed-loop mode, and m increases with each sample received during the closed-loop mode). DeltaGlu(n) is forced to zero when m>1 as well as in the following situation described in Equation 52.

Force DeltaGlu to zero if it is less than a certain threshold set in the controller **900** (referred to as MinDeltaGlu). Otherwise, it remains as DeltaGlu(n) if it is more than the threshold set in the controller **900**, as described in Equation 52:

$$DeltaGlu(n) = \begin{cases} 0, & DeltaGlu \le MinDeltaGlu \\ DeltaGlu(n), & DeltaGlu > MinDeltaGlu \end{cases} \quad \text{(eq 52)}$$

Here DeltaGlu is the difference between the current SG value **940** and the defined target glucose setpoint value **944**, calculated from Equation 51 above, and MinDeltaGlu is the minimum difference (set in the controller **900**) allowable between the current SG value **940** and the target glucose setpoint value **944**.

The dynamic setpoint (DynSP) is calculated based on a discretized second order transfer function model as indicated in Equation 53:

$$DynSP(n) = cd_1 \cdot DynSP(n-1) + cd_2 \cdot DynSP(n-2) + cn_0 \cdot DeltaGlu(n) + cn_1 \cdot DeltaGlu(n-1) \quad \text{(eq 53)}$$

Here, DynSP is the dynamic setpoint value, n is the current sampling point, n−1 is the last sampling point, and n−2 is the second to last sampling point. The parameters cd_1, cd_2, cn_0, and cn_1 are the coefficients of the setpoint model. These parameters are calculated based on the two time constants (τ_{sp1} and τ_{sp2}) of the setpoint model, as indicated below:

$$cd_1 = eaxx1 + eaxx2$$

$$cd_2 = -eaxx1 \times eaxx2$$

$$cn_0 = 1$$

$$cn_1 = \frac{(axx1 \times eaxx1 - axx2 \times eaxx2)}{daxx21}$$

Where:

$$axx1 = 1/\tau_{sp1}$$

$$axx2 = 1/\tau_{sp2}$$

$$eaxx1 = e^{-axx1 \cdot Ts}$$

$$eaxx2 = e^{-axx2 \cdot Ts}$$

$$daxx21 = axx2 - axx1$$

In the above equations Ts indicates the sampling interval in minutes, and τ_{sp1} and τ_{sp2} are the time constants of the set-

point model. Moreover, axx1 is the reciprocal of the time constant τ_{sp1}, axx2 is the reciprocal of the time constant τsp2, eaxx1 is the exponential decay factor for τ_{sp1}, eaxx2 is the exponential decay factor for τ_{sp2}, and daxx21 is the difference between the reciprocal of τ_{sp1} and τ_{sp2}.

The final target glucose value **946** is obtained by adding the dynamic setpoint value (calculated in Equation 53) with the target glucose setpoint value **944** as shown in Equation 54:

$$\text{Final Target}=\text{Setpoint}+\text{DynSP}(n) \quad \text{(eq 54)}$$

In particular implementations, some of the parameters mentioned above for the start-up module **904** can be fixed. In this regard, the following values may be utilized in an exemplary embodiment. It should be appreciated that these values are provided here for illustrative purposes only, and that an implementation of the start-up module **904** may utilize different values if so desired.

Setpoint=120 mg/dL

MinDeltaGlu=30 mg/dL (nominal); 0 mg/dL (lower bound); 600 mg/dL (upper bound)

τ_{sp1}=25 minutes (nominal); 0.1 minute (lower bound); 250 minutes (upper bound)

τ_{sp2}=30 minutes (nominal); 0.1 minute (lower bound); 250 minutes (upper bound)

PID-IFB Control Module

The PID-IFB control module **906** calculates the insulin infusion rate (final insulin dose **962**) based on the current and past sensor glucose values **940**, the sensor Isig values **950**, the rate of change of the sensor glucose values, the sensor calibration factor **952**, the final target glucose value **946**, the target glucose setpoint value **944**, insulin limits such as the upper insulin limit, and the insulin delivered **954** in order to achieve euglycemia. In certain embodiments, the PID-IFB control module **906** receives its inputs every five minutes, therefore the calculation of the insulin feedback components considers how often the input data is being received by the controller **900**.

The PID-IFB control module **906** calculates the final insulin dose **962** in accordance with Equation 55:

$$u(n)=P(n)+I(n)+D(n)-\gamma_1 I_{SC}\gamma_2 I_P-\gamma_3 I_{EFF} \quad \text{(eq 55)}$$

Note that PIDRate(n)≡u(n). In Equation 55, the insulin infusion rate u(n) represents the final insulin dose **962** shown in FIG. **49**. In Equation 55, P(n), I(n), and D(n) are, respectively, the proportional, integral, and derivative components of the PID controller. The insulin feedback components correspond to the remaining terms. The variables γ_1, γ_2, and γ_3 represent tuning coefficients. In accordance with some embodiments, γ_1=0.64935, γ_2=0.34128, and γ_3=0.0093667, although other values may be used. The parameters I_{SC}(n), I_P(n), and I_{EFF}(n) correspond to the states of the insulin pharmacokinetic model corresponding to, respectively, the subcutaneous, plasma, and effective site compartments. Therefore, the amount of insulin delivered is reduced in proportion to the predicted insulin concentration in the different compartments.

The exemplary implementation of the control algorithm employed by the PID-IFB control module **906** is implemented in discrete (sampled) time. In the notation used, n is the current time step, where $t=nT_s$, and t is the continuous time (in minutes) when using a sampling period of T_s.

The proportional component P(n) is calculated as follows:

$$P(n)=Kp[SG(n)-\text{Final Target}(n)] \quad \text{(eq 56)}$$

Here, Kp is the overall controller gain (expressed in Units/hour per mg/dL), SG(n) is the current sensor glucose, n indicates the current sampling point, and Final Target(n) is the calculated final target glucose setpoint from Equation 54. It should be appreciated that Kp is a patient-specific value and, therefore, the actual value of Kp will vary from one person to another. Although the range can vary depending upon the patient, in most typical scenarios, the value of Kp may be within the range of 0.008 to 0.200.

The integral component I(n) can be calculated as follows:

$$I(n) = I(n-1) + \frac{K_p \cdot T_s}{T_I}[SG(n) - \text{Final Target}(n)] \quad \text{(eq 57)}$$

Here, I(n−1) is the integral component from the previous sampling point, n indicates the current sampling point, n−1 indicates the previous sampling point, Kp is the overall controller gain, Ts is the sampling period, T_1 is the integral time constant, SG(n) is the current sensor glucose, and Final Target (n) is the calculated final target glucose setpoint from Equation 54.

The derivative component D (n) can be calculated as follows:

$$D(n)=Kp\times T_D\times dSGdt(n) \quad \text{(eq 58)}$$

Here, Kp is the overall controller gain, T_D is the derivative time constant, dSGdt(n) is derivative of the sensor glucose value (pre-filtered to remove noise), and n indicates the current sampling point.

The parameters that need to be set (tuned) for the controller **900** are: K_P, τ_I, and τ_D (see Equations 56, 57, and 58). For the first three PID parameters, they will be calculated in accordance with the previous studies mentioned below (these previous approaches have resulted in good controller performance). The nominal (i.e., for the case with no insulin feedback) controller gain K_{P0} is calculated based on the subject's insulin total daily dose I_{TDD}, (in Units/day), as indicated in Equation 59:

$$K_{P0} = \frac{60}{(90)(1500)} I_{TDD} \quad \text{(eq 59)}$$

Here, K_{P0} is the default controller gain, and I_{TDD} is the subject's insulin total daily dose in Units/Day.

The purpose of insulin feedback is to allow the controller **900** to deliver more insulin up-front (e.g., at the onset of a meal disturbance), but to prevent over-infusion of insulin, in a similar fashion to the bolus estimator calculations used in existing insulin pumps to prevent the stacking of boluses. Therefore, when insulin feedback is used, the controller gain K_P can be adjusted so that at steady state (i.e., basal delivery conditions) the insulin delivery system will deliver the same amount of insulin as in the nominal case. This is accomplished by multiplying the nominal controller gain K_{P0} (calculated for no insulin feedback) by $(1+\gamma_1+\gamma_2+\gamma_3)$ as indicated below:

$$K_P=K_P\text{factor}\cdot K_{P0}\cdot(1+\gamma_1+\gamma_2+\gamma_3) \quad \text{(eq 60)}$$

Here, K_P is the overall controller gain, $K_P$factor is the gain factor for K_P, K_{P0} is the default controller gain, γ_1 (0.64935) is a tuning coefficient for the subcutaneous insulin concentration, γ_2 (0.34128) is a tuning coefficient for plasma insulin concentration, and γ_3 (0.0093667) is a tuning coefficient for effective insulin concentration.

The integral component I(n) is also equipped with anti-windup and saturation constraints to address integral windup issues. This is achieved by calculating an integral clip value (upper limit for the integral component, IClip) as indicated by the following equations:

$$IClip(n) = \begin{cases} Imax(n), & (SG(n) > UnwindHigh) \\ Iramp(n), & (SG(n) > UnwindLow) \text{ and } (SG(n) < UnwindHigh) \\ Ilow(n), & (SG(n) < UnwindLow) \end{cases} \quad \text{(eq 61)}$$

$$Imax(n) = Imaxfactor \times \text{Basal} \times (1 + \gamma_1 + \gamma_2 + \gamma_3) \quad \text{(eq 61a)}$$

Here, Imaxfactor is the gain factor for Imax, and Basal is the subject's night time basal rate. In accordance with these expressions, IClip becomes equal to the Imax (which is a constant value) when the sensor glucose value is greater than an upper threshold (UnwindHigh). In certain embodiments, the value of (expressed in Units/hour) may reach about 15. In a typical case, Imax may have a default value of 5.0. When the sensor glucose value is between the upper and lower threshold (UnwindLow), then IClip becomes equal to Iramp (n), which is calculated as indicated in Equation 62.

$$Iramp(n) = Kp \cdot [SG(n) - UnwindLow] \cdot \left(\frac{SG(n) - UnwindLow}{UnwindHigh - UnwindLow}\right) \cdot (Imax - Kp \cdot [Setpoint(n) - UnwindLow]) \quad \text{(eq 62)}$$

Here, Kp is the overall controller gain, SG(n) is the current sensor glucose, UnwindLow is the sensor glucose lower threshold, UnwindHigh is the sensor glucose upper threshold, Imax is a constant value, and Setpoint(n) is a user-defined target glucose setpoint.

Finally, if sensor glucose is below the UnwindLow threshold, IClip assumes the value of Ilow(n), which can be calculated by Equation 61:

$$Ilow(n) = Kp[\text{Setpoint}(n) - \text{Unwindlow}] \quad \text{(eq 63)}$$

Here, Kp is the overall controller gain, Setpoint is the target glucose defined by the user, and UnwindLow is the sensor glucose lower threshold.

FIG. **51** is a graph of IClip (in Units/Hour) versus sensor glucose level (in mg/dL) in accordance with one example. FIG. **51** depicts the relationships between Imax, Ilow, UnwindLow, and UnwindHigh for this particular example.

The integral component I(n) as calculated in Equation 57 must be less than or equal to the IClip value as shown in Equation 64:

$$I(n) = \begin{cases} IClip(n), & I(n) > IClip(n) \\ I(n), & I(n) \le IClip(n) \end{cases} \quad \text{(eq 64)}$$

The insulin feedback components correspond to the remaining terms. As mentioned above, for this particular example γ_1=0.64935, γ_2=0.34128, and γ_3=0.0093667 (the tuning coefficients), while the parameters I_{SC}(n), I_P(n), and I_{EFF}(n) correspond to the states of the insulin pharmacokinetic model corresponding to, respectively, the subcutaneous, plasma, and effective site compartments. Therefore, the amount of insulin delivered is reduced in proportion to the predicted insulin concentration in the different compartments.

The model describing the insulin pharmacokinetics (insulin PK) is given by the following expressions:

$$I_{SC}(n) = \alpha_{11} \times I_{SC}(n-1) + \beta_1 \times I_D(n) \quad \text{(eq 65)}$$

where:

$$\alpha_{11} = \exp\left(-\frac{Ts}{\tau_s}\right) \quad \text{(eq 65a)}$$

$$\beta_1 = \left(\frac{60}{1}\right) \cdot \left[1 - \exp\left(-\frac{Ts}{\tau_s}\right)\right] \quad \text{(eq 65b)}$$

Here, Ts is the sampling time (which is five minutes for this example), and τ_s is the time constant for estimated subcutaneous insulin level in minutes (which is set to 50 minutes for this example).

$$I_P(n) = \alpha_{21} \times I_{SC}(n-1) + \alpha_{22} \times I_P(n-1) + \beta_2 \times I_D(n) \quad \text{(eq 65c)}$$

where:

$$\alpha_{21} = \tau_s \cdot \left[\exp\left(-\frac{Ts}{\tau_s}\right) - \exp\left(-\frac{Ts}{\tau_p}\right)\right] \Big/ (\tau_s - \tau_p) \quad \text{(eq 65d)}$$

$$\alpha_{22} = \exp\left(-\frac{Ts}{\tau_p}\right) \quad \text{(eq 65e)}$$

$$\beta_2 = \left(\frac{60}{1}\right) \cdot \left(\tau_s \cdot \left[1 - \exp\left(-\frac{Ts}{\tau_s}\right)\right] - \tau_p \cdot \left[1 - \exp\left(-\frac{Ts}{\tau_p}\right)\right]\right) \Big/ (\tau_s - \tau_p) \quad \text{(eq 65f)}$$

Here, Ts is the sampling time, which is five minutes for this example, τ_s is the time constant for estimated subcutaneous insulin level in minutes, which is set to 50 for this example, and τ_p is the time constant for estimated plasma insulin level in minutes, which is set to 70 for this example.

$$I_{EFF}(n) = \alpha_{31} \times I_{SC}(n-1) + \alpha_{32} \times I_P(n-1) + \alpha_{33} \times I_{EFF}(n-1) + \beta_3 \times I_D(n) \quad \text{(eq 66)}$$

For Equation 66:

$$\alpha_{31} = \tau_s \cdot \left[\tau_s \cdot (\tau_p - \tau_e) \cdot \exp\left(-\frac{Ts}{\tau_s}\right) - \tau_p \cdot (\tau_p - \tau_e) \cdot \exp\left(-\frac{Ts}{\tau_p}\right) + \tau_e \cdot (\tau_s - \tau_p) \cdot \exp\left(-\frac{Ts}{\tau_e}\right)\right] \Big/ [(\tau_s - \tau_p) \cdot (\tau_s - \tau_e) \cdot (\tau_p - \tau_e)] \quad \text{(eq 66a)}$$

$$\alpha_{32} = \tau_p \cdot \left[\exp\left(-\frac{Ts}{\tau_p}\right) - \exp\left(-\frac{Ts}{\tau_e}\right)\right] \Big/ (\tau_p - \tau_e) \quad \text{(eq 66b)}$$

$$\alpha_{33} = \exp\left(-\frac{Ts}{\tau_e}\right) \quad \text{(eq 66c)}$$

$$\beta_3 = \left(\frac{60}{1}\right) \cdot \left(\left[\tau_s^2 \cdot (\tau_p - \tau_e) \cdot \left(1 - \exp\left(-\frac{Ts}{\tau_s}\right)\right)\right] - \tau_p^2 \cdot (\tau_s - \tau_e) \cdot \left[1 - \exp\left(-\frac{Ts}{\tau_p}\right)\right] + \tau_e^2 \cdot (\tau_s - \tau_p) \cdot \left[1 - \exp\left(-\frac{Ts}{\tau_e}\right)\right]\right) \Big/ (\tau_s - \tau_p) \cdot (\tau_s - \tau_e) \cdot (\tau_p - \tau_e) \quad \text{(eq 66d)}$$

Here, Ts is the sampling time, which is five minutes for this example, τ_s is the time constant for estimated subcutaneous insulin level in minutes, which is set to 50 for this example, τ_p is the time constant for estimated plasma insulin level in minutes, which is set to 70 for this example, and τ_e is the time

constant for estimated interstitial insulin level in minutes, which is set to 55 for this example.

ID(n) is the calculated and administered insulin infusion.

The notation (n−1) indicates values at the previous time step.

I_{SC} is the subcutaneous insulin model estimate/prediction.

I_P is the plasma insulin model estimate/prediction.

I_{EFF} is the effective site insulin model estimate/prediction.

For this particular example, the insulin PK model parameters α_{11}, α_{21}, α_{22}, α_{31}, α_{32}, α_{33}, β_1, β_2, and β_3 are set to 0.9802, 0.014043, 0.98582, 0.000127, 0.017889, 0.98198, 1.1881, 0.0084741, and 0.00005, respectively. These values were calculated from PK-PD data for insulin as part of an empirical study and investigation. It should be appreciated that the specific values presented here merely reflect one possible set of suitable values, and that any one or more of these values may be adjusted as appropriate for the particular embodiment.

Insulin Limit

The final infusion rate as calculated by Equation 55 is limited such that is does not exceed the maximum upper insulin limit (Umax) as indicated below in Equation 67:

$$u(n) = \begin{cases} Umax, & u(n) > Umax \\ u(n), & u(n) \le Umax \end{cases} \quad \text{(eq 67)}$$

Umax is calculated as indicated by Equation 68:

$$Umax = I_{basal,0} + \frac{BG_{LBL} - FBG_0}{KI} \quad \text{(eq 68)}$$

Here, Umax is the upper insulin limit bounded at BG_{LBL} (see Equation 68a below), and $I_{basal,0}$ is the basal rate defined for the user to bring the patient to a Fasting Blood Glucose (FBG) of the value FBG_0 mg/dL. BG_{LBL} (mg/dL) is the lower buffer limit BG when reaching Umax, FBG_0 is the estimated blood glucose using meter blood glucose readings at the end of the night period, and KI is insulin gain as calculated by Equation 69 below.

$$BG_{LBL} = \text{Setpoint} - \text{ILB} \quad \text{(eq 68a)}$$

Here, BG_{LBL} (mg/dL) is the lower buffer limit BG when reaching Umax, Setpoint is the target glucose setpoint value **944** (FIG. **49**) that is defined by the user, and ILB is the insulin limit buffer, which is an amount (in mg/dL) that the system allows as an additional buffer to handle higher insulin needs. For example, an ILB of 50 allows the system to deliver additional insulin to lower by 50 mg/dL from the Setpoint.

$$KI = -IS * 3\left(\frac{\text{mg}}{\text{dL}} \text{ per } \frac{U}{h}\right) \quad \text{(eq 69)}$$

Here, KI is insulin gain, and IS is the insulin sensitivity estimated by the 1800 rule as IS=1800/TDI (Total Daily Insulin). In certain embodiments, the value of Umax may reach 150 Units/hour. In a typical implementation, the value of Umax is calculated on a per-patient basis, and the typical range for Umax is between 0.5 to 3.0 Units/hour.

Moreover, if the insulin limit is active, then the integral component of the PID algorithm is frozen to its previous value. This feature can be employed to assist in the prevention of integral wind up. This information is passed back to the PID-IFB control module **906** for use during the next PID calculation.

$$I(n) = \begin{cases} I(n-1), & u(n) = Umax \\ I(n), & u(n) < Umax \end{cases} \quad \text{(eq 70)}$$

As mentioned above, previous studies may be leveraged for purposes of configuring and/or operating the PID-IFB control module **906**. A first study (Study 1; Panteleon et al., 2006) looked at the effect of changing the controller gain in a study on eight diabetic dogs. The nominal gain was calculated based on the total daily dose of insulin for one experiment; in duplicate experiments this nominal gain was increased and decreased by fifty percent. Insulin delivery in the six-hour postprandial period tended to increase with increasing gain, but this did not achieve statistical significance. This was due to feedback, with lower insulin delivered as glucose levels fell. In essence, the higher gains tended to give more insulin earlier (achieving much better glucose regulation), and reducing the infusion later, whereas the lower gains tended to keep insulin infusion above basal for a longer period of time due to the glucose levels remaining significantly above target. Note that the controller gain affects all of the components of the PID algorithm, including the integral and derivative terms.

A second study (Study 2; Steil et al., 2006) applied a PID controller to ten human subjects. In this study the nominal controller gain was about 42 percent higher than that proposed here, with the integral time constants the same (therefore also a higher integral response), but slightly lower derivative time constants (defined in terms of rising or falling blood glucose, instead of day or night response). In the proposed embodiment presented here, the night-time derivative time constant is just slightly lower than that used in Study 2.

A third study (Study 3; Weinzimer et al., 2008) applied a PID controller to seventeen human subjects. For a subset of eight subjects, no pre-meal bolus was given, while in the remaining nine subjects about 50 percent of the standard meal bolus was given about fifteen minutes before the meal. The controller tuning was the same as that proposed herein. In both cases, performance was acceptable, with the pre-meal bolus helping to lower the postprandial peak glucose excursion. When compared with home treatment using standard pump therapy, both closed-loop algorithms were superior, reducing both glucose excursions above 180 mg/dl and below 70 mg/dl.

One of the observations from Study 3 was that the meal-related insulin infusion persisted above pre-meal levels for at least four hours after the meal. This result led to the introduction of insulin feedback to the algorithm, which serves to compensate for insulin already delivered, while at the same time allowing for more aggressive action at the start of meals, where it is needed.

In particular implementations, some of the parameters mentioned above for the PID-IFB control module **906** can be fixed. In this regard, the following values may be utilized in an exemplary embodiment. It should be appreciated that these values are provided here for illustrative purposes only, and that an implementation of the PID-IFB control module **906** may utilize different values if so desired.

γ_1=0.64935
γ_2=0.34128
γ_3=0.0093667
α_{11}=0.90483741803596
α_{12}=0.065563404170158
α_{22}=0.931062779704023
α_{31}=0.00297495042963571
α_{32}=0.083822962634882
α_{33}=0.083822962634882
β_1=5.70975491784243
β_2=0.202428967549153
β_3=0.202428967549153

The values of the PID parameters mentioned above (K_P, τ_I, and τ_D) are not expected to change, but it may be desirable to adjust them if doing so would improve the response of the glucose excursion. The nominal values for these PID parameters, together with exemplary allowable ranges, are shown in Table 2.

TABLE 2

Adjustable Parameters For the PID-IFB Control Module

Parameter	Nominal Value	Lower Bound	Upper Bound
Controller gain: K_P	$1 \times K_{P0} \times (1 + \gamma_1 + \gamma_2 + \gamma_3)$	$0.05 \times K_{P0} \times (1 + \gamma_1 + \gamma_2 + \gamma_3)$	$20 \times K_{P0} \times (1 + \gamma_1 + \gamma_2 + \gamma_3)$
Integral time constant: τ_1	250 min	10 min	1500 min
Derivative time constant: τ_D	75 min	10 min	500 min
UnwindLow (mg/dL)	80	0	200
UnwindHigh (mg/dL)	100	0	200
Imax	$2.5 \times (1 + \gamma_1 + \gamma_2 + \gamma_3) \times$ Basal Rate	0	$10 \times (1 + \gamma_1 + \gamma_2 + \gamma_3) \times$ Basal Rate

The lower bound for the controller gain K_{P0} would lower it by 95 percent from the nominal, resulting in an overall less aggressive response of the controller **900**, and resulting in less insulin delivered for the same glucose level and trend. The upper bound allows this gain to be increased up to 20 times from the nominal. Although this would result in more insulin being given, this is always with respect to the actual glucose level and its derivative, rapidly falling blood glucose, even with an elevated blood glucose level, results in a decreased delivery of insulin due to the derivative component.

The integral time constant τ_I determines how fast a deviation in the blood glucose from the desired glucose target accumulates. A higher value results in a slower response to persistent deviations in glucose from target. Lastly, the derivative time constant τ_D can safely be decreased all the way to zero, as the lower it is the less insulin will be delivered. Anything much higher than the upper bound of 500 minutes would make the controller too sensitive to small changes in the rate of change of the sensor glucose, which even though it is not necessarily dangerous, is still undesirable in terms of overall performance.

IOB Compensation Module

FIG. **52** is a block diagram that schematically depicts one suitable embodiment of the IOB compensation module **910** in additional detail. As mentioned briefly above, the IOB compensation module **910** adjusts the current insulin dose **958** (i.e., the insulin infusion rate as computed by the PID-IFB control module **906**) as needed to generate the final insulin dose **962** (i.e., the final adjusted infusion rate used by the insulin infusion device). The IOB compensation module **910** may also receive basal rate data **990** and the information related to the manual boluses delivered **960** as input for purposes of calculating the current value of the final insulin dose **962** and/or for purposes of calculating future values of the final insulin dose **962**. The basal rate data **990** may indicate the current basal rate of insulin being delivered to the user, and the manual boluses delivered **960** may indicate the amount for each bolus administered to the user, along with timestamp data corresponding to the delivery date/time of each bolus. In this regard, the manual boluses delivered **960** may include information for any number of boluses delivered in the past, and the manual boluses delivered **960** can be updated as needed in response to each bolus that is delivered going forward. Moreover, the basal rate could be dynamically adjusted if needed or desired (automatically by the system, by the user, by a caregiver, etc.).

The manual boluses delivered **960** may be collected and saved in association with the IOB compensation module **910** for use as bolus history **992**. In this regard, the bolus history **992** may include any number of past bolus amounts administered during a given period of time. The IOB compensation module **910** may also use a number of constants, parameters, coefficients, configuration settings, gain values, or the like (for simplicity, the constants **994** shown in FIG. **52** are intended to encompass these and any other quantities that might be used by the IOB compensation module **910** to calculate the final insulin dose **962**. FIG. **52** also depicts IOB history **996**, which represents previously calculated IOB values (i.e., historical IOB values calculated for past sampling times). As explained in more detail below, the IOB history **996** and the bolus history **992** may influence the determination of the final insulin dose **962**. It should be appreciated that the bolus history **992**, the constants **994**, and the IOB history **996** can be stored and maintained in one or more memory storage elements of the host system. FIG. **52** shows these data items "inside" the IOB compensation module **910** for simplicity and ease of description.

The IOB compensation module **910** provides an additional safeguard that estimates the insulin on board the body of the patient from manual boluses that were delivered prior to activation of the closed-loop mode, to compensate the final insulin dose **962** and help avoid over-delivery of insulin. When the system initially enters the closed-loop mode, the IOB compensation module **910** considers the manual boluses delivered **960** that have been administered over a defined period of time (e.g., the last eight hours), and subtracts the manual boluses. Thereafter, during the closed-loop mode, the IOB compensation module adjusts for manual boluses that were delivered during each sampling period (e.g., every five minutes).

FIG. **53** is a flow chart that illustrates an exemplary embodiment of an IOB compensation process **1100**, which may be performed by the IOB compensation module **910**. The process **1100** represents one iteration that is performed for a current sampling point or time, n. Accordingly, the process **1100** receives, obtains, or accesses a variety of inputs that may have an influence on the output of the IOB compensation module (task **1102**). For example, the process **1100** may utilize the current value of the uncompensated insulin infusion rate, PIDRate(n), as generated by the PID-IFB control module **906**. The process **1100** may also use the current basal rate (provided with the basal rate data **990**), some of the bolus history **992**, and/or some of the IOB history **996** as needed.

In the context of the process **1100**, the IOB compensation module **910** calculates insulin on board from manual boluses at each cycle and compensates the controller output rate (insulin infusion rate) if active IOB is greater than a certain threshold. Accordingly, the process **1100** calculates, generates, or otherwise obtains a current IOB value (task **1104**) that represents an estimate of active insulin in the body of the user. In certain embodiments, the active IOB is estimated in accordance with a discretized three-compartment insulin pharmacokinetic (PK) model, as indicated below:

$$IOB(n)=ci_1 \cdot IOB(n-1)+ci_2 \cdot IOB(n-2)+ci_3 \cdot IOB(n-3)+cb_0 \cdot U\text{bolus}(n)+cb_1 \cdot U\text{bolus}(n-1)+cb_2 \cdot U\text{bolus}(n-2) \quad \text{(eq 71)}$$

Here, IOB is the active insulin on board, Ubolus is the amount of manual bolus delivered in units per sample, n is the current sampling point, n−1 is the last sampling point, n−2 is

the second to last sampling point, and n−3 is the third to last sampling point. Accordingly, the process **1100** obtains the current IOB value, IOB(n), based at least in part on historical bolus delivery data for the user (see the manual boluses delivered **960** and the bolus history **992** in FIG. **52**). The parameters ci_1, ci_2, ci_3, cb_0, cb_1, and cb_2 are the coefficients of the insulin absorption model. These parameters are calculated based on the three time constants (τ_{sc}, τ_p, and τ_{eff}) of the insulin pharmacokinetic model, as indicated below:

$$ci_1 = eaxx3 + eaxx4 + eaxx5 \quad \text{(eq 71a)}$$

$$ci_2 = -(eaxx3 \times eaxx4 + (eaxx3 + eaxx4) \times eaxx5) \quad \text{(eq 71b)}$$

$$ci_3 = eaxx3 \times eaxx4 \times eaxx5 \quad \text{(eq 71c)}$$

$$cb_0 = 1$$

$$cb_1 = dprod \times (-(daxx22 \times eaxx3 + daxx22 \times eaxx4) \times axx3 \times axx4 + (daxx31 \times eaxx3 + daxx31 \times eaxx5) \times axx3 \times axx5 - (daxx32 \times eaxx4 + daxx32 \times eaxx5) \times axx4 \times axx5) \quad \text{(eq 71d)}$$

$$cb_2 = dprod \times (daxx22 \times eaxx3 \times eaxx4 \times axx3 \times axx4 + daxx32 \times eaxx4 \times eaxx5 \times axx4 \times axx5 - daxx31 \times eaxx3 \times eaxx5 \times axx3 \times axx5) \quad \text{(eq 71e)}$$

Where:

$$axx3 = 1/\tau_{SC} \quad \text{(eq 71f)}$$

$$axx4 = 1/\tau_p \quad \text{(eq 71g)}$$

$$axx5 = 1/\tau_{eff} \quad \text{(eq 71h)}$$

$$eaxx3 = e^{-axx3 \cdot TsC} \quad \text{(eq 71i)}$$

$$eaxx4 = e^{-axx4 \cdot TsC} \quad \text{(eq 71j)}$$

$$eaxx5 = e^{-axx5 \cdot TsC} \quad \text{(eq 71k)}$$

$$daxx22 = axx4 - axx3 \quad \text{(eq 711)}$$

$$daxx31 = axx5 - axx3 \quad \text{(eq 71m)}$$

$$daxx32 = axx5 - axx4 \quad \text{(eq 71n)}$$

$$dprod = -1/(daxx22 \times daxx31 \times daxx32) \quad \text{(eq 71o)}$$

In the above equations TsC indicates a modified sampling interval in minutes, which can be calculated as TsC=Ts*6/CurveSpeed, where Ts is the sampling interval and CurveSpeed is the insulin on board decay speed rate in hours. τ_{SC}, τ_p, and τ_{eff} are the respective time constants of the subcutaneous, plasma, and effective compartments of the insulin PK model.

IOB (in Units) as calculated by Equation 71 represents the residual active insulin in the body from manual boluses (that may have been administered before the start of the closed-loop mode or during closed-loop operation) which must be taken into account for calculation of the final insulin delivery rate. This is achieved by first calculating the IOB rate (task **1106**) and then deducting the IOB rate from the PID-IFB calculated infusion rate, as indicated below. Accordingly, in certain situations the process **1100** determines an adjusted insulin infusion rate (task **1108**) based at least in part on the calculated IOB rate and the uncompensated insulin infusion rate, PIDRate(n):

$$IOBRate(n) = \begin{cases} GainIOB \times IOB(n), & IOB(n) > MinIOB \\ 0, & IOB(n) \le MinIOB \end{cases} \quad \text{(eq 72)}$$

$$AdjustedRate(n) = \max(0, PIDRate(n) - IOBRate(n)) \quad \text{(eq 73)}$$

Note that the process **1100** calculates the IOB rate, IOBRate (n), based at least in part on the current IOB value, IOB(n). The IOB rate, which is expressed in Units per hour (U/h), represents the amount of active insulin accumulated from manual boluses in the body per unit of time. Hence, this additional insulin which is already present in the body is deducted from the controller delivery rate (PIDRate). This accounts for all the manual boluses that have been administered by the user, and minimizes the possibility of over-delivery by the controller. Here, GainIOB is the IOB decay rate in h^{-1}, and MinIOB is the minimum IOB required to compensate the PIDRate (where MinIOB is expressed in Units). Thus, the IOB rate is calculated to be equal to the current IOB value multiplied by an IOB decay rate when the current IOB value is greater than a minimum IOB value, and is calculated to be equal to zero when the current IOB value is less than or equal to the minimum IOB value. In this regard, MinIOB is a minimum threshold for IOB, below which the effect of IOB on glucose is considered to be negligible; hence not needed to be compensated.

As reflected in Equation 73, the process **1100** selects the adjusted insulin infusion rate to be the maximum of zero or the difference between the uncompensated insulin infusion rate and the calculated IOB rate (from task **1106**). Note that the difference between PIDRate and IOBRate could be negative, as these values are calculated from different sources. PIDRate is the controller calculated infusion rate and IOBRate is the accumulated active insulin in the body obtained from manual boluses. Accordingly, Equation 73 ensures that the AdjustedRate does not fall below zero.

Next, the process **1100** may calculate, select, or otherwise determine a final insulin infusion rate (task **1110**). In certain embodiments, the final insulin infusion rate (the final insulin dose **962** in FIG. **49**) is calculated as indicated below:

$$FinalRate(n) = \begin{cases} \max(\text{Basal}, AdjustedRate(n)), & PIDRate > \text{Basal} \\ PIDRate(n), & PIDRate \le \text{Basal} \end{cases} \quad \text{(eq 74)}$$

As indicated by this expression, the process **1100** selects either the adjusted insulin infusion rate (AdjustedRate(n)), the uncompensated insulin infusion rate (PIDRate(n)), or the current basal rate (Basal) to serve as the final insulin infusion rate (FinalRate(n)) for the insulin infusion device. Here, PIDRate is the insulin infusion rate as calculated by the PID-IFB control module **906** and Basal is the current pre-programmed pump basal rate. Accordingly, task **1110** selects the final insulin infusion rate to be equal to the uncompensated insulin infusion rate when the current basal rate is greater than or equal to the uncompensated insulin infusion rate. In contrast, when the current basal rate is less than the uncompensated insulin infusion rate, task **1110** selects the final insulin infusion rate to be either the current basal rate or the adjusted insulin infusion rate, whichever is higher.

In the context of task **1110**, the PIDRate is used as the FinalRate (when PIDRate is less than or equal to Basal) to allow the controller to "apply brakes" (in other words, suppress insulin delivery rate) in order to prevent any potential hypoglycemia. On the other hand, when PIDRate is greater than Basal, the FinalRate will be the maximum of Basal or

AdjustedRate, which ensures that the insulin adjustment only accounts for the insulin coming from boluses, and not the basal. A lower bound (i.e., the value of Basal) is applied to the FinalRate when PIDRate is greater than Basal; this lower bound is utilized to prevent over-compensation of insulin on board under these circumstances.

The process **1100** may continue by communicating or otherwise providing the final insulin infusion rate, FinalRate(n), to the insulin infusion device (task **1112**). For embodiments where the process **1100** is executed natively by the insulin infusion device itself, then the process **1100** may simply provide the final insulin infusion rate to the processing logic or fluid delivery control module of the infusion device. In turn, the insulin infusion device responds by regulating delivery of insulin in accordance with the final insulin infusion rate.

This description assumes that the process **1100** is repeated for each sampling time. For the next sampling time, therefore, the value of n may be incremented by one (or by any desired amount) to establish an index for the next iteration of the process **1100** (task **1114**). Thereafter, the process **1100** may return to task **1102** to obtain the newest input data values and to repeat the various tasks described above. Accordingly, the process **1100** facilitates regulation of insulin delivery to the body of the user in a controlled and ongoing manner by continuously adjusting the final insulin infusion rate while the system is operating in the closed-loop mode.

In certain embodiments, it may be desirable to adjust some of the parameters utilized by the IOB compensation module **910** if doing so would improve performance. The nominal values for these parameters, together with exemplary allowable ranges, are shown in Table 3.

TABLE 3

Adjustable Parameters For the IOB Compensation Module

Parameter	Nominal Value	Lower Bound	Upper Bound
Curve Speed	6	1	8
GainIOB	1.25	0	5
MinIOB	1	0	500

Insulin Delivery Timeout Module

The insulin delivery timeout module **912** is suitably designed and configured to continuously monitor (during the closed-loop mode) if the patient is receiving insulin at the insulin limit (Umax) or no insulin (Umin, which may be defined as insulin delivery at little to no Units/Hour) for a prolonged period of time. If one of these insulin delivery conditions is detected, the system will issue a warning and continue operating under the closed-loop mode. As mentioned previously, the insulin delivery timeout module **912** may process the insulin delivered **960** as an input.

Accordingly, the insulin delivery timeout module **912** introduces an additional safeguard that checks for a series of steps as described below for the delivery of insulin at the insulin limit (Umax Timeout) or no insulin (Umin Timeout) for a prolonged period of time. This is achieved by calculating the total amount of insulin delivered by the system during the closed-loop mode in a pre-specified moving window that is identified as the insulin time window.

Regarding the Umin Timeout condition, once the insulin time window for Umin (which may be defined as delivering insulin at zero Units/Hour) has been reached from the start of the closed-loop mode, the system will monitor the amount of insulin being delivered at the user specified insulin time window and compare it with the amount that could have been delivered if operating at the patient's basal rate for the same time span, as shown in the following logical expression.

$$\text{Pump Delivery Rate} = \begin{cases} FinalRate, & \text{if } U_{Tot}^{WinMin} > (MinDeliveryTol/100) \times U_{Basal}^{WinMin} \\ \text{Alert}, & \text{if } U_{Tot}^{WinMin} \leq (MinDeliveryTol/100) \times U_{Basal}^{WinMin} \end{cases} \quad \text{(eq 75)}$$

Here, Pump Delivery Rate (Units/Hour) is the infusion rate, which is either equal to the FinalRate from Equation 74 (i.e., the infusion rate calculated by the controller during the closed-loop mode), or a pre-programmed overnight basal rate that is used during open-loop operation. The quantity U_{Tot}^{WinMin} is the total amount of insulin delivered (in Units) by the closed-loop control algorithm in a user-specified insulin time window for Umin, and the quantity U_{Basal}^{WinMin} is the total amount of insulin that could be delivered if operating at a pre-programmed overnight basal rate in the same insulin time window for Umin. The parameter MinDeliveryTol is a user-specified tolerance, in percentage of U_{Basal}^{WinMin}, that the system has to deliver in order to stay in the closed-loop mode.

In accordance with this particular example, closed-loop control continues as long as the total amount of insulin delivered during the insulin time window (which is set to 120 minutes for this example) by the system is greater than the total amount of insulin that might have been delivered if operating at five percent (which is the default minimum tolerance for this example) of basal. Moreover, a fail-safe alert is triggered once the total amount of insulin delivered during the insulin time window (120 minutes) by the system is less than five percent of basal.

Regarding the Umax Timeout condition, once the insulin time window for Umax has been reached from the start of the closed-loop mode, the system will monitor the amount of insulin being delivered at the user specified insulin time window and compare it with the amount that might be delivered if operating at the Umax rate for the same time span, as shown in the following logical expression.

$$\text{Pump Delivery Rate} = \begin{cases} FinalRate, & \text{if } U_{Tot}^{WinMax} < (MaxDeliveryTol/100) \times U_{max}^{WinMax} \\ \text{Alert}, & \text{if } U_{Tot}^{WinMax} \geq (MaxDeliveryTol/100) \times U_{max}^{WinMax} \end{cases} \quad \text{(eq 76)}$$

Here, Pump Delivery Rate is the infusion rate, which is equal to either the FinalRate or a pre-programmed overnight basal rate that is used during operation in the open-loop mode. The quantity U_{Tot}^{WinMax} is the total amount of insulin delivered (in Units) by the closed-loop control algorithm in a user-specified insulin time window for Umax, and the quantity U_{max}^{WinMax} is the total amount of insulin that could have been delivered in the user-specified moving window for Umax if operating at a calculated Umax rate. The parameter MaxDeliveryTol is a user-specified tolerance, in percentage of U_{max}^{WinMax} the system must adhere to in order to stay in the closed-loop mode.

In accordance with this particular example, closed-loop control continues as long as the total amount of insulin delivered during the insulin time window (which is set to 600 minutes for this example) by the system is less than the total amount of insulin that might have been delivered if operating at 95% (which is the default maximum tolerance for this

example) of Umax. Moreover, a fail-safe alert is triggered once the total amount of insulin delivered during the insulin time window (600 minutes) by the system is greater than the total amount that might have been delivered if operating at 95% of Umax.

In certain embodiments, it may be desirable to adjust some of the parameters utilized by the insulin delivery timeout module **912** if doing so would improve performance. The nominal values for these parameters, together with exemplary allowable ranges, are shown in Table 4.

TABLE 4

Adjustable Parameters For the Insulin Delivery Timeout Module

Parameter	Nominal Value	Lower Bound	Upper Bound
Insulin Time Window for Umin	120 minutes	30 minutes	600 minutes
Insulin Time Window for Umax	600 minutes	30 minutes	600 minutes
MinDeliveryTol	5%	0%	100%
MaxDeliveryTol	95%	0%	100%

Model Supervisor Module

The model supervisor module **914** is similar to the insulin delivery timeout module **912** in that it monitors and polices the system during closed-loop operation. In practice, closed-loop systems are only aware of signals (inputs) that are being provided by the measurement device(s). If measurements deviate from true values, the control system may react to the deviation. When using continuous glucose sensors for diabetes, the sensors provide the measurements to the closed-loop control system and, based on these measurements, insulin is delivered to the subject. Accordingly, sensor performance and integrity should be closely monitored. Fortunately, there is a relationship between the insulin and meal intake to the glycemic response. This relationship can be translated into a mathematical model that is able to predict the sensor glucose response based upon the insulin delivered. The sensitivity of sensor glucose to insulin delivered is patient-specific (the sensitivity can usually be learned over a period of three to six days for each patient).

The model supervisor module **914** uses a mathematical model that enables individualization of a patient's unique blood glucose time-dependent response. The model describes the sensor glucose time-dependent response as a function of insulin and meal intake. The exemplary mathematical model described herein has a number of benefits and advantages: it is linear, physiologically-based, and includes only parameters that have direct connection to measurable data (sensor glucose and insulin delivered). These features are important because a linear model is easy to analyze and predict. Moreover, a physiological-based model facilitates an understanding of the origin of the predictions (e.g., insulin sensitivity, meal intake, etc.), and use of measureable data reduces the need to estimate unobserved variables (e.g., metabolism, cell activity, etc.).

FIG. **54** is a diagram that defines certain time events for the model supervision. The label "present" indicates the most recent sampling time or sampling period **1120**, and k is equal to the present sampling time minus a period corresponding to a length of prediction horizon (LPH) in sampling times. FIG. **54** also indicates a period corresponding to a length of training horizon (LTH) in sampling times, which refers to a model training period. Insulin history is defined as the length of data needed to estimate the plasma insulin. In order for the model supervisor module **914** to be able to estimate a fault, it considers the records of the insulin delivered over the past insulin history plus the LTH and the LPH sampling periods, and at least 80 percent of the Isig (electrical signal) measurements from k-LTH and k.

As described in more detail below, the model supervisor module **914** considers a "moving window" that includes a historical time period **1122** that is defined from the present (most recent sampling period **1120**) back to the beginning of the LTH. The moving window considered by the model supervisor module **914** may also include insulin history that precedes the LTH, as depicted in FIG. **54**. Data obtained during each window of time is processed and analyzed at or near the present time and preferably before the next sampling period has ended. Thus, at the end of each new sampling period, the "moving window" shifts by one sampling period such that the model supervisor module **914** can consider the most recently obtained data for the current sampling period while disregarding the data that no longer appears within the updated window of time (i.e., the oldest data is no longer considered). The historical time period **1122** may be defined by the LTH and the LPH, which for this example immediately follows the LTH (as shown in FIG. **54**). The LPH may also be referred to herein as the "recent history period" or the "model prediction period" for reasons that will become apparent from the following description. The LTH may also be referred to herein as the "distant history period" or the "model training period" for reasons that will become apparent from the following description. In this regard, the LTH (distant history period) corresponds to a period of time from a begin-training sampling period **1124** to an end-training sampling period **1126**, inclusive, while the LPH (recent history period) corresponds to a period of time from a begin-prediction sampling period **1128** to the most recent sampling period **1120**, inclusive. Accordingly, by definition the current sampling period (i.e., the most recent sampling period **1120**) resides within the LPH. For this particular example, the begin-prediction sampling period **1128** corresponds to the end-training sampling period **1126**. Alternatively, the begin-prediction sampling period **1128** may immediately follow the end-training sampling period **1126**.

FIG. **55** is a flow chart that illustrates an exemplary embodiment of a sensor model supervision process **1150**, which may be performed by the model supervisor module **914**. The process **1150** is shown and described in a simplified manner that focuses on functionality for ease of understanding. Certain aspects of the process **1150** are addressed in more detail below with reference to particular representations of the model supervisor module **914**.

The process **1150** represents one iteration that is performed for a current sampling point or time, which corresponds to the most recent sampling period. This example assumes that the insulin infusion device is already operating in the closed-loop mode (task **1152**) to deliver insulin to the body of the user, and that the process **1150** receives relevant data in accordance with a predetermined schedule (e.g., a sampling period of five minutes). Accordingly, the process **1150** receives, obtains, or accesses a variety of inputs that may have an influence on the operation of the model supervisor module **914** (task **1154**). For example, the process **1150** may receive at least the following data for the current sampling period: current insulin-delivered data that indicates an amount of insulin delivered by the insulin infusion device during the most recent sampling period; current sensor data that indicates a current sensor glucose value for the user, which corresponds to the most recent sampling period; and a current sensor calibration factor, which may be needed to compensate for recent meter-based calibrations. Any amount of historical data could also

be received during task **1154** if so desired. Thus, some amount of redundancy may be built into the system (which may be desirable to account for missed transmissions, lost packets, or the like). The sensor data may be received and processed in any suitable form. For example, a continuous glucose sensor may generate Isig (electrical current) values that can be mapped to sensor glucose values. The model supervisor module **914** may be suitably configured to process Isig values directly, or it could translate or map the raw Isig values into any desired representation.

The process **1150** may also access or retrieve historical data that was received for past sampling periods (task **1156**). Task **1156** may represent an initialization routine that populates a grid, matrix, or other type of database structure as needed to prepare the model supervisor module **914** for the various calculations, analyses, and functions described in more detail below. It should be appreciated that subsequent iterations of the process **1150** (which are performed in an ongoing manner during the closed-loop mode) need not repeat the initialization of the historical data. Rather, task **1156** may simply adjust the data history to reflect newly received data. For the embodiments described here, the following historical data may be processed by the model supervisor module **914**, without limitation: historical insulin-delivered data for the user; and historical sensor glucose values for the user. The historical insulin-delivered data may correspond to amounts of insulin delivered by the insulin infusion device during each historical sampling period of interest, and the historical sensor glucose values may correspond to respective sensor glucose measurements obtained during each historical sampling period of interest. In certain implementations, each historical sensor glucose value may be associated with or derived from a historical Isig value and a sensor calibration factor.

The process **1150** is iterative in nature, and each iteration considers data associated with the defined historical period of time (see FIG. **54**). Accordingly, the process **1150** may define the model training period and the model prediction period for the historical period of time (task **1158**). In this regard, task **1158** may identify or designate which data samples fall within the model training period (the LTH in FIG. **54**) and/or which data samples fall within the model prediction period (the LPH in FIG. **54**). Task **1158** may also serve to identify or designate "stale" data samples that need not be considered going forward. In practice, if data for the oldest sampling period is missing for some reason, then the process **1150** can make appropriate adjustments (e.g., search for the closest available data sample, wait for the next sampling period, or the like).

Next, the process **1150** processes at least some of the historical data to determine a best-matched solution to a sensor glucose prediction model (task **1160**). Task **1160** may be considered to be a training procedure that finds the best-fitting sensor glucose prediction function, which in turn can be used to check (predict) the integrity and quality of the glucose sensor. In certain embodiments, the sensor glucose prediction model is expressed as a fourth order ordinary differential equation that, when solved given the initial conditions, provides model-predicted sensor glucose values. Notably, task **1160** uses the actual sensor glucose values obtained during the model training period (and does not use any of the actual sensor glucose values obtained during the model prediction period) to determine which candidate solution will be selected as the best-matched solution. Conceptually, task **1160** generates a plurality of curves (or discrete values that may be used to visualize curves for purposes of this explanation) and compares the portion of the curves within the model training period to the actual sensor glucose values obtained during the model training period. In an ideal scenario with a perfect match, one of the generated curves will precisely track the actual sensor glucose values within the model training period. In practice, however, the generated curves will deviate from the actual sensor glucose values. Accordingly, task **1160** identifies the calculated curve that best matches the actual sensor values. It should be appreciated that this best-matching curve also includes model-predicted sensor glucose values that extend beyond the model training period and into the model prediction period.

The process **1150** may continue by comparing at least one historical sensor glucose value obtained during the model prediction period to at least one corresponding predicted sensor glucose value of the best-matched solution (task **1162**). In certain embodiments, task **1162** checks only one actual sensor glucose value: the current sensor glucose value obtained for the most recent sampling period. In other embodiments, any or all of the sensor glucose values obtained during the model prediction period could be analyzed during task **1162**. The straightforward example described here only considers the current sensor glucose value such that the comparison in task **1162** is simple and straightforward. In this regard, task **1162** may calculate a difference between the current sensor glucose value (i.e., the most recent historical value) and the predicted current glucose value for the most recent sampling period (the difference may be expressed as an absolute value), and the process **1150** may continue by comparing the calculated difference to a threshold error amount (query task **1164**). In other embodiments, the comparison performed during task **1162** may involve a more advanced methodology, e.g., curve-fitting that considers more than one sampling point in the model prediction period, statistical analyses, or the like. For example, rather than calculating error on a point-by-point basis, the process **1150** could utilize any appropriate methodology to determine whether or not the historical sensor glucose values in the model prediction period deviate (by at least a threshold amount) from the corresponding model-predicted values in the best-matched solution.

If the calculated error between the model-predicted glucose value(s) and the corresponding actual historical sensor glucose value(s) is less than or equal to the error threshold, or otherwise satisfies the predetermined criteria monitored by the model supervisor module **914**, then the "No" branch of query task **1164** is followed and the process **1150** continues to the next sampling period (task **1166**). At this point, the process **1150** returns to task **1152** such that the core of the process **1150** can be repeated to consider the data received for the next sampling period. Thus, the oldest data considered by the previous iteration of the process **1150** is disregarded, the newly received data is designated as the "most recent" data, and the historical time period or "analysis window" for the current iteration of the process **1150** shifts by one sampling period (see FIG. **54**).

If the calculated error exceeds the threshold error amount (the "Yes" branch of query task **1164**), then the process **1150** may generate an alert, an alarm, and/or a message (task **1168**). In practice, an alert, alarm, or message can be initiated by the model supervisor module **914** for rendering, annunciation, delivery, playback, etc. For example, an alert could be presented at the insulin infusion device, at a remote monitoring station, at a handheld controller device, or the like. In certain embodiments, the process **1150** switches from the closed-loop mode to the open-loop mode (or to some type of safe operating mode with reduced insulin delivery) when the threshold error amount is exceeded (task **1170**).

One important aspect of the process **1150** relates to the manner in which the best-matched sensor glucose prediction

model is chosen (see task **1160**). In this regard, FIG. **56** is a flow chart that illustrates an exemplary embodiment of a sensor model training process **1180**, which may be performed in conjunction with the sensor model supervision process **1150** depicted in FIG. **55**. The process **1180** is shown and described in a simplified manner for ease of understanding. Certain aspects of the process **1180** are addressed in more detail below with reference to particular implementations of the model supervisor module **914**.

As mentioned previously, the exemplary sensor glucose prediction model utilized here is expressed as a fourth order ordinary differential equation. In accordance with conventional mathematics, the model-predicted sensor glucose values (G) in time are calculated as a function of the two model prediction initial conditions G_0 and dG_0. Here, G_0 is the estimated sensor glucose value for the begin-training sampling period **1124** (the start of LTH in FIG. **54**), and dG_0 is the derivative of G_0. Therefore, different initial condition values result in different solutions to the sensor glucose prediction model; each distinct set of initial conditions corresponds to a different prediction model. For the sake of processing efficiency, the model supervisor module **914** imposes limits and boundaries on the initial condition values to calculate and analyze a manageable number of candidate solutions. In this regard, the sensor model training process **1180** may begin by calculating a range or boundary for each bounded initial condition (task **1182**).

For the exemplary embodiment presented here, the initial condition dG_0 is bounded in a simple manner that is based on a predetermined parameter (which may be adjustable): $dG_0=\pm grad_bound$. In contrast, the boundary for the initial condition G_0 is based on (or is otherwise influenced by) a baseline historical sensor glucose value obtained during the model training period, such as the sensor glucose value that was obtained during the begin-training sampling period **1124**. Thus, the process **1180** may identify, from the historical sensor glucose values, the baseline sensor glucose value to be used for purposes of calculating the boundary for the initial condition G_0: $G_0=SG_{k\text{-}LTH}\pm 0.14\cdot SG_{k\text{-}LTH}$, where $SG_{k\text{-}LTH}$ is the baseline sensor glucose value obtained for the earliest sampling period in the historical time period under analysis (see FIG. **54**). Notably, the boundary for G_0 is a function of the baseline sensor glucose value, which may vary in an ongoing manner during operation of the system, and which may vary from one iteration of the process **1180** to another. In practice, if the sensor glucose data is missing for the begin-training sampling period **1124**, then the process **1180** can take appropriate measures, e.g., search for the nearest available sensor glucose data point, wait for the next sampling period, etc.

The process **1180** may then continue by determining, calculating, or otherwise obtaining the next set of initial conditions (task **1184**). The manner in which the process **1180** selects and steps through the different initial conditions is unimportant in this context. The current set of initial conditions is used to calculate a candidate solution to the sensor glucose prediction model (task **1186**). As mentioned above, each candidate solution is calculated as a function of the two bounded initial conditions. Moreover, each candidate solution is calculated as a function of estimated plasma insulin for the user, which in turn is calculated as a function of an amount of insulin delivered to the user. Accordingly, task **1186** may estimate plasma insulin for the user based on: the current insulin-delivered data (obtained for the most recent sampling period); the historical insulin-delivered data; and an insulin basal rate for the user. In practice, task **1186** considers the total insulin (basal, bolus, and any other insulin delivered) for all sampling periods. This allows the process **1180** to obtain the candidate solution to the sensor glucose prediction model based at least in part on the estimated plasma insulin and based at least in part on the baseline sensor glucose value obtained at the earliest sampling period under analysis.

The process **1180** may continue by generating a training error value, quantity, or function for the candidate solution (task **1188**). The training error may be calculated by comparing predicted sensor glucose values from the candidate solution to the corresponding historical sensor glucose values, to obtain a metric that indicates how closely the predicted values match the actual values. In certain embodiments, the training error is based only on predicted values and actual values for the model training period (LTH in FIG. **54**), and, therefore, task **1188** does not consider any predicted or actual values for the model prediction period (LPH in FIG. **54**).

If the process **1180** has considered all of the initial condition combinations (the "Yes" branch of query task **1190**), then the process **1180** may proceed to a task **1192**. If more sets of initial conditions remain (the "No" branch of query task **1190**), then the process **1180** may return to task **1184**, retrieve the next set of initial conditions, and continue as described above. Task **1192** is performed after a plurality of different candidate solutions have been calculated, using the different sets of initial conditions. Task **1192** may be performed to select the best-matching candidate solution from the plurality of calculated solutions. For this particular embodiment, the selection is based on the training errors generated during task **1188**. For example, the candidate solution having the lowest training error may be selected as the best-matching solution.

It should be appreciated that the process **1180** need not be performed in the illustrated sequence, and that some tasks could be performed in parallel. For example, the calculation of the training errors (task **1188**) may instead be performed after all of the candidate solutions have been obtained and saved. Moreover, the process **1180** could be designed to immediately eliminate candidate solutions (following completion of task **1188**) that have a training error that exceeds a predetermined error threshold. As another option, the process **1180** could be designed to immediately designate a candidate solution as the best-matched solution if the associated training error satisfies certain criteria.

The foregoing concepts and methodologies may be implemented in a practical embodiment of the model supervisor module **914**. The following description relates to two possible embodiments that implement the general concepts presented above. It should be appreciated that the particular embodiments described below are not exhaustive, and that the description of the embodiments is not intended to limit or restrict the scope or application of the subject matter presented here.

Model Supervisor Module: First Representation

The model supervisor module **914** is suitably designed and configured to detect potentially faulty sensor measurements. The model supervisor module **914** may utilize a mathematical model that is trained offline. For example, parameters that could be estimated offline estimated include, without limitation: K_I (insulin gain in mg/dL per U/h; τ_1 (first insulin time constant, in minutes); τ_2 (second insulin time constant, in minutes); Ibasal (basal insulin, in U/h); and SGbase (blood glucose (BG) at fasting, in mg/dL, when Ibasal insulin is delivered.

The model supervisor module **914** trains the model prediction initial conditions, G_0 and dG_0 every sampling time. G_0 and dG_0 represent the BG (mg/dL) and BG derivative (mg/dL/min) estimate values at k-LTH (see FIG. **54**), where LTH is the length of the training data (sampling times) and k is equal to the present sampling time minus LPH. In this con-

text, LPH is the length of the prediction horizon in sampling times. G_0 and dG_0 estimations are bounded as formulated by the expressions collectively identified below as Equation 77. Note that these initial conditions and their boundaries were also described above with reference to task **1182** of the sensor model training process **1180**.

$$G_0 = CGM_{k\text{-}LTH} \pm 0.14\ CGM_{k\text{-}LTH}$$

$$dG_0 = \pm \text{grad_bound} \qquad \text{(eq 77)}$$

For Equation 77, $CGM_{k\text{-}LTH}$ is the CGM measurement at sampling time k-LTH, and grad_bound is a predefined absolute maximum BG derivative in time (mg/dL/min).

The model supervisor module **914** estimates plasma insulin, I_p, at k-LTH using the insulin history records from k-LTH-insulin history and k-LTH (see FIG. **54**) in accordance with Equation 81. Having the estimated I_p, G_0, and dG_0, a model prediction is generated from present-LTH-LPH, until present (as described above for task **1186** of the sensor model training process **1180**). The model prediction enables the calculation of two values: Terr and Perr. Terr is defined as the mean sum square of errors between the model prediction and the CGM records from k-LTH and k (Equation 78). Perr is defined as the absolute mean error between the model prediction and the CGM records from k and present (Equation 79). Note that Terr is one type of training error, which was described above for task **1188** of the process **1180**, and Perr is one type of prediction error, as described above for task **1162** and query task **1164** of the sensor model supervision process **1150**. A fault is defined when Perr<err1 and Terr>err2 (Equation 80).

$$Terr = \sqrt{\frac{\sum_{i=k-LTH}^{k} (Model_i - CGM_i)^2}{LTH}} \qquad \text{(eq 78)}$$

$$Perr = \text{abs}\left(\frac{\sum_{i=k}^{k+LPH} Model_i - CGM_i}{LPH}\right) \qquad \text{(eq 79)}$$

$$\text{Fault} = \begin{cases} 1, & \text{if } Terr < err1 \text{ and } Perr > err2 \\ 0, & \text{else if } Terr \le err2 \text{ or } Perr \ge err1 \\ -1, & \text{if not enough data records available} \end{cases} \qquad \text{(eq 80)}$$

In Equation 80, Fault 1 indicates a faulty sensor, Fault 0 indicates a non-faulty sensor, and Fault −1 indicates that there is not enough information to decide. Referring again to FIG. **55**, Fault 1 corresponds to the "Yes" branch of query task **1164**.

In certain embodiments, some of the parameters used by the model supervisor module **914** may be adjustable. Table 5 identifies the adjustable parameters, along with some exemplary values for the parameters.

TABLE 5

Adjustable Parameters For the Model Supervisor Module

Parameter	Symbol	Typical Starting Value	Minimum Value	Maximum Value
Insulin gain	K_I	−100	−500	−1
Insulin time constant	τ_1	30	0.1	150
Insulin time constant	τ_2	150	0.1	150
Fasting BG	SGbase	120	50	300

TABLE 5-continued

Adjustable Parameters For the Model Supervisor Module

Parameter	Symbol	Typical Starting Value	Minimum Value	Maximum Value
Basal insulin at fasting BG	Ibasal	1	0.1	3
Training data error	err1	5	1	100
Prediction data error	err2	20	1	100
Length of training data	LTH	8	5	30
Length of prediction data	LPH	3	1	20
Length of insulin data	Insulin History	48	30	60
BG maximum absolute derivative	grad_bound	5	1	8

The following equations describe the mathematical model equations in Laplace transform form:

$$\hat{I}_p(s) = \frac{1}{(50\ s+1)(70\ s+1)}\left(\hat{I}_D + \hat{I}_{P0} s\alpha\alpha + dI_{P0}\beta\right) \qquad \text{(eq 81)}$$

In this expression, α=3500, β=120, and $\hat{I}_P$ is the I_P in deviation form. $\hat{I}_{P0}$ and dI_{P0} are the $\hat{I}_P$ and derivative initial conditions, respectively.

All the insulin states are formulated in deviation form from the given insulin value Ibasal as it is expressed by the following Equation 82:

$$\hat{I}_x = I_x - I\text{basal} \qquad \text{(eq 82)}$$

In Equation 82, x represents D, in, or P.

The following Equation 83 expresses BG in deviation form from SGbase. Note that Equation 83 represents one suitable expression for the sensor glucose prediction model, which is a fourth order ordinary differential equation.

$$\hat{G}(s) = \frac{1}{(\tau_1 s+1)\cdot(\tau_2 s+1)} \left(K_I \cdot \hat{I}_P - \frac{1}{(50\ s+1)(70\ s+1)}\left(\hat{G}_0 \cdot \alpha + \left(\hat{G}_0 \cdot s + d\hat{G}_0\right)\cdot\beta + \left(\hat{G}_0 \cdot s^2 + d\hat{G}_0 \cdot s\right)\cdot\chi + \left(\hat{G}_0 \cdot s^3 + d\hat{G}_0 \cdot s^2\right)\cdot\delta\right)\right) \qquad \text{(eq 83)}$$

In Equation 83, the following relationships hold:

$$\alpha = 120 + \tau_1 + \tau_2$$

$$\beta = 3500 + 120\tau_1 + 120\tau_2 + \tau_1\tau_2$$

$$\chi = 3500\tau_1 + 3500\tau_2 + 120\tau_1\tau_2$$

$$\delta = 3500\tau_1\tau_2$$

Moreover, in Equation 78, $\hat{G}$, K_I, $\hat{G}_0$, dG_0, τ_1, and τ_2 are the BG in deviation form from SGbase, the insulin gain, the BG initial conditions in deviation form, the BG derivative initial conditions, and two time constants, respectively.

Model Supervisor Module: Second Representation

In accordance with some embodiments, the functionality of the model supervisor module **914** can be represented as follows. As mentioned above, the model supervisor module

914 estimates the user's glucose concentration in real-time based on the insulin delivered, the sensor Isig values, and sensor calibration factors. If the model-predicted sensor glucose value (SG) and the actual SG value differ significantly, the system will trigger a fail-safe alert that indicates that the collected data contains unexplained behavior, which may in turn be associated with a faulty sensor and/or insulin delivery, or an unannounced meal intake.

The time frames and reference time periods for the model supervisor module **914** are defined as shown in FIG. **54**. The methodology performed by the model supervisor module **914** uses data packets received for past time frames to estimate plasma insulin and model-predicted glucose in order to estimate the fault conditions. The sampling time is the time interval between two consecutive data packets, which for this particular example is five minutes. The insulin history in FIG. **54** corresponds to a defined past time frame that is needed to estimate plasma insulin (for this example, the insulin history corresponds to four hours or 48 sampling periods). The length training horizon (LTH) for this example includes 24 data packets, which corresponds to a past time frame of 120 minutes. The length of predicted horizon (LPH) for this example includes 24 data packets, which corresponds to a past time frame of 120 minutes. In FIG. **54**, k is equal to the present number of data packets minus LPH, and "present" indicates the most recent sampling time.

The following equations describe the mathematical model in Laplace transform form. Equation 84 provides an estimate of the plasma insulin, and Equation 85 provides the model-predicted SG values. Accordingly, the model supervisor module **914** in accordance with this particular embodiment estimates the plasma insulin as follows:

$$\hat{I}_p(s) = \frac{1}{(50\ s+1)(70\ s+1)}\left(\hat{I}_D + \hat{I}_{P0}s\varepsilon + dI_{P0}\gamma\right) \quad \text{(eq 84)}$$

For this example, ϵ=3500, γ=120, $\hat{I}_P$ is the estimated plasma insulin in deviation form, (s) refers to Laplace transform form, and $\hat{I}_D$ is the insulin delivered from the system in deviation form. Moreover, $\hat{I}_{P0}$ is the estimated plasma insulin in deviation form for the sampling time identified as k-LTH (see FIG. **54**), dI_{P0} is the derivative of the estimated plasma insulin, and α and β are constants.

The insulin states described above are formulated in deviation form from a given insulin value Ibasal as it is expressed by the following equation:

$$\hat{I}_x = I_x - I\text{basal} \quad \text{(eq 85)}$$

In Equation 85, x represents D or P (where D refers to insulin delivered and P refers to plasma insulin), and $I_{basal,0}$ is the estimated basal rate defined for each user to bring the patient to a fasting blood glucose (FBG) of the value FBG_0 (in mg/dL).

For this second embodiment, the model-predicted sensor glucose value, $\hat{G}$, in time is calculated in accordance with Equation 83 and the associated relationships, as described for the first embodiment of the model supervisor module **914**. In this regard, $\hat{G}$ is the model-predicted SG value in deviation form from FBG_0 (estimated blood glucose using meter blood glucose readings at the end of the night period), (s) refers to Laplace transform form, τ_1, and τ are the two insulin time constants identified for each patient, which are related to how fast a patient reacts to insulin, K_I is the insulin gain, and $\hat{I}_P$ is the estimated plasma insulin in deviation form. Moreover, $\hat{G}_0$ is the estimated SG value (in mg/dL) in deviation form for the sampling time of k-LTH (see FIG. **54**), as calculated in accordance with Equation 86 below, and dG_0 (calculated by Equation 87 below) is the derivative of the estimated SG value (in mg/dL/min) for the sampling time of k-LTH. The constants α, β, χ, and δ are calculated as set forth above in the context of Equation 83. The estimated blood glucose values are calculated as a function of the model prediction initial conditions, G_0 and dG_0. For this particular embodiment, the estimations for G_0 and dG_0 are bounded as formulated by the following equations. Note that these initial conditions and their boundaries were also described above with reference to task **1182** of the sensor model training process **1180**.

$$G_0 = SG_{k\text{-}LTH} \pm 0.14 \cdot SG_{k\text{-}LTH} \quad \text{(eq 86)}$$

$$dG_0 = \pm\text{grad_bound} \quad \text{(eq 87)}$$

Here, G_0 is the estimated SG value (in mg/dL) value for the sampling time of k-LTH, $SG_{k\text{-}LTH}$ is the SG measurement for the sampling time of k-LTH, dG_0 is the derivative of the estimated SG value (in mg/dL/min) for the sampling time of k-LTH, and grad_bound is a predefined absolute maximum SG derivative in time (mg/dL/min). For certain embodiments, grad_bound is a fixed parameter. For the example presented here, grad_bound has a value of 5 mg/dL/min.

The model prediction facilitates the calculation of two values: Terr and Perr. Terr is defined as the mean absolute error between the model predicted SG values and the actual SG records for the sampling time identified as k-LTH and k as calculated by Equation 88 below. Perr is defined as the mean absolute error between the model predicted SG values and the actual SG records for sampling times identified as k to present (see FIG. **54**) as calculated by Equation 89 below.

$$Terr = \frac{\sum_{i=k-LTH}^{k} \text{abs}(Model_i - SG_i)}{LTH} \quad \text{(eq 88)}$$

Here, Terr is defined as the mean absolute error between the model predicted SG values ($Model_i$) and the SG records (SG_i) for the sampling time identified as k-LTH and k.

$$Perr = \frac{\text{abs}(Model_{present} - SG_{present})}{SG_{present}} \cdot 100\% \quad \text{(eq 89)}$$

Here, Perr is defined as the percentage of error between the model prediction and the SG measurement at the present (most recent) sampling time.

In accordance with this particular implementation, the model supervisor module **914** estimates the fault scenario based on Equation 90, where Fault 1 signifies a faulty sensor, Fault 0 indicates a non-faulty sensor, Fault 3 indicates a training error, and Fault −1 indicates that there is not enough data available to make a determination.

$$\text{Fault} = \begin{cases} 1, & \text{if } Terr < err1 \text{ and } Perr > err2 \\ 0, & \text{if } Perr \le err2 \text{ or } Terr \ge err1 \\ 3, & \text{if } Terr > err3 \\ -1, & \text{if not enough data available} \end{cases} \quad \text{(eq 90)}$$

In Equation 90, err1 is the upper threshold for the mean absolute error (see Equation 88). Thus, if the training error is

above this threshold, a fault cannot be triggered because the credibility of the training is suspect. The err2 is the lower threshold for Equation 89. If the prediction value of the model and the sensor measurement at present are above this threshold and the training error is less than err1, then a fault will be triggered. The err3 defines a lower threshold for the training period. If Equation 88 indicates a value that is above this threshold, then a warning associated with poor training can be triggered.

FIG. **57** is a diagram that illustrates exemplary sensor conditions corresponding to a non-faulty sensor (Fault 0) and a faulty sensor (Fault 1). The common horizontal axis indicates the present sampling time at the far right, along with the time periods identified by LPH and LTH. The sampling time **1202** corresponds to the oldest data considered by the model supervisor module **914** at the present time. Accordingly, historical data **1204** for sampling times that occurred before the sampling time **1202** is disregarded.

The top plot **1206** in FIG. **57** is indicative of a non-faulty sensor (Fault 0), the middle plot **1208** is indicative of a faulty sensor (Fault 1), and the bottom plot **1210** depicts the insulin administered, which is needed in order to estimate the plasma insulin and to generate the model predicted SG values. In the plots **1206**, **1208**, the solid line **1212** represents the model-predicted SG values, and the dots represent the actual SG measurements. The dashed vertical line **1214** represents the demarcation between the LTH time frame and the LPH time frame. The lines between the solid line **1212** and the dots represent the difference (error) between the model-predicted SG values and the actual SG measurements. Dashed lines are utilized in the LPH time frame, which corresponds to fifteen minutes or three sampling periods for this example.

Referring to the top plot **1206**, there is good agreement between the model predicted SG values (represented by the solid line **1212**) and the actual SG measurements (represented by the dots). In other words, the actual measurements do not deviate significantly from the predicted values. In certain embodiments, the model supervisor module **914** only compares actual measurement values that are within the LPH time frame. In accordance with one exemplary embodiment, the model supervisor module **914** determines the fault status based solely on the most recently obtained data, i.e., the information received for the last sampling time. For this example depicted in FIG. **55**, Perr is less than or equal to err2. Thus, in accordance with Equation 90, the model supervisor module **914** returns Fault 1 and the system is commanded to remain in the closed-loop mode.

Referring to the middle plot **1208**, of FIG. **57**, there is good agreement between the model predicted SG values and the actual SG measurements in the LTH time period (for this period, Terr is less than err1 in Equation 90). Note, however, that there is a significant difference observed between the model predicted SG last value and the actual last SG measurement **1218** (Perr is greater than err2 in Equation 90). In this scenario, therefore, the model supervisor module **914** will issue a fail-safe alert and/or take other appropriate measures.

In certain embodiments, some of the parameters used by the model supervisor module **914** may be adjustable. Table 6 identifies some adjustable parameters for this embodiment, along with some exemplary values for the parameters.

TABLE 6

Adjustable Parameters For the Model Supervisor Module

Parameter	Default Value	Lower Bound	Upper Bound
K_I (mg/dL/U/H)	−100	−360	−49
FBG_0 (mg/dL)	120	50	300

TABLE 6-continued

Adjustable Parameters For the Model Supervisor Module

Parameter	Default Value	Lower Bound	Upper Bound
Ibasal (U/H)	1	0.1	3
err1 (mg/dL)	5	1	30
err2 (%)	50	20	100
err3 (mg/dL)	10	1	30
LTH (sampling times)	24	4	48
LPH (sampling times)	24	1	48

Missed Transmission Module

The missed transmission module **916** continuously checks whether the controller receiving data packets (including SG values) for processing. The missed transmission module **916** keeps the system operating in the closed-loop mode for when less than a stated number of data packets are missed (e.g., less than four data packets in a row, a total number of data packets that represent a timespan of less than 15 minutes, or the like). During this time, the system will continue to calculate the insulin dose using the closed-loop control algorithm based on the last valid sensor glucose value or sensor Isig value. For missed data packets that represent a time longer than a lower time threshold and longer than an upper time threshold (e.g., between 15 and 60 minutes), the missed transmission module **916** switches the system to a pre-programmed safe basal rate, which may be defined as half the patient's nighttime basal rate. If the controller starts receiving data packets during the safe basal rate timeframe, the system will switch back to the closed-loop mode. For missed data packets that represent a time longer than the upper time threshold, however, the missed transmission module **916** switches the system to the open-loop mode to deliver a pre-programmed nighttime basal rate, which may be set by a healthcare provider or a caregiver.

The missed transmission module **916** checks for different scenarios pertaining to when and what kind of packet is lost during transmission. Different steps are executed depending on the type of lost transmission. The details of four different scenarios are described below.

Case 1

If the sensor Isig value and the SG value are both received by the controller, then:

(a) the sensor Isig is saved by the controller;

(b) the SG value is saved by the controller;

(c) a Zero Order Hold (ZOH) count is set to zero; and

(d) the system remains in the closed-loop mode as described previously.

Case 2

If the sensor Isig value is not received, but the SG value is received by the controller, then:

(a) the ZOH count is set to zero;

(b) Isig is calculated by Equation 91 (see below) using the SG value and the sensor calibration factor; and

(c) the system remains in the closed-loop mode.

$$Isig_{calc}=(SG/CF')+2 \quad \text{(eq 91)}$$

Case 3

If the sensor Isig value is received, but the SG value is not received by the controller, then:

(a) the ZOH count is set to zero;

(b) SG is calculated by Equation 92 (see below) using the Isig value and the sensor calibration factor; and

(c) the system remains in the closed-loop mode.

$$SG_{calc}=(Isig-2)\times CF' \quad \text{(eq 92)}$$

Case 4a

If neither the sensor Isig value nor the SG value are received by the controller (i.e., both values are not received), and if:

$$ZOH\ \text{Count} \leq ZOH\ \text{Count Max}$$

then:

(a) the ZOH count for the sensor Isig and SG is calculated based on previous values;

(b) ZOH Count=ZOH Count+1;

(c) TimeoutCount=0; and

(d) the system remains in the closed-loop mode.

Case 4b

If neither the sensor Isig value nor the SG value are received by the controller (i.e., both values are not received), and if:

$$ZOH\ \text{Count} > ZOH\ \text{Count Max}$$

then:

(a) an "invalid" place holder for the sensor Isig and SG value is saved;

(b) the system remains in the closed-loop mode, but switches to a temporary safe basal rate, which is half the patient's night time basal rate when in the open-loop mode;

(c) if a packet is received by the system while it is delivering the safe basal rate, the system will transition back to the closed-loop mode;

(d) for every minute that the system is delivering the safe basal rate, a TimeoutCount

is incremented: TimeoutCount=TimeoutCount+1;

(e) if TimeoutCount>Timeout Count Max, then the system switches to the open-loop mode.

In accordance with certain embodiments, ZOH Count Max has a fixed value of two, and Timeout Count Max has a fixed value of 45, although different values may be used as appropriate to the particular implementation. Moreover, the safe basal rate used by the missed transmission module **916** may be adjustable. In this regard, the safe basal rate may be adjustable within a range of about zero to five Units/Hour.

While at least one exemplary embodiment has been presented in the foregoing detailed description, it should be appreciated that a vast number of variations exist. It should also be appreciated that the exemplary embodiment or embodiments described herein are not intended to limit the scope, applicability, or configuration of the claimed subject matter in any way. Rather, the foregoing detailed description will provide those skilled in the art with a convenient road map for implementing the described embodiment or embodiments. It should be understood that various changes can be made in the function and arrangement of elements without departing from the scope defined by the claims, which includes known equivalents and foreseeable equivalents at the time of filing this patent application.

What is claimed is:

1. An electronic insulin infusion device comprising:

an insulin reservoir for insulin to be delivered from the insulin infusion device to a body of a user;

a processor architecture comprising at least one processor device; and at least one memory element associated with the processor architecture, the at least one memory element storing processor-executable instructions that, when executed by the processor architecture, perform a method of controlling closed-loop delivery of insulin from the insulin reservoir to the body of the user, the method comprising:

computing a current insulin on board (IOB) value that indicates an amount of active insulin in the body of the user;

calculating an IOB rate based at least in part on the computed IOB value, wherein the IOB rate represents an amount of active insulin accumulated from manual boluses in the body of the user per unit of time;

determining an adjusted insulin infusion rate based at least in part on the calculated IOB rate and an uncompensated insulin infusion rate;

selecting a final insulin infusion rate for the insulin infusion device, wherein the selecting selects either the determined adjusted insulin infusion rate, the uncompensated insulin infusion rate, or a current basal rate as the final insulin infusion rate, wherein selecting the final insulin infusion rate is in accordance with either expression FinalRate(n)=max(Basal; AdjustedRate(n)) when PIDRate>Basal, or expression FinalRate(n)=PIDRate(n) when PIDRate Basal, wherein:

FinalRate(n) is the selected final insulin infusion rate;

Basal is the current basal rate;

AdjustedRate(n) is the determined adjusted insulin infusion rate; and

PIDRate(n) is the uncompensated insulin infusion rate; and

operating the insulin infusion device in a closed-loop mode to continuously deliver insulin from the insulin reservoir to the body of the user in accordance with the final insulin infusion rate that is selected, wherein the final insulin infusion rate represents an amount of insulin to be delivered per unit of time.

2. The insulin infusion device of claim **1**, wherein the method performed by the processor-executable instructions further comprises:

repeating the computing, the calculating, the determining, the selecting, and the operating in accordance with a predetermined schedule to adjust the final insulin infusion rate in an ongoing manner.

3. The insulin infusion device of claim **1**, wherein the current IOB value is calculated based at least in part on historical bolus delivery data for the user.

4. The insulin infusion device of claim **3**, wherein the current IOB value is calculated in accordance with a three-compartment insulin pharmacokinetic model.

5. The insulin infusion device of claim **3**, wherein determining the adjusted insulin infusion rate comprises:

selecting the adjusted insulin infusion rate in accordance with the expression AdjustedRate(n)=max(0; PIDRate(n)−IOBRate(n)), wherein:

AdjustedRate(n) is the selected adjusted insulin infusion rate;

PIDRate(n) is the uncompensated insulin infusion rate; and

IOBRate(n) is the calculated IOB rate.

6. A closed-loop insulin infusion system comprising:

a continuous glucose sensor that generates sensor data indicative of sensor glucose values for a user; and

an insulin infusion device coupled to receive the sensor data generated by the continuous glucose sensor, the insulin infusion device comprising an insulin reservoir for insulin to be delivered from the insulin infusion device to the user, a processor architecture comprising at least one processor device and further comprising at least one memory element associated with the processor architecture, the at least one memory element storing processor-executable instructions that, when executed by the processor architecture, cause the insulin infusion device to perform a method comprising:

initiating a closed-loop operating mode of the insulin infusion device; in response to initiating the closed-loop operating mode, obtaining a most recent sensor glucose value for the user;

computing a current insulin on board (IOB) value that indicates an amount of active insulin in the body of the user;

calculating an IOB rate based at least in part on the computed IOB value, wherein the IOB rate represents an amount of active insulin accumulated from manual boluses in the body of the user per unit of time;

determining an adjusted insulin infusion rate based at least in part on the calculated IOB rate and an uncompensated insulin infusion rate;

selecting a final insulin infusion rate for the insulin infusion device, wherein the selecting selects either the determined adjusted insulin infusion rate, the uncompensated insulin infusion rate, or a current basal rate as the final insulin infusion rate; wherein selecting the final insulin infusion rate is in accordance with either expression FinalRate(n)=max(Basal; AdjustedRate(n)) when PIDRate>Basal, or expression FinalRate(n)=PIDRate(n) when PIDRate≤Basal, wherein:

FinalRate(n) is the selected final insulin infusion rate;

Basal is the current basal rate;

AdjustedRate(n) is the determined adjusted insulin infusion rate; and

PIDRate(n) is the uncompensated insulin infusion rate;

and operating the insulin infusion device in the closed-loop operating mode to continuously deliver insulin from the insulin reservoir to the body of the user in accordance with the final insulin infusion rate that is selected, wherein the final insulin infusion rate represents an amount of insulin to be delivered per unit of time.

7. The closed-loop insulin infusion system of claim **6**, wherein the current IOB value is calculated based at least in part on historical bolus delivery data for the user.

8. The closed-loop insulin infusion system of claim **7**, wherein the current IOB value is calculated in accordance with a three-compartment insulin pharmacokinetic model.

9. The closed-loop insulin infusion system of claim **6**, wherein determining the adjusted insulin infusion rate comprises:

selecting the adjusted insulin infusion rate in accordance with the expression

$$\text{AdjustedRate}(n)=\max(0;\text{PIDRate}(n)-\text{IOBRate}(n)),$$

wherein:

AdjustedRate(n) is the selected adjusted insulin infusion rate;

PIDRate(n) is the uncompensated insulin infusion rate; and

IOBRate(n) is the calculated IOB rate.

10. The closed-loop insulin infusion system of claim **6**, wherein the method performed by the processor-executable instructions further comprises:

repeating the computing, the calculating, the determining, the selecting, and the operating in accordance with a predetermined schedule to adjust the final insulin infusion rate in an ongoing manner.

* * * * *